1-1-2013

New Ruthenium and Osmium Carbonyl Cluster Complexes With Main Group Bridging Ligands Having Unusual Structures and Bonding

Yuwei Kan
University of South Carolina

NEW RUTHENIUM AND OSMIUM CARBONYL CLUSTER COMPLEXES WITH MAIN GROUP BRIDGING LIGANDS HAVING UNUSUAL STRUCTURES AND BONDING

by

Yuwei Kan

Bachelor of Engineering
Jilin University, 2008

Submitted in Partial Fulfillment of the Requirements

For the Degree of Doctor of Philosophy in

Chemistry

College of Arts & Sciences

University of South Carolina

2013

Accepted by:

Richard D. Adams, Major Professor

Hans-Conrad Zur Loye, Committee Member

Qian Wang, Committee Member

Timir Datta, Committee Member

Lacy Ford, Vice Provost and Dean of Graduate Studies

ACKNOWLEDGEMENTS

I would like to express my most sincere gratitude and appreciation to my advisor, Professor Richard Adams, for his guidance, patient and support throughout my research over the past five years. His dedication, passion and expertise in cluster chemistry made me always want to think and explore more. My sincere appreciation is extended to my committee members: Prof. Hans-Conrad Zur Loye, Prof. Qian Wang and Prof. Timir Datta for their time and valuable advice to my research.

I would like to thank Prof. Vitaly Rassolov, Prof. Michael B. Hall (Texas A&M University) and Dr. Eszter Trufan (Texas A&M University) for the DFT calculations on the $Ru_4(CO)_{12}(\mu_4\text{-GePh})$ and $[Ru_3(CO)_8(\mu_3\text{-CMe})(\mu\text{-H})_2(\mu_3\text{-H})]_2$. I am also thankful to Qiang Zhang, who is a great companion in Adams group and my life (my dear husband), for his help with crystals that were difficult to handle and the DFT calculations on the OsAu and OsBi compounds.

I wish to thank the past and present members of Adams group. Dr. Minglai Fu and Dr. Eszter Trufan for guiding my first steps in research; Gaya Elpitiya for the best time we had in the lab and the most precious friendship; Dr. Mingwei Chen, Yuen Onn Wong and Joeseph Kiprotich for being great teammates; and the new members Jonathan Tedder and Dr. Juliet Hahn for making me realize how much I have learnt.

These years wouldn't have been as great if without the support from my family. I wish to express my deepest gratitude to my dear husband, Qiang Zhang, for being extremely supportive to my research and the family: you are the reason I am writing this,

I would not be able to done all of this without you. I thank my son, Jason Zhang, for being a good boy and not making too much trouble; my mom Wanhua Li, dad Qiang Kan and mother in-law Xuehua Na for helping me take care of my son and being so supportive for my research. Thank my grandfather, Xueda Li, for your understanding and support to study in the US: I miss you so much. Thank my precious daughter: we'll be able to see you in one month.

I would also like to thank my friends Xin Li, Nan Jiang, Suning Wang, Yun Wu, Xiaofang Zhang, Pei Tang, Hong Guan, Xiaoguang Ma, Di Song, Chen Zhao, Zhichao Shan, Xiaolong Bai, Ron Parker and Marianne Parker for all the wonderful time we spent together. Especially I would like to thank Gaya Elpitiya and Prasanna Malinda Witharana for the delicious Sri Lankan food.

Last but not least, I would like to thank National Science Foundation for the financial support to my research.

ABSTRACT

The reaction of $IrRu_3(CO)_{13}(\mu\text{-}H)$, **2.1** with $HSnPh_3$ in hexane solvent at reflux has provided the new mixed metal cluster compounds $Ir_2Ru_2(CO)_{11}(SnPh_3)(\mu\text{-}H)_3$, **2.2** and $IrRu_3(CO)_{11}(SnPh_3)_3(\mu\text{-}H)_4$, **2.3** containing $SnPh_3$ ligands. Compound **2.2** which was obtained in low yield (3%) contains a closed cluster having two iridium and two ruthenium atoms, one $SnPh_3$ ligand and three bridging hydride ligands. Compound **2.3** has a butterfly structure for the four metal atoms with three $SnPh_3$ ligands and four bridging hydride ligands around the periphery of the cluster. When compound **2.3** was heated to 97 ^oC for 30min, $IrRu_3(CO)_9(\mu\text{-}\eta^2\text{-}C_6H_5)(\mu_4\text{-}SnPh)_2(\mu\text{-}SnPh_2)$, **2.4** was formed by cleavage of phenyl rings from the $SnPh_3$ ligands in low yield. Compound **2.4** contain square $IrRu_3$ clusters of the metal atoms with quadruply bridging SnPh ligands on opposite sides of the cluster, one bridging $SnPh_2$ ligand on one of the Ir-Ru bonds and also a rare η^2-bridging phenyl ligand.

The new compound $IrRu_3(CO)_{11}(GePh_3)_3(\mu\text{-}H)_4$, **3.1** was obtained in 64% yield from the reaction of $IrRu_3(CO)_{13}(\mu\text{-}H)$ with $HGePh_3$ at room temperature. Compound **3.1** is the Ge analog of compound **2.3**, which contains an open cluster of one iridium and three ruthenium atoms with three $GePh_3$ ligands and four hydride ligands. When the reaction was performed at hexane reflux for 10 min a second minor $Ir_2Ru_2(CO)_{11}(GePh_3)(\mu\text{-}H)_3$, **3.2** was formed. Compound **3.2** is two iridium atoms and two ruthenium atoms in a tetrahedral structure which must have formed by some metal-metal exchange process. When compound **3.1** was heated to 68 ^oC for 6h, two new

compounds: $IrRu_3(CO)_{10}(\mu\text{-}\eta^2\text{-}C_6H_5)(\mu_4\text{-}GePh)_2$, **3.3** and $IrRu_3(CO)_9(\mu\text{-}\eta^2\text{-}C_6H_5)(\mu_4\text{-}GePh)_2(\mu\text{-}GePh_2)$, **3.4** were formed by cleavage of phenyl rings from the $GePh_3$ ligands. Compound **3.3** and **3.4** contain square $IrRu_3$ clusters of the metal atoms with quadruply bridging GePh germylyne ligands on opposite sides of the cluster. Both compounds also contain a rare η^2-bridging phenyl ligand. Compound **3.4** was found to react with dimethylacetylenedicarboxylate DMAD to yield new compound $IrRu_3(CO)_9([\mu_4\text{-}Ge(Ph)C(CO_2Me)C(CO_2Me)](\mu\text{-}GePh_2)_2$, **3.5** by addition of DMAD to one of the bridging germylyne ligands. In the process the bridging phenyl ligand was transferred to the other bridging germylyne ligand to form a bridging germylene ligand.

The compounds $Ru_4(CO)_{12}(GePh_3)_2(\mu\text{-}H)_4$, **4.1** and $Ru_4(CO)_{12}(SnPh_3)_2(\mu\text{-}H)_4$, **4.2** were obtained from the reactions of $Ru_4(CO)_{13}(\mu\text{-}H)_2$ with $HGePh_3$ and $HSnPh_3$, respectively. Both compounds contain a nearly planar butterfly structure for the four metal atoms with two $GePh_3$ / $SnPh_3$ ligands and four bridging hydride ligands around the periphery of the cluster. When heated, **4.1** and **4.2** were converted into the complexes $Ru_4(CO)_{12}(\mu_4\text{-}EPh)_2$, **4.3**, E = Ge, and **4.4**, E = Sn, by cleavage of two phenyl groups from each of the $GePh_3$ ligands. Compounds **4.3** and **4.4** contain square planar arrangements of the four ruthenium atoms with quadruply bridging germylyne and stannylyne ligands on opposite sides of the square plane. The bonding and electronic transitions of **4.3** were analyzed by DFT computational analyses.

The electronically unsaturated complex $[Ru_3(CO)_8(\mu_3\text{–}CMe)(\mu\text{–}H)_2(\mu_3\text{–}H)]_2$, **5.1** was obtained by silica gel induced reaction of $Ru_3(CO)_8(\mu_3\text{–}CMe)(\mu\text{–}H)_3$, **5.2**. Compound **5.1** can be viewed as a dimer of the 46 electron fragment $Ru_3(CO)_8(\mu_3\text{–}CMe)(\mu\text{–}H)_3$, is held together by a delocalized bonding involving two triply-bridging hydride ligands.

Compound **5.1** exhibits a dynamical activity in solution that equilibrates two of the three types of hydride ligands. Compound **5.1** reacts with 1,1–bis(diphenyphosphino)methane to form the macrocyclic complex $[Ru_3(CO)_7(\mu_3\text{–}CMe)(\mu\text{–}H)_3]_2(\mu\text{–}dppm)_2$, **5.3**. Compound **5.3** is a centrosymmetrical dimer linked by two bridging dppm ligands, each phosphorus atom of the dppm is coordinated to a different Ru_3 cluster. However, $Ru_3(CO)_7(\mu_3\text{-}CMe)(\mu\text{-}H)_3(\mu\text{-}dppm)$, **5.4**, was obtained from the reaction of Compound **5.2** with dppm.

Reactions of $Os_3(CO)_{10}(NCMe)_2$ with $HGePh_3$ have yielded the compounds $Os_3(CO)_{10}(NCMe)(GePh_3)(\mu\text{-}H)$, **6.1** and $Os_3(CO)_{10}(GePh_3)_2(\mu\text{-}H)_2$, **6.2** by the sequential replacement of the NCMe ligands and the oxidative addition of the GeH bonds of one and two $HGePh_3$ molecules, respectively, to the osmium atoms of the cluster. Compound **6.2** exists as two isomers in solution at low temperatures which interconvert rapidly on the ^1H NMR time scale at room temperature. When heated, **6.1** was transformed into the pentaosmium complex $Os_5(CO)_{17}(\mu\text{-}GePh_2)$, **6.3** which exhibits a planar raft structure with one bridging $GePh_2$ ligand. Compound **6.1** reacts with the compound $PhAu(PPh_3)$ to yield the compound $Os_3(CO)_8(\mu\text{-}CO)(\mu\text{-}O{=}CPh)(\mu\text{-}GePh_2)(\mu\text{-}AuPPh_3)$, **6.4** which contains a bridging O=CPh ligand and a $Au(PPh_3)$ group that bridges an Os-Ge bond, and compound $PhOs_4(CO)_{13}(\mu\text{-}GePh2)(\mu\text{-}AuPPh_3)$, **6.6** which contains four osmium atoms in a butterfly arrangement with one bridging $GePh_2$ ligand, one bridging $AuPPh_3$ ligand and one σ-bonded phenyl ligand to one of the osmium atoms. A minor product, $Os(CO)_4(GePh_3)(AuPPh_3)$, **6.5** was also obtained in this reaction. Compound **6.4** was also obtained from the reaction of **6.1** with $CH_3Au(PPh_3)$. Compound **6.4** reacted with PhC_2Ph to yield the complex $Os_3(CO)_7(\mu\text{-}GePh_2)(\mu\text{-}AuPPh_3)[\mu\text{-}(O)CPhCPhCPh)]$, **6.7** which

contains a novel bridging oxa-metallacycle formed by the coupling of PhC_2Ph to the bridging O=CPh ligand **6.4** and another example of a $Au(PPh_3)$ group that bridges an Os-Ge bond. The bonding of the bridging $Au(PPh_3)$ group to the Os – Ge bonds in **6.4** and **6.7** was investigated by DFT computational analyses.

Three new compounds were obtained from the reaction of $Os_3(CO)_{10}(NCMe)_2$, **7.1** with $BiPh_3$ in a methylenechloride solution at reflux. These have been identified as $Os_3(CO)_{10}(\mu_3\text{-}C_6H_4)$, **7.2**, $Os_3(CO)_{10}Ph(\mu\text{-}\eta^2\text{-}O{=}CPh)$, **7.3**, and $HOs_6(CO)_{20}(\mu\text{-}\eta^2\text{-}C_6H_4)(\mu_4\text{-}Bi)$, **7.5**. A fourth product $HOs_5(CO)_{18}(\mu\text{-}\eta^2\text{-}C_6H_4)(\mu_4\text{-}Bi)$, **7.4** was also obtained from the reaction of $Os_3(CO)_{11}(NCMe)$ with $BiPh_3$. Cleavage of the phenyl groups from the $BiPh_3$ was the dominant reaction pathway and two of the products **7.2** and **7.3** contain rings but no bismuth. Each of the new compounds was characterized structurally by single-crystal X-ray diffraction methods. Compound **7.2** contains a triply bridging benzyne (C_6H_4) ligand that exhibits a pattern of alternating long and short C – C bonds that can be attributed to partial localization of the π-bonding in the C_6 ring. The localization in the π-bonding was supported by DFT calculations. Compound **7.3** contains a triangular cluster of three osmium atoms with a bridging benzoyl ligand and a terminally coordinated phenyl ligand. Compound **7.5** contains six osmium atoms divided into two groups of four and two and the two groups are linked by a spiro-bridging bismuth atom. The group of two osmium atoms contains a bridging C_6H_4 ligand. When heated, compound **7.3** was converted into **7.2** and the compound $Os_3(CO)_{10}(\mu\text{-}\eta^2\text{-}O{=}CPh)_2$, **7. 6**. Compound **7.6** contains two bridging benzoyl ligands.

TABLE OF CONTENTS

LIST OF TABLES

LIST OF FIGURES

LIST OF SCHEMES

CHAPTER 1

INTRODUCTION

Metal cluster chemistry has been developed rapidly over the last five decades.[1] A metal cluster compound can be defined as the compound that contains two or more metal atoms that are held together by direct and substantial metal-metal bonds.[2] Ligated transition metal clusters, such as transition metal carbonyl complexes, which can be used as synthetic organometallic reagents, are usually synthesized by thermal or photochemical activation of mononuclear metal precursors.[3] Transition metal carbonyl complexes are coordination complexes with carbon monoxide ligands that are bonded terminally to one transition metal atom or bridging to two or more transition metal atoms. The transition metal – carbonyl bonding interaction involves σ-bonding of the CO ligand to the empty d orbital of the transition metal, as well as the π back bonding of a filled metal d orbital to an empty π* orbital.[4] The CO ligand has a high tendency to stabilize metal-metal bonding in cluster compounds because they are capable of reducing the electron density on the metal by π-backbonding to the CO ligand. The first metal carbonyl complex, $Ni(CO)_4$, was discovered by Ludwig Mond in 1890, which is an intermediate used to produce pure nickel metal by the Mond process.[5] Polynuclear metal carbonyl cluster compounds include not only electron-precise polyhedral cluster complexes in which all the metal atoms have the closed shell 18 electron configuration, but also compounds in which the metal atoms interact with each other by forming delocalized bonds that can be explained by polyhedral skeletal electron pair theory.[6] Transition metal cluster chemistry has

aroused interest over the years for the following reasons:

1. This area of chemistry can serve as effective structural model to the study on metal surfaces in chemisorbed processes, which is known as the cluster-surface analogy.[7] As an example, the high-nuclearity cluster $[Os_{20}(CO)_{40}]^{2-}$ (Figure.1.1) was synthesized and characterized by Johnson and Lewis in 1991.[8] This cluster contains a tetrahedron of 20 osmium atoms with 40 terminal CO ligands, arranged like the unit cell of cubic close-packed metal atoms with chemisorbed molecules. The size of some transition metal cluster compounds spans the range from the small ligated clusters and the colloidal metals, and large enough to make the valuable comparisons to the bulk metal and metal surfaces regarding to the structure, electronic and chemical characteristics, as well as the catalytic transformations of small molecules.[3] The characterization of cluster compounds in solution and the solid state by the use of spectroscopic (particularly IR, NMR and mass spectrometry) and diffraction techniques (single-crystal X-ray diffraction) can provide a useful understanding for metal surfaces at the atomic and molecular level.

2. Transition metal cluster complexes are able to act as good homogeneous catalysts.[7] Although in some metal cluster catalytic system, it is the mononuclear metal fragment which is formed after the loss of ligands from the cluster that acts as the catalysts,[9] there are some examples where catalysis is achieved by intact clusters complexes. In the homogenous metal cluster catalyzed reaction, one or more metal atoms in the cluster can serve as an active site to convert the reactants into products, and the cluster catalyst is an integral part of the catalytic cycle.[10] For example, the complex $Pt_3Ru_6(CO)_{20}(\mu_3\text{-}PhC_2Ph)(\mu_3\text{-}H)(\mu\text{-}H)$ has been shown to be an effective catalyst for the hydrogenation of diphenylacetylene to (Z)-stilbene[11]. In this layer segregated metal

cluster complex, the central triangular layer contains three platinum atoms while each of the two outer triangle layers contains three ruthenium atoms. In the hydrogenation of diphenylacetylene, the formation of (Z)-stilbene was observed at a turn over frequency of $47h^{-1}$. The kinetic studies also showed that it was the whole cluster complex itself that acted as the active catalyst in the catalytic cycle instead of metal-containing-fragments, see Scheme 1.1.

3. Many transition metal cluster complexes have been shown to serve as precursors to heterogeneous catalysts for a variety of important industrial processes.[12] It is believed that metal carbonyl clusters on metal supports such as silica, alumina, can form highly dispersed metallic catalysts in low oxidation states. Parkyns reported the first example to prepare highly dispersed catalysts by using metal carbonyls as the precursors. They prepared an alumina supported metallic nickel from the decomposition of $Ni(CO)_4$.[13] Since this discovery, there has been significant interest in this research field.

Recently, much more attention has been focused on the study of the synthesis and characterization of mixed-metal cluster complexes for the applications in catalysis.[14] The presence of two or more types of metals can improve the catalytic properties, including increasing product selectivity, enhancing the catalyst lifetime and increasing activity.[15] The improvement is often produced by cooperative interactions between the different types of metal atoms.[16] It is widely believed that the investigation of heteronuclear transition metal cluster complexes can provide a deeper insight into such synergistic effects due to the fact that cluster complexes can be better characterized at the atomic and molecular level and can be used directly as precursors to nanoscale heterogeneous heterometallic catalysts.[17] One great advantage to prepare heterogeneous catalysts

derived from transition metal complexes is that the stoichiometry of the heterometallic catalysts on the support can be controlled, because the mixed-metal cluster complexes contain direct bonds between the metal atoms.

It is well known that bimetallic catalysts are widely used in many industrial processes, for example bimetallic catalysts containing platinum are extensively used in petroleum reforming which refers to the process of converting low-octane rating petroleum naphtha to high-octane gasoline.[18] Reforming reactions include isomerization, dehydrogenation, and dehydrocyclization to produce aromatic hydrocarbons from the hydrocarbon feedstocks. The first industrial bimetallic catalyst used in petroleum reforming is alumina-supported Pt-Re catalysts in 1969.[14] Later it was also discovered that alumina-supported Pt-Ir and Pt-Sn bimetallic catalysts exhibit superior catalytic properties to monometallic Pt catalysts.[19] Since 1970s, the development of EXAFS (extended X-ray absorption fine structure) greatly improved the study of bimetallic clusters. EXAFS provides the structural information of catalytic materials to investigate the dispersion of the bimetallic clusters over the surface of an oxide support.[20]

Main group metals, such as Ge,[21] Sn,[22] Bi,[23] have been shown to be valuable modifiers for transition metal based catalysts to enhance their catalytic performance. Platinium-tin nanoparticles supported on alumina that are used as dehydrogenation and aromatization catalysts have been shown to be even more effective than Pt-Re and Pt-Ir bimetallic catalysts in petroleum reforming.[19] The platinum-tin catalysts possess increased reforming selectivity and reduced poisoning by weakening Pt-C bonds that lead to the formation of coke. Many studies have been conducted to try to understand the role of tin in bimetallic catalysts considering the fact that Pt surface should be poisoned by

even small traces of metallic tin.[21] Dautzenberg *et al.* and Biloen *et al.* have suggested that tin divides the surface to very small ensembles of platinum atoms (ensemble effect), thus the hydrogenolysis and isomerization can be suppressed to reduce coke formation.[24] However, Burch and Garla proposed that tin modifies the electronic properties of the small platinum particles (ligand effect), which is attributed to the higher stability and selectivity.

Tin has also been shown to be valuable modifier to many other transition metal catalysts. Iridium-tin catalysts have been shown to have high selectivity for dehydrogenation of propane to propene.[25] Nickel-tin catalysts have been shown to produce hydrogen catalytically from biomass-derived oxygenated hydrocarbons.[26] Recently, Adams *et. al.* showed that the tin-containing nanoscale catalysts platinum-tin, rhodium-tin, and ruthenium-tin anchored with mesoporous silica exhibit remarkable selectivity for the selective hydrogenation of 1,5,9-cyclododecatriene (CDT) to produce cyclododecene (CDE), which is the vital feedstock in many industrial processes (Scheme 1.2).[27] These bimetallic catalysts are more effective than the traditional monometallic catalysts which lack selectivity and produce considerable amounts of the undesired product cyclododecane (CDA). Bimetallic organometallic transition metal carbonyl complexes are used as precursors to prepare the catalysts, following by their deposition from solution onto silica supports such as Davison type 911 and ligand removal by heating in vacuo for 1h at 473 K. The corresponding precursors complexes were used as precursors for the nanocatalysts $PtSn_2$, $RhSn_2$ and $RuSn_2$ are $(COD)Pt(SnPh_3)_2$, (COD = 1,5-cyclooctadiene), $Rh_3(CO)_6(SnPh_3)_2(\mu\text{-}SnPh)_2$ and $Ru(CO)_4(SnPh_3)_2$, respectively. To compare the catalytic performance to the pure PGM (platinum group metals), $Pt(COD)_2$,

$Rh_4(CO)_{12}$, and $Ru_3(CO)_{12}$ were used as the precursors to prepare the corresponding monometallic catalysts. The result of the catalytic performance is shown in Figure 1.2. The $PtSn_2$ catalyst on the silica support was characterized by using electron-induced energy-dispersive X-ray (EDX) emission spectroscopy.

Another Group 14 element germanium has also been shown to exhibit interesting catalytic properties when introduced to monometallic catalysts. The alumina supported rhodium-germanium bimetallic catalysts prepared by surface redox reaction have been shown to improve the selectivity of citral hydrogenation to the unsaturated alcohols (nerol and geraniol) which are of importance in several industries, such as flavor, fragrance and pharmaceutical industry., whereas the monometallic rhodium catalysts lead to saturated aldehyde (citronellal) as main product.[21]

Bismuth on oxide supports is of great interest recently because it has been shown to catalyze the oxidation of certain hydrocarbons efficiently.[23] Transition metal – bismuth bimetallic catalysts also attracted significant attention since the discovery of bismuth-molybdate catalysts in the 1980s which catalyze the important industrial process for the ammoxidation of propylene to acrylonitrile.[28] Studies of the mechanism of this reaction have been suggested that bismuth is responsible for the abstraction of hydrogen from propylene through the Bi-O bond.[28]

Niacin (3-picolinic acid or nicotinic acid), produced commercially both by the gas-phase ammoxidation and liquid-phase oxidation of 3-picoline (Figure 1.3), is known as vitamin B_3 and plays an essential role in human metabolism.[29] It is also been extensively used as a cholesterol-lowing agent.[30] Thus, it is desired to find environmentally-friendly and one-step syntheses for niacin from 3-picoline. It has been

shown recently by Raja and Adams that silica-supported bimetallic rhenium-bismuth and rhenium-antimony nanocluster catalysts, Re_2Bi_2, Re_2Sb_2, Re_2Sb, derived from $Re_2(CO)_8(\mu\text{-}BiPh_2)_2$, $Re_2(CO)_8(\mu\text{-}SbPh_2)_2$ and $Re_2(CO)_8(\mu\text{-}SbPh_2)(\mu\text{-}H)$, respectively can improve the activity and selectivity for the liquid-phase ammoxidation of 3-picoline to nicotinonitrile (an intermediate to niacin) under mild condition, see Figure 1.4.[31] This result is attributed to the significant synergistic effects produced by combining two metallic elements, and the intimate bonding in Re-Sb/Bi complexes precursor prior to the conversion into nanoparticles.

Due to the excellent catalytic performance of precious metal - heavy main group metal, there have been major efforts to synthesize and characterize main group metal containing mixed metal cluster complexes. The heavy main group metals (Ge, Sn, Bi) with alkyl substituents attract most interest because the alkyl groups are easily removed under thermal treatment when preparing the multi-metallic catalysts. The important synthetic routes for tri-alkyl transition metal-tin/germanium complexes include halide displacement and oxidative addition.[32] The halide displacement is a nucleophilic displacement process in which the electron-rich nucleophilic anion bond displaces a halide anion from a metal halide complex. For example, the Ir-E (E = Ge, Sn) cluster $Ir(COD)(CO)_2EPh_3$ were obtained by the reaction of $[Ir(COD)Cl]_2$ with Ph_3ELi (prepared by reacting Ph_3EH with PhLi) under the purge with CO, see Scheme 1.3.[33] In this process, the halide Cl^- which is known to be a good leaving group forms LiCl with Li^+, accompanied by the simultaneous formation of Ir-E bond to yield this Ir-E complexes. There are numerous examples for the oxidative addition reaction for the synthesis of transition metal-tin/germanium complexes.[34] For example, the Sn-H bond in Ph_3SnH

readily react with $Ru(CO)_5$ after the loss of one CO via oxidative addition to give the stable stannyl hydride complex $Ru(CO)_4(SnPh_3)H$.[35]

In addition to terminally-coordinated triphenylgermyl or triphenylstannyl ligands EPh_3, the bridging EPh_2 ligands, triply-bridging EPh ligands, and quadruply-bridging ligands EPh can be formed by the cleavage of phenyl groups from the EPh_3 ligands and subsequent elimination of benzene when hydrides are present, the bridging modes are shown in Figure 1.5.[36] Recently, the computational analysis of the α-cleavage of a phenyl group from $GePh_3$ ligand has been studied in the transformation of the complex $Ir_3(CO)_6(\mu\text{-}CO)(\mu\text{-}GePh_2)_2(GePh_3)_3$ into the complex $Ir_3(CO)_6(\eta^1\text{-}Ph)(\mu\text{-}GePh_2)_3(GePh_3)_2$, see Scheme 1.4.[37] In this transformation, the α-cleavage of the phenyl group occurs at one single iridium atom. The first example of triply-bridging SnPh ligands was for the complex $Rh_3(CO)_3(SnPh_3)_3(\mu\text{-}SnPh_2)_3(\mu_3\text{-}SnPh)_2$, which contains three terminal $SnPh_3$ ligands, three edge-bridging $SnPh_2$ ligands, and two triply bridging SnPh ligands.[38] This complex was made from the reaction of $Rh_4(CO)_{12}$ with Ph_3SnH by forming $Rh_3(CO)_6(\mu\text{-}SnPh_2)_3(SnPh_3)_3$ as intermediate. The first example of quadruply-bridging EPh ligands was found in the complex $Ru_5(CO)_{11}(C_6H_6)(\mu_4\text{-}SnPh)(\mu_3\text{-}CPh)$ which was obtained by the cleavage of phenyl groups from the $SnPh_3$ ligand in the complex $Ru_5(CO)_{11}(C_6H_6)(SnPh_3)(\mu\text{-}H)(\mu_5\text{-}C)$.[39] The quadruply bridging EPh is not uncommon. For example, a series of tetraruthenium complexes containing quadruply bridging EPh ligands, **1.1**-**1.4**, were obtained from the reactions of $Ru_4(CO)_{12}(\mu\text{-}H)_4$ with $HEPh_3$, see Scheme 1.5. [40] The quadruply bridging EPh ligands serve as a three-electron donor, thus three of the ruthenium atoms achieve an 18-electron configuration, but the fourth ruthenium atom has only 16 electrons. Alternatively, a delocalized bonding model as

represented by the polyhedral skeletal electron approach would predict a total valence electron count of 62 electrons for an arachnooctahedron of four metal atoms, which is precisely the number of valence electrons found in compounds **1.1**-**1.4**.

As previously discussed, the addition of the Group VB heavy metal bismuth to transition metal catalysts can improve catalytic properties. $BiPh_3$ has been shown to be the major source of Bi for the addition of bismuth to transition metal carbonyl complexes. However, unlike $SbPh_3$, it is very difficult to introduce $BiPh_3$ to transition metal cluster complexes. There are only a few examples of transition metal cluster complexes with terminally-coordinated $BiPh_3$ ligand reported so far. These include $Cr(CO)_5(BiPh_3)$,[41] $M(CO)_5(BiPh_3)$, (M = Mo or W),[42] and $[(\eta^5\text{-}C_5H_5)Fe(CO)_2(BiPh_3)]BF_4$.[43] Attempts have been made to mimic the reaction of $Ni(CO)_4$, $Co_2(CO)_8$, $Fe(CO)_5$, $Fe_2(CO)_9$/THF and $Mn_2(CO)_{10}$ with $SbPh_3$ by using $BiPh_3$, but all failed to add bismuth to the complexes.[44] This is mainly a result of the poor σ-donor ability of the bismuth and the weak Bi-C bond which is easily cleaved.[45] For example, the reaction of $Os_3(CO)_{11}(NCMe)$ with $BiPh_3$ yielded five compounds $Os_2(CO)_8(\mu\text{-BiPh})$, **1.5**, $Os(CO)_4Ph_2$, **1.6**, $Os_4(CO)_{14}(\mu\text{-}\eta^3\text{-}O{=}CC_6H_5)(\mu_4\text{-Bi})$, **1.7**, $Os_4(CO)_{15}Ph(\mu_4\text{-Bi})$, **1.8**, and $Os_5(CO)_{19}Ph(\mu_4\text{-Bi})$, **1.9**, but none of them contains $BiPh_3$ ligand.[46] The products are formed by the fragmentation of Os_3 cluster and the facile phenyl cleavage from $BiPh_3$. In compound **1.5**, the BiPh ligand serves as a two-electron donor to the two osmium atoms, while in compound **1.7**-**1.9** the spiro μ_4-Bi serve as five-electron donor to the osmium atoms with proper distribution, all those compounds achieve 18 electron configuration.

The design and synthesis of main group (especially heavy main group metal) containing mixed metal cluster complexes is essential to further facilitate an

understanding of the synergistic effect of the metals. In addition, the investigation of the bonding and reactivity in such cluster complexes is also of great important. In this thesis, a large number of novel ruthenium and osmium carbonyl cluster complexes with bridging main group ligand were synthesized and characterized, some with unusual bonding have also been studied as well.

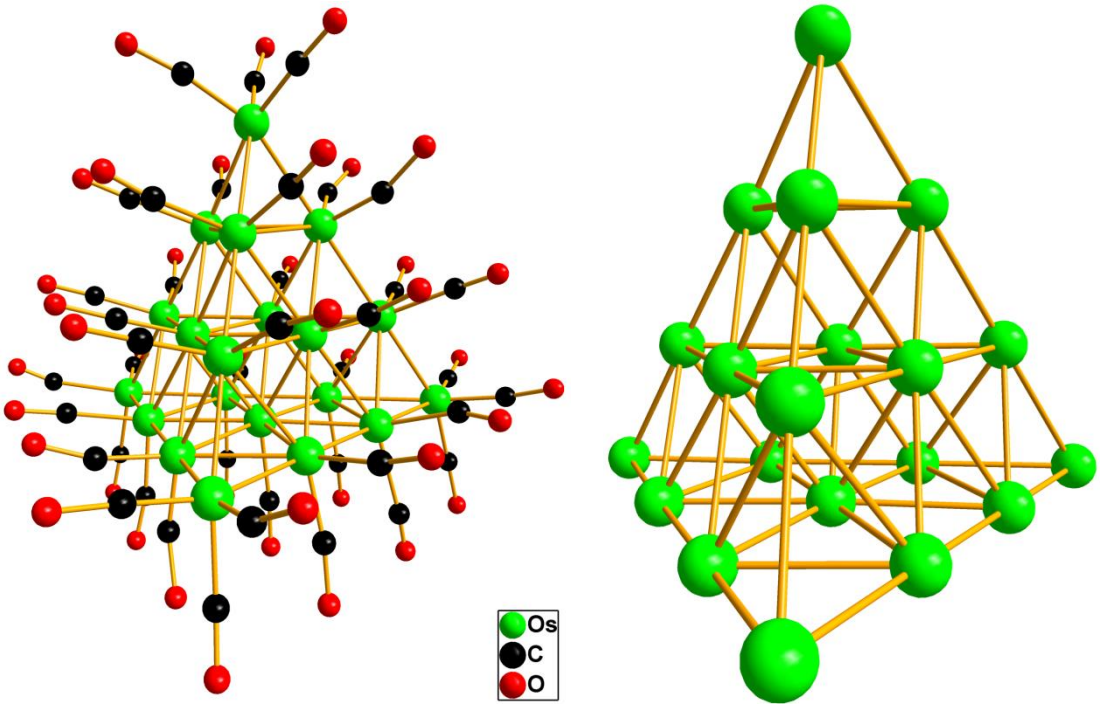

Figure 1.1. (Left) The ν_3 tetrahedral structure of $[Os_{20}(CO)_{40}]^{2-}$; (Right) View of the metal core.[8]

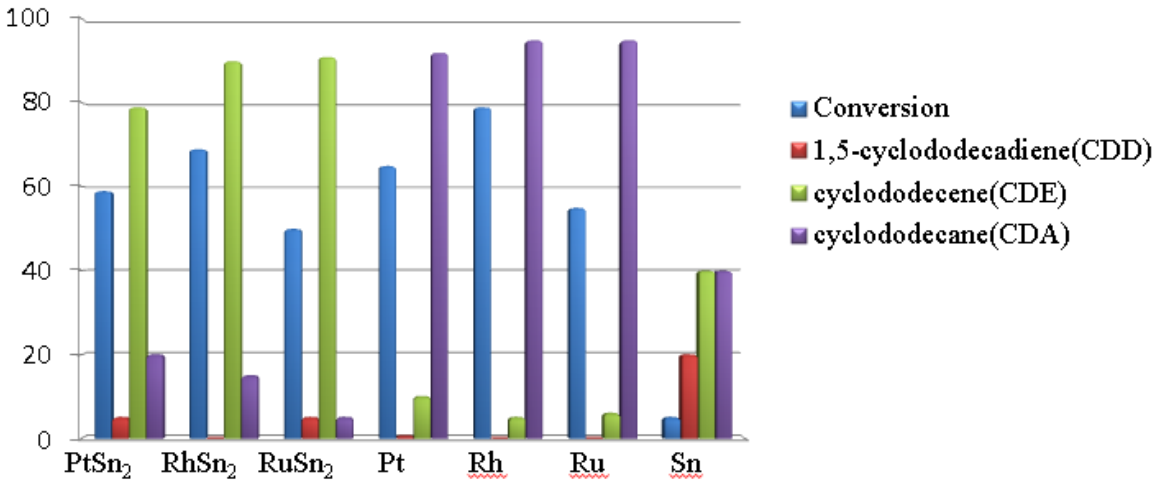

Figure 1.2. Effect of tin in the selective hydrogenation of 1,5,9-cyclododecatriene (CDT) using anchored monometallic and bimetallic cluster catalysts.[27]

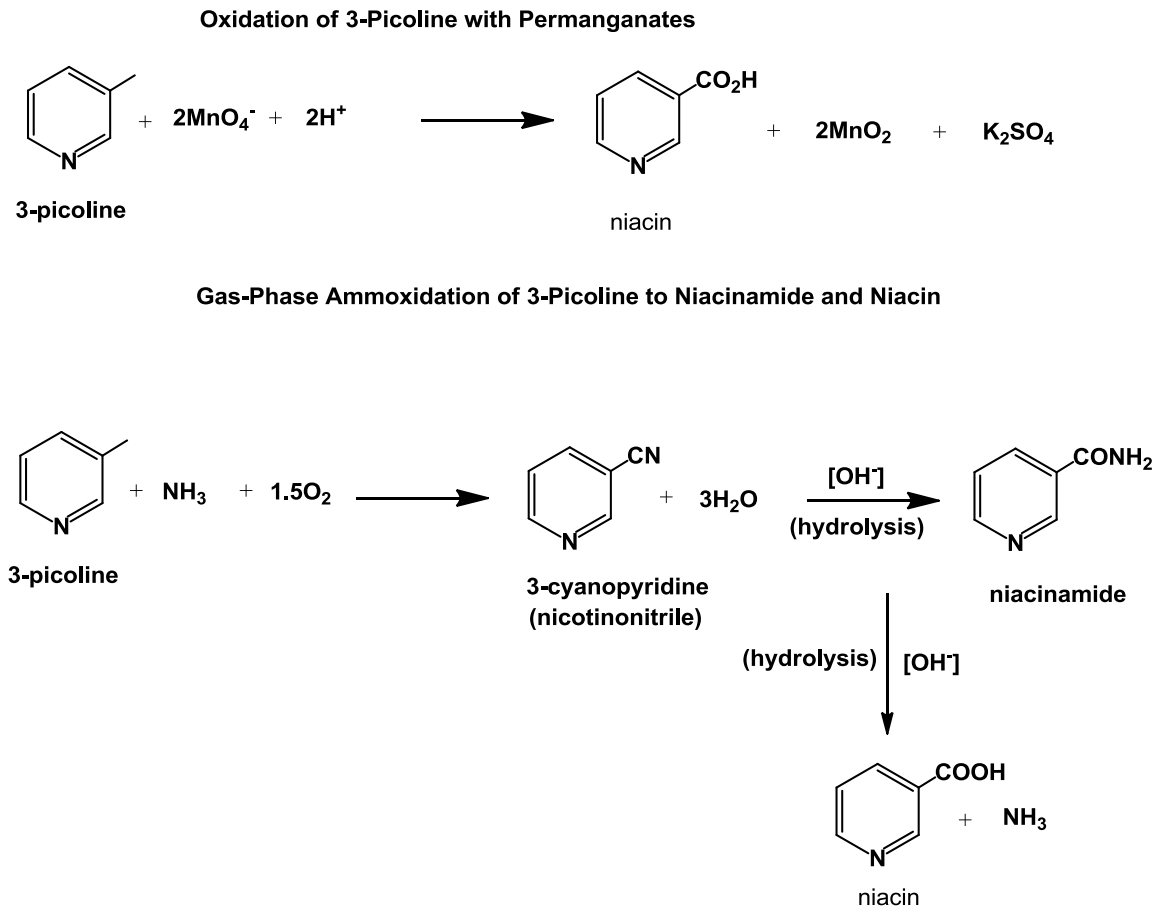

Figure 1.3. Gas-phase ammoxidation and liquid-phase oxidation of 3-picoline.[31]

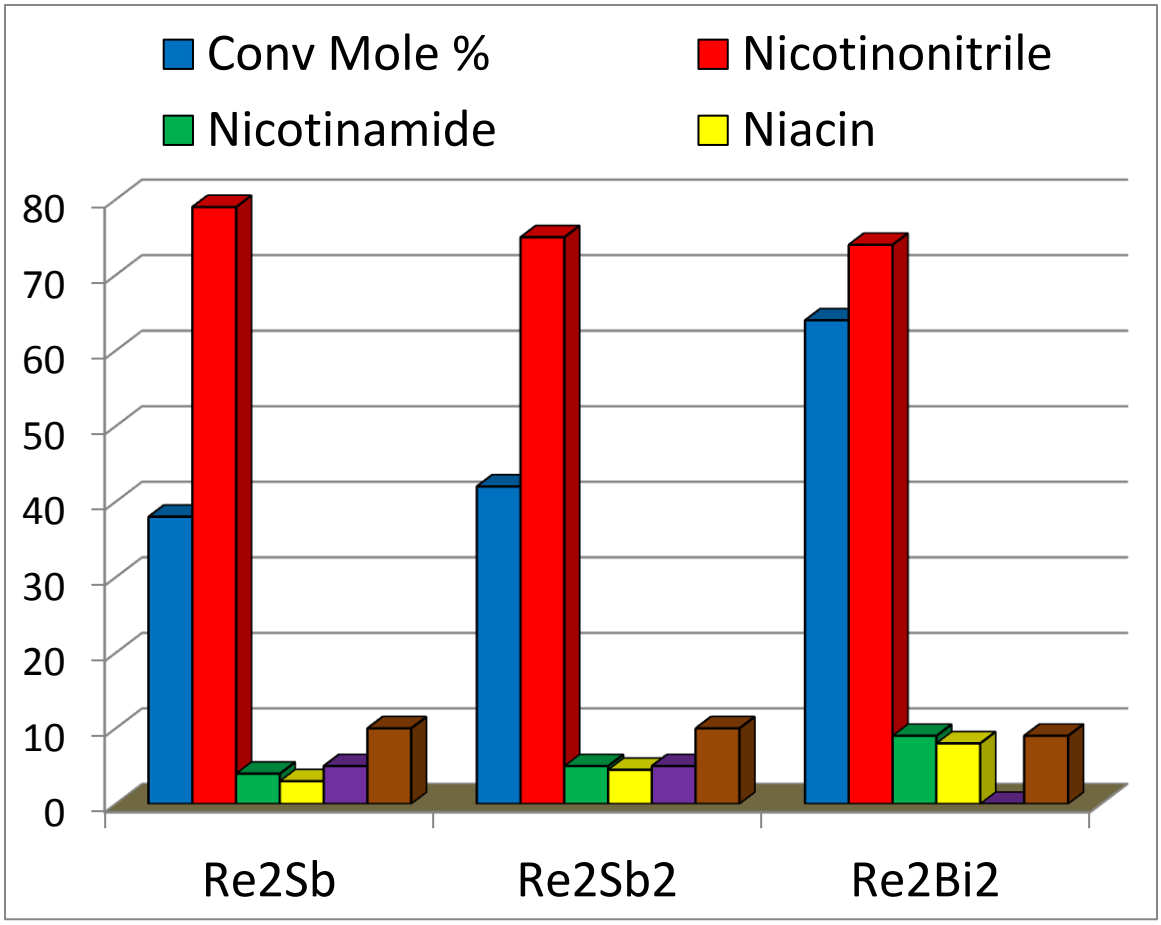

Figure1.4. Catalytic behavior of the bimetallic Re-Sb/Bi catalysts with differenct Re-Sb ratio.[31]

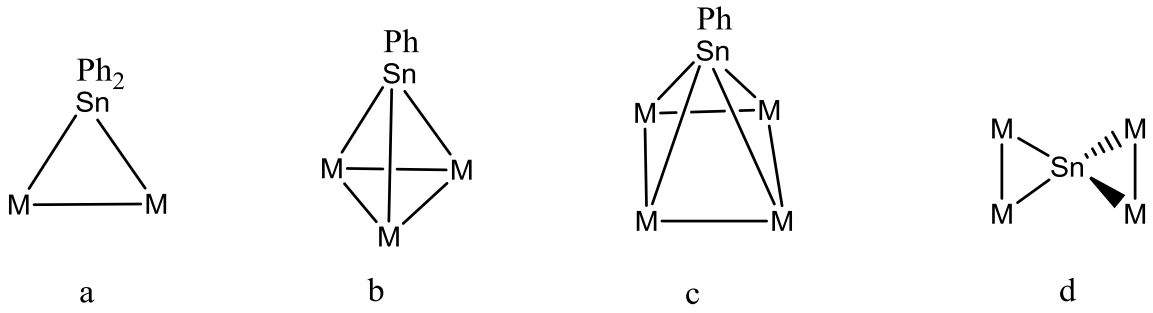

Figure 1.5. Four phenyltin bridging mode to transition metal clusters.[36]

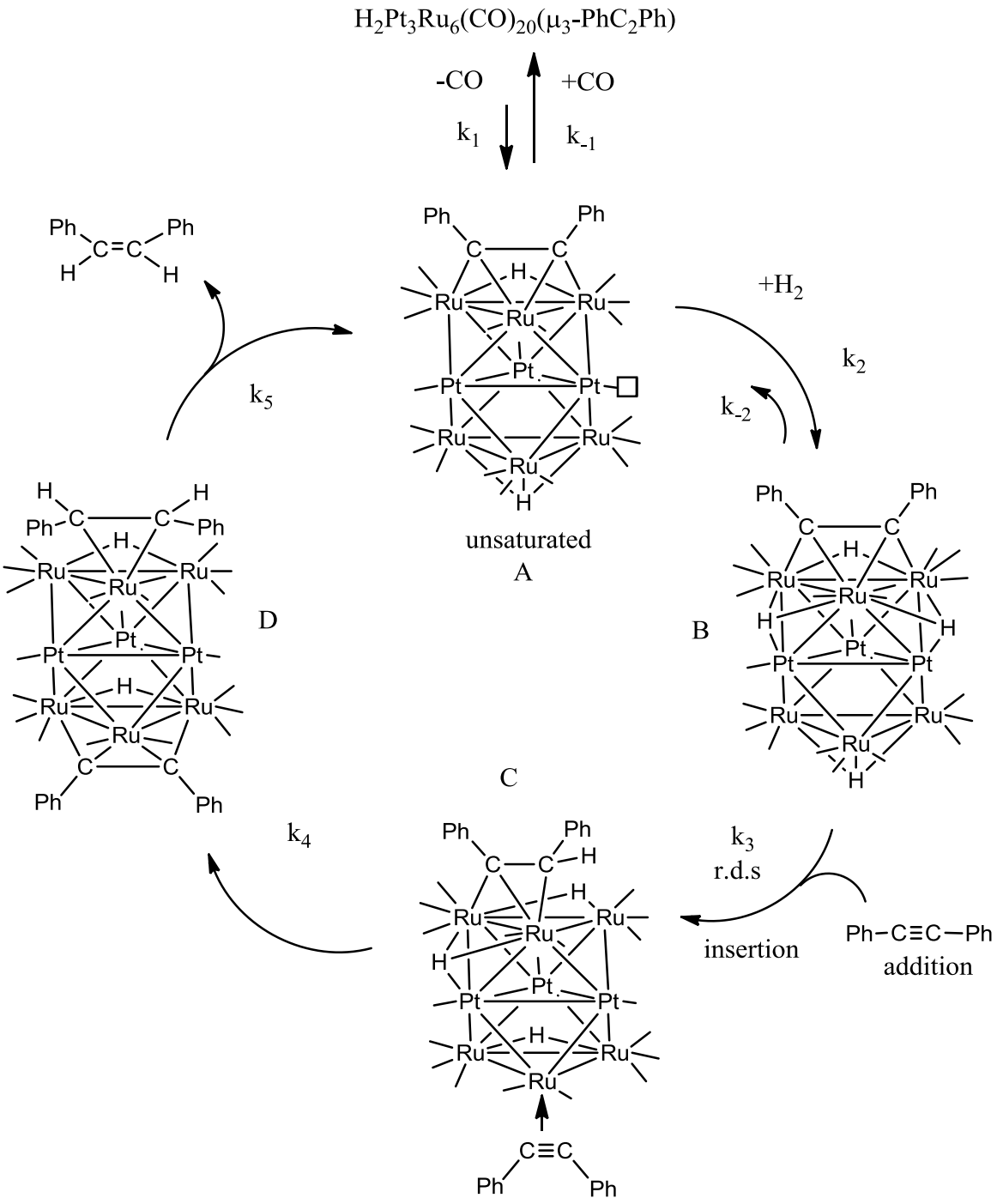

Scheme 1.1. The mechanism for the catalytic process of hydrogenation of diphenylacetylene to (Z)-Stilbene by use of $Pt_3Ru_6(CO)_{20}(\mu_3\text{-}PhC_2Ph)(\mu_3\text{-}H)(\mu\text{-}H)$ complex as catalysts.[11]

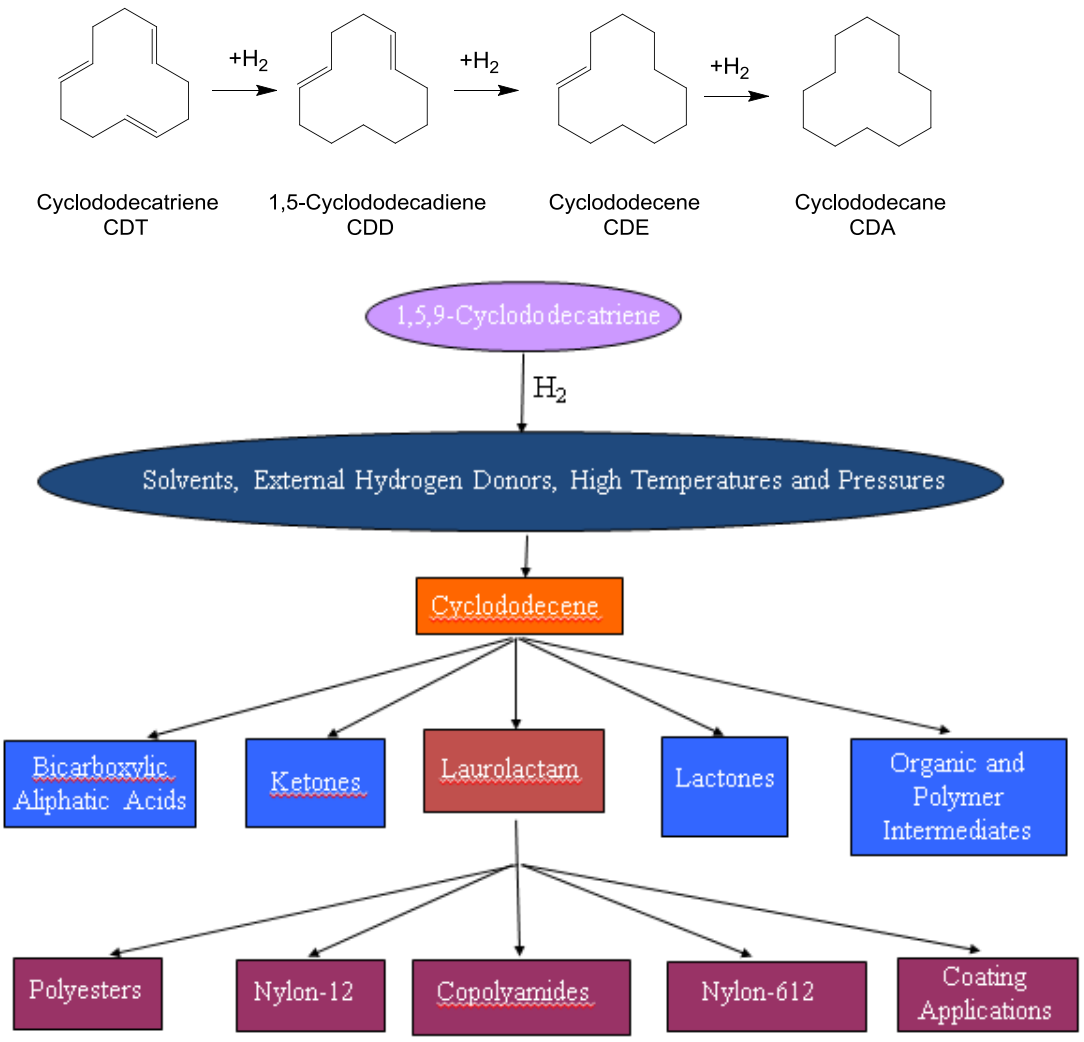

Scheme 1.2. Range of Commodity and Specialty Chemicals That Can Be Derived from the Selective Partial Hydrogenation of Cyclododecatriene (CDT).[27]

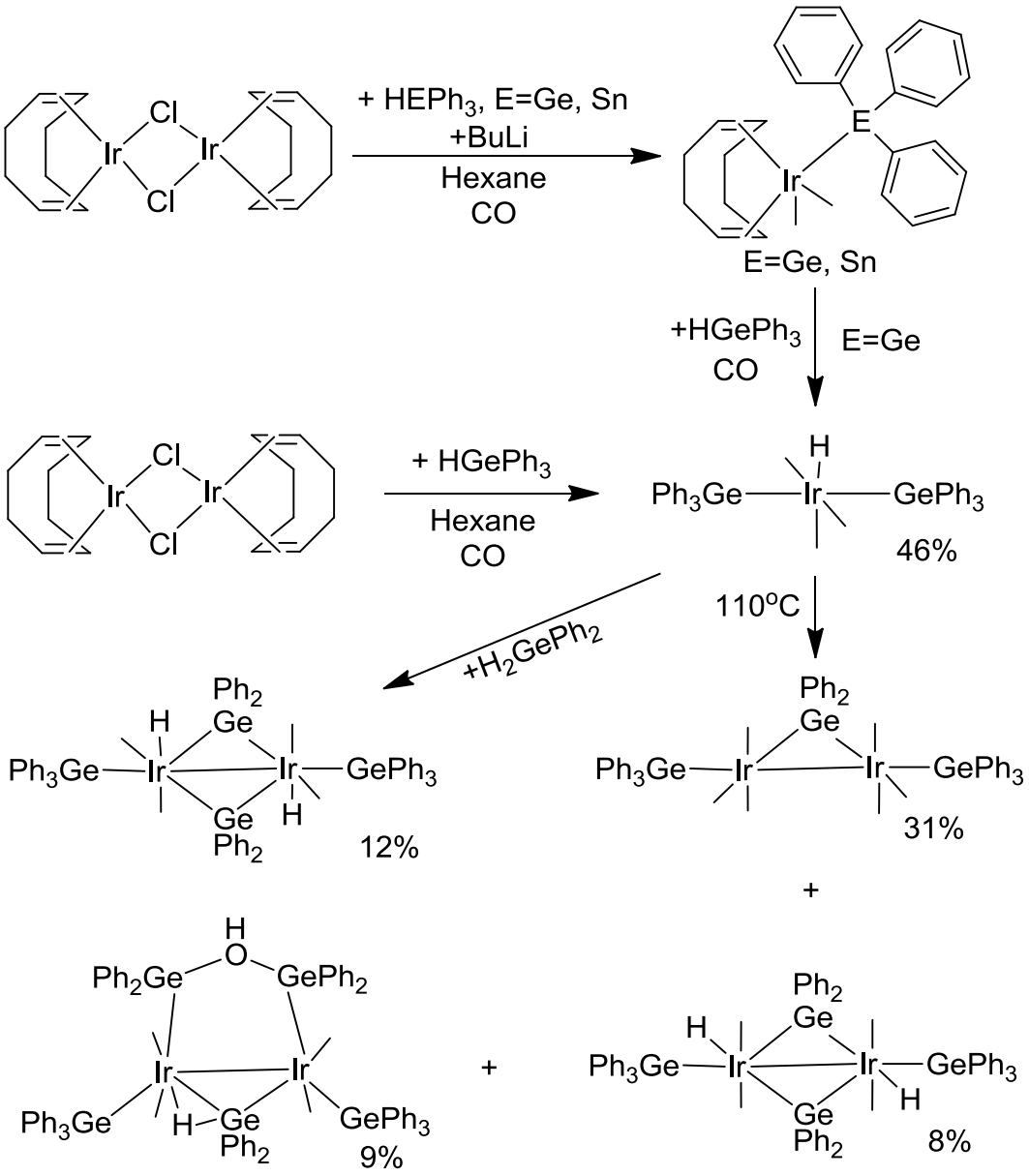

Scheme 1.3. Synthesis of $Ir(COD)(CO)_2EPh_3$ from the reaction of $[Ir(COD)Cl]_2$ with Ph_3Eli and some transformation of Ir-E cluster complexes, (E = Ge or Sn).[33]

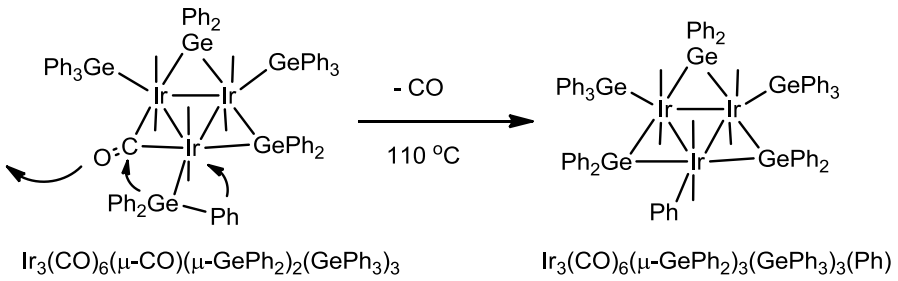

Scheme 1.4. $Ir_3(CO)_6(\mu\text{-}GePh_2)_3(GePh_3)_3(Ph)$ is obtained by α-phenyl cleavage from $Ir_3(CO)_6(\mu\text{-}CO)(\mu\text{-}GePh_2)_2(GePh_3)_3$ upon heating under 110°C .[37]

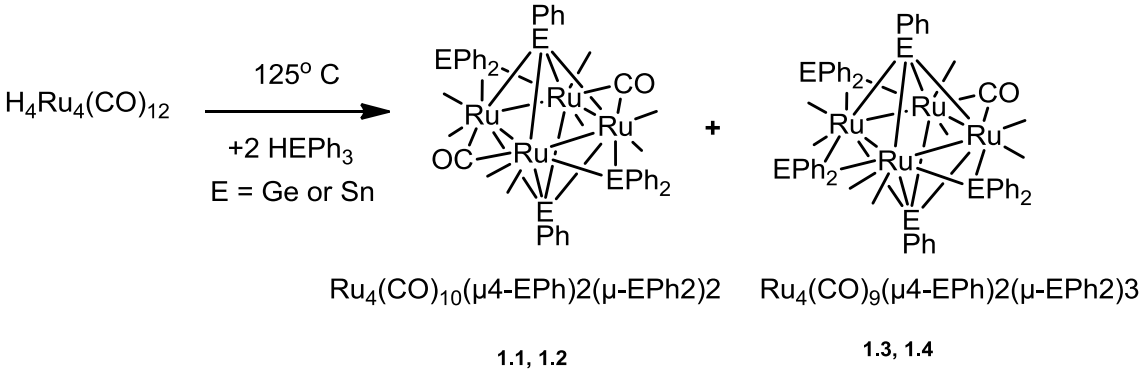

Scheme 1.5. Quadruply bridging EPh compounds $Ru_4(CO)_{10}(\mu_4\text{-EPh})_2(\mu\text{-EPh}_2)_2$ and $Ru_4(CO)_9(\mu_4\text{-EPh})_2(\mu\text{-EPh}_2)_3$ are obtained from the reaction of $H_4Ru_4(CO)_{12}$ with excess Ph_3EH in octane reflux.[40]

REFERENCES

1. (a) Dine, T. J.; Rochester, C. H.; Thomson, J. *Catalysis and surface characterization*; The Royal Society of Chemistry, Cambride, 1992. (b) Shriver, D. F.; Kaesz, H. D.; Adams, R. D. *The Chemistry of Metal Cluster Complexes*; VCH Publisher, Weinheim, 1990. (c) Mingos, D. M. P.; Wales, D. J. *Introduction of Cluster Chemistry*; Prentice Hall, New York, 1990. (d) Knozinger, H.; Guczi, L.; Gates, B. C. *Metal Clusters in Catalysis*; Elsevier, New York, 1986. (e) Johnson, B. F. G., *Transition Metal Clusters*; Wiley, New York, 1980

2. Chisholm, M. H.; Early Transition Metal Clusters with π-Donor Ligands; VCH Publishers, New York, 1995.

3. Johnson, B. F. G. *Coord. Chem. Rev.* **1999**, *190-192*, 1269.

4. Cotton, F. A.; Wilkinson, G.; Murillo, C. A.; Bochmann, M.; *Advanced Inorganic Chemistry*, six ed., Wiley, New York, 1999.

5. (a) Thayer, J. S. *Organometallic Chemistry*, VCH Publishers, 1988. (b) Mond, L.; Langer, C.; Quincke, F. *J. Chem. Soc.* **1890**, 749. (c) Abel, E. *J. Organomet. Chem.* **1990**, *383*, 11.

6. Mingo, D. M. P. *Accts. Chem. Res.* **1984**, *17*, 311.

7. (a) Muetterties, E. L.; Rhodin, T. N.; Band, E.; Brucker, C. F.; Retzer, W. R. *Chem. Rev.* **1979**, *79*, 91. (b) Muetterties, E. L. *Bull. Soc. Chim. Belg.* **1976**, *85*, 451. (c) Muetterties, E. L. *Bull Soc. Chim. Belg.* **1975**, *84*, 959.

8. Amoroso, A. J.; Gade, L. H.; Johnson, B. F. G.; Lewis, J.; Raithby, P. R.; Wong, W. T. *Angew. Chem. Int. Ed. Engl.* **1991**, *24*, 697.

9. Bradley, J. S. *J. Am. Chem. Soc.* **1966**, *88*, 3491.

10. Adams, R. D.; Cotton, F. A. *Catalysis by Di- and Polynuclear Metal Cluster Complexes*, Wiley-VCH, New York, 1998, chapter1, p4

11 Adams, R. D.; Barnard, T. S.; Li, Z.; Wu, W.; Yamamoto, J. H. *J. Am. Chem. Soc.* **1994**, *116*, 9103.

12. Shephard, D. S.; Maschmeyer, T.; Thomas, J. M.; Sankar, G.; Ozkaya, D.; Zhou, W.; Oldroyd, R. D.; Bell, R. G. *Angew. Chem. Int. Ed. Engl.* **1997**, *36*, 2242.

13. (a) Parkyns, N. D. in *Proceddings, 3rd International Congress on Catalysis.* (b) Sachtler, W. H. M.; Schuit, G. C. A.; Zwietering, P. Eds. North-Holland, Amsterdam, 1965, p. 164.

14. (a) Sinfelt, J. H. *Bimetallic Catalysts: Discoveries, Concepts, and Applications*; Wiley, New York, 1983. (b) Sinfelt, J. H. *Adv. Chem. Eng.* 1964, *5*, 37.

15. Ichikawa, M. *Adv. Catal.* **1992**, *38*, 283.

16. Goodman, D. W.; Houston, J. E. *Science*, **1987**, *236*, 403

17. (a) Adams, R. D.; Babin, J. E.; Tasi, M.; Wang, J. G. *Organometallics* **1988**, *7*, 755. (b) Castiglioni, M.; Giordano, R.; Sappa, E. *J. Organomet. Chem.* **1988**, *342*, 111. (c) Castiglioni, M.; Giordano, R.; Sappa, E. *J. Organomet. Chem.* **1987**, *319*, 167. (d) Dombek, B. D. *Organometallics* **1985**, *4*, 1707.

18. (a) Xiao. J.; Puddephatt, R. J. *Coord. Chem. Rev.* **1995**, *143*, 457. (b) Dees, M. J.; Ponec, V. *J. Catal.* **1989**, *115*, 347. (c) Rice, R. W.; Lu, K. *J. Catal.* **1982**, *77*, 104. (d) Rasser, J. C.; Beindorff, W. H.; Scholten, J. F. *J. Catal.* **1979**, *59*, 211.

19. (a) Sinfelt, J. H. *Sci. Am.* **1985**, *253*, 90. (b) Sinfelt, J. H.; Via, G. H. *J. Catal.* **1979**, *56*, 1.

20. (a) Nashner, M. S.; Frenkel, A. I.; Adler, D. L.; Shapley, J. R.; Nuzzo, R. G. *J. Am. Chem. Soc.* **1997**, *119*, 7760. (b) Hills, C. W.; Nashner, M. S.; Frenkel, A. I.; Shapley, J. R. Nuzzo, R. G. *Langmuir*, **1999**, *15*, 690.

21. (a) Ekou, T.; Vicente, A.; Lafaye, G.; Especel, C.; Marecot, P. *Appl Catal. A Gen.*. **2006**, *314*, 73-80. (b) Lafaye, G.; Micheaud-Especel, C.; Montassier, C.; Marecot, P. *Appl. Catal. A Gen.* **2002**, *230*, 19-30. (c) Lafaye, G.; Micheaud-Especel, C.; Montassier, C.; Marecot, P. *Appl. Catal. A Gen.* **2004**, *257*, 107-117. (d) Macleod, N.; Fryer, J. R.; Stirling, D.;Webb, G. *Catal. Today* **1998**, *46*, 37-54.

22. (a) Burch, R. *J. Catal.* **1981**, *71*, 348-359. (b) Burch, R.; Garla, L. C. *J. Catal.* **1981**, *71*,360-372. (c) Srinivasan, R.; Davis, B. H. *Platinum Metals Rev.* **1992**, *36*, 151-163. (d) Fujikawa, T.; Ribeiro, F. H.; Somorjai, G. A. *J. Catal.* **1998**, *178*, 58-65. (e) Park, Y.-K.; Ribeiro, F. H.; Somorjai, G. A. *J. Catal.* **1998**, *178*, 66-75. (f) Epron, F.; Carnevillier, C.; Marecot, P. *Appl. Catal.* **2005**, *295*, 157-169. (g) Cortright, R. D.; Dumesic, J. A. *J. Catal.* **1994**, *148*, 771-778. (h) Huber, G. W.; Shabaker, J. W.; Dumesic, J. A. *Science* **2003**, *300*, 2075-2077. (i)Cortright, R. D.; Hill, J. M.; Dumesic, J. A. *Catal. Today* **2000**, *55*, 213-223. (j) Hermans, S.; Raja, R.; Thomas, J. M.; Johnson, B. F. G.; Sankar, G.; Gleeson, D. *Angew. Chem., Int. Ed.* **2001**, *40*, 1211-1215. (k) Johnson, B. F. G.; Raynor, S. A.; Brown, D. B.; Shephard, D. S.; Mashmeyer, T.; Thomas, J. M.; Hermans, S.; Raja, R.; Sankar, G. *J. Mol. Catal. A: Chem* **2002**, *182-183*, 89-97. (l) Hermans, S.; Johnson, B. F. G. *Chem. Commun.* **2000**, 1955-1956.

23. (a) Dumitriu, D.; B âjega, R.; Frunza, L.; Macovei, D.; Hu, T.; Xie, Y; P ârvulescu, V.I.; Kaliaguine, S. *J. Catal.* **2003**, *219*, 337–351. (b) Zhao, J.; Qian, G., Li, F.; Zhu J.; Ji ,S.; Li, L. *Chin. J. Catal.*, **2012**, *33*, 771–776. (c) Qian, G.; Ji, D.; Lu, G.; Zhao, R.; Qi, Y.; Suo, J, *J. Catal.* **2005**, *232*, 378–385.

24. (a) Dautzenberg, F. M.; Helle, J. N.; Biolen, P.; Sachtler, W. M. H. *J. Catal.* **1980**, *63*, 119-128. (b) Biloen, P.; Helle, J. N.; Verbeek, H.; Dautzenberg, F. M.; Sachtler, W. M. H. J. Catal, 1980, 63, 112.

25. Guidotti, M.; Dal Aanto, V.; Gallo, A.; Gianotti, E.; Peli, G.; Psaro, R.; Sordelli, L. *Catal. Lett.* **2006**, *112*, 89-95.

26. Shabaker, J. W.; Simonetti, D. A.; Cortright, R. D.; Dumesic, J. A. *J. Catal.* **2005**, *231*, 67-76.

27. Adams, R. D.; Blom, D. A.; Captain, B.; Raja, R.; Thomas, J. M.; Trufan, E. *Langmuir*, **2008**, *24*, 9223-9226.

28. Grasselli, R. K. *J. Chem. Ed.* **1986**, *63*, 216-221.

29. Kirkland, J. B., Niacin, in *Handbook of Vitamins*, Rucker, R.; Zempleni, J.; Suttie, J.W.; McCormick, D.B. (Eds.), 4th ed., Taylor and Francis, New York, **2007**, pp 191–232. *Catal. Lett.* **2006**, *112*, 89-95.

30. (a) Ali, K. M.; Wonnerth, A.; Huber, K.; Wojta, J. *Brit. J. Pharmacology* **2012**, *167*, 1177-1194. (b) Grundy, S. M. *Am. J. Cardiol.* **1992**, *70*, I27-I32.

31. Raja, R.; Adams, R. D.; Blom, D. A.; Pearl, Jr., W. C.; Gianotti, E.; Thomas, J. M. *Langmuir* **2009**, *25*, 7200–7204.

32. Holt, M. S.; Wilson, W. L.; Helson, J. H. *Chem. Rev.* **1989**, 89, 11-49.

33. Adams, R. D.; Trufan, E. *Organometallics* **2010**, *29*, 4346-4353.

34. (a) Adams, R. D.; Trufan, E. *Phil. Trans. R. Soc. A* **2010**, *368*, 1473–1493. (b) Thomas, J. M.; Johnson, B. F. G.; Raja, R.; Sankar, G.;Midgley, P. A. *Acc. Chem. Res.* **2003**, *36*, 20. (c) Braunstein, P. Rose, J. In Catalysis by Di- and Polynuclear Metal Cluster Complexes; Adams, R. D.; Cotton, F. A., Eds.;Wiley-VCH: New York, **1998**; Chapter 13. (d) Braunstein, P.; Rose, J. Metal Clusters in Chemistry; Braunstein, P.; Oro, L.A.; Raithby, P. R., Eds.; Wiley-VCH: Weinheim, **1999**; Vol. 2, Chapter 2.2, pp 616-677.

35. Adams, R. D.; Captain, B.; Trufan, E.; Zhu, L. *J. Am. Chem. Soc.*, **2007**, *129*, 7545.

36. Adams, R. D.; Captain, B.; Zhu, L. *Organometallics*, **2006**, *25*, 4183-4187.

37. Adams, R. D.; Fang, F.; Zhang, Q. *Organometallics*, **2012**, *31*, 2621-2630.

38. Adams, R. D.; Captain, B.; Smith, J. L., Jr.; Hall, M. B.; Beddie, C. L.; Webster, C. E. *Inorg. Chem.* **2004**, *43*, 7576.

39. Adams, R. D.; Captain, B.; Fu, W.; Smith, M. D. *Inorg. Chem.* **2002**, *41*, 5593.

40. (a) Adams, R. D.; Boswell, E. M.; Captain, B.; Hungria, A. B.; Midgley, P. A.; Raja, R.; Thomas, J. M. *Angew. Chem. Int. Ed.* **2007**, *46*, 8182. (b) Adams, R. D.; Boswell, E. M.; Captain, B.; Patel. M. A. *Inorg. Chem.* **2007**, *46*, 533.

41. Carty, A. J.; Taylor, N. J.; Coleman, A. W.; Lappert, M. F.; *J. Chem. Soc. Chem. Commun.* **1979**, 639.

42. Holmes, N. J.; Levason, W.; Webster, M. *J. Organomet. Chem.* **1997**, *545-546*, 111.

43. Schumann, H.; Eguren, L. *J. Organomet. Chem.* **1991**, *403*, 183.

44. Holmes, N. J.; Levason, W.; Webster, M. *J. Organomet. Chem.* **1999**, *584*, 179-184.

45. (a) Champness, N. R.; Levason, W. *Coord. Chem. Rev.* **1994**, 133, 115 (b) Gemelin Handbuch der Anorganische Chemie, Bismut Organischen Verbindungen. Springer, New York 1977.

46. Adams, R. D.; Pearl, Jr., W. C. *Inorg. Chem.* **2010**, *49*, 7170–7175.

CHAPTER 2

New Iridium-Ruthenium-Tin Cluster Complexes from the Reaction of $HSnPh_3$ with $HIrRu_3(CO)_{13}$

Introduction

Tin is well known to be an effective modifier of transition metal catalysts.[1,2,3,4,5] Recent studies have shown that polynuclear metal carbonyl cluster complexes containing tin ligands can serve as effective precursors to multimetallic heterogeneous catalysts that exhibit high activity and improved selectivity for certain types of catalytic hydrogenation reactions.[2-5] Adams *et. al.* have recently shown that the phenylstannanes, $HSnPh_3$ and H_2SnPh_2, are good reagents for introducing phenyltin ligands into polynuclear metal carbonyl cluster complexes, e.g. Scheme 2.1[6] and Scheme 2.2[7].

Bridging $SnPh_2$ and SnPh ligands are often formed by cleavage of phenyl groups from the $SnPh_3$ ligands by mild heating. In some cases, the number of tin ligands that can ultimately be added to a complex is quite large. For example, the complexes $Ru_5(CO)_{10}(SnPh_3)(\mu\text{-}SnPh_2)_4(\mu_5\text{-}C)(\mu\text{-}H)$,[8] $Ru_4(CO)_8(\mu\text{-}SnPh_2)_4(\mu_3\text{-}SnPh)_2$[2] and $Rh_3(CO)_3(SnPh_3)_3(\mu\text{-}SnPh_2)_3(\mu_3\text{-}SnPh)_2$[7] contain five, six and eight tin ligands, respectively.

Adams group has been focused on polynuclear ruthenium carbonyl complexes containing $SnPh_3$, $SnPh_2$ and SnPh ligands.[9] Studies have investigated the reaction of the mixed metal complex $HIrRu_3(CO)_{13}$, **2.1** with $HSnPh_3$ in this chapter. Two new compounds were obtained: $Ir_2Ru_2(CO)_{11}(SnPh_3)(\mu\text{-}H)_3$, **2.2** and $IrRu_3(CO)_{11}(SnPh_3)_3(\mu$-

$H)_4$, **2.3**. The major product **2.3** was formed by the addition of three equivalents of the Ph_3SnH to **2.1** in a process that resulted in an opening of the $IrRu_3$ cluster. When compound **2.3** was heated to 97 ^oC for 30min, $IrRu_3(CO)_9(\mu\text{-}\eta^2\text{-}C_6H_5)(\mu\text{-}SnPh)_2(\mu\text{-}SnPh_2)$, **2.4** was formed by cleavage of phenyl rings from the $SnPh_3$ ligands. The syntheses and characterizations of these new compounds are described in this chapter.

Experimental

General Data.

Reagent grade solvents were dried by the standard procedures and were freshly distilled prior to use. Infrared spectra were recorded on a Thermo Nicolet Avatar 360 FT-IR spectrophotometer. ^1H NMR spectra were recorded on a Varian Mercury 300 spectrometer operating at 300.1 MHz. Mass spectrometric (MS) measurements performed by a direct-exposure probe using electron impact ionization (EI) electrospray techniques (ES) were made on a VG 70S instrument. $Ru_3(CO)_{12}$ and $Ir_4(CO)_{12}$ were purchased from STREM. $HSnPh_3$ was purchased from Aldrich and was used without further purification. $IrRu_3(CO)_{13}(\mu\text{-}H)$ was prepared according to a previously reported procedure.[10] Product separations were performed by TLC in air on Analtech 0.25 and 0.5 mm silica gel 60 Å F_{254} glass plates.

Reaction of $HIrRu_3(CO)_{13}$ with $HSnPh_3$.

A 48.89 mg (0.1394 mmol) of $HSnPh_3$ were added to 30.0 mg (0.0349 mmol) of $HIrRu_3(CO)_{13}$ in 30 mL of hexane. The reaction solution was heated to reflux for 10 min. The color of the solution changed from red to dark brown. After cooling, the solvent was removed *in vacuo*, and the products were separated by TLC using a 3:1

hexane/methylene chloride solvent mixture to yield in order of elution 1.3 mg of yellow $Ir_2Ru_2(CO)_{11}(SnPh_3)(\mu\text{-}H)_3$, **2.2** (3.0% yield) and 12.1 mg of brown $IrRu_3(CO)_{11}(SnPh_3)_3(\mu\text{-}H)_4$, **2.3** (19% yield).

Spectral data for **2.2**. IR *vCO* (cm^{-1} in methylene chloride): 2106(m), 2081(vs), 2074(s), 2048(m), 2037(m), 2028(m). ^1H NMR (CD_2Cl_2, in ppm) at 25°C: δ = 7.12-7.53(m, 15H, Ph), -18.05(s, hydride), -19.31(s, hydride). Mass Spec. EI/MS *m*/*z*. 1248, M^+.

Spectral data for **2.3**. IR *vCO* (cm^{-1} in hexane): 2115(vw), 2093(w), 2084(vw), 2073(w), 2051(m), 2044(vs), 2028(w), 2015(m). ^1H NMR (CD_2Cl_2, in ppm) at 25 ℃: δ= 7.30-7.55 (m, 45H, Ph), δ= -12.09 (s, hydride), δ= -15.45 (s, hydride). Negative ion ES/MS *m*/*z* 1856, $M^+ - 2H$; 1507, $M^+ - SnPh_3$; 1479, $M^+ - SnPh_3$ - CO.

Thermal Transformations of 2.3.

A 22.4 mg (0.0130 mmol) amount of **2.3** was dissolved in 30 mL of hepane in a 100 mL three neck flask. The solution was heated to reflux for 30min. After cooling, the solvent was removed *in vacuo*, and the products were then separated by TLC using a 6:1 hexane/methylene chloride solvent mixture to yield 0.77 mg of dark green $IrRu_3(CO)_9(\mu\text{-}\eta^2\text{-}C_6H_5)(\mu\text{-}SnPh)_2(\mu\text{-}SnPh_2)$, **2.4** (4% yield).

Spectral data for **2.4**. IR *vCO* (cm^{-1} in methylene chloride): 2058(s), 2030(vs), 1997(s). Mass Spec. EI/MS *m*/*z*. 1489, M^+.

Crystallographic Analyses

Yellow single crystals of **2.2** and black crystals of **2.4** suitable for x-ray diffraction analyses were obtained by slow evaporation of solvent from a hexane/methylene chloride solvent mixture at room temperature. Purple-brown single crystals of **2.3** suitable for x-ray diffraction analyses were obtained by slow evaporation of solvent from a hexane solvent at room temperature. Each data crystal was glued onto the end of a thin glass fiber. X-ray diffraction intensity data were measured by using a Bruker SMART APEX CCD-based diffractometer using Mo Kα radiation (λ = 0.71073 Å). The raw data frames were integrated with the SAINT+ program by using a narrow-frame integration algorithm.[11] Corrections for Lorentz and polarization effects were also applied with SAINT+. An empirical absorption correction based on the multiple measurement of equivalent reflections was applied using the program SADABS.[11] Both structures were solved by a combination of direct methods and difference Fourier syntheses, and refined by full-matrix least-squares on F^2 y using the SHELXTL software package.[12] All non-hydrogen atoms were refined with anisotropic thermal parameters. Hydrogen atoms on the phenyl rings were placed in geometrically idealized positions and included as standard riding atoms during the least-squares refinements.

Compound **2.2** and **2.4** crystallized in the triclinic crystal system. The space group $P\bar{1}$ was assumed and confirmed by the successful solution and refinement for the structure. For compound **2.2**, each hydride ligand was located, and refined by using geometric restraints (i.e. fixed Ir – H, Ru – H bond distances of 1.75 Å) and an isotropic thermal parameter.

Compound **2.3** crystallized in the monoclinic system. The space group *P*n was indicated by the systematic absences in the data and confirmed by the successful solution

and refinement for the structure. The hydride ligands were located and refined by using geometric restraints (i.e. fixed Ir – H, Ru – H bond distances of 1.75 Å) and an isotropic thermal parameter. Crystal data, data collection parameters, and results of the analyses are listed in Tables 2.1.

Results

Two new compounds: $Ir_2Ru_2(CO)_{11}(SnPh_3)(\mu\text{-}H)_3$ (**2.2**) and $IrRu_3(CO)_{11}(SnPh_3)_3(\mu\text{-}H)_4$, (**2.3**) were obtained from the reaction of **2.1** with $HSnPh_3$ in hexane when heated to reflux for 10 min. Compound **2.3** is the major product, but the yield is only 19%. Compound **2.2** is a minor side product, 3% yield. Both compounds were characterized by a combination of IR, ^1H NMR, mass spectra and by a single crystal x-ray diffraction analyses. An ORTEP diagram of the molecular structure of **2.2** is shown in Figure 2.1. Compound **2.2** contains a tetrahedral cluster of four metal atoms: two of iridium and two of ruthenium. There are three bridging hydrido ligands. They were located and refined with bond distance restraints (1.75 Å). One hydrido ligand bridges the Ir – Ir bond. The other two bridge the two Ir – Ru bonds to atom Ir(1). The Ir – Ir distance, Ir(1)-Ir(2)= 2.7450(9) Å, is significantly longer than that found in $Ir_4(CO)_{12}$ (2.693 Å).[13] The Ru – Ir bonds that have bridging hydride ligands, Ru(1)-Ir(1)= 2.8847(13) Å, Ru(2)-Ir(1) =2.9003(15) Å are significantly longer than the Ru – Ir bonds that do not have bridging hydride ligands, Ru(1)-Ir(2)= 2.7419(15) Å and Ru(2)-Ir(2)=2.7446(16) Å. It is well known that bridging hydride ligands increase the length of the associated metal – metal bonds.[14] The Ru – Ru distance Ru(1)-Ru(2)= 2.9095(19) Å is slightly longer than that in $Ru_3(CO)_{12}$ (2.854(1) Å).[15] Similar Ru – Ir distances were observed in the iridium-ruthenium complexes $IrRu_3(CO)_{11}(L)(\mu\text{-}H)_3$, L = PMe_3, $P(OPh)_3$

and $AsPh_3$.[16] Compound **2.2** contains one $SnPh_3$ ligand that is coordinated to one of the iridium atoms, Ir(1). The Ir – Sn distance, Ir(1) - Sn(1) = 2.6782(12) Å, is similar to the Ir – Sn distances found in the triiridium complex $Ir_3(CO)_6(\mu\text{-}SnPh_2)_3(SnPh_3)_3$: 2.6736(9) Å, 2.6981(11) Å and 2.6888(10) Å.[7] There are eleven linear terminal carbonyl ligands distributed among the metal atoms as shown in Figure 2.1. Overall, the cluster contains a total of 60 valence electrons which is exactly the number required for a tetrahedral cluster complex in which each of the metal atoms obeys the 18 electron rule.

An ORTEP diagram of the molecular structure of **2.3** is shown in Figure 2.2. Compound **2.3** consists of an open "butterfly" cluster of four metal atoms consisting one iridium and three ruthenium atoms. The cluster is nearly planar; the dihedral angle between the planes Ru(1) - Ru(2) – Ir(1) and Ru(2) - Ru(3) – Ir(1) is 179.4°. There are four bridging hydride ligands that go around the periphery of the cluster. The hydride-bridged Ir – Ru bond distances, Ir(1)-Ru(1)= 2.9695(9) Å and Ir(1)-Ru(3)= 2.9684(9) Å, are significantly longer than hydride-bridged Ir – Ru bonds observed in **2.2**, and are much longer than the nonhydride bridged Ir – Ru bond, Ir(1)-Ru(2)= 2.8489(6) Å, that occupies the hinge of the butterfly. The latter is also much longer than the non-hydride bridged Ru – Ir bonds in **2.2**. The hydride-bridged Ru – Ru bonds are the longest in the molecule, Ru(1) - Ru(2) = 3.0283(12) Å, Ru(2) - Ru(3) = 3.0275(11) Å. This is due first to the bond lengthening effects of the hydride ligands,[14] but may also be due in part to steric crowding effects that result from the presence of three $SnPh_3$ ligands. By symmetry the hydride ligands are exist it two pairs, those that bridge Ir – Ru bonds and those that bridge Ru – Ru bonds and the ^1H NMR spectrum of 3 exhibits two high-field singlets at δ = -12.09 and 15.45 in a 2:2 ratio. The tin atoms of all three $SnPh_3$ ligands lie essentially

in the plane of the cluster. There is one $SnPh_3$ ligand on the iridium atom and one on each of the ruthenium atoms on the "wing-tip" of the butterfly. The Ir – Sn distance, Ir(1)-Sn(1)= 2.6588(6) Å, is similar to that in **2.2**. The Ru – Sn distances are slightly longer than the Ir – Sn distance, Ru(1) - Sn(2) = 2.6851(11) Å and Ru(3) - Sn(3) = 2.6835(11) Å, but are similar to the Ru – Sn distances observed in a number of triruthenium complexes containing $SnPh_3$ ligands that have been characterized recently, e. g. $Ru_3(CO)_9(SnPh_3)_2(NCMe)(\mu\text{-}H)_2$: Ru(1) – Sn(1) = 2.6773(6), Ru(2) – Sn(2) = 2.6488(6), Ru(4) – Sn(3) = 2.6799(6), Ru(5) – Sn(4) = 2.6553(6);[6] $Ru_3(CO)_{10}(SnPh_3)_2(\mu\text{-}H)_2$: Ru(1) – Sn(1) = 2.6891(7), Ru(2)- Sn(2) = 2.6565(7); [6] $Ru_3(CO)_7(SnPh_3)_3(NCMe)_2(\mu\text{-}H)_3$: Ru(1) – Sn(1) = 2.6610(6), Ru(2) – Sn(2) = 2.6681(6), Ru(3) – Sn(3) = 2.6745(6);[6] $Ru_3(CO)_9(SnPh_3)_3(\mu\text{-}H)_3$: Ru(2) – Sn(2) = 2.6892(7).[6] The cluster contains a total of 62 valence electrons which is consistent with a four metal cluster having five metal – metal bonds as found in **2.3**.

The new compound $IrRu_3(CO)_9(\mu\text{-}\eta^2\text{-}C_6H_5)(\mu\text{-}SnPh)_2(\mu\text{-}SnPh_2)$, **2.4** (4% yield) was obtained when a solution of **2.3** in heptane solvent was heated to reflux (97 ^oC) for 30min. This compound was characterized by a combination of IR, mass spec and single-crystal x-ray diffraction analyses. Compound **2.4** contains 9 linear terminal carbonyl ligands distributed as shown in Figure 2.3. Compound **2.4** contains a planar cluster of four metal atoms, one of iridium and three of ruthenium. There are two quadruply bridging SnPh ligands on opposite sides of the cluster and an edge-bridging $SnPh_2$ ligand on one of the Ir-Ru bonds that were formed by cleavage of phenyl groups from the $SnPh_3$ ligands in **2.3**. The SnPh ligands and the bridging $\mu\text{-}\eta^2$-bridging phenyl ligand on Ru(2)-Ru(3) bond each serve as a three-electron donor. The phenyl-bridged metal-metal bond,

Ru(2)-Ru(3)=2.7468(10)Å, is considerably shorter than the unbridged Ru-Ru bond, Ru(1)-Ru(2)= 2.9605(9)Å. Compound **2.4** contains a total of 62 valence electrons, which is consistent with the bonding model represented by the polyhedral skeletal electron pair approach.[17] The cluster complexes, $Ru_4(CO)_{12}(\mu_4\text{-}SnPh)_2$, **2.11**, $Ru_4(CO)_8(\mu\text{-}CO)_2(\mu_4\text{-}SnPh)_2(\mu\text{-}SnPh_2)_2$, **2.12**, $Ru_4(CO)_8(\mu\text{-}CO)(\mu_4\text{-}SnPh)_2(\mu\text{-}SnPh_2)_3$, **2.13** and $Ru_4(CO)_8(\mu_4\text{-}SnPh)_2(\mu\text{-}SnPh_2)_4$, **2.14** also have quadruply bridging SnPh ligands on opposite sides of a similar arrangement of four metal atoms, Scheme 2.3.[2]

The bridging phenyl ligand observed in **2.4** is unusual because two of its carbon atoms, C(57) and C(58), are coordinated to the metal atoms. The ipso carbon C(57) is bonded to the two metal atoms Ru(2) and Ru(3) (Ru(2)-C(57)= 2.222(6)Å, Ru(3)-C(57) = 2.133(6)Å), while C(58) is bonded only to Ru(2) (Ru(2)-C(58)=2.389(7)Å). There are very few examples of a $\mu\text{-}\eta^2$-bridging phenyl ligand in the literature. These include $MoRhPt(C_5H_5)(PPh_3)_2(\mu\text{-}CO)_2(\mu\text{-}PPh_2)(\mu\text{-}\eta^2\text{-}C_6H_5)$,[18] $Ru_3(CO)_7(PPh_3)(\mu\text{-}PPh_2)(\mu\text{-}\eta^2\text{-}C_6H_5)(\mu_3\text{-}S)$,[19] and $RuIr(C_5Me_5)_2(PPh_3)_2(\mu\text{-}H)(\mu\text{-}PPh_2)(\mu\text{-}\eta_2\text{-}C_6H_5)$,[20] all of which were formed by the cleavage of a phenyl ring from a PPh_3 ligand, and $Ru_2(C_5H_5)_2(CO)_2(SnMePh_2)(\mu\text{-}\eta^2\text{-}C_6H_5)_{18}$ and $Mo_2(C_5H_5)_2(NO)_2[\mu\text{-}P(C_6H_{11})_2](\mu\text{-}\eta^2\text{-}C_6H_5)$.[21]

Discussion

A summary of the reactions described in this chapter is shown in the Scheme 2.4. Two new iridium-ruthenium cluster compounds **2.2** and **2.3** containing $SnPh_3$ ligands were obtained by the reaction of **2.1** with $HSnPh_3$. Compound **2.2** contains two iridium atoms and must have been formed by an unobserved metal – metal exchange process of

some sort because the reagent **2.1** contains only one iridium atom. Compound **2.2** contains one $SnPh_3$ that is coordinated to one of the iridium atoms. The major product **2.3** was formed as a result of the addition of three equivalents of $HSnPh_3$ to **2.1** and the elimination of two CO ligands. In order to accommodate the net increase in ligands, the metal cluster has opened to form a butterfly cluster with five metal – metal bonds that is nearly planar.

When compound **2.3** was heated to 97 ^{o}C for 30min, the phenyl groups were cleaved from the $SnPh_3$ ligands and the complexes **2.4** was formed. This complex contains two quadruply bridging SnPh ligands positioned on opposite sides of square cluster of four metal atoms and an edge-bridging $SnPh_2$ ligand. Interestingly, one of the cleaved phenyl groups was retained in the product in the form of a rare η^2-bridging ligand.

As we have recently shown for a number of related compounds, it is anticipated that these new trimetallic complexes will also serve as precursors to new nanoscale heterogeneous particles[17] and hydrogenation catalysts when deposited and activated on suitable supports.[2,3,4,5]

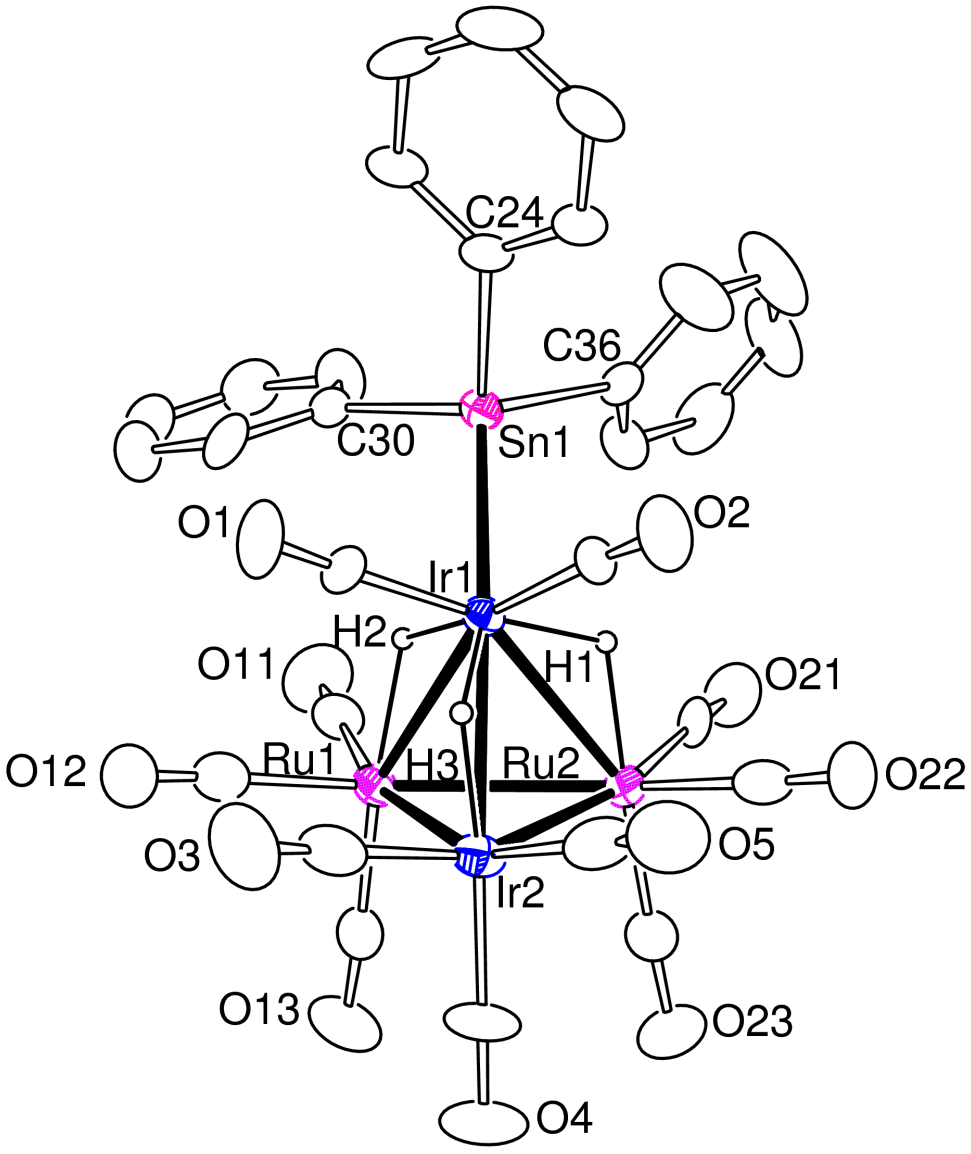

Figure 2.1. An ORTEP diagram of $H_3Ru_2Ir_2(CO)_{11}SnPh_3$, **2.2** showing 40% probability thermal ellipsoids.

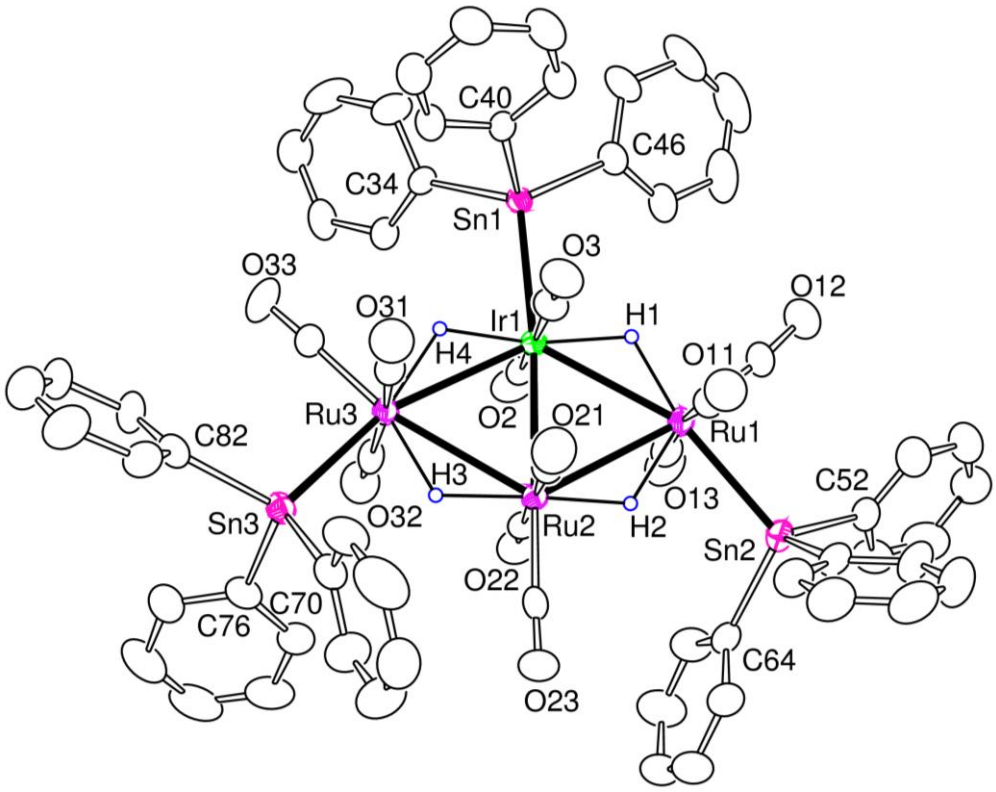

Figure 2.2. An ORTEP diagram of $H_4Ru_3Ir(CO)_{11}(SnPh_3)_3$, **2.3** showing 30% probability thermal ellipsoids.

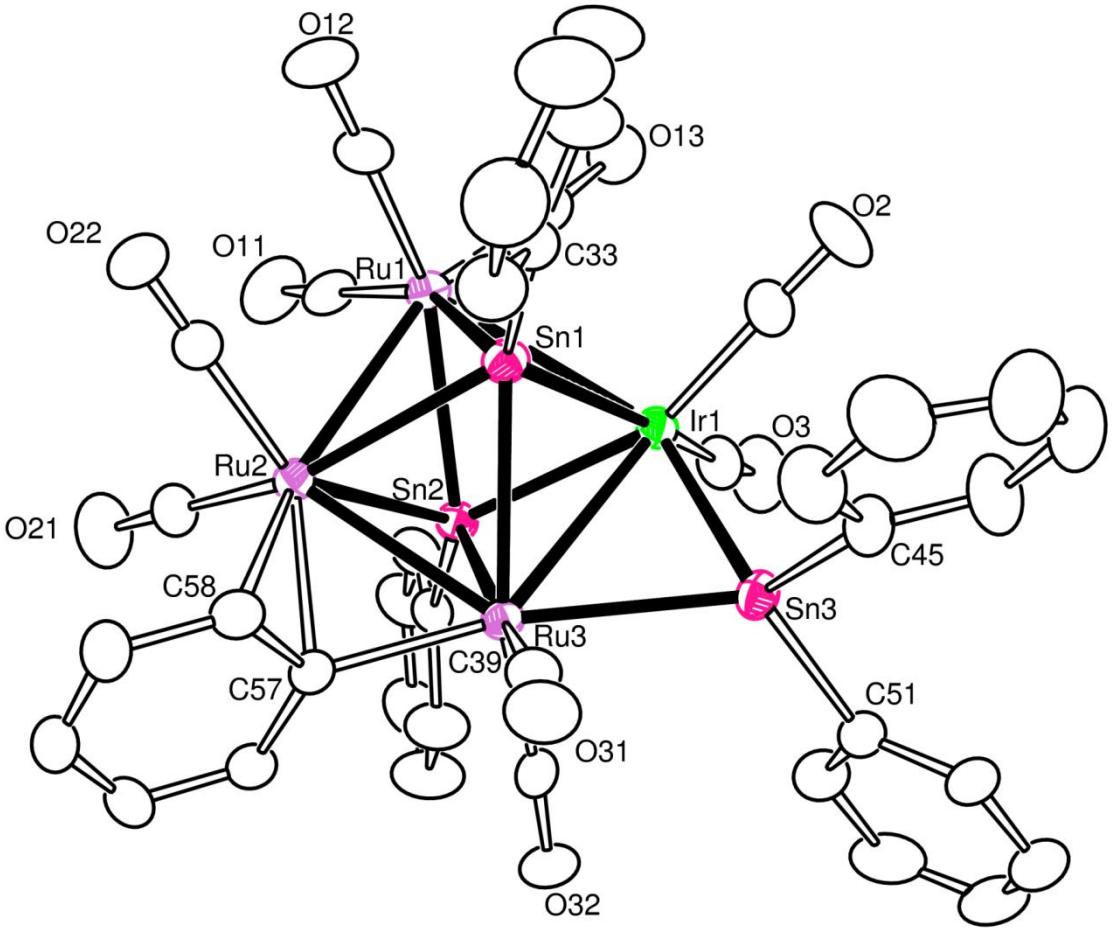

Figure 2.3. An ORTEP diagram of $IrRu_3(CO)_9(\mu\text{-}\eta^2\text{-}C_6H_5)(\mu\text{-}SnPh)_2(\mu\text{-}SnPh_2)$, **2.4** showing 25% probability thermal ellipsoids. The hydrogen atoms are omitted for clarity.

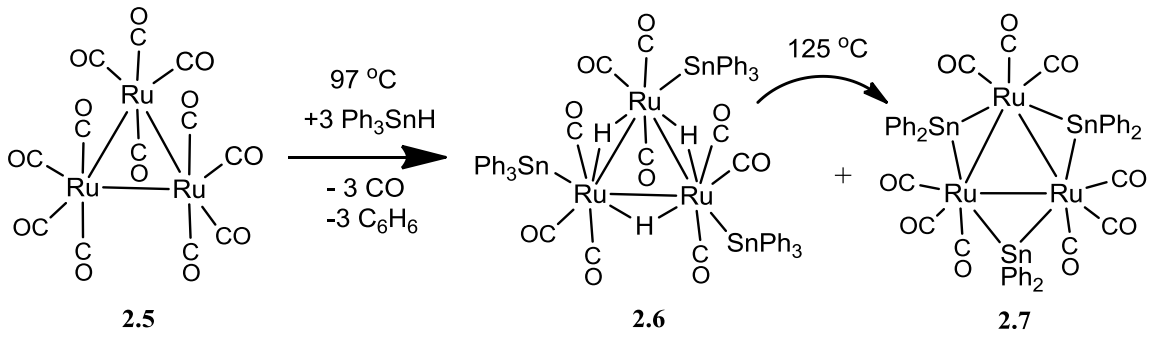

Scheme 2.1. $Ru_3(CO)_{12}$, **2.5** reacts with Ph_3SnH at 97 °C under hydrogen atmosphere to yield $Ru_3(CO)_9(SnPh_3)_3(\mu\text{-}H)_3$, **2.6** and $Ru_3(CO)_9(\mu\text{-}SnPh_2)_3$, **2.7**. **2.6** can be converted to **2.7** by heating to reflux in an octane solution.

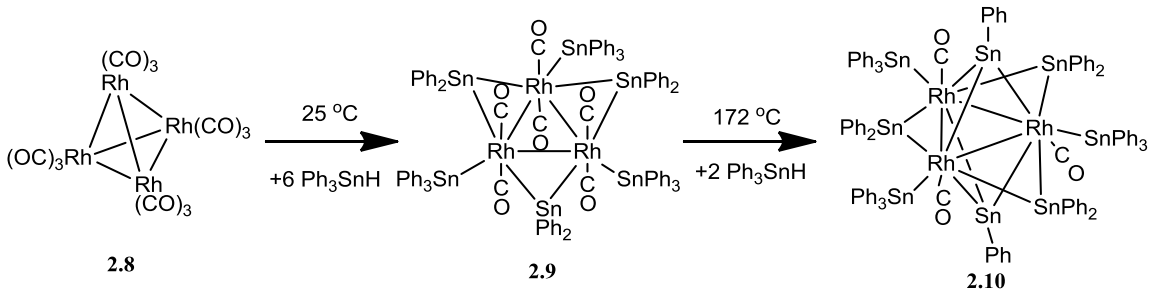

2.8 **2.9** **2.10**

Scheme 2.2. $Rh_4(CO)_{12}$, **2.8** reacts with Ph_3SnH at room temperature to yield $Rh_3(CO)_6(\mu\text{-}SnPh_2)_3(SnPh_3)_3$, **2.9**. Reaction of **2.9** with Ph_3SnH at reflux in 1,2-dichlorobenzene solvent yielded the complex $Rh_3(CO)_3(SnPh_3)_3(\mu\text{-}SnPh_2)_3(\mu_3\text{-}SnPh)_2$, **2.10**.

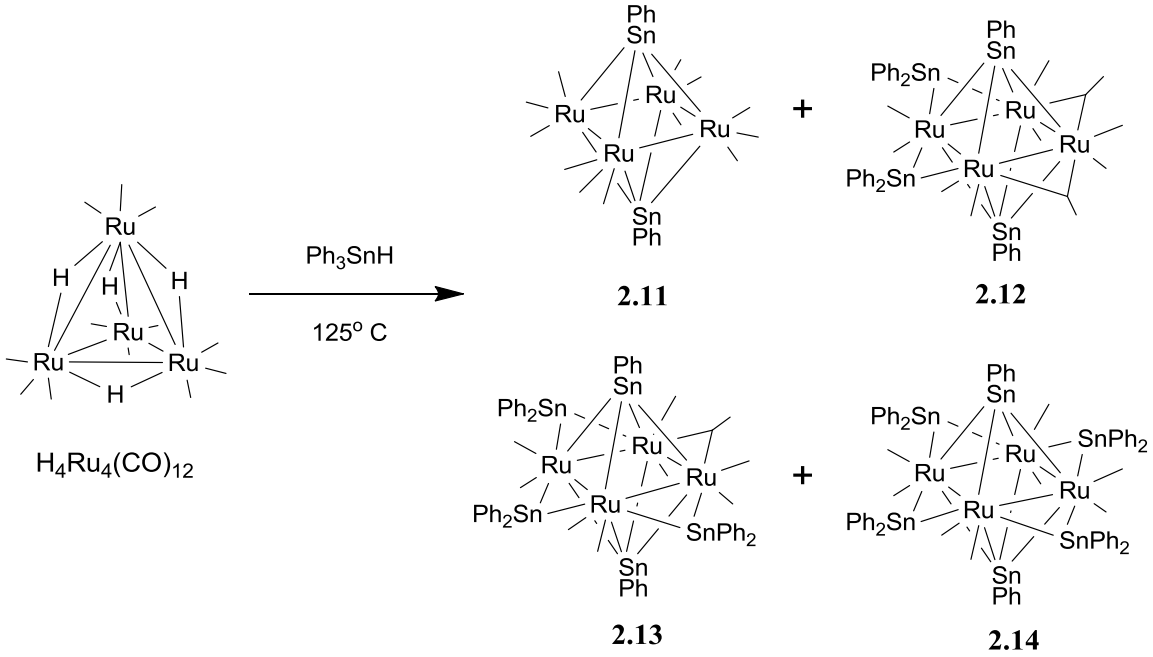

Scheme 2.3. The compounds $[Ru_4(\mu_4\text{-}SnPh)_2(CO)_{12}]$ (**2.11**), $[Ru_4(\mu_4\text{-}SnPh)_2(\mu\text{-}SnPh_2)_2(\mu\text{-}CO)_2(CO)_8]$ (**2.12**), $[Ru_4(\mu_4\text{-}SnPh)_2\text{-}(\mu\text{-}SnPh_2)_3(\mu\text{-}CO)(CO)_8]$ (**2.13**), and $[Ru_4(\mu_4\text{-}SnPh)_2(\mu\text{-}SnPh_2)_4(CO)_8]$ (**2.14**) were obtained from the reaction of $[Ru_4(CO)_{12}(\mu\text{-}H)_4]$ with Ph3SnH in octane solvent at reflux (125 ^oC).

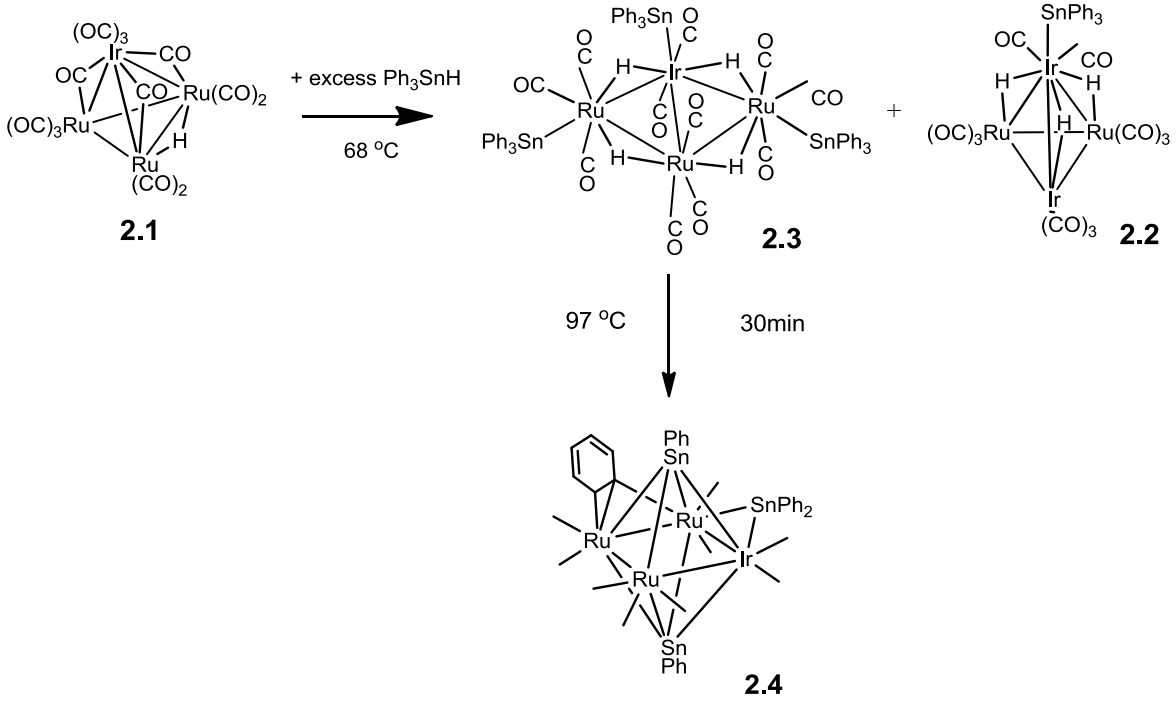

Scheme 2.4. $HIrRu_3(CO)_{13}$, **2.1** react with $HSnPh_3$ to yield $Ir_2Ru_2(CO)_{11}(SnPh_3)(\mu\text{-}H)_3$, **2.2** and $IrRu_3(CO)_{11}(SnPh_3)_3(\mu\text{-}H)_4$, **2.3**. $IrRu_3(CO)_9(\mu\text{-}\eta^2\text{-}C_6H_5)(\mu\text{-}SnPh)_2(\mu\text{-}SnPh_2)$, **2.4** was formed when compound **2.3** was heated to 97 °C for 30min.

Table 2.1 Crystallographic Data for Compounds **2.2**, **2.3** and **2.4**.

Compound	**2.2**	**2.3**	**2.4**
Empirical formula	$Ir_2Ru_2SnO_{11}C_{29}H_{18}$	$IrRu_3Sn_3O_{11}C_{65}H_{49}$	$IrRu_3Sn_3O_9C_{39}H_{25}$
Formula weight	1247.66	1857.52	1489.07
Crystal system	Triclinic	Monoclinic	Triclinic
Lattice parameters			
a (Å)	8.4546(4)	9.1810(7)	12.624(3)
b (Å)	9.6129(4)	20.5121(16)	12.676(3)
c (Å)	22.4078(10)	17.4468(13)	14.666(2)
α (deg)	82.499(1)	90.00	89.527(8)
β (deg)	82.078(1)	98.839(2)	87.456(7)
γ (deg)	68.605(1)	90.00	64.546(6)
V ($Å^3$)	1673.10(13)	3246.6(4)	2116.8(8)
Space group	*P*-1	*P*n	*P*-1
Z value	2	2	2
ρ_{calc} (g / cm^3)	2.477	1.900	2.336
μ (Mo Kα) (mm^{-1})	9.599	3.911	5.962
Temperature (K)	294(2)	294(2)	294(2)
$2\Theta_{max}$ (°)	52.74	53.74	50.06
No. Obs. ($I > 2\sigma(I)$)	4868	15003	26406
No. Parameters	415	764	496
Goodness of fit (GOF)	1.140	1.036	1.051
Max. shift in final cycle	0.000	0.001	0.001
Residuals*: R1; wR2	0.0661; 0.1217	0.0414; 0.0972	0.0332; 0.0689
Absorption Correction Max/min	Multi-scan 1.000/0.772	Multi-scan 1.000/0.707	Multi-scan 1.000/0.789
Largest peak in Final Diff. Map ($e^- / Å^3$)	1.448	1.941	0.808

[a] $R = \Sigma_{hkl}(\,|\,|F_{obs}| - |F_{calc}|\,|)/\Sigma_{hkl}|F_{obs}|$; $R_w = [\Sigma_{hkl} w(|F_{obs}| - |F_{calc}|)^2/\Sigma_{hkl} w F^2_{obs}]^{1/2}$; $w = 1/\sigma^2(F_{obs})$; GOF = $[\Sigma_{hkl} w(|F_{obs}| - |F_{calc}|)^2/(n_{data} - n_{vari})]^{1/2}$.

Table 2.2. Selected intramolecular angles and bond distances for compound **2.2**.[a]

Distances			**Angles**			
Atom	Atom	Distance(Å)	Atom	Atom	Atom	Angle(deg)
Ir1	Sn1	2.6782(12)	Sn1	Ir1	Ru1	109.40(4)
Ru1	Ru2	2.9095(19)	Sn1	Ir1	Ru2	112.89(4)
Ru1	Ir1	2.8847(13)				
Ru1	Ir2	2.7419(15)				
Ir1	Ru2	2.9003(15)				
Ir1	Ir2	2.7450(9)				
Ru2	Ir2	2.7446(16)				

[a] Estimated standard deviations in the least significant figure are given in parentheses.

Table 2.3. Selected intramolecular angles and bond distances for compound **2.3**.[a]

Distances			**Angles**			
Atom	Atom	Distance(Å)	Atom	Atom	Atom	Angle(deg)
Ir1	Ru1	2.9695(9)	Sn3	Ru3	Ru2	103.85(3)
Ir1	Ru2	2.8489(6)	Sn1	Ir1	Ru3	111.44(2)
Ir1	Ru3	2.9684(9)	Sn1	Ir1	Ru1	123.08(2)
Ru1	Ru2	3.0283(12)	Sn2	Ru1	Ru2	102.90(3)
Ru2	Ru3	3.0275(11)				
Ir1	Sn1	2.6588(6)				
Ru1	Sn2	2.6851(11)				
Ru3	Sn3	2.6835(11)				

[a] Estimated standard deviations in the least significant figure are given in parentheses.

Table 2.4. Selected intramolecular angles and bond distances for compound **2.4**.[a]

Distances			**Angles**			
Atom	Atom	Distance(Å)	Atom	Atom	Atom	Angle(deg)
Ir1	Sn3	2.5736(7)	Ir1	Sn3	Ru3	71.06(2)
Ir1	Sn1	2.6570(7)	Ru2	C57	Ru3	78.2(2)
Ir1	Sn2	2.6690(6)				
Ir1	Ru1	3.0190(10)				
Ir1	Ru3	3.0935(7)				
Ru1	Sn2	2.6713(8)				
Ru1	Sn1	2.6847(8)				
Ru1	Ru2	2.9605(9)				
Ru2	Sn2	2.7301(8)				
Ru2	Ru2	2.7468(10)				
Ru2	Sn1	2.7602(8)				
Ru3	Sn3	2.7442(8)				
Ru3	Sn2	2.7776(8)				
Ru3	Sn1	2.7788(8)				
Ru3	C57	2.133(6)				
Ru2	C57	2.222(6)				
Ru2	C58	2.389(7)				

[a] Estimated standard deviations in the least significant figure are given in parentheses.

REFERENCES

1. (a) Burch, R.; Garla, L. C. *J. Catal.* **1981**, *71*, 360-372. (b) Srinivasan, R.; Davis, B. H. *Platinum Metals Rev.* **1992**, *36*, 151-163. (c) Cortright, R. D.; Dumesic, J. A. *J. Catal.* **1995**, *148*, 771-778. (d) Cortright, R. D.; Dumesic, J. A. *Appl. Catal. A General* **1995**, *129*, 101-115. (e) Cortright, R. D.; Dumesic, J. A. *J. Catal.* **1995**, *157*, 576-583. (f) Mallat, T.; Baiker, A. *Appl. Catal. A General* **2000**, *200*, 3-22. (g) Yoshikawa, K.; Iwasawa, Y. *J. Molec. Catal.* **1995**, *100*, 115-127. (h) Gerstosio, V.; Santini, C. C.; Taoufik, M.; Bayard, F.; Basset, J.-M.; Buendia, J.; Vivat, M. *J. Catal.* **2001**, *199*, 1-8. (i) Ruiz-Martinez, J.; Sepulveda-Escribano, A.; Anderson, J. A; Rodriguez-Reinoso, F. *Catal. Today* **2007**, *123*, 235-244.

2. Adams, R. D.; Boswell, E. M.; Captain, B.; Hungria, A. B.; Midgley, P. A.; Raja, R.; Thomas, J. M. *Angew. Chem. int. Ed.,* **2007**, *46*, 8182-8185.

3. Hungria, A. B.; Raja, R.; Adams, R. D.; Captain, B.; Thomas, J. M.; Midgley, P. A.; Golvenko, V.; Johnson, B. F. G. *Angew. Chem. int. Ed.*, **2006**, *45*, 4782-4785.

4. (a) Thomas, J. M.; Adams, R. D.; Boswell, E. M.; Captain, B.; Grönbeck, H.; Raja, R. *Faraday Disc.* **2008**, *138*, 301-315. (b) Hungria, A. B.; Raja, R.; Adams, R. D.; Captain, B.; Thomas, J. M.; Midgley, P. A.; Golvenko, V.; Johnson, B. F. G. *Angew. Chem. int. Ed.*, **2006**, *45*, 4782-4785.

5. Adams, R. D.; Blom, D. A.; Captain, B.; Raja, R.; Thomas, J. M.; Trufan, E. *Langmuir*, **2008**, *24*, 9223-9226.

6. Adams, R. D.; Captain, B.; Trufan, E. *J. Organomet. Chem.* **2008**, *693*, 3593-3602.

7. Adams, R. D.; Captain，B.; Smith, Jr. J. L.; Hall, M. B.; Webster, C. E. *Inorg. Chem.* **2004**, *43*, 7576-7578.

8. Adams, R. D.; Captain, B.; Fu, W.; Smith，M. D. *Inorg. Chem.*, **2002**, *41*, 2302-2303.

9. Adams, R. D.; Trufan, E. *Phil. Trans. R Soc. A*, **2010**, *368*, 1473-1493.

10. Suss-Fink, G.; Haak, S.; Ferrand, V.; Stoeckli-Evans, H. *Dalton Trans.* **1997**, 3861-3865.

11. SAINT+ Version 6.2a. Bruker Analytical X-ray System, Inc., Madison, Wisconsin, USA, **2001**.

12. Sheldrick, G. M. SHELXTL Version 6.1; Bruker Analytical X-ray Systems, Inc., Madison, Wisconsin, USA, **1997**.

13. Churchill, M. R.; Hutchinson, J. P. *Inorg. Chem.*, **1978**, *17*, 3528-3535.

14. (a) Bau, R.; Drabnis, M. H. *Inorg. Chim. Acta* **1997**, *259*, 27-50. (b) Teller, R. G.; Bau, R. *Struc. Bonding*, **1981**, *41*, 1-82.

15. Churchill, M. R.; Hollander, F. J.; Hutchinson, J. P. *Inorg. Chem.* **1977**, *16*, 2655.

16. Suss-Fink, G.; Haak, S.; Ferrand, V.; Neels, A.; Stoeckli-Evans, H. *J. Organomet. Chem.* **1999**, 580, 225-233.

17. Mingos, D. M. P. *Acc. Chem. Res.* **1984**, *17*, 311-319.

18. Farrugia, L. J.; Miles, A. D.; Stone, F. G. A. *J. Chem. Soc., Dalton Trans.* **1984**, 2415-2422.

19. Hoferkamp, L. A.; Rheinwald, G.; Stoeckli-Evans, H.; Suss-Fink, G. *Organometallics* **1996**, *15*, 704-712.

20. Shima, T.; Suzuki, H. *Organometallics* **2005**, *24*, 1703-1708.

21. Alvarez, M. A.; Garcia, M. E.; Martinez, M.E.; Ramos, A.; Ruiz, M.A. *Organometallics* **2009**, *28*, 6293-6307.

CHAPTER 3

Transformations of Triphenylgermyl Ligands in New Iridium-Ruthenium Carbonyl Cluster Complexes

Introduction

The coordination chemistry of germylenes has attracted considerable interest in recent years.[1] Power has synthesized the first examples of mononuclear organometallic complexes containing germylyne ligands by using sterically encumbered aryl substituents.[2] Germanium has been shown to be an modifier of important heterogeneous catalysts.[3,4] Mixed metal carbonyl cluster complexes are known to be precursors to superior bi- and multimetallic heterogeneous catalysts.[5] Adams *et. al.* have been investigating the synthesis and structures of polynuclear metal carbonyl complexes containing organogermanium ligands for possible use a new heterogeneous catalysts.[5] They have recently shown that $HGePh_3$ reacts with polynuclear ruthenium and iridium carbonyl complexes by cleavaged phenyl groups from the germanium atoms to yield complexes containing edge-bridging germylene ligands and triply-bridging and quadruply-bridging germylyne ligands, scheme 3.1-3.3.[6,7]

In this chapter, the reaction of the mixed-metal iridium-ruthenium complex $IrRu_3(CO)_{13}(\mu\text{-}H)$[8] with $HGePh_3$ have been investigated. Facile oxidative-addition of $HGePh_3$ to the $IrRu_3(CO)_{13}(\mu\text{-}H)$ that leads to an opening of the cluster has been observed. Further treatment leads to cleavage of phenyl rings from the $GePh_3$ ligands with formation of bridging germylene and germylyne ligands. Interestingly, a phenyl ring

was also observed as a bridging ligand in two of the new $IrRu_3$ complexes. Upon treatment with dimethylacetylene dicarboxylate, the phenyl ring of one of these complexes was shifted back from the metal atoms to a germylyne ligand. The results of these studies are discussed in this chapter.

Experimental Section

General Data.

Reagent grade solvents were dried by the standard procedures and were freshly distilled prior to use. Infrared spectra were recorded on a Thermo Nicolet Avatar 360 FT-IR spectrophotometer. ^1H NMR spectra were recorded on a Varian Mercury 300 spectrometer operating at 300.1 MHz. Mass spectrometric (MS) measurements were performed either by a direct-exposure probe using electron impact ionization (EI) or by electrospray techniques (ES) were made on a VG 70S instrument. $Ru_3(CO)_{12}$ and $Ir_4(CO)_{12}$ were purchased from STREM. $HGePh_3$ and dimethylacetylenedicarboxylate (DMAD) were purchased from Aldrich and were used without further purification. $IrRu_3(CO)_{13}(\mu\text{-}H)$ was prepared according to a previously reported procedure.[8] Product separations were performed by TLC in air on Analtech 0.25 and 0.5 mm silica gel 60 Å F_{254} glass plates.

Reaction of $IrRu_3(CO)_{13}(\mu\text{-}H)$ with $HGePh_3$.

A 20.4 mg (0.0237 mmol) amount of $IrRu_3(CO)_{13}(\mu\text{-}H)$ was dissolved in 30 mL of hexane in a 100mL three neck flask. To this solution was added 30.4 mg (0.1000 mmol) of $HGePh_3$, and the mixture was stirred for 8h in room temperature. The color of

the solution changed from red to dark green. The solvent was then removed *in vacuo*, and the products were separated by TLC using a 6:1 hexane/methylene chloride solvent mixture to yield 26.0 mg of dark green $IrRu_3(CO)_{11}(GePh_3)_3(\mu\text{-}H)_4$, **3.1** (64% yield).

Spectral data for **3.1**. IR *vCO* (cm^{-1} in methylene chloride): 2118(vw), 2098(m), 2074(m), 2046(vs), 2030(w), 2017(m), 1998 (vw). ^1H NMR (CD_2Cl_2, in ppm) at 25 ℃: δ= 7.30-7.55 (m, 45H, Ph), δ= -12.33 (s, hydride), δ= -15.68 (s, hydride). Negative ion ES/MS *m*/*z* 1719, $M^+ - CO$; 1691, $M^+ - CO - GePh_3$; 1388.

Preparation of $Ir_2Ru_2(CO)_{11}(GePh_3)(\mu\text{-}H)_3$, 3.2.

A 20.4 mg (0.0237 mmol) amount of $IrRu_3(CO)_{13}(\mu\text{-}H)$ was dissolved in 30 mL of hexane in a 100mL three neck flask. To this solution was added 30.4 mg (0.100 mmol) of $HGePh_3$, and the mixture was heated to reflux for 10 min. The color of the solution changed from red to dark green. After cooling, the solvent was then removed *in vacuo*, and the products were separated by TLC using a 6:1 hexane/methylene chloride solvent mixture to yield in order of elution 0.9 mg of yellow $Ir_2Ru_2(CO)_{11}(GePh_3)(\mu\text{-}H)_3$, **3.2** (3% yield) and 4.7 mg of **3.1** (12% yield).

Spectral data for **3.2**. IR *vCO* (cm^{-1} in methylene chloride): 2106(m), 2082(vs), 2071(s), 2057(m), 2047(m), 2028(m). ^1H NMR (CD_2Cl_2, in ppm) at 25°C: δ = 7.32-7.51(m, 15H, Ph), -17.81(s, 1H, hydride), -18.79(s, 2H, hydride). Mass Spec. EI/MS *m*/*z*. 1202, M^+.

Thermal Transformations of 3.1.

An 11.2 mg (0.0065 mmol) amount of **3.1** was dissolved in 30 mL of hexane in a 100 mL three neck flask. The solution was heated to reflux for 6 h. After cooling, the solvent was removed *in vacuo*, and the products were then separated by TLC using a 6:1 hexane/methylene chloride solvent mixture to yield in order of elution 1.06 mg of green $IrRu_3(CO)_{10}(\mu\text{-}\eta^2\text{-}C_6H_5)(\mu_4\text{-}GePh)_2$, **3.3** (16.0% yield) and 2.85 mg of dark green $IrRu_3(CO)_9(\mu\text{-}\eta^2\text{-}C_6H_5)(\mu_4\text{-}GePh)_2(\mu\text{-}GePh_2)$, **3.4** (32.4% yield).

Spectral data for **3.3**. IR *vCO* (cm^{-1} in hexane): 2083(vw), 2072(m), 2056(w), 2047(vs), 2036(m), 2013(m), 2005(m), 1986 (w), 1974 (w). Mass Spec. EI/MS *m*/*z*. 1153, M^+.

Spectral data for **3.4**. IR *vCO* (cm^{-1} in hexane): 2059(s), 2032(vs), 2028(vs), 2011(w), 2002(s), 1987(w), 1977(vw), 1973(vw). Mass Spec. EI/MS *m*/*z*. 1352, M^+.

Reaction of 4 with DMAD

An 11.0 mg (0.0081 mmol) amount of **3.4** was dissolved in 30 mL of heptane in a 100 mL three neck flask. To this solution was added 0.01 mL (0.0813 mmol) of DMAD via syringe, and the mixture was heated to reflux for 30 min. The color was changed from dark green to yellow. After cooling, the solvent was then removed *in vacuo*, and the products were separated by TLC using a 4:1 hexane/methylene chloride solvent mixture to yield 1.02 mg of yellow $IrRu_3(CO)_9([\mu_4\text{-}Ge(Ph)C(CO_2CH_3)C(CO_2CH_3)](\mu\text{-}GePh_2)_2$, **3.5** (8.4% yield).

Spectral data for **3.5**. IR *vCO* (cm^{-1} in methylene chloride): 2076 (m), 2050(vs), 2023(vs), 2014(vs), 1985 (m), 1966 (m). ^1H NMR (CD_2Cl_2, in ppm) at 25 ℃: δ= 7.36-

7.78 (m, 25H, Ph), δ= 3.77 (s, methyl), δ= 3.61 (s, methyl). Mass Spec. EI/MS *m*/*z*. 1466, M - CO.

Crystallographic Analyses:

Black-green single crystal of **3.1** suitable for x-ray diffraction analyses were obtained by slow evaporation of solvent from a hexane solvent at room temperature. Orange single crystals of **3.2** suitable for x-ray diffraction analyses were obtained by slow evaporation of solvent from a hexane/methylene chloride solvent mixture at room temperature. Black-green single crystals of **3.3** and **3.4** suitable for x-ray diffraction analyses were obtained by slow evaporation of solvent from a hexane/methylene chloride solvent mixture at -30 ℃. Orange single crystals of **3.5** suitable for x-ray diffraction analyses were obtained by slow evaporation of solvent from a hexane/methylene chloride solvent mixture at -30 ℃. Each data crystal was glued onto the end of a thin glass fiber. X-ray diffraction intensity data were measured by using a Bruker SMART APEX CCD-based diffractometer by using Mo Kα radiation (λ = 0.71073 Å). The raw data frames were integrated with the SAINT+ program by using a narrow-frame integration algorithm.[9] Corrections for Lorentz and polarization effects were also applied with SAINT+. An empirical absorption correction based on the multiple measurement of equivalent reflections was applied using the program SADABS.[9] All structures were solved by a combination of direct methods and difference Fourier syntheses, and refined by full-matrix least-squares on F^2 by using the SHELXTL software package.[10] All non-hydrogen atoms were refined with anisotropic thermal parameters. Hydrogen atoms on

the phenyl rings were placed in geometrically idealized positions and included as standard riding atoms during the least-squares refinements.

Compound **3.1** crystallized in the monoclinic system. The space groups *P*2/n and *P*n were indicated by the systematic absences in the data. Efforts to solve the structure in the space group *P*2/n were unsuccessful. A successful solution and refinement for the structure was subsequently achieved by using the space group groups *P*n. The hydride ligands were located and refined by using geometric restraints (i.e. fixed Ir – H, Ru – H bond distances of 1.75 Å) and isotropic thermal parameters.

Compound **3.2** crystallized in the triclinic crystal system. The space group P $\bar{1}$ was assumed and confirmed by the successful solution and refinement for the structure. Each hydride ligand was located, and refined by using geometric restraints (i.e. fixed coordinates) and an isotropic thermal parameter.

Compound **3.3** crystallized in the monoclinic crystal system. The systematic absences in the intensity data indicate the unique space group $P2_1/n$.

Compounds **3.4** and **3.5** both crystallized in the triclinic crystal system. The centrosymmetric space group *P* $\bar{1}$ was selected and confirmed by the successful solution and refinement of the structure. The iridium atom Ir(1) and the ruthenium atom Ru(1) in compound **3.5** were disordered. These two atoms were refined by using EXYZ and EADP constraints and the occupancies refined to nearly equal values of 0.529/0.471 on each site. Two molecules of methylene chloride from the crystallization solvent cocrystallized in the lattice with **3.5**. They were added to the structure factor calculation and were suitably refined by using anisotropic parameters. Crystal data, data collection parameters, and results of the analyses are listed in Tables 3.1 and 3.2.

Results and Discussion

The new compound $IrRu_3(CO)_{11}(GePh_3)_3(\mu\text{-}H)_4$, **3.1** was obtained in 64% yield from the reaction of $IrRu_3(CO)_{13}(\mu\text{-}H)$ with $HGePh_3$ in hexane solvent in room temperature over a period of 8 h. Compound **3.1** was characterized by a combination of IR, ^1H NMR and single-crystal x-ray diffraction analyses. An ORTEP diagram of the molecular structure of **3.1** is shown in Figure 3.1. Compound **3.1** consists of a butterfly cluster of one iridium and three ruthenium atoms. Atoms Ir(1) and Ru(2) occupy the "hinge" sites of the cluster and Ru(1) and Ru(3) occupy the "wingtips" sites. The cluster is nearly planar; the dihedral angle between the planes Ru(1) - Ru(2) – Ir(1) and Ru(2) - Ru(3) – Ir(1) is 179^o. The molecule contains three terminal $GePh_3$ ligands. Two of the $GePh_3$ ligands are coordinated to ruthenium atoms Ru(1) and Ru(3) and lie approximately trans to the Ir – Ru bond. The Ru – Ge distances in **3.1**, Ru(1)-Ge(2) = 2.5430(9) Å, Ru(3)-Ge(3) = 2.5431(9) Å, are similar to those found in the complexes $Ru_2(CO)_8(GePh_3)_2$,[11] Ru(1) – Ge(1) = 2.5457(6) Å, Ru(2) – Ge(2) = 2.5413(6) Å, and $Ru_3(CO)_9(GePh_3)_3(\mu\text{-}H)_3$,[11] Ru – Ge = 2.5491(6) Å, 2.5433(6) Å, 2.5352(16) Å. The third $GePh_3$ ligand is coordinated to the iridium atom. The Ir – Ge distance, Ir(1)-Ge(1) = 2.5130(7) Å, is slightly shorter than the Ir - Ge distances found to the terminal $GePh_3$ ligands in the triiridium complex $Ir_3(CO)_6(GePh_3)_3(\mu\text{-}GePh_2)_3$,[7] 2.5754(7) Å, 2.5959(7) Å and 2.5534(8) Å.[7] Compound **3.1** contains four bridging hydride ligands, one on each metal – metal bond around the periphery of the cluster. The hydride-bridged metal – metal bond distances, Ir(1)-Ru(1) = 2.9932(6) Å, Ir(1)-Ru(2) = 2.8625(5) Å, Ir(1)-Ru(3) = 3.0041(6) Å, Ru(1)-Ru(2) = 3.0305(9), Ru(2)-Ru(3) = 3.0316(9) are significantly

longer than the hinge bond Ir(1)-Ru(2) = 2.8625(5) Å which has no bridging ligand. Bridging hydride ligands are well known to cause lengthening to the associated metal – metal bonds.[12] The metal – metal bond distances in **3.1** are slightly shorter than the corresponding metal – metal bond distances in the compound $IrRu_3(CO)_{11}(SnPh_3)_3(\mu\text{-}H)_4$ which is the $SnPh_3$ homologue of **3.1**.[13] All of the hydride ligands were located in the structure analysis. They exist as two inequivalent pairs in the molecule and appear as two high-field resonances of equal intensity in the ^{1}H NMR spectrum, δ = -12.33 and -15.68.

When solutions of $IrRu_3(CO)_{13}(\mu\text{-}H)$ with $HGePh_3$ in hexane solvent were heated to reflux 1 h. Compound **3.1** (12% yield) together with a small amount of the new compound $Ir_2Ru_2(CO)_{11}(GePh_3)(\mu\text{-}H)_3$, **3.2** in 3% yield were formed. Compound **3.2** was characterized by a combination of IR, ^{1}H NMR and single-crystal x-ray diffraction analyses. An ORTEP diagram of the molecular structure of **3.2** is shown in Figure 3.2. Compound **3.2** contains a cluster of four metal atoms: two of iridium and two of ruthenium. The cluster of **3.2** is closed. There are six metal – metal bonds: Ru(1)-Ru(2) = 2.8928(15) Å, Ru(1)-Ir(1) = 2.8923(12) Å, Ru(1)-Ir(2) = 2.7514(13) Å, Ir(1)-Ru(2) = 2.9007(12) Å, Ir(1)-Ir(2) = 2.7506(8) Å, Ru(2)-Ir(2) = 2.7429(13) Å. Compound **3.2** contains one $GePh_3$ ligand that is coordinated to the iridium atom Ir(1). The Ir(1)-Ge(1) = 2.5149(15) distance the same as that found in **3.1** within experimental error. Compound **3.2** contains three bridging hydrido ligands; one on each of the Ir – Ru bonds, Ru(1)-Ir(1) Ir(1)-Ru(2) and one on the Ir(1)-Ir(2) bond. As expected, the hydride bridged metal – metal bonds are significantly longer than the unbridged bonds.[12] The ^{1}H NMR spectrum exhibits two high-field resonances, δ = -17.81(s, 1H), -18.79 (s, 2H) that are assigned to the three hydride ligands. There are eleven linear terminal carbonyl ligands distributed

among the metal atoms as shown in Figure 3.2. Overall, the cluster contains a total of 60 valence electrons which is exactly the number required for a tetrahedral cluster complex in which each of the metal atoms obeys the 18 electron rule. Compound **3.2** is remarkably similar to its tin homolog $Ir_2Ru_2(CO)_{11}(SnPh_3)(\mu\text{-}H)_3$ which was recently obtained from the reaction of $IrRu_3(CO)_{13}(\mu\text{-}H)$ with $HSnPh_3$.[13]

Two new compounds $IrRu_3(CO)_{10}(\mu\text{-}\eta^2\text{-}C_6H_5)(\mu_4\text{-}GePh)_2$, **3.3** (16% yield) and $IrRu_3(CO)_9(\mu\text{-}\eta^2\text{-}C_6H_5)(\mu_4\text{-}GePh)_2(\mu\text{-}GePh_2)$, **3.4** (32% yield) were obtained when a solution of **3.1** in hexane solvent was heated to reflux (68 ^oC) for 6 h. Both compounds were characterized by a combination of IR, ^1H NMR, mass spec and single-crystal x-ray diffraction analyses. An ORTEP diagram of the molecular structure of **3.3** is shown in Figure 3.3. Compound **3.3** contains a planar cluster of four metal atoms, one of iridium and three of ruthenium. There are two quadruply bridging phenylgermylyne ligands on opposite sides of the cluster that were formed by cleavage of phenyl groups from the $GePh_3$ ligands in **3.1**. The Ru – Ru bond distances are significantly different, Ru(1)-Ru(3) = 2.9823(6) Å while Ru(2)-Ru(3) is 2.8690(6) Å. The difference in lengths may be related to steric effects, in particular, atoms Ru(1) and Ru(3) both contain three terminal carbonyl ligands, while Ru(2) has only two carbonyl ligands. The cluster complexes, $Ru_4(CO)_8(\mu\text{-}CO)_2(\mu_4\text{-}GePh)_2(\mu\text{-}GePh_2)_2$, **3.6**, $Ru_4(CO)_8(\mu\text{-}CO)(\mu_4\text{-}GePh)_2(\mu\text{-}GePh_2)_3$, **3.7** and $Ru_4(CO)_8(\mu_4\text{-}GePh)_2(\mu\text{-}GePh_2)_4$, **3.8** also have quadruply bridging germylyne ligands on opposite sides of a similar arrangement of four metal atoms, scheme 3.1.[6] The Ir – Ru bond distances also have significantly different lengths. The Ir(1)-Ru(2) bond distance of 2.6485(5) Å is nearly 0.30 Å shorter than the Ir(1)-Ru(1) distance of 2.9368(5) Å. The short length of the Ir(1)-Ru(2) bond can be attributed to the presence of a bridging phenyl

ligand across that bond. The Ru – Ge bond distances span a considerable range, 2.4582(7) Å - 2.7147(7) Å, which is probably due to sterics and asymmetrical bonding introduced by the presence of the bridging phenyl ligand across the Ir(1)-Ru(2) bond. The Ir – Ge distances are of similar lengths, Ir(1)-Ge(1) = 2.5737(6) Å, Ir(1)-Ge(2) = 2.5138(6) Å, and are slightly longer than those observed for the quadruply bridging germylyne ligands in the complex in the tetrairidium complex, $H_4Ir_4(CO)_4(\mu_4\text{-}GePh)_2(\mu\text{-}GePh_2)_4$, 2.44 Å – 2.47 Å.[7] Although bridging phenyl rings are not common, a number of examples have been structurally characterized in metal carbonyl cluster complexes and polynuclear metal coordination complexes.[14]

The bridging phenyl ligand observed in **3.3** unusual because two of its carbon atoms, C(46) and C(51) are coordinated to the metal atoms. The ipso carbon C(46) is bonded to two metal atoms Ir(1) and Ru(2), Ir(1) – C(46) = 2.083(6) Å, Ru(2) – C(46) = 2.260(5) Å, while C(51) is bonded only to Ru(2), Ru(2) – C(51) = 2.441(6) Å. There are very few examples of $\mu\text{-}\eta^2$-bridging phenyl ligand in the literature. These include: $MoRhPt(C_5H_5)(PPh_3)_2(\mu\text{-}CO)_2(\mu\text{-}PPh_2)(\mu\text{-}\eta^2\text{-}C_6H_5)$,[15] $Ru_3(CO)_7(PPh_3)(\mu\text{-}PPh_2)(\mu\text{-}\eta^2\text{-}C_6H_5)(\mu_3\text{-}S)$,[16] and $RuIr(C_5Me_5)_2(PPh_3)_2(\mu\text{-}H)(\mu\text{-}PPh_2)(\mu\text{-}\eta^2\text{-}C_6H_5)$,[17] all of which were formed by the cleavage of a phenyl ring from a PPh_3 ligand, and $Ru_2(C_5H_5)_2(CO)_2(SnMePh_2)(\mu\text{-}\eta^2\text{-}C_6H_5)$[18] and $Mo_2(C_5H_5)_2(NO)_2[\mu\text{-}P(C_6H_{11})_2](\mu\text{-}\eta^2\text{-}C_6H_5)$.[19]

Compound **3.3** contains 10 linear terminal carbonyl ligands distributed as shown in Figure 3.3. The GePh ligands and the bridging phenyl ligand each serve as a 3-electron donor. Each of the ruthenium atoms thus achieves an 18 electron configuration but the iridium atom has only 16 electrons. Alternatively, a delocalized bonding model as

represented by the Polyhedral Skeletal Electron Pair approach would predict a total valence electron count of 62 electrons for an arachno-octahedron of four metal atoms which is precisely the number valence electrons found in complex **3.3**.[20]

An ORTEP diagram of the molecular structure of **3.4** is shown in Figure 3.4. The structure of **3.4** is somewhat similar to **3.3**. Compound **3.4** contains four metal atoms, one of iridium and three of ruthenium in a square arrangement, and two quadruply bridging phenylgermylyne ligands. However, compound **3.4** has an edge-bridging $GePh_2$ ligand on one of the Ir – Ru bonds and one less terminal CO ligand. Like **3.3**, compound **3.4** also contains a μ-η^2-bridging phenyl ligand, but in **3.4**, this ligand bridges a Ru – Ru bond instead of the Ir – Ru bond as found in **3.3**. As found in **3.3**, the phenyl-bridged metal - metal bond, Ru(2)-Ru(3) = 2.6994(4) Å, is considerably shorter than the unbridged Ru – Ru bond, Ru(1)-Ru(2) = 2.8932(4) Å. As with **3.3**, compound **3.4** contains a total of 62 valence electrons, which is consistent with the bonding model represented by the Polyhedral Skeletal Electron Pair Approach.[20]

In order to investigate its reactivity, a solution of compound **3.4** in heptane solvent was treated with $(MeO_2C)C_2(CO_2Me)$, DMAD and heated to reflux for 30 min. From this reaction mixture, the new compound $IrRu_3(CO)_9([\mu_4$-$Ge(Ph)C(CO_2Me)C(CO_2Me)](\mu GePh_2)_2$, **3.5** was obtained in 8.4% yield. Compound **3.5** was characterized by a combination of IR, ^{1}H NMR, mass spec and single-crystal x-ray diffraction analyses. An ORTEP diagram of the molecular structure of **3.5** is shown in Figure 3.5. Compound **3.5** contains a butterfly cluster of four metal atoms, one of iridium and three of ruthenium. The iridium atom occupies one of the wingtip positions and in the crystal, Ir(1) and Ru(3) in the other wingtip position are equally disordered. There are

two $GePh_2$ ligands that bridge the adjacent hinge-wingtip bonds Ru(1) – Ir(1) and Ru(1) – Ru(3). One of these $GePh_2$ ligands was evidently formed by a shift of the bridging phenyl ligand in **3.4** to one of the bridging GePh ligands because **3.4** has only one $GePh_2$ ligand. One equivalent of DMAD was added to **3.4** in the reaction. The DMAD has formed a bond to one of the GePh ligands by using one of the alkyne carbon atoms, Ge(3) – C(1) = 1.947(6) Å. The entire $(CH_3O_2C)C(CO_2CH_3)CGePh$ group serves a quadruply-bridging ligand across all four metal atoms and alkyne C – C bond, C(1) – C(4), has lengthened to 1.448(9) Å due to the coordination. This C – C distance is similar to the C – C distances found for the quadruply bridging DMAD ligands found in the complex $CoRh_3(CO)_9[\mu_4\text{-}(CH_3O_2C)C_2(CO_2CH_3)]_2[\mu_4\text{-}(CH_3O_2C)C_2(CO_2CH_3)]$, 1.411(6) Å and 1.428(6) Å.[21] The formation of germanium – carbon bonds is central to reactions such as the hydrogermylation of alkynes.[22] Mochida et al. has shown that digermanes can be added alkynes catalytically in the presence of certain platinum complexes.[23]

If one counts the $(CH_3O_2C)C(CO_2CH_3)CGePh$ ligand as a five electron donor, then the cluster has a total of 60 valence electrons which is two short of the requirements for an 18 electron configuration at each metal atom in a cluster of four metal atoms with five metal – metal bonds. Alternatively, if one views the germanium atom and carbon atoms C(1) and C(4) as part of the cluster then the cluster could be regarded as a closo-pentagonal bipyramidal framework and the total valence electron count would be 70 which is exactly the number predicted for this delocalized bonding model by the Polyhedral Skeletal Electron Pair theory.[20]

Summary

A summary of the reactions reported here is shown in Scheme 3.4. The closed cluster complex $IrRu_3(CO)_{13}(\mu\text{-}H)$ eliminated two equivalents of CO and was opened to form the tris-$GePh_3$ complex **3.1** in good yield by the oxidative addition of three equivalents of $HGePh_3$ when the reaction was performed at room temperature. Compound **3.1** was also formed but in a significantly lower yield together with minor coproduct **3.2** when the reaction was performed at 68 ^oC. Compound **3.2** has a different metal composition than **3.1** which is obviously the result of a complex metal – metal exchange reaction that could also account for its low yield.

When compound **3.1** was heated to 68 ^oC for an extended period, the phenyl groups were cleaved from the $GePh_3$ ligands and the complexes **3.3** and **3.4** were formed. Both of these complexes contain two quadruply bridging germylyne ligands positioned on opposite sides of square cluster of four metal atoms. Compound **3.4** also contains an edge-bridging $GePh_2$ ligand. Interestingly, one of the cleaved phenyl groups was retained in each of these products in the form of a rare η^2-bridging ligand. Even more interestingly, it was found that the bridging phenyl ligand in **3.4** could be passed back to one of the bridging germylyne ligands upon addition of DMAD to the complex and the added DMAD formed a bond to the other germylyne ligand. It is hoped that these new mixed-metal germanium complexes will prove to be useful precursors to new heterogeneous catalysts for the hydrogenation of unsaturated hydrocarbons.[3-4]

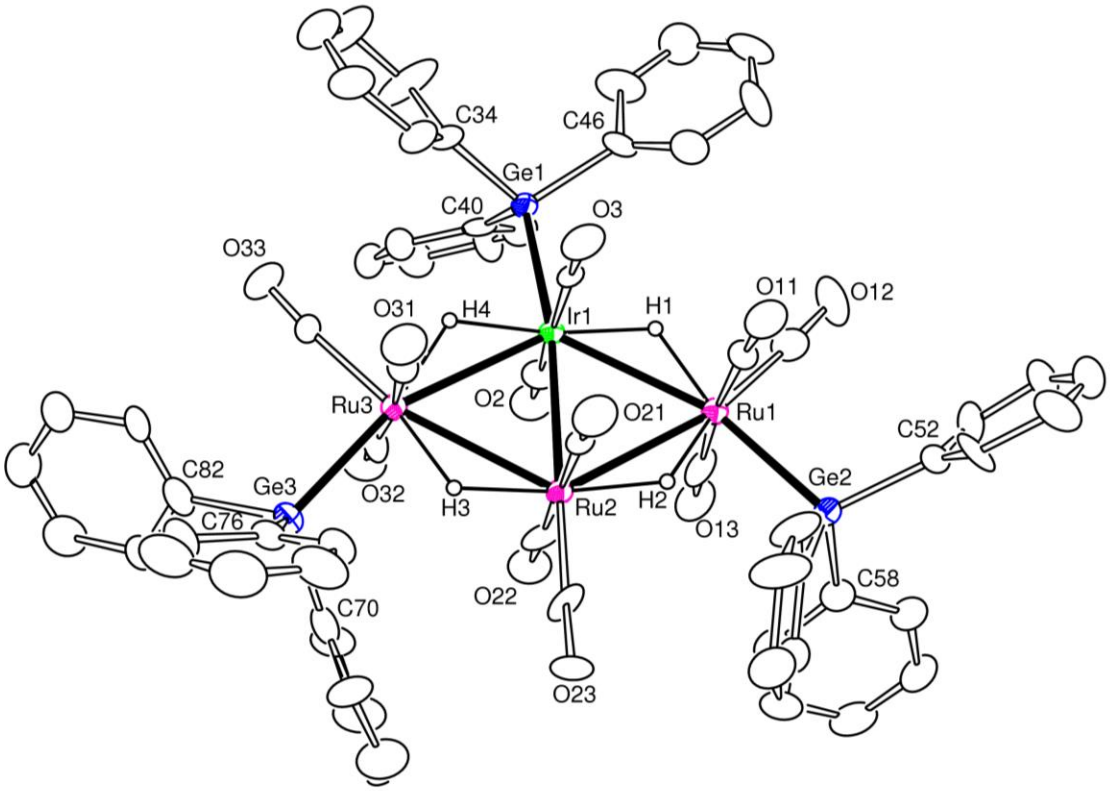

Figure 3.1. An ORTEP diagram of $IrRu_3(CO)_{11}(GePh_3)_3(\mu\text{-}H)_4$, **3.1** showing 30% probability thermal ellipsoids.

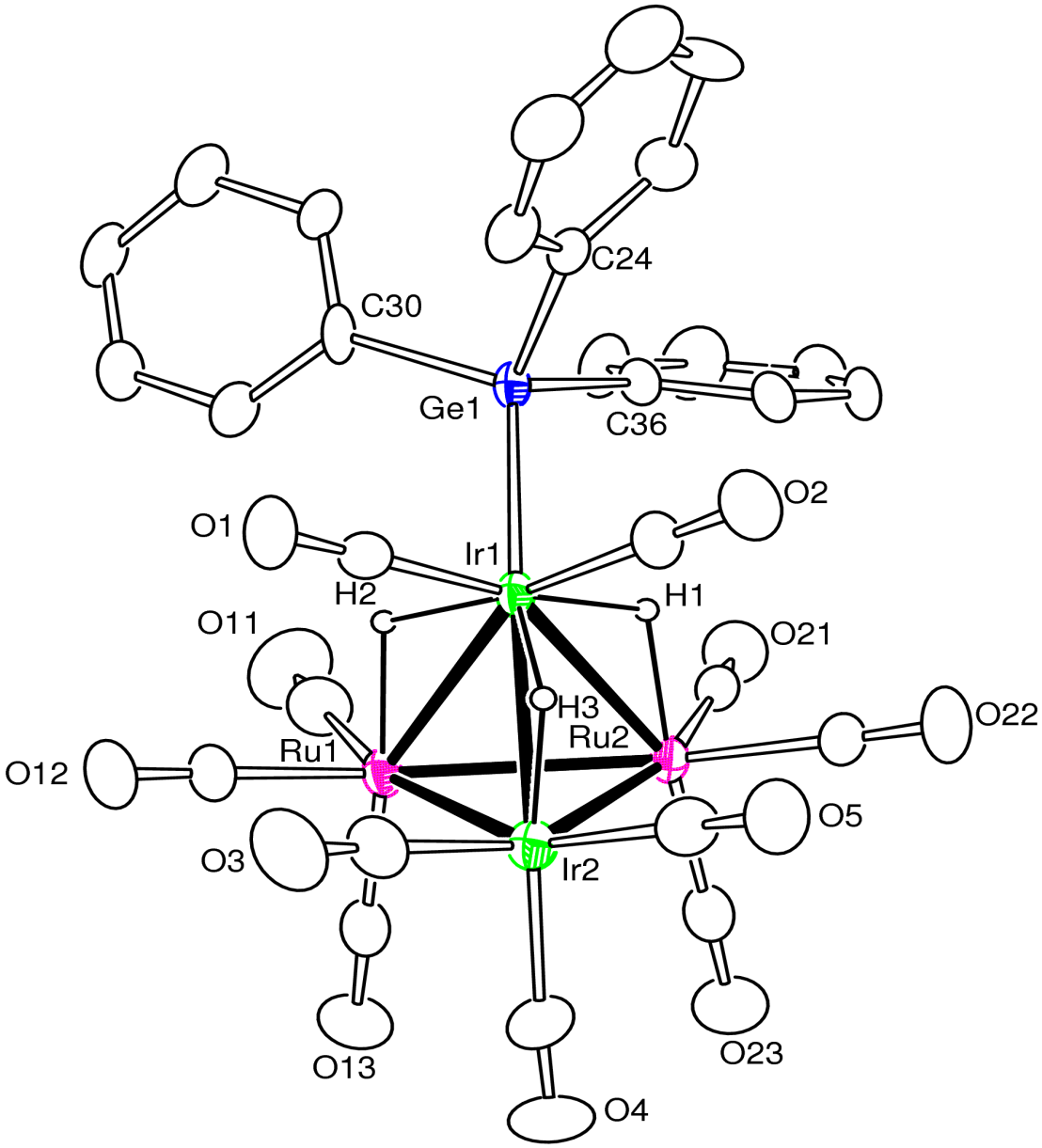

Figure 3.2. An ORTEP diagram of $Ir_2Ru_2(CO)_{11}(GePh_3)(\mu\text{-}H)_3$, **3.2** showing 30% probability thermal ellipsoids.

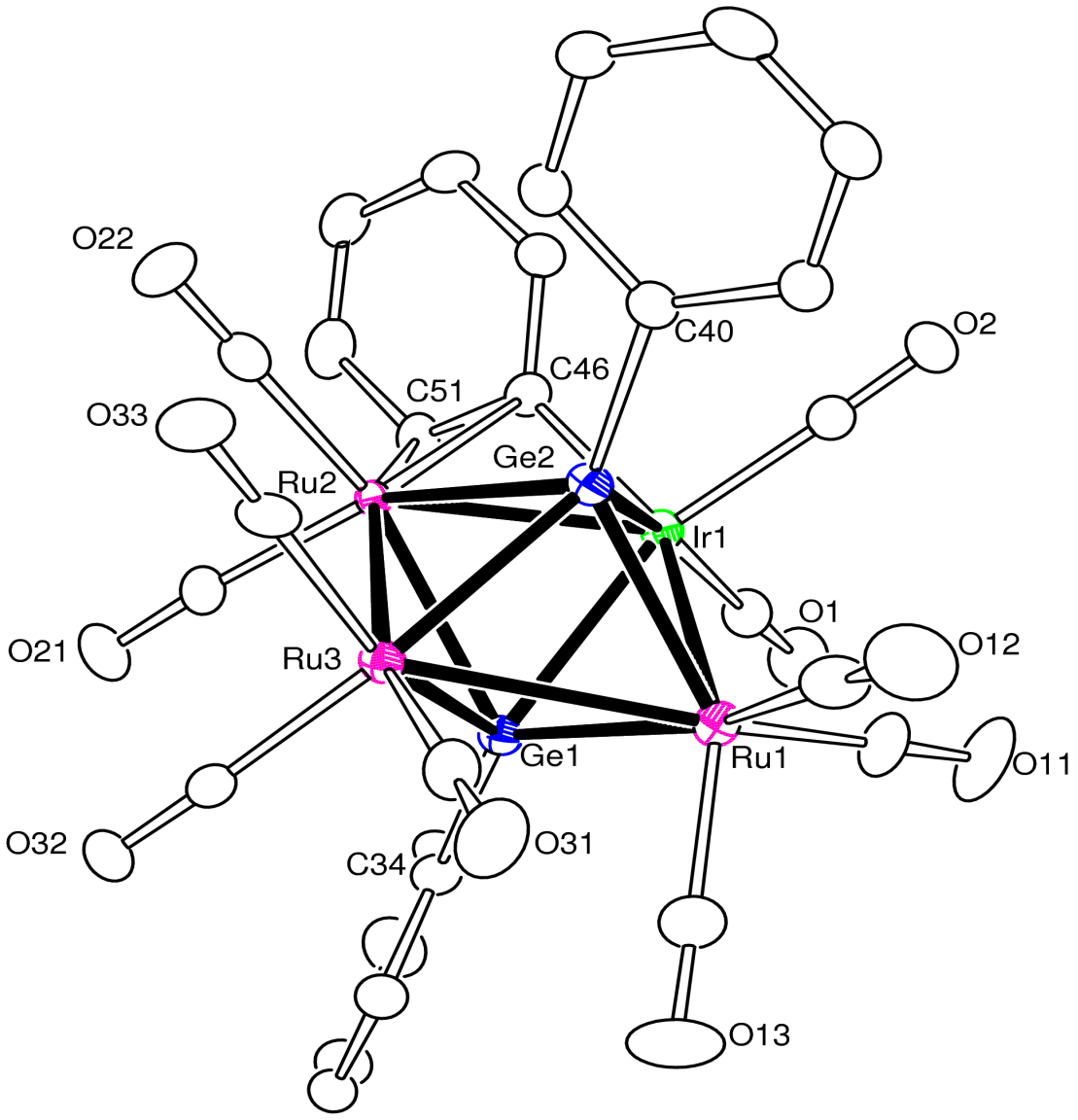

Figure 3.3. An ORTEP diagram of $IrRu_3(CO)_{10}(\mu\text{-}\eta^2\text{-}C_6H_5)(\mu_4\text{-}GePh)_2$, **3.3** showing 40% probability thermal ellipsoids. The hydrogen atoms are omitted for clarity.

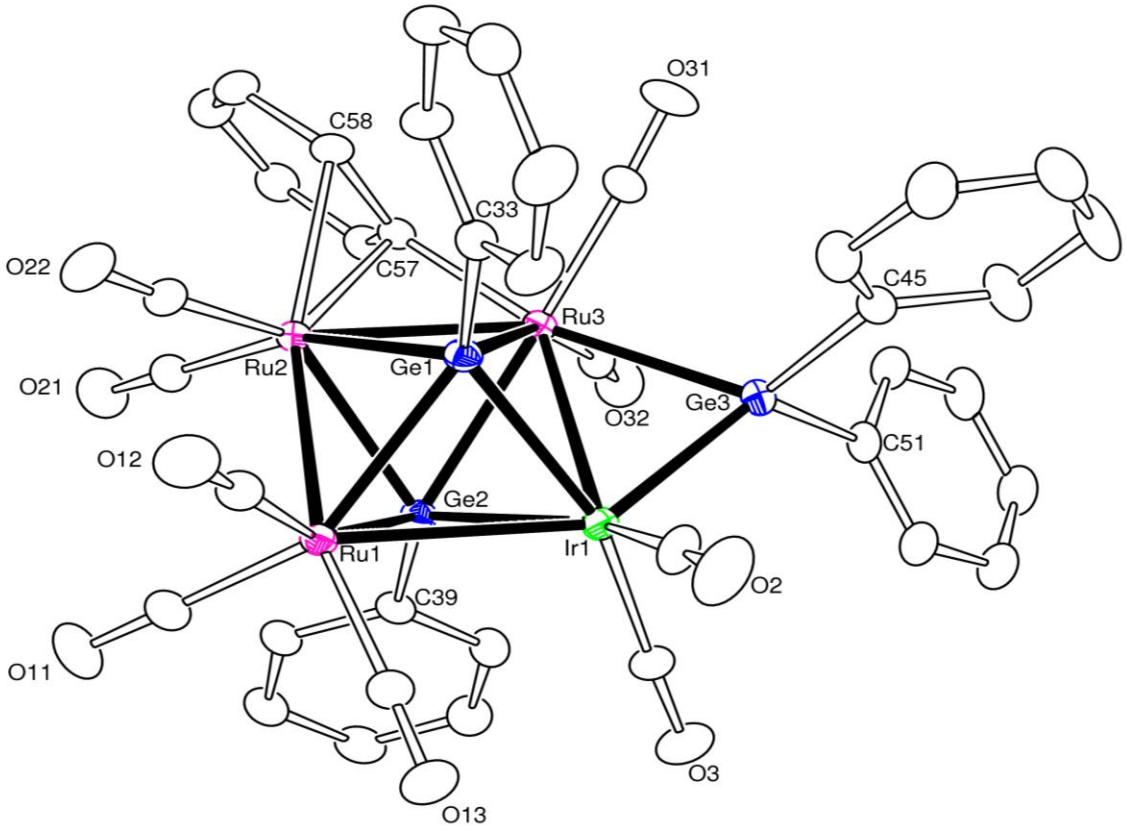

Figure 3.4. An ORTEP diagram of $IrRu_3(CO)_9(\mu\text{-}\eta^2\text{-}C_6H_5)(\mu_4\text{-}GePh)_2(\mu\text{-}GePh_2)$, **3.4** showing 20% probability thermal ellipsoids. The hydrogen atoms are omitted for clarity.

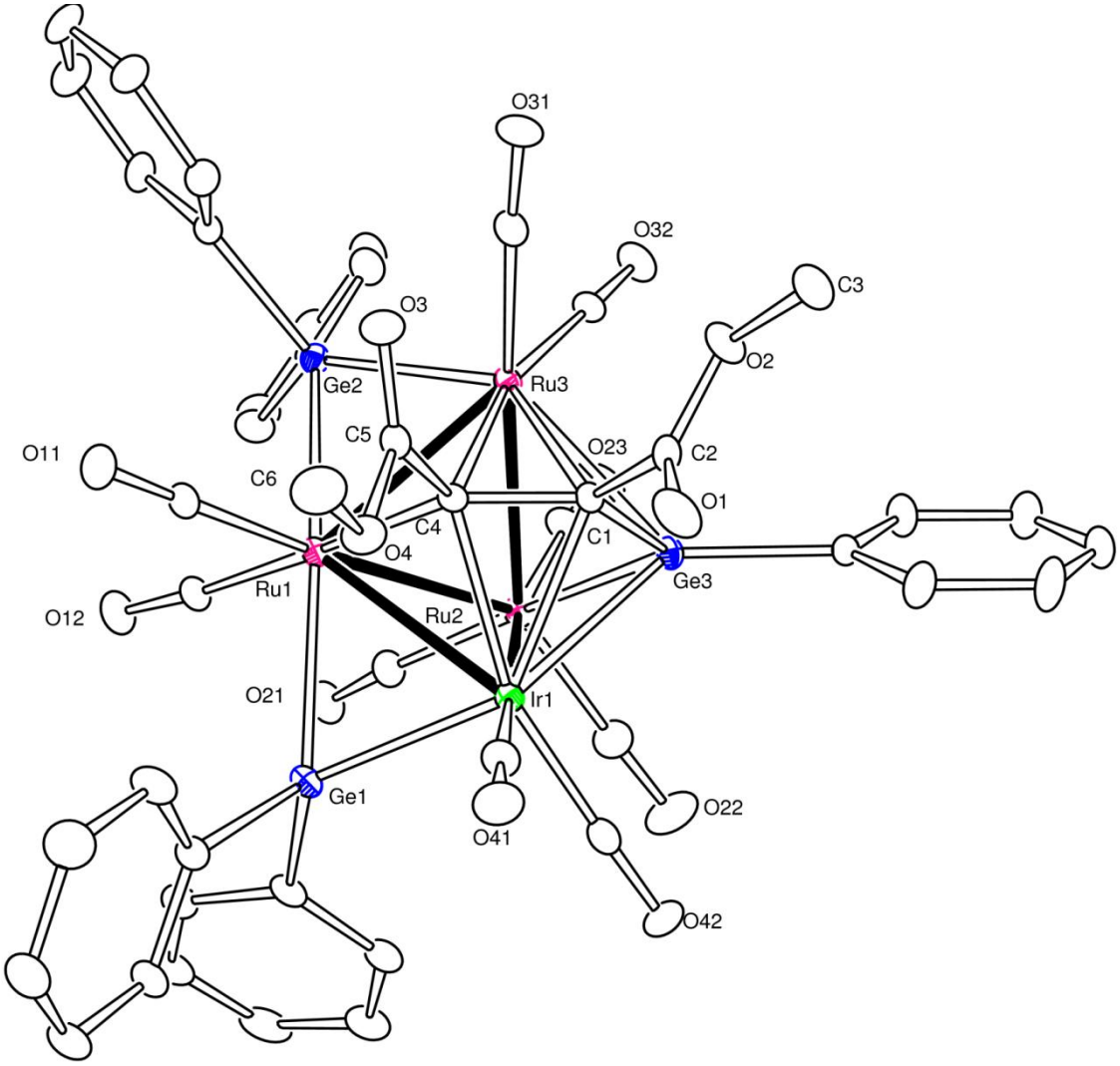

Figure 3.5. An ORTEP diagram of $IrRu_3(CO)_9(\mu\text{-}GePh_2)_2[\mu_4\text{-}Ge(Ph)C(CO_2CH_3)C(CO_2CH_3)]$, **3.5** showing 10% probability thermal ellipsoids. The hydrogen atoms are omitted for clarity.

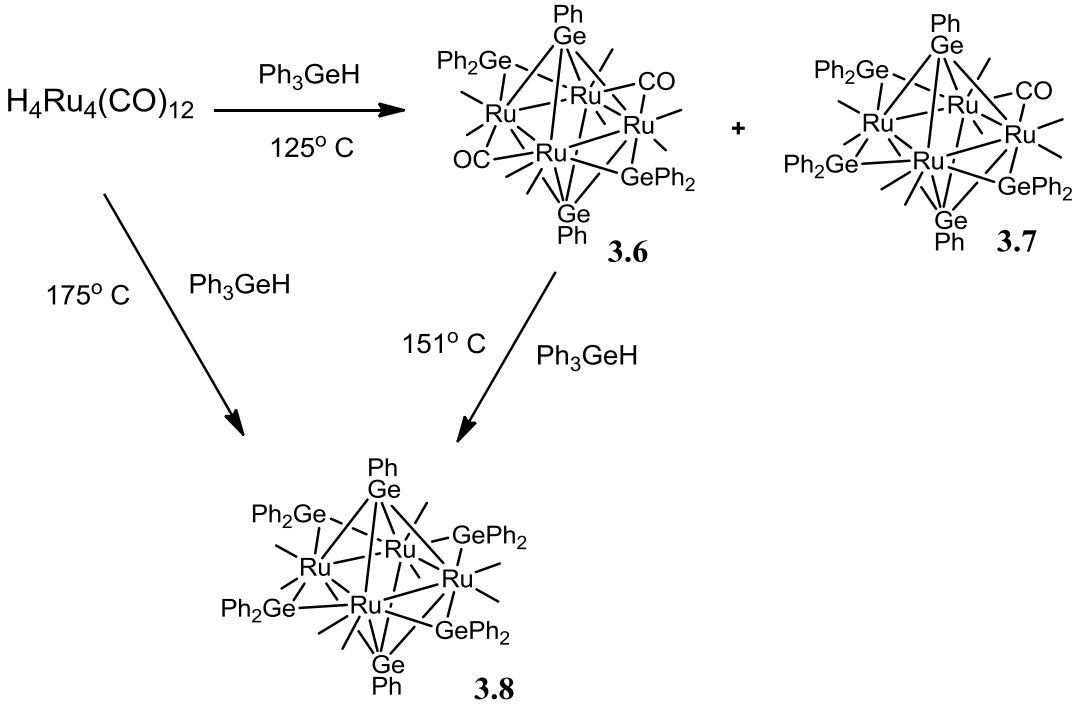

Scheme 3.1. $Ru_4(CO)_8(\mu\text{-}CO)_2(\mu_4\text{-}GePh)_2(\mu\text{-}GePh_2)_2$, **3.6**, $Ru_4(CO)_8(\mu\text{-}CO)(\mu_4\text{-}GePh)_2(\mu\text{-}GePh_2)_3$, **3.7,** and $Ru_4(CO)_8(\mu_4\text{-}GePh)_2(\mu\text{-}GePh_2)_4$, **3.8** are obtained from the reaction of H4Ru4(CO)12 with excess Ph3GeH in octane reflux.

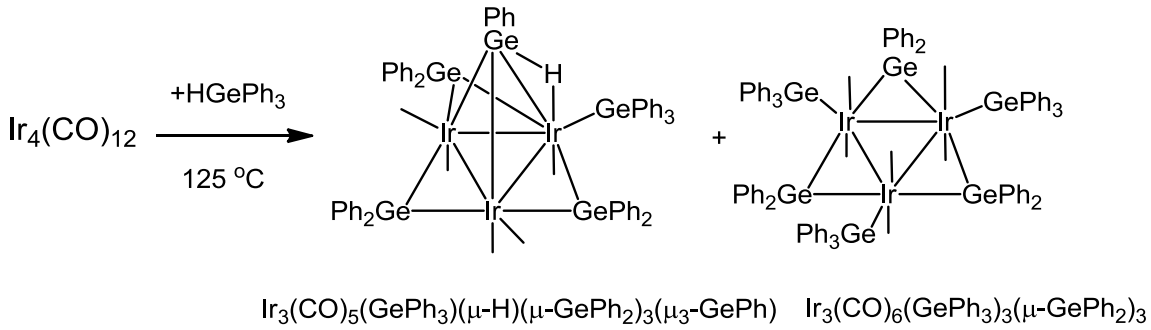

Scheme 3.2. $Ir_4(CO)_{12}$ react with $HGePh_3$ under octane reflux to yield $Ir_3(CO)_5(GePh_3)(\mu\text{-}H)(\mu\text{-}GePh_2)_3(\mu_3\text{-}GePh)$ and $Ir_3(CO)_6(GePh_3)_3(\mu\text{-}GePh_2)_3$.

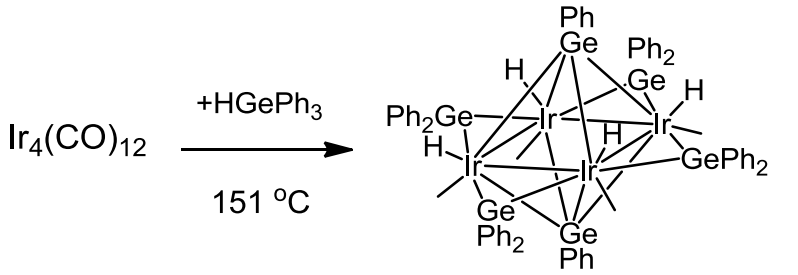

Scheme 3.3. $Ir_4(CO)_{12}$ react with $HGePh_3$ under nonane reflux to yield $H_4Ir_4(CO)_4(\mu\text{-}GePh_2)_4(\mu_4\text{-}GePh)_2$.

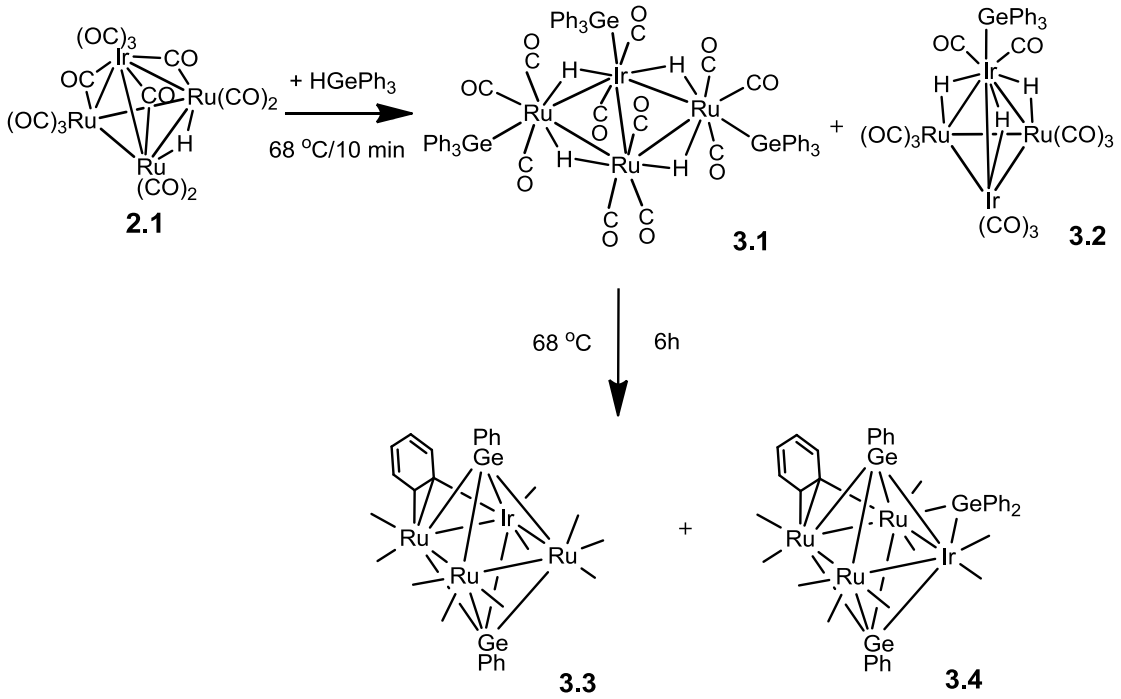

Scheme 3.4. $IrRu_3(CO)_{13}(\mu\text{-}H)$ reacts with $HGePh_3$ to yield the compound $IrRu_3(CO)_{11}(GePh_3)_3(\mu\text{-}H)_4$, **3.1** and $Ir_2Ru_2(CO)_{11}(GePh_3)(\mu\text{-}H)_3$, **3.2**. Compound **3.1** was transformed into $IrRu_3(CO)_{10}(\mu\text{-}\eta^2\text{-}C_6H_5)(\mu_4\text{-}GePh)_2$, **3.3** and $IrRu_3(CO)_9(\mu\text{-}\eta^2\text{-}C_6H_5)(\mu_4\text{-}GePh)_2(\mu\text{-}GePh_2)$, **3.4** upon heating to hexane reflux for 6h. Compound **3.4** reacts with dimethylacetylenedicarboxylate to yield the new compound $IrRu_3(CO)_9([\mu_4\text{-}Ge(Ph)C(CO_2Me)C(CO_2Me)](\mu\text{-}GePh_2)_2$, **3.5**.

Table 3.1. Crystallographic Data for Compounds **3.1** and **3.2**.

Compound	**3.1**	**3.2**
Empirical formula	$IrRu_3Ge_3O_{11}C_{65}H_{49}$	$Ir_2Ru_2GeO_{11}C_{29}H_{18}$
Formula weight	1719.22	1201.56
Crystal system	Monoclinic	Triclinic
Lattice parameters		
a (Å)	9.1558(5)	8.5766(11)
b (Å)	20.1898(12)	9.4559(12)
c (Å)	17.0198(10)	22.096(3)
α (deg)	90.00	88.520(2)
β (deg)	98.3440(10)	89.436(2)
γ (deg)	90.00	67.579(2)
V ($Å^3$)	3112.9(3)	1656.0(4)
Space group		
Z value	2	2
ρ_{calc} (g / cm^3)	1.834	2.410
μ (Mo Kα) (mm^{-1})	4.324	9.851
Temperature (K)	294(2)	293(2)
$2\Theta_{max}$ (°)	56.54	50.06
No. Obs. ($I > 2\sigma(I)$)	10920	5832
No. Parameters	765	406
Goodness of fit (GOF)	1.010	1.065
Max. shift in final cycle	0.007	0.001
Residuals*: R1; wR2 ($I > 2\sigma(I)$)	0.0522; 0.1075	0.0633; 0.1797
Absor.Corr, Max/min	1.000/0.760	1.000/0.587
Largest peak in Final Diff. Map ($e^- / Å^3$)	1.686	4.104

*$R1 = \Sigma_{hkl}(\,|\,|F_{obs}| - |F_{calc}|\,|)/\Sigma_{hkl}|F_{obs}|$; $wR2 = [\Sigma_{hkl}w(|F_{obs}| - |F_{calc}|)^2/\Sigma_{hkl}wF^2_{obs}]^{1/2}$; $w = 1/\sigma^2(F_{obs})$; $GOF = [\Sigma_{hkl}w(|F_{obs}| - |F_{calc}|)^2/(n_{data} - n_{vari})]^{1/2}$.

Table 3.2. Crystallographic Data for Compounds **3.3**, **3.4** and **3.5**.

Compound	**3.3**	**3.4**	**3.5**
Empirical formula	$IrRu_3Ge_2O_{10}C_{28}H_{15}$	$IrRu_3Ge_3O_9C_{39}H_{25}$	$IrRu_3Ge_3Cl_4O_{13}C_{14}H_{35}$
Formula weight	1151.99	1350.77	1662.73
Crystal system	Monoclinic	Triclinic	Triclinic
Lattice parameters			
a (Å)	9.8825(4)	9.4226(3)	11.4182(3)
b (Å)	17.5216(7)	11.6333(3)	14.0029(4)
c (Å)	17.8167(7)	19.3885(6)	18.3262(5)
α (deg)	90.00	87.376(1)	103.039(1)
β (deg)	94.503(1)	87.887(1)	107.564(1)
γ (deg)	90.00	69.714(1)	96.185(1)
V ($Å^3$)	3075.6(2)	1990.87(10)	2672.30(13)
Space group	$P2_1/n$, No. 14	*P*-1, No. 2	*P*-1, No. 2
Z value	4	2	2
ρ_{calc} (g / cm^3)	2.488	2.253	2.066
μ (Mo K_α) (mm^{-1})	7.730	6.722	5.228
Temperature (K)	150(2)	294(2)	293(2)
$2\Theta_{max}$ (°)	56.76	56.64	50.06
No. Obs. ($I > 2\sigma(I)$)	7702	9922	9461
No. Parameters	397	496	616
Goodness of fit (GOF)	1.063	1.044	1.080
Max. shift in cycle	0.001	0.001	0.001
Residuals*: R1; wR2	0.0346, 0.0772	0.0257, 0.0602	0.0393, 0.0897
Absor.Corr, Max/min	1.000/0.585	1.000/ 0.649	1.000/0.804
Largest peak in Final Diff. Map (e^- / $Å^3$)	1.991	0.971	1.926

*$R1 = \Sigma_{hkl}(||F_{obs}| - |F_{calc}||)/\Sigma_{hkl}|F_{obs}|$; $wR2 = [\Sigma_{hkl}w(|F_{obs}| - |F_{calc}|)^2/\Sigma_{hkl}wF^2_{obs}]^{1/2}$; $w = 1/\sigma^2(F_{obs})$; $GOF = [\Sigma_{hkl}w(|F_{obs}| - |F_{calc}|)^2/(n_{data} - n_{vari})]^{1/2}$.

Table 3.3. Selected intramolecular angles and bond distances for compound **3.1**.[a]

Distances			**Angles**			
Atom	Atom	Distance(Å)	Atom	Atom	Atom	Angle(deg)
Ir1	Ru1	2.9932(6)	Ge1	Ir1	Ru3	62.17(4)
Ir1	Ru2	2.8625(5)	Ge1	Ir1	Ru1	125.04(4)
Ir1	Ru3	3.0041(6)	Ge2	Ru1	Ru2	102.96(6)
Ru1	Ru2	3.0305(9)	Ge2	Ru3	Ru2	104.01(6)
Ru2	Ru3	3.0316(9)				
Ir1	Ge1	2.5130(7)				
Ru1	Ge2	2.5430(9)				
Ru3	Ge3	2.5431(9)				

[a] Estimated standard deviations in the least significant figure are given in parentheses.

Table 3.4. Selected intramolecular angles and bond distances for compound **3.2**.[a]

Distances			**Angles**			
Atom	Atom	Distance(Å)	Atom	Atom	Atom	Angle(deg)
Ir1	Ge1	2.5149(15)	Ge1	Ir1	Ru2	111.58(4)
Ru1	Ru2	2.8928(15)	Ge1	Ir1	Ru1	113.92(4)
Ru1	Ir1	2.8923(12)				
Ru1	Ir2	2.7514(13)				
Ir1	Ru2	2.9007(12)				
Ir1	Ir2	2.7506(8)				
Ru2	Ir2	2.7429(13)				

[a] Estimated standard deviations in the least significant figure are given in parentheses.

Table 3.5. Selected intramolecular angles and bond distances for compound **3.3**.[a]

Distances			**Angles**			
Atom	Atom	Distance(Å)	Atom	Atom	Atom	Angle(deg)
Ir1	Ru1	2.9368(5)	Ir1	C46	Ru2	75.04(18)
Ir1	Ru2	2.6485(5)	C46	C51	Ru2	65.5(3)
Ir1	Ge1	2.5737(6)				
Ir1	Ge2	2.5138(6)				
Ru1	Ru3	2.9823(6)				
Ru1	Ge1	2.4582(7)				
Ru1	Ge2	2.5253(7)				
Ru2	Ru3	2.8690(6)				
Ru2	Ge1	2.6035(7)				
Ru2	Ge2	2.7147(7)				
Ru3	Ge1	2.5422(7)				
Ru3	Ge2	2.4693(7)				
Ir1	C46	2.083(6)				
Ru2	C46	2.260(5)				
Ru2	C51	2.441(6)				

[a] Estimated standard deviations in the least significant figure are given in parentheses.

Table 3.6. Selected intramolecular angles and bond distances for compound **3.4**.[a]

Distances			**Angles**			
Atom	Atom	Distance(Å)	Atom	Atom	Atom	Angle(deg)
Ir1	Ru1	2.9519(3)	Ru2	C57	Ru3	76.99(11)
Ir1	Ru3	2.9188(3)	C57	C58	Ru2	66.36(18)
Ir1	Ge1	2.4920(4)	Ir1	Ge3	Ru3	71.468(11)
Ir1	Ge2	2.5228(4)				
Ir1	Ge3	2.4098(4)				
Ru1	Ru2	2.8932(4)				
Ru1	Ge1	2.5267(4)				
Ru1	Ge2	2.4943(4)				
Ru2	Ru3	2.6994(4)				
Ru2	Ge1	2.5956(5)				
Ru2	Ge2	2.5555(4)				
Ru3	Ge1	2.6203(4)				
Ru3	Ge2	2.6058(4)				
Ru3	Ge3	2.5822(5)				
Ru2	C57	2.215(3)				
Ru3	C57	2.121(3)				
Ru2	C58	2.360(3)				

[a] Estimated standard deviations in the least significant figure are given in parentheses.

Table 3.7. Selected intramolecular angles and bond distances for compound **3.5**.[a]

Distances			**Angles**			
Atom	Atom	Distance(Å)	Atom	Atom	Atom	Angle(deg)
Ir1	Ru1	2.8428(7)	Ru1	Ge1	Ir1	69.55(2)
Ir1	Ge1	2.4384(8)	Ru1	Ge2	Ru3	69.47(2)
Ir1	Ge3	2.6475(9)	Ru3	Ge3	Ir1	88.84(2)
Ru1	Ru2	2.9094(8)	C4	C1	Ge3	119.4(4)
Ru1	Ru3	2.8302(7)	C1	C4	Ru1	132.1(4)
Ru1	Ge1	2.5434(10)				
Ru1	Ge2	2.5294(10)				
Ru2	Ru3	2.9677(7)				
Ru2	Ge3	2.3820(9)				
Ru3	Ge2	2.4356(8)				
Ru3	Ge3	2.5906(9)				
Ge3	C1	1.947(6)				
C1	C4	1.448(9)				

[a] Estimated standard deviations in the least significant figure are given in parentheses.

REFERENCE

1. Takaoka, Mendiratta, A.; Peters, J. C. *Organometallics* **2009**, *28*, 3744–3753. (b) Feldman, J. D.; Peters, J. C.; Tilley, T. D., *Organometallics* **2002**, *21*, 4065-4075. (c) Litz, K.E.; Banaszak Holl, M. M.; Kampf, J. W.; Carpenter, G. B. *Inorg. Chem.*, **1998**, *37*, 6461–6469. (d) Tokitoh, N.; Manmaru, K.; Okazaki, R., *Organometallics* **1999**, *13*, 167–171.

2. Pu, L.; Twamley, B.; Haubrich, S.T.; Olmstead, M. M.; Mork, B. V.; Simons, R. S.; Power, P. P., *J. Am. Chem. Soc.* **2000**, *122*, 650-656.

3. (a) Macleod, N.; Fryer, J. R.; Stirling, D.; Webb, G. *Catal. Today* **1998**, *46*, 37-54. (b) Ponec, V. and Bond, G. C. in *Catalysis by Metals and Alloys*, *Stud. Surf. Sci. Catal.* **1998**, *95*, Ch. 13. (c) Tiong Sie, S. in *Catalytic Naphtha Reforming*, G.J. Antos, A.M. Aitani, J.M. Parera (Eds.), Science and Technology, Marcel Dekker Inc., New York, **1995**, Ch. 6.

4. (a) Ekou, T.; Vicente, A.; Lafaye, G.; Especel, C.; Marecot, P. *Appl Catal. A Gen.*. **2006**, *314*, 73-80. (b) Lafaye, G.; Micheaud-Especel, C.; Montassier, C.; Marecot P., *Appl. Catal. A Gen.* **2002**, *230*, 19-30. (c) Lafaye, G.; Micheaud-Especel, C.; Montassier, C.; Marecot P., *Appl. Catal. A Gen.* **2004**, *257*, 107-117.

5. (a) Adams, R. D.; Trufan, E., *Phil. Trans. R. Soc. A* (2010) **368**, 1473–1493 (b) J. M. Thomas, B. F. G. Johnson, R. Raja, G. Sankar, P. A. Midgley, *Acc. Chem. Res.* **2003**, *36*, 20-30. (c) Braunstein, P. and Rose, J. in *Catalysis by Di- and Polynuclear Metal Cluster Complexes*, R.D. Adams and F. A. Cotton, Eds, Wiley-VCH, New York, 1998, Ch. 13. (d) P. Braunstein and J. Rose, *Metal Clusters in Chemistry*, P. Braunstein, L.A. Oro, P.R. Raithby, Wiley-VCH, Weinheim, Vol. 2, 1999, Ch. 2.2, pp 616-677.

6. Adams, R. D.; Boswell, E. M.; Captain, B.; Patel, M. A. *Inorg. Chem.* **2007**, *46*, 533 - 540.

7. Adams, R. D.; Captain, B.; Smith, Jr., J. L. *Inorg. Chem.* **2005**, *44*, 1413 – 1420.

8. Suss-Fink, G.; Haak, S.; Ferrand, G.; Stoeckli-Evans, H. *Dalton Trans.* **1997**, 3861-3865.

9. SAINT+, version 6.2a, Bruker Analytical X-ray Systems, Inc., Madison, WI, 2001.

10. G. M. Sheldrick, SHELXTL, version 6.1, Bruker Analytical X-ray Systems, Inc., Madison, WI, 1997.

11. Adams, R. D.; Captain, B.; Trufan, E. *J. Cluster Sci.* **2007**, *18*, 642-659.

12. Bau, R.; Drabnis, M. H. *Inorg. Chim. Acta* **1997**, *259*, 27-50. (b) Teller, R. G.; Bau, R., *Struc. Bonding* **1981**, 41, 1-82.

13. Adams, R. D.; Kan Y., Trufan, E.; Zhang, Q. *J. Cluster Sci.* **2010**, *21*, 371-378.

14. (a) Adams, R. D.; Pearl Jr., W. C. *J. Organomet. Chem.* **2011**, *696*, 1198-1210. (b) Adams, R. D.; Captain, B.; Zhu, L. *Organometallics*, **2006**, *25*, 4183-4187. (c) Cabeza, J. A.; Franco, R. J.; Llamazares, A.; Riera, V.; Perez-Carreiio, E.; Van der Maelen, J. F. *Organometallics* **1994**, *13*, 55-59. (d) Delavaux, B.; Chaudret, B.; Dahan, F.; Poilblanc, R. *Organometallics* **1985**, *4*, 935-937. (e) Harding, M. M.; Nicholls, B. S.; Smith, A. K. *J. Chem. Soc. Dalton* Trans. **1983**, 1479-1481. (f) Jans, J.; Naegeli, R.; Venanzi, L. M.; Albinati, A. *J. Organomet. Chem.* **1983**, *247*, C37-C41. (g) Taylor, N. J.; Chieh, P. C.; Carty, A. J. *J. Chem. Soc. Chem. Commun.* **1975**, 448. (h) Bradford, C. W.; Nyholm, R. S.; Gainsford, G. J.; Guss, J. M.; Ireland, P. R.; Mason, R. *J. Chem. Soc., Chem. Commun.* **1972**, 87-89. (i) Bradford, C. W.; Nyholm, R. S. *J. Chem. Soc. Dalton* Trans. **1973**, 529-533.

15. Farrugia, L. J.; Miles, A. D.; Stone, F. G. A. *J. Chem. Soc., Dalton Trans.* **1984**, 2415-2422.

16. Hoferkamp, L. A.; Rheinwald, G.; Stoeckli-Evans, H.; Suss-Fink, G. *Organometallics* **1996**, *15*, 704-712.

17. Shima, T.; Suzuki, H. *Organometallics* **2005**, *24*, 1703-1708.

18. Akita, M.; Hua, R.; Oku, T.; Tanaka, M.; Moro-oka, Y. *Organometallics* **1996**, *15*, 4162-4177.

19. Alvarez, M. A.; Garcia, M. E.; Martinez, M.E.; Ramos, A.; Ruiz, M.A. *Organometallics* **2009**, *28*, 6293-6307.

20. Mingos, D. M. P. *Acc. Chem. Res.* **1984**, *17*, 311-319.

21. Watson, W. H.; Poola, B.; Richmond, M.G., *Organometallics* **2005**, *24*, 4687-4690.

22. (a) Takanori Matsuda, T.; Kadowaki, S.; Yamaguchi, Y.; Murakami, M. *Org. Lett.* **2010** , *12*, 1056-1058. (b) Corriu, R. J. P.; Moreau, J. J. E. *J. Chem. Soc., D* **1971**, 812. (c) Esteruelas, M. A.; Martin, M.; Oro, L. A. *Organometallics* **1999**, *18*, 2267-2270. (d) Kinoshita, H.; Nakamura, T.; Kakiya, H.; Shinokubo, H.; Matsubara, S.; Oshima, K. *Org. Lett.* **2001**, *3*, 2521-2524. (e) Marciniec, B .; Lawicka, H.; Majchrzak, M.; Kubicki, M.; Kownacki, I. *Chem. Eur. J.* **2006**, *12*, 244-250. (f) David-Quillot, F.; Thiery, V.; Abarbri, M.; Thibonnet, J.; Besson, T.; Duchene, A. *Trans. Metal Chem.* **2007**, *30*, 235-244. (g) Ichinose, Y.; Oda, H.; Oshima, K.; Utimoto, K. *Bull. Chem. Soc. Jpn.* **1987**, *60*, 3468-3470.

23. Mochida, K.; Wada, T.; Suzuki, K.; Hatanaka, W.; Nishiyama , Y.; Nanjo, M.; Sekine, A.; Ohashi, Y.; Masato Sakamoto, M.; Yamamoto, A., *Bull. Chem. Soc. Jpn.* **2001**, *74*, 123-137.

CHAPTER 4

New Tetraruthenium Carbonyl Complexes Containing Germyl and Stannyl Ligands from the Reactions of $Ru_4(CO)_{13}(\mu\text{-}H)_2$ with $HGePh_3$ and $HSnPh_3$

Introduction

Studies have shown that mixed metal cluster complexes can serve as precursors to superior bi- and multi-metallic nanoscale heterogeneous catalysts.[1] Germanium[2] and tin[1a,3] are well known to serve as excellent modifiers for heterogeneous transition metal catalysts. Adams *et. al.* have been investigating the synthesis and structures of metal carbonyl cluster complexes containing phenylgermanium[4] and phenyltin[5] ligands for use as precursors to new nanoscale particles[5a] and heterogeneous catalysts when placed on supports[3r].

As shown in Scheme 4.1, polynuclear transition metal carbonyl cluster complexes containing terminally-coordinated EPh_3 ligands **A**, E = Ge or Sn, bridging EPh_2 ligands, **B**, triply-bridging EPh ligands, **C** and quadruply-bridging ligands EPh, **D** have been obtained from reactions of a variety of transition metal carbonyl cluster complexes with $HGePh_3$, Scheme 4.2-4.5[4a,6,7,8].

When using $HEPh_3$ as a reagent, it is not uncommon to obtain metal carbonyl products containing terminally coordinated EPh_3 ligands[9]. For example, the reaction of $Ru_3(CO)_{12}$ with $HEPh_3$ yields the product $Ru_3(CO)_9(EPh_3)_3(\mu\text{-}H)_3$, among many others, which contains three EPh_3 ligands[4c,5b]. When heated, $Ru_3(CO)_9(EPh_3)_3(\mu\text{-}H)_3$ eliminates one phenyl ring from each EPh_3 ligand and the three hydride ligands to form tris-

germylene and tris-stannylene complex $Ru_3(CO)_9(\mu\text{-}EPh_2)_3$, Scheme 4.6[4c,5b].

The $IrRu_3$ complex $IrRu_3(CO)_{11}(GePh_3)_3(\mu\text{-}H)_4$ was recently obtained from the reaction of $IrRu_3(CO)_{13}(\mu\text{-}H)$ with $HGePh_3$. When heated, $IrRu_3(CO)_{11}(GePh_3)_3(\mu\text{-}H)_4$ was converted to the compounds $IrRu_3(CO)_{10}(\mu\text{-}\eta^2\text{-}C_6H_5)(\mu_4\text{-}GePh)_2$ and $IrRu_3(CO)_9(\mu\text{-}\eta^2\text{-}C_6H_5)(\mu_4\text{-}GePh)_2(\mu\text{-}GePh_2)$, Scheme 4.7[9]. These products contain quadruply-bridging germylyne ligands formed by cleavage of the phenyl groups from the $GePh_3$ ligands. Each product also contains one of the cleaved phenyl ring that serves as a bridging $\mu\text{-}\eta^2\text{-}C_6H_5$ ligand.

Recently, it has been shown by a computational analysis that the α-cleavage of a phenyl group from a $GePh_3$ ligand in the transformation of the triiridium complex $Ir_3(CO)_6(\mu\text{-}CO)(\mu\text{-}GePh_2)_2(GePh_3)_3$ into the complex $Ir_3(CO)_6(\eta^1\text{-}Ph)(\mu\text{-}GePh_2)_3(GePh_3)_2$, Scheme 4.8, occurs at a single iridium atom[10].

A series of tetraruthenium complexes containing both edge-bridging EPh_2 ligands and quadruply bridging EPh ligands have been obtained recently, E = Ge or Sn, from the reactions of $Ru_4(CO)_{12}(\mu\text{-}H)_4$ with $HGePh_3$ and $HSnPh_3$, Scheme 4.5 [3r, 4a]. No intermediates containing $GePh_3$ or $SnPh_3$ ligands were observed in these reactions. A number of cobalt complexes containing quadruply bridging germylyne ligands have been prepared by using alkylgermanes[11].

In this chapter, the reactions of $Ru_4(CO)_{13}(\mu\text{-}H)_2$ with $HGePh_3$ and $HSnPh_3$ have been investigated, and the new tetrahydridotetraruthenium complexes $Ru_4(CO)_{12}(EPh_3)_2(\mu\text{-}H)_4$ are obtained, **4.1**, E = Ge, and **4.2**, E = Sn. When heated, **4.1** and **4.2** are converted into the complexes $Ru_4(CO)_{12}(\mu_4\text{-}EPh)_2$, **4.3**, E = Ge, and **4.4**, E = Sn having quadruply bridging EPh ligands. Because of the unusual quadruply bridging

coordination of the EPh groups in **4.3** and **4.4**, we have performed DFT calculations of the molecular orbitals (MOs) of **4.3** in order to understand the bonding of these unusual ligands to the planar Ru_4 cluster.

Experimental Section

General Data.

Reagent grade solvents were dried by the standard procedures and were freshly distilled prior to use. Infrared spectra were recorded on a Thermo Nicolet Avatar 360 FT-IR spectrophotometer. ^{1}H NMR spectra were recorded on a Varian Mercury 300 spectrometer operating at 300.1 MHz. Mass spectral (MS) measurements were performed by a direct-exposure probe by using electron impact ionization (EI) or electrospray techniques (ES) were made on a VG 70S instrument. UV–vis spectra of **4.3** and **4.4** were recorded on a Jasco V-530 UV–vis spectrometer in methylene chloride solvent at a concentration of 7.94×10^{-4} M and 1.77×10^{-3} M, respectively. $Ru_3(CO)_{12}$ was purchased from STREM. $HGePh_3$ and $HSnPh_3$ were purchased from Aldrich and were used without further purification. $Ru_4(CO)_{13}(\mu\text{-}H)_2$ was prepared according to a previously reported procedure[12]. Product separations were performed by TLC in air on Analtech 0.25 and 0.5 mm silica gel 60 Å F_{254} glass plates.

Synthesis of $Ru_4(CO)_{12}(GePh_3)_2(\mu\text{-}H)_4$, 4.1.

A 23.7 mg (0.0778 mmol) of $HGePh_3$ were added to 30.0 mg (0.0389 mmol) of $Ru_4(CO)_{13}(\mu\text{-}H)_2$ in 30 mL of hexane solvent. The reaction solution was stirred at room temperature for 6 h. An additional 6.0 mg (0.0197 mmol) of $HGePh_3$ were added to the

reaction mixture six times at 3 h intervals. The color of the solution changed from red to dark orange. After the IR spectrum showed that all of the $Ru_4(CO)_{13}(\mu\text{-}H)_2$ had been consumed, the solvent was removed in vacuo. The residue was then extracted with methylene chloride, transferred to silica TLC plates and then separated by using a 6:1 hexane/methylene chloride solvent mixture to yield in order of elution: 2.5 mg of yellow $Ru_4(CO)_{12}(\mu\text{-}H)_4$ (8.6% yield) and 17.9 mg of red $Ru_4(CO)_{12}(GePh_3)_2(\mu\text{-}H)_4$, **4.1** (34% yield).

Spectral data for **4.1**: IR *vCO* (cm^{-1} in hexane): 2098(w), 2058(m), 2046(vs), 2023(w), 2008(w), 1998(vw). ^1H NMR (CD_2Cl_2, in ppm) at 25°C: δ = 7.18-7.46 (m, 30H, Ph), -15.10 (d, $J_{H\text{-}H}$ = 12 Hz, 2H, hydride), -16.15 (d, $J_{H\text{-}H}$ = 12 Hz, 2H, hydride). Negative ion ES/MS m/z 1352, M+ – CO; 1324, M+ – CO – $GePh_3$; 1020.

Synthesis of $Ru_4(CO)_{12}(SnPh_3)_2(\mu\text{-}H)_4$, 4.2.

An 18.9 mg (0.0540 mmol) of $HSnPh_3$ were added to 20.0 mg (0.0259 mmol) of $Ru_4(CO)_{13}(\mu\text{-}H)_2$ in 30 mL of hexane. The reaction solution was stirred at room temperature for 6 h. An additional 5.0 mg (0.0142 mmol) of $HSnPh_3$ were added to the reaction mixture six times at 3 h intervals. The color of the solution changed from red to a dark orange. After the IR spectrum showed that all of the $Ru_4(CO)_{13}(\mu\text{-}H)_2$ had been consumed, the solvent was removed in vacuo. The residue was then extracted with methylene chloride, transferred to silica TLC plates and then separated by using a 6:1 hexane/methylene chloride solvent mixture to yield in order of elution: 1.3 mg of yellow $Ru_4(CO)_{12}(\mu\text{-}H)_4$, (6.7% yield) and 10.1 mg of red $Ru_4(CO)_{12}(SnPh_3)_2(\mu\text{-}H)_4$, **4.2** (27% yield).

Spectral data for **4.2**. IR *vCO* (cm^{-1} in hexane): 2092(w), 2059(m), 2043(vs), 2031(m), 2020(w), 2009(vw). ^1H NMR (CD_2Cl_2, in ppm) at 25°C: δ = 7.10-7.54(m, 30H, Ph),-14.54 (d, J_{H-H} = 11 Hz, 2H, hydride), -16.22 (d, J_{H-H} = 11Hz, 2H, hydride). Negative ion ES/MS m/z 1444, M+ – CO; 1416, M+ – CO –$SnPh_3$; 1066.

Synthesis of $Ru_4(CO)_{12}(\mu_4\text{-}GePh)_2$, 4.3.

A 24.7 mg (0.0183mmol) of **4.1** was dissolved in hexane and heated to reflux for 1 h. The solvent was then removed in vacuo, and the residue was extracted by methylene chloride and separated by TLC using a 6:1 hexane/methylene chloride solvent mixture to yield in order of elution 1.3 mg of green $Ru_4(CO)_{12}(\mu_4\text{-}GePh)_2$, **4.3** (7% yield), 1.7 mg of the previously reported orange compound $Ru_3(CO)_{10}(\mu\text{-}GePh_2)_2$ (7% yield) [4c], 2.9 mg of the previously reported pale yellow compound *trans*-$Ru(CO)_4(GePh_3)_2$ (5% yield) [4c], and 0.4 mg of the previously reported purple compound $Ru_4(CO)_8(\mu\text{-}CO)_2(\mu_4\text{-}GePh)_2(\mu\text{-}GePh_2)_2$ (1.5% yield) [4a].

Spectral data for **4.3**. IR *vCO* (cm^{-1} in hexane): 2052(vs), 2013(s). The UV-vis absorption spectrum of **4.3** in CH_2Cl_2 solvent shows two broad absorptions in the visible region of the spectrum, λ_{max} = 453 nm, ϵ = 974 $cm^{-1}M^{-1}$, λ_{max} = 667 nm, ϵ = 893 $cm^{-1}M^{-1}$. Mass Spec. EI/MS, *m*/*z*. 1040, M^+.

Synthesis of $Ru_4(CO)_{12}(\mu_4\text{-}SnPh)_2$, 4.4.

A 55 mg (0.0381mmol) of **4.2** was dissolved in hexane and heated to reflux for 40 min. The solvent was then removed in vacuo, and the residue was extracted by methylene chloride and separated by TLC by using a 6:1 hexane/methylene chloride solvent mixture

to yield in order of elution 1.3 mg of purple $Ru_4(CO)_{12}(\mu_4\text{-}SnPh)_2$, **4.4** (3% yield)[3r]; 7.9 mg of the previously reported yellow compounds $Ru_3(CO)_9(\mu\text{-}SnPh_2)_3$ (11% yield)[13], and $Ru_3(CO)_9(SnPh_3)_3(\mu\text{-}H)_3$ (17% yield)[5b]. The UV-vis absorption spectrum of **4.4** in CH_2Cl_2 solvent shows two broad absorptions in the visible region of the spectrum, λ_{max} = 530 nm, ϵ = 245 $cm^{-1}M^{-1}$, λ_{max} = 680 nm, ϵ = 153 $cm^{-1}M^{-1}$.

Crystallographic Analyses.

Red crystals of **4.1** and **4.2** suitable for x-ray diffraction analyses were obtained by slow evaporation of solvent from solutions of the pure compound in a hexane/methylene chloride solvent mixture at room temperature. Dark purple single crystals of **4.3** suitable for x-ray diffraction analyses were obtained by slow evaporation of solvent from a hexane/methylene chloride solvent at -30 ℃. Each data crystal was glued onto the end of a thin glass fiber. X-ray diffraction intensity data were measured by using a Bruker SMART APEX CCD-based diffractometer using Mo Kα radiation (λ = 0.71073 Å). The raw data frames were integrated with the SAINT+ program by using a narrow-frame integration algorithm[14]. Corrections for Lorentz and polarization effects were also applied with SAINT+. An empirical absorption correction based on the multiple measurement of equivalent reflections was applied using the program SADABS[14]. All structures were solved by a combination of direct methods and difference Fourier syntheses, and refined by full-matrix least-squares on F^2 by using the SHELXTL software package[15]. All non-hydrogen atoms were refined with anisotropic thermal parameters. Hydrogen atoms on the phenyl rings were placed in geometrically

idealized positions and included as standard riding atoms during the least-squares refinements.

Compounds **4.1** and **4.2** are isomorphous. They crystallized in the orthorhombic crystal system. The space group *P*bcn was established by the pattern of systematic absences observed in the data and was confirmed by the successful solution and refinement of the structure in both cases. The hydride ligands in compounds **4.1** and **4.2** were located, and refined without restraints by using isotropic thermal parameters.

Compound **4.3** crystallized in the triclinic system. The space group $P\bar{1}$ was assumed and confirmed by the successful solution and refinement for the structure. Crystal data, data collection parameters, and results of the analyses are listed in Table 4.1.

Computational Details.

All density functional theory (DFT) calculations were performed with the ADF suite of programs using the PBEsol functional with Slater-type triple-zeta polarized TZP basis sets with small frozen cores, and scalar relativistic correction[16]. We performed an extensive study of various functionals (B3LYP, M06 family, TPSS family, PBE family) and all-electron vs. frozen core basis sets, and the chosen model provides an optimum compromise between the accuracy and the computational cost, although we found that it is necessary to increase the default numerical integration accuracy parameter to 6. The geometric structure of **4.3** was optimized as gas-phase with point symmetric group of C_{2h}. The time-dependent DFT (TDDFT) calculation was performed at the same theory level. The transitions to triplet and higher order multiplet excited states from the ground state are forbidden because the ground states of the species in this study are singlets. Even if

some of these forbidden transitions gain intensity by spin-orbit splitting, their intensities in absorption spectrum should still be very weak relative to the transitions to the singlet excited states.

Results and Discussion

The compounds $Ru_4(CO)_{12}(GePh_3)_2(\mu\text{-}H)_4$, **4.1** (34% yield) and $Ru_4(CO)_{12}(SnPh_3)_2(\mu\text{-}H)_4$, **4.2** (27% yield) were obtained from the reactions of $Ru_4(CO)_{13}(\mu\text{-}H)_2$ with $HGePh_3$ and $HSnPh_3$, respectively. Compounds **4.1** and **4.2** were both characterized by a combination of IR, ^1H NMR and single-crystal x-ray diffraction analyses. Compounds **4.1** and **4.2** are isomorphous and crystallized in the orthorhombic crystal system. Both compounds are structurally similar. ORTEP diagrams of the molecular structure of **4.1** and **4.2** are shown in Figures 4.1 and 4.2, respectively. Both compounds consist of a butterfly cluster of four ruthenium atoms. In the solid state the molecule sits on a center of symmetry and the cluster of four ruthenium atoms is thus planar in the solid state. Both molecules are similar to the planar $IrRu_3$ cluster complex $IrRu_3(CO)_{11}(GePh_3)_3(\mu\text{-}H)_4$, **4.5** that was obtained from the reaction of $IrRu_3(CO)_{13}(\mu\text{-}H)$ with $HGePh_3$ [9]. Compound **4.5** differs from **4.1** by the replacement of one of the hinge-positioned $Ru(CO)_3$ groups with an $Ir(CO)_2(GePh_3)$ group.

There are five Ru – Ru bonds in each molecule, only three are symmetry independent: for **4.1**: Ru(1) - Ru(2) = 3.0734(9) Å, Ru(1) - Ru(2^i) = 3.0130(9) Å, Ru(2) - Ru(2^i) = 2.8744(12) Å; for **4.2**: Ru(1) - Ru(2) = 3.0434(12) Å, Ru(1) - Ru(2^i) = 3.0031(13) Å, Ru(2) - Ru(2^i) = 2.8796(16) Å. The Ru -Ru bond distances in **4.5** have similar lengths: Ru(1)-Ru(2) = 3.0305(9) Å, Ru(2)-Ru(3) = 3.0316(9) Å. Each of the

peripheral Ru – Ru bonds in **4.1** and **4.2** contains a bridging hydride ligand that was located and refined crystallographically. They exist as two inequivalent pairs and thus exhibit two resonances in the ^{1}H NMR spectrum: for **4.1**: δ = -15.10 (d, J_{H-H} = 12 Hz), -16.15 (d, J_{H-H} = 12 Hz); for **4.2**: δ = -14.54 (d, J_{H-H} = 11 Hz), -16.22 (d, J_{H-H} = 11 Hz). As expected, the hydride-bridged Ru – Ru bonds are significantly longer than the diagonal hinge Ru – Ru bond[17].

Each ruthenium atom contains three linear terminal carbonyl ligands. The two wing-tip Ru atoms, Ru(1) and Ru(1^i), also contain an additional EPh_3 ligand, E = Ge or Sn, that lies in the plane of the cluster in the position trans to the Ru(1) – Ru(2) bond, for **4.1**: Ru(1) – Ge(1) = 2.5501(10) Å, Ru(2) – Ru(1) – Ge(1) = 157.94(3)^o, for **4.2**: Ru(1)-Sn(1) = 2.6894(11), Ru(2) – Ru(1) – Sn(1) = 157.73(4)^o. The Ru – Ge bond distances in **4.1** are very similar to those in **4.5**: Ru(1)-Ge(2) = 2.5430(9) Å, Ru(3)-Ge(3) = 2.5431(9) Å.

When a solution of **4.1** was heated to reflux for 1 h in a hexane solution, it was converted into the new compound $Ru_4(CO)_{12}(\mu_4\text{-}GePh)_2$, **4.3** in 7% yield. Several previously reported coproducts: $Ru_3(CO)_{10}(\mu\text{-}GePh_2)_2$ (7% yield)[4c], *trans*-$Ru(CO)_4(GePh_3)_2$ (5% yield)[4c], and $Ru_4(CO)_8(\mu\text{-}CO)_2(\mu_4\text{-}GePh)_2(\mu\text{-}GePh_2)_2$, **4.6** (1.5% yield)[4a] were also obtained. Compound **4.3** was characterized by IR spectroscopy, ν(CO), 2052 cm^{-1}, 2013 cm^{-1}, UV-vis spectroscopy, mass spectrometry and single-crystal x-ray diffraction analyses.

An ORTEP diagram of the molecular structure of **4.3** is shown in Figure 4.3. In the solid state the molecule sits on a center of symmetry and is thus crystallographically centrosymmetric. The cluster contains four ruthenium atoms in a square planar

arrangement. The two independent Ru - Ru distances are equivalent within experimental error, Ru(1)-Ru(2) = 2.8830(4) Å, Ru(2)-Ru(1*) = 2.8850(3) Å. There are two quadruply bridging GePh ligands that lie on each side of the Ru_4 plane. These distances are shorter than the $GePh_2$ bridged Ru – Ru bond distance in **4.6**, 2.9508(9) Å, and longer than the CO-bridged Ru – Ru bond in **4.6**, 2.8188(7) Å [4a]. The four independent Ru – Ge distances are not significantly different: Ru(1)-Ge(1) = 2.5586(3) Å, Ru(2)-Ge(1) = 2.5559(4) Å, Ru(1)-Ge(1') = 2.5571(6) Å, Ru(2)-Ge(1') = 2.5563(6) Å and they are very similar to the Ru – Ge distances to the quadruply-bridging GePh ligands in **4.6**: 2.5497(10) Å, 2.5565(10) Å and 2.5580(8) Å. The Ge – C distance to the phenyl ring, Ge(1) – C(24) = 1.944(3) Å in **4.3** is the same as that found for the Ge – C distance for the quadruply bridging GePh ligand in **4.6**, 1.940(7) Å. Each Ru atoms contains three linear carbonyl ligands. One CO ligand lies in the Ru_4 plane. The other two lie symmetrically on either side of the Ru_4 plane such that the molecule overall has an approximate C_{4h} symmetry.

When heated to reflux in hexane solvent, compound **4.2** was converted into the previously reported compound $Ru_4(CO)_{12}(\mu_4\text{-}SnPh)_2$, **4.4** but the yield was very low (3%) [3r]. Two other previously reported compounds $Ru_3(CO)_9(\mu\text{-}SnPh_2)_3$ (11% yield)[12] and $Ru_3(CO)_9(SnPh_3)_3(\mu\text{-}H)_3$ (17% yield)[5b] were also obtained. Compound **4.4** is structurally similar to **4.3**.

The bonding of the GePh and SnPh ligands to the $Ru_4(CO)_{12}$ cluster is somewhat unconventional because the GePh/SnPh ligands are each bonded to five atoms: the four Ru atoms and one carbon atom of its attached phenyl ring. Square planar, tetranuclear transition metal cluster complexes can be viewed has having four metal – metal bonds.

When the metal atoms in these complexes obey the 18-electron rule, the metal atoms generally have a total of 64 valence electrons[18]. However, there are a number of examples of square planar, tetranuclear transition metal cluster complexes containing bridging ligands that have only 62 valence electrons[19]. Compound **4.3** belongs to the family of 62 valence electron tetranuclear metal complexes and is "formally" electron deficient.

In order to understand the bonding of the quadruply-bridging GePh and SnPh ligands to the four metal atoms in **4.3**, DFT molecular orbitals were calculated by using the PBEsol functional of the ADF library[16]. To explain the bonding in compound **4.3** we will consider the molecule as a combination of two face to face GePh fragments interacting with a square planar $Ru_4(CO)_{12}$. The $Ru_4(CO)_{12}$ fragment has approximate C_{4h} symmetry. If one includes the eclipsed phenyl groups on the Ge atoms, compound **4.3** has an idealized symmetry of C_{2h}. Our DFT analysis of compound **4.3** was performed in the following way. The molecular orbitals and their energies were obtained from a geometry-optimized structure for **4.3** by starting with the positional parameters obtained from the crystal structure analysis. Molecular orbitals for the $Ru_4(CO)_{12}$ fragment were then obtained by deleting the two GePh ligands and performing a single point calculation on the remaining atoms. Molecular orbitals for the suitably-oriented GePh fragments were obtained by deleting the $Ru_4(CO)_{12}$ fragment of the optimized **4.3** and performing a single point calculation on the remaining atoms. A molecular energy level correlation diagram is shown in Figure 4.4.

The atomic orbital (AO) combinations of the two GePh fragments that are available for bonding to the metal atoms are sketched at the far right of Figure 4.4. Each GePh fragment has one orbital which can be viewed as a sp hybrid that is pointing toward

the Ge atom of the other GePh fragment and also two p-orbitals that are perpendicular to the Ge – Ge vector. Symmetry assignments are based on the point group C_{2h} because of the presence of the two eclipsed phenyl rings. The calculated energies of these orbital combinations and their symmetries are shown in Figure 4 to the left of the sketches of the two GePh fragments. The sp hybrids form a pair of orbitals; the symmetric a_g (HOMO-4) and the antisymmetric a_u (HOMO-1) which are interleaved by two phenyl ring orbitals. The latter are not shown because they are not important for understanding the bonding of the GePh fragments to the metal atoms. The four p-orbitals give four binary combinations: two of b_u symmetry and two of b_g symmetry. The two b_u orbitals are not equal in energy due to different interactions between them and the phenyl rings. For the same reason the two higher energy b_g orbitals are also not of equal in energy.

The energy levels of MOs for the $Ru_4(CO)_{12}$ fragment are shown on the far left of Figure 4. Selected MOs for the $Ru_4(CO)_{12}$ fragment are shown in Figure 4.5. The symmetry of these MOs has been assigned by using the idealized point group C_{4h} but the energies of the two components of the e_u and e_g orbitals are not identical because our arrangement of the atoms was not exactly according to C_{4h} symmetry.

The selected MOs for a geometry-optimized version **4.3** are shown in Figure 4.6. The energy and their symmetry assignments are based on idealized C_{2h} symmetry. These orbitals and their correlations to the appropriate MOs of the fragments are shown in center of Figure 4.4. Note: The e_u and e_g orbitals of the $Ru_4(CO)_{12}$ fragment split and are converted into two orbitals of b_u symmetry and two orbitals of b_g symmetry, respectively, upon crossing over from the C_{4h} symmetry of the $Ru_4(CO)_{12}$ fragment to the C_{2h} symmetry of **4.3**, and the a_g and b_g representations of C_{4h} symmetry both become a_g in

C_{2h} and the a_u and b_u orbitals both become a_u in C_{2h}. The a_g HOMO-4 of the GePh fragments forms a strong bonding interactions to the a_g, HOMO-1 and HOMO-15, of the $Ru_4(CO)_{12}$ fragment to form the strongly bonding HOMO-28 in **4.3**. The b_g HOMO-3 of the $Ru_4(CO)_{12}$ fragment is predominantly metal – metal bonding and becomes the a_g HOMO-17 in **4.3**, see Figure 4.6. The a_u HOMO-1 of the GePh fragments forms strong bonding interactions to the A_u HOMO-2 and HOMO-6 of the $Ru_4(CO)_{12}$ fragment to form the strongly bonding HOMO-26 and the HOMO-15 in **4.3**. The b_u orbitals, HOMO and LUMO, of the GePh fragments form strong bonding interactions to the e_u, HOMO and LUMO, of the $Ru_4(CO)_{12}$ fragment to form the bonding pair HOMO-3 and HOMO-4 and the unoccupied LUMO+1 in **4.3**. The two b_g orbitals, LUMO+1 and LUMO+2, of the GePh fragments form bonding interactions to the e_g orbitals, LUMO+1 and LUMO+2, of the $Ru_4(CO)_{12}$ fragment to form the bonding pair HOMO and HOMO-1 in **4.3**. They also complement the bonding pair of e_g orbitals, HOMO-9 and HOMO-11, of the $Ru_4(CO)_{12}$ fragment to create the strongly bonding pair of b_g orbitals, HOMO-19 and HOMO-21 in **4.3**.

A number of years ago, Halet *et. al* examined the bonding of the complexes of this type by extended Hückel methods[20]. Specifically, they considered the 64 electron model compound $Fe_4(CO)_{12}(\mu_4\text{-}PH)_2$, **4.7**. In **4.7** the HOMO was a b_u orbital (C_{4h} symmetry) analogous to our a_u LUMO (C_{2h} symmetry) for **4.3** because **4.7** has two more electrons that **4.3**. Because they are "formally" unsaturated the 62 electron cluster complexes have a smaller HOMO – LUMO gap and these compounds turn out to be highly colored. For this reason we have also measured the UV-vis absorption spectra of **4.3** and **4.4**.

Compounds **4.3** (blue) and **4.4** (purple) both exhibit two broad absorptions in the visible region: for **3**, λ_{max} = 453 nm, ϵ = 974 $cm^{-1}M^{-1}$, λ_{max} = 667 nm, ϵ = 893 $cm^{-1}M^{-1}$; for **4.4**, λ_{max} = 530 nm, ϵ = 245 $cm^{-1}M^{-1}$, λ_{max} = 680 nm, ϵ = 153 $cm^{-1}M^{-1}$. The observed spectrum of **4.3** is shown in Figure 4.7.

The UV – vis absorption spectrum for **4.3** was calculated from our geometry-optimized structure by using a time-dependent PBEsol calculation. The computed spectrum of **4.3** is shown in Figure 4.8. The observed absorption at 667 nm is attributed to two transitions HOMO-1 to LUMO and HOMO to LUMO that are based in the Ru_4 core of the cluster. They are calculated to be 560 nm, f = 0.047 and 604 nm, f = 0.030, respectively. The observed absorption at 453 nm is attributed to the HOMO-8 (π-ring atomic orbitals) to LUMO transition and is calculated to be 450 nm, f = 0.012. A high energy absorption at approx. 370 nm (calcd) is due to transitions within the phenyl rings.

Summary

The new planar butterfly cluster complexes **4.1** and **4.2** have been obtained from the reactions of $Ru_4(CO)_{13}(\mu\text{-}H)_2$ with $HGePh_3$ and $HSnPh_3$, respectively. When heated, two phenyl rings were cleaved from each of the two EPh_3 ligands, see Scheme 4.9. These phenyl rings were combined with the four hydride ligands and were eliminated as benzene and the complexes **4.3** and **4.4** that contain square planar arrangements of the four ruthenium atoms with quadruply bridging EPh ligands on opposite sides of the Ru_4 plane were formed. A mechanism for the α-cleavage of a phenyl group from a $GePh_3$ ligand in a triiridium cluster complex has recently been established by a computational analysis[10].

The bonding and electronic transitions in **4.3** was also investigated by computational analyses. It has been shown that the quadruply-bridging GePh ligands form delocalized bonding MOs to the $Ru_4(CO)_{12}$ cluster by using a_g and a_u combinations from two "σ-type" sp-hydrid orbitals and two b_g and two b_u orbitals by using unhybridized "π-like" p-orbitals on the two Ge atoms. The color observed for these complexes is due to symmetry-allowed electronic transitions in the Ru_4Ge_2 cluster core of the molecule.

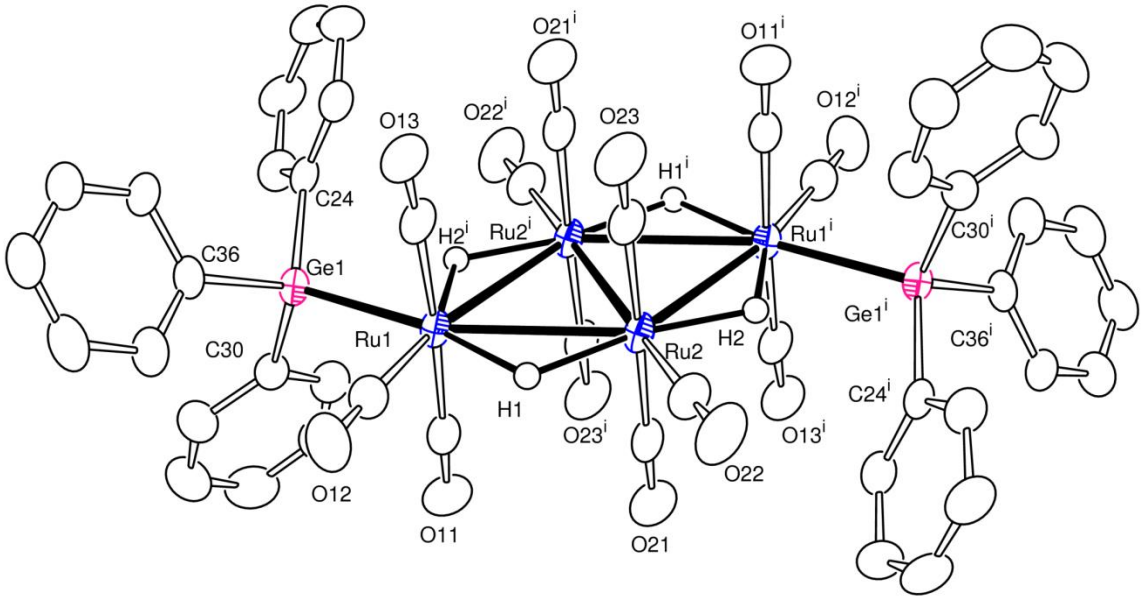

Figure 4.1. An ORTEP diagram of $Ru_4(CO)_{12}(GePh_3)_2(\mu\text{-}H)_4$, **4.1** showing 30% probability thermal ellipsoids. The hydrogen atoms on phenyl groups are omitted for clarity.

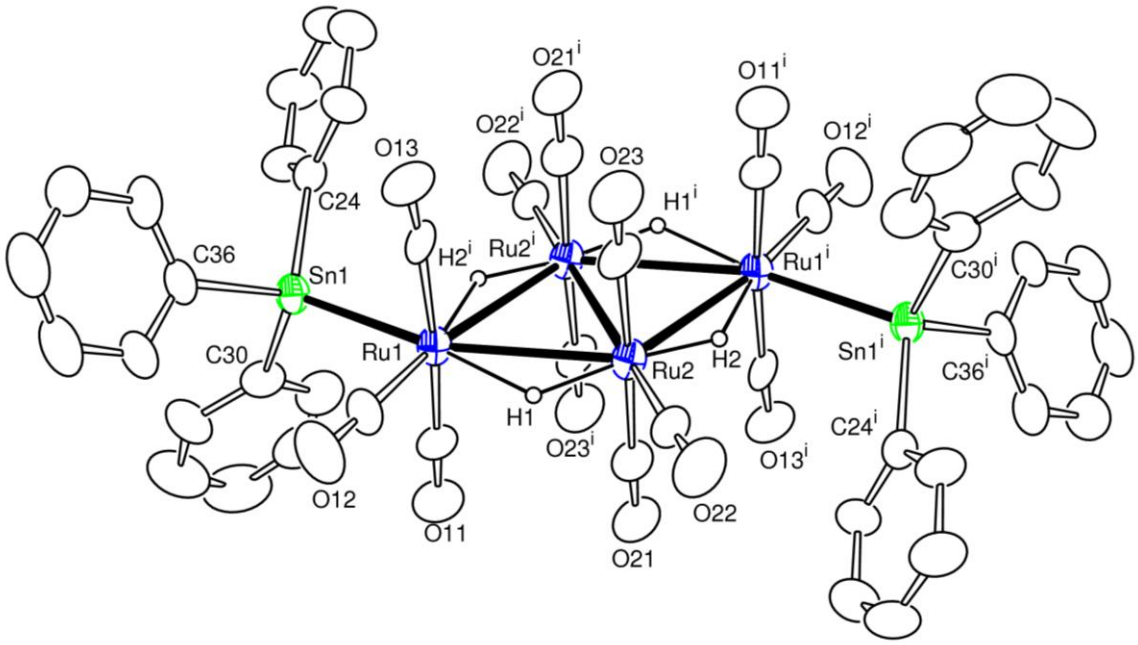

Figure 4.2. An ORTEP diagram of $Ru_4(CO)_{12}(SnPh_3)_2(\mu\text{-}H)_4$, **4.2** showing 20% probability thermal ellipsoids. The hydrogen atoms on phenyl groups are omitted for clarity.

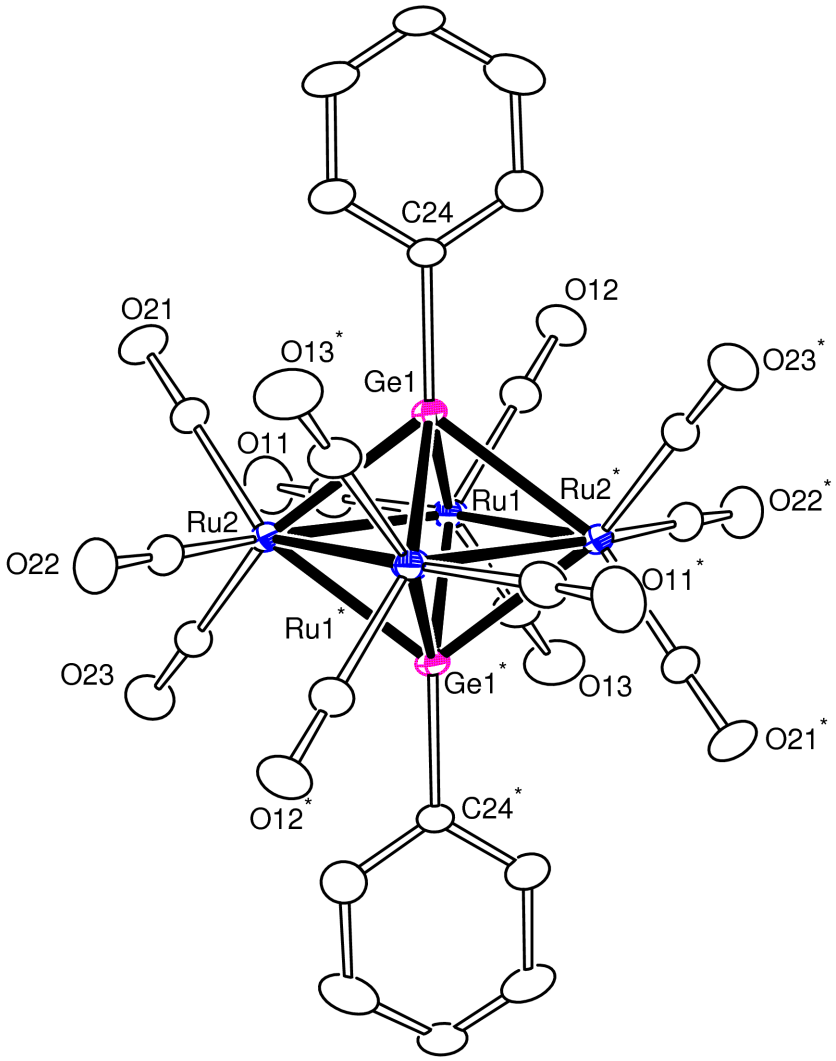

Figure 4.3. An ORTEP diagram of $Ru_4(CO)_{12}(\mu_4\text{-}GePh)_2$, **4.3** showing 20% probability thermal ellipsoids. The hydrogen atoms are omitted for clarity

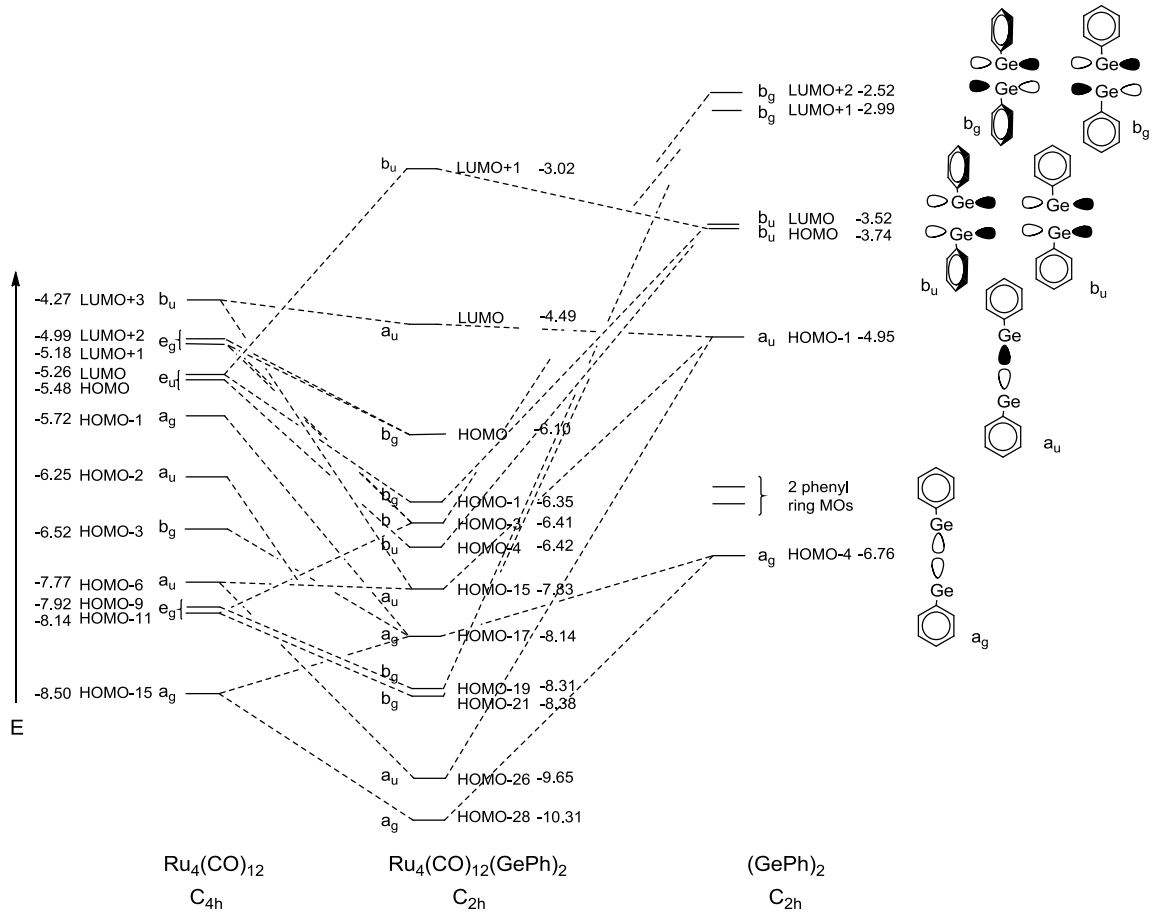

Figure 4.4. A molecular orbital energy level diagram in eV for compound **4.3** and selected molecular fragments. The symmetry correlations $C_{4h} \rightarrow C_{2h}$ are as follow: $A_g \rightarrow A_g$, $B_g \rightarrow A_g$, $E_g \rightarrow 2B_g$, $A_u \rightarrow A_u$, $B_u \rightarrow A_u$, $E_u \rightarrow 2B_u$.

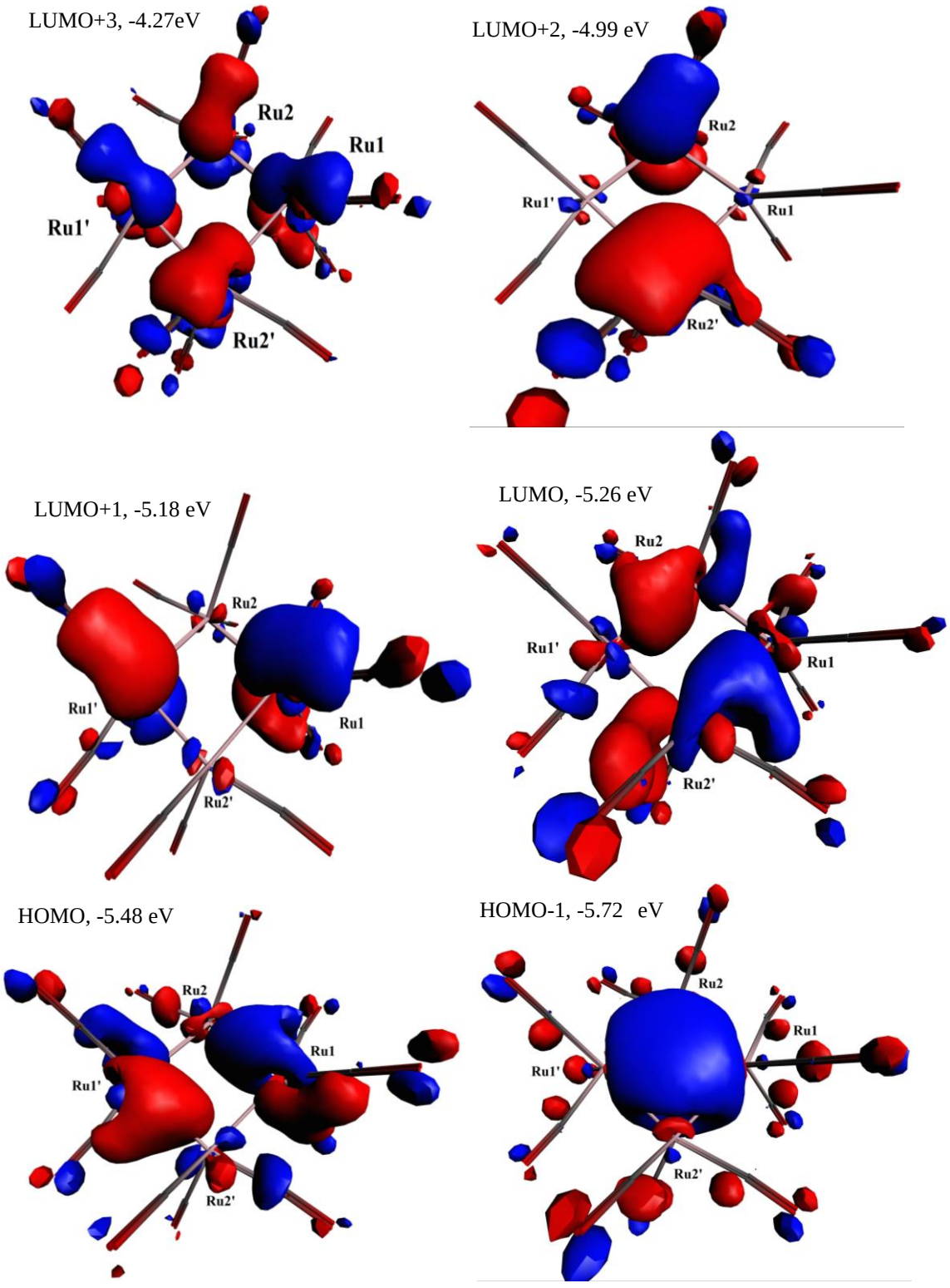

Figure 4.5. Selected molecular orbitals for the $Ru_4(CO)_{12}$ fragment of compound **4.3**.

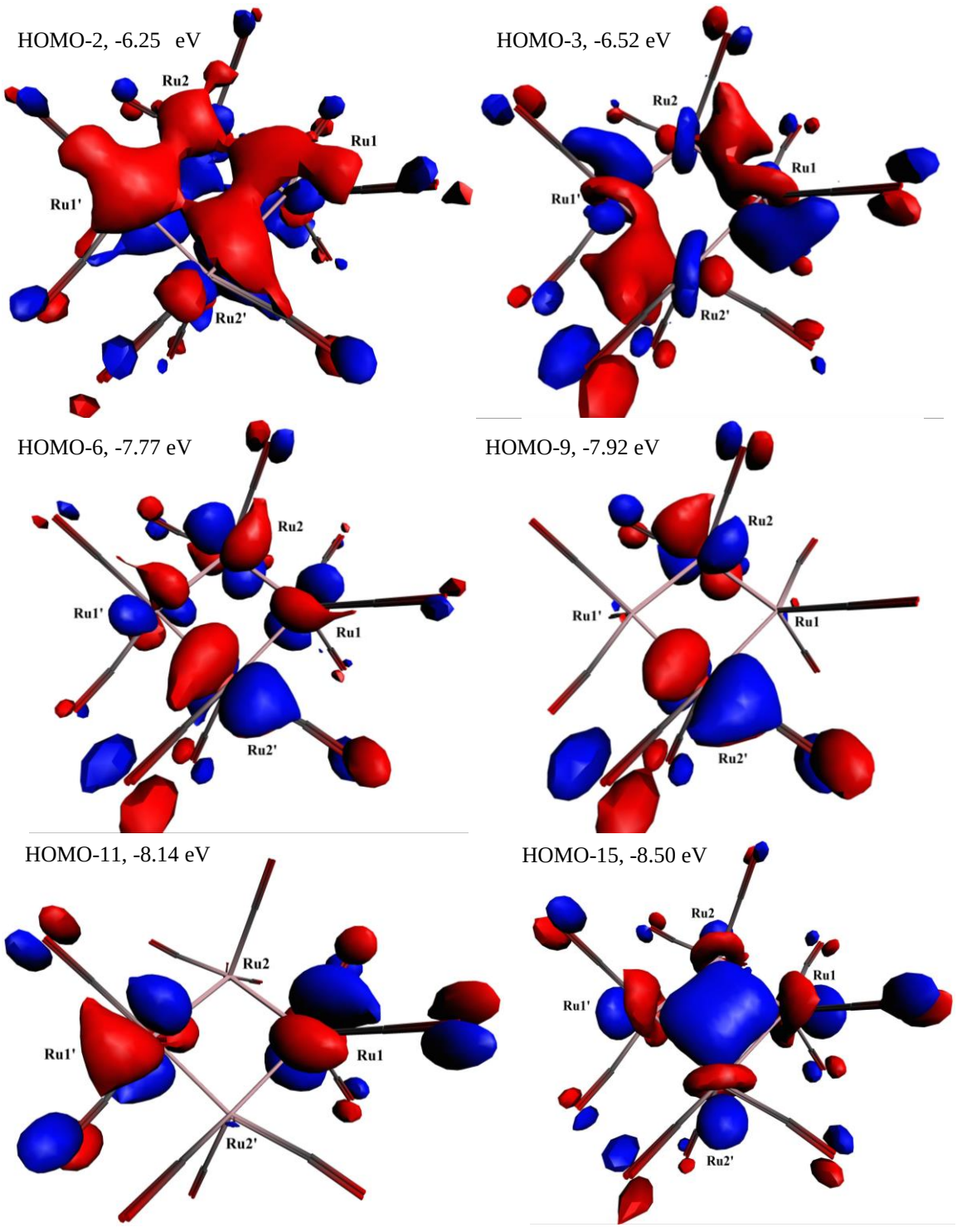

Figure 4.5. (*Continued*).

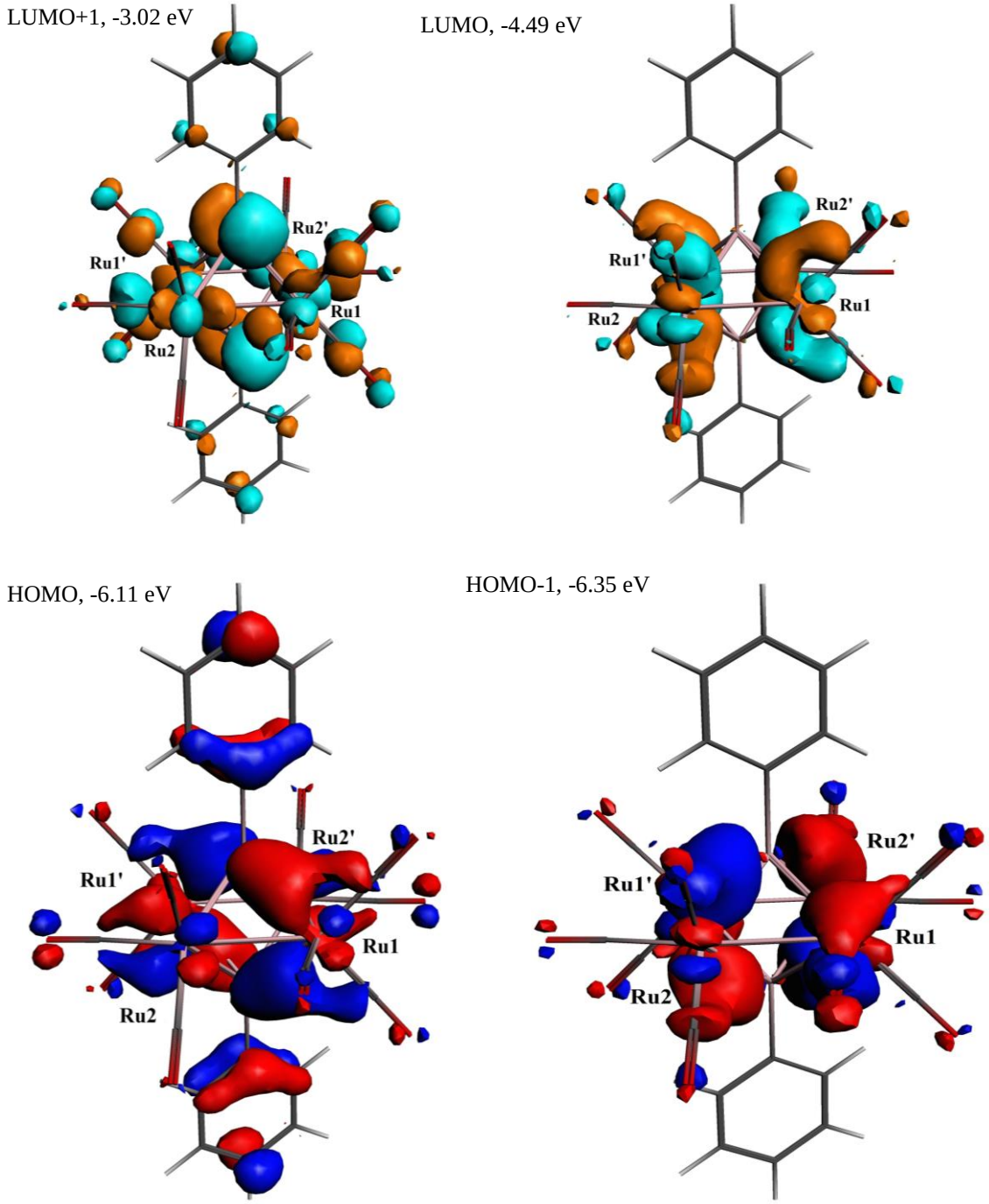

Figure 4.6. Selected molecular orbitals for compound **4.3**

HOMO-4, -6.66 eV

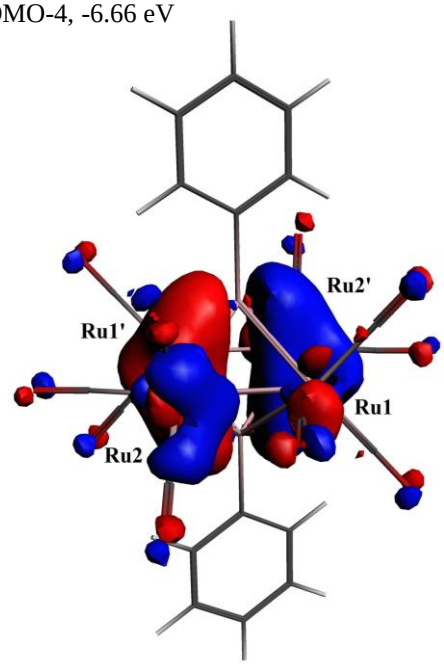

HOMO-15, -7.83 eV

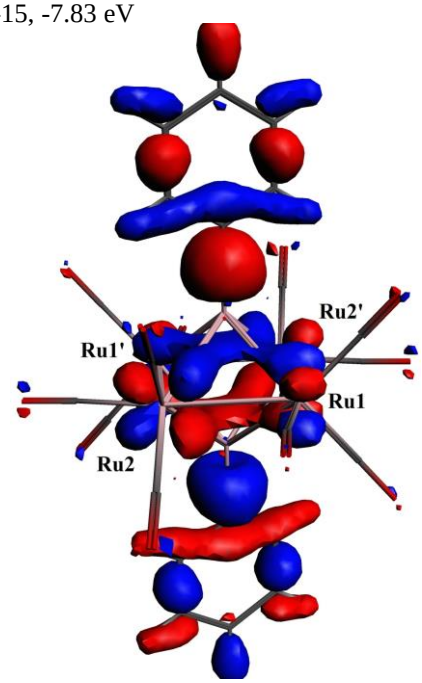

HOMO-19, -8.31 eV

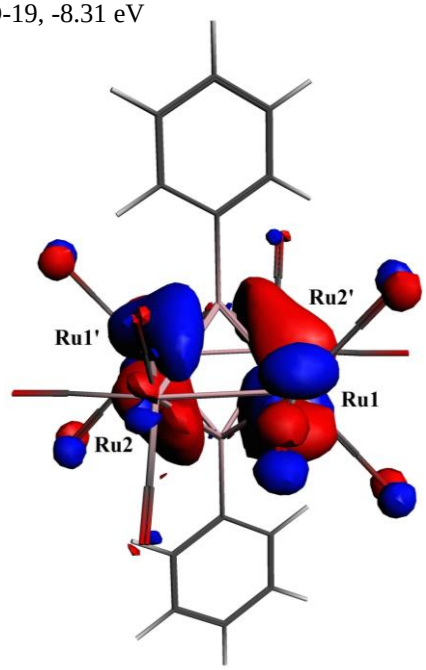

HOMO-21, -8.38 eV

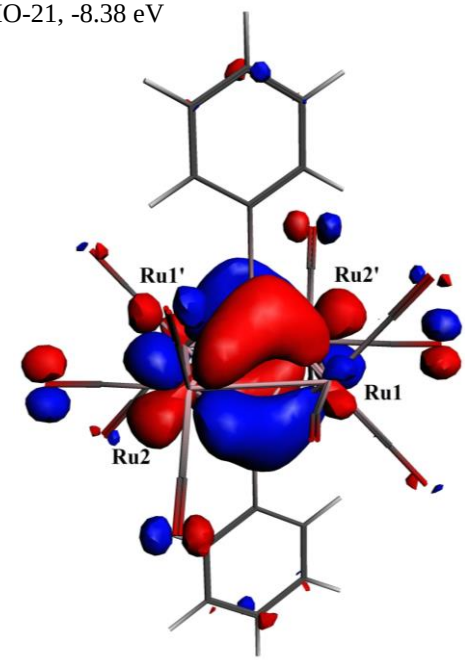

Figure 4.6. (*Continued*).

HOMO-26, -9.65 eV

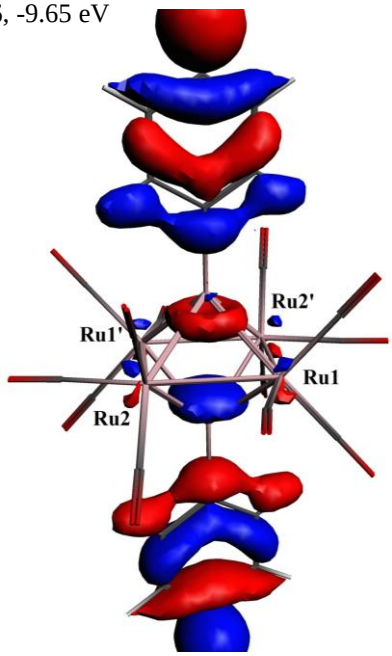

HOMO-28, -10.31 eV

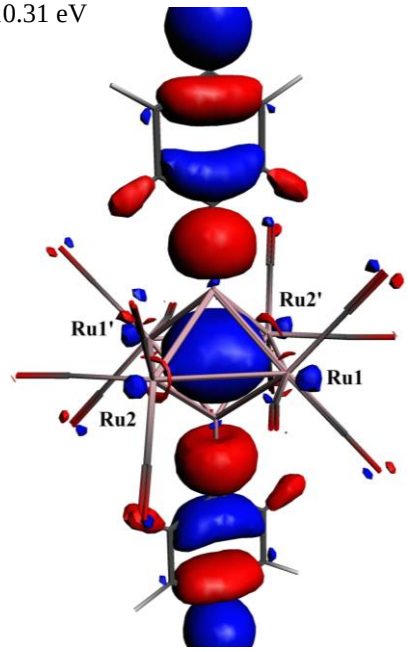

Figure 4.6. (*Continued*).

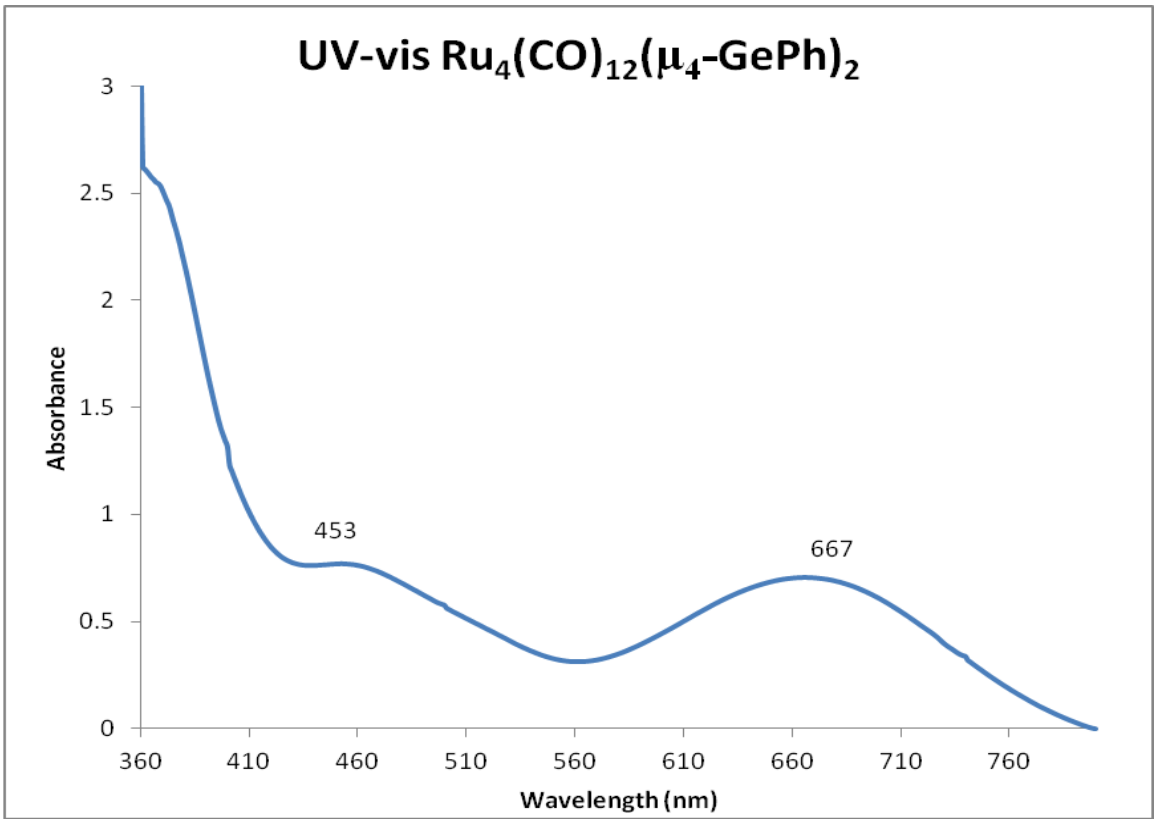

Figure 4.7. UV–vis spectrum of **4.3** in methylene chloride solution.

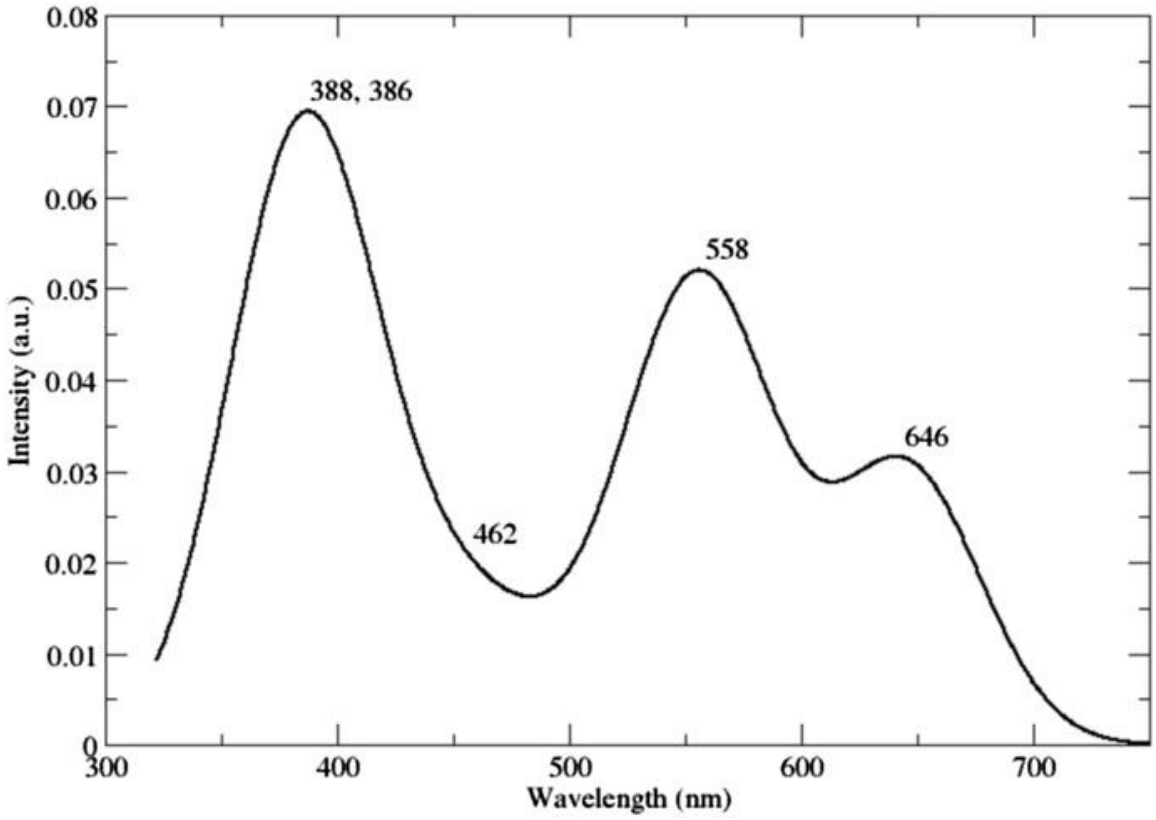

Figure 4.8. TD-PBEsol calculated UV–vis spectrum of compound **4.3**.

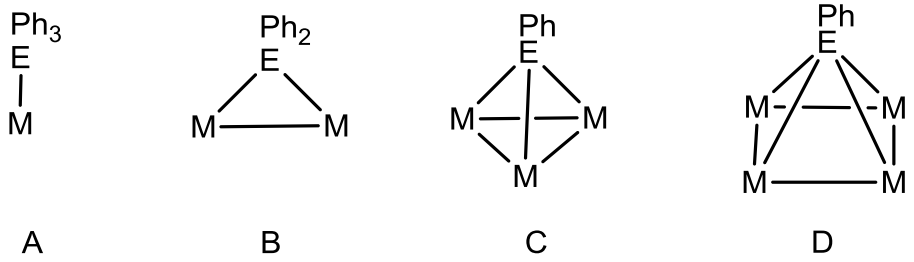

Scheme 4.1. Four PhSn or PhGe bridging mode to transition metal.

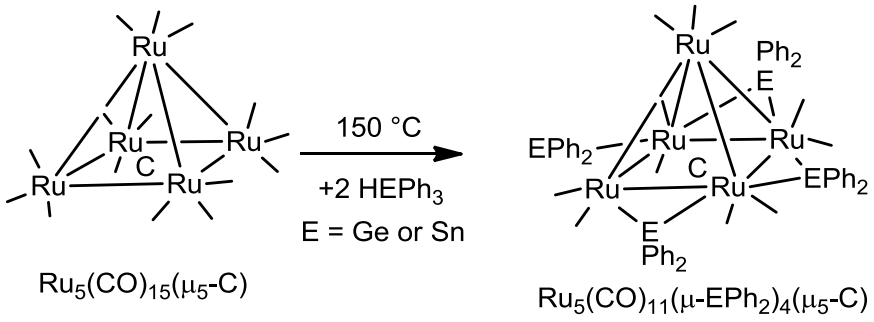

Scheme 4.2. $Ru_5(CO)_{15}(\mu_5\text{-}C)$ reacts with $HGePh_3$ or $HSnPh_3$ in nonane reflux to yield $Ru_5(CO)_{11}(\mu\text{-}EPh_2)_4(\mu_5\text{-}C)$.

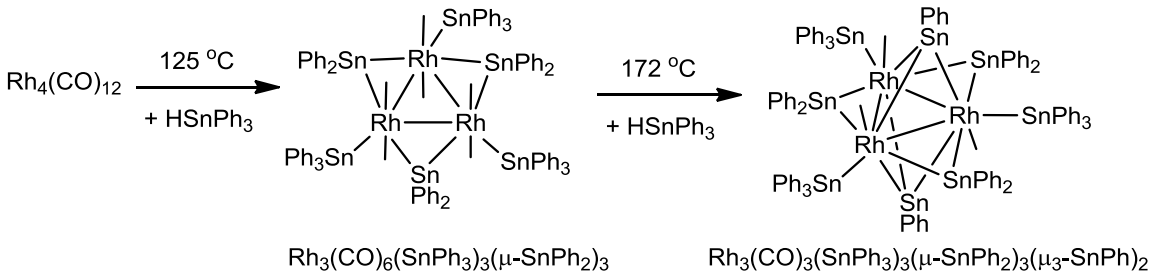

Scheme 4.3. $Rh_4(CO)_{12}$ reacts with $HSnPh_3$ in octane reflux to yield $Rh_3(CO)_6(SnPh_3)_3(\mu\text{-}SnPh_2)_3$. Triply bridging PhSn compound $Rh_3(CO)_3(SnPh_3)_3(\mu\text{-}SnPh_2)_3(\mu_3\text{-}SnPh)_2$ is obtained when $Rh_3(CO)_6(SnPh_3)_3(\mu\text{-}SnPh_2)_3$ reacts with more $HSnPh_3$ under 172°C.

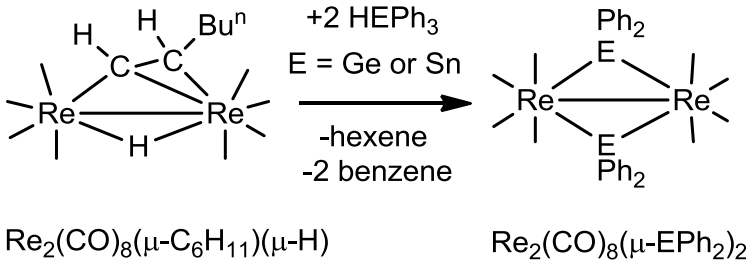

$Re_2(CO)_8(\mu\text{-}C_6H_{11})(\mu\text{-}H)$ $Re_2(CO)_8(\mu\text{-}EPh_2)_2$

Scheme 4.4. $Re_2(CO)_8(\mu\text{-}C_6H_{11})(\mu\text{-}H)$ reacts with $HEPh_3$ (E = Ge or Sn) to yield $Re_2(CO)_8(\mu\text{-}EPh_2)_2$.

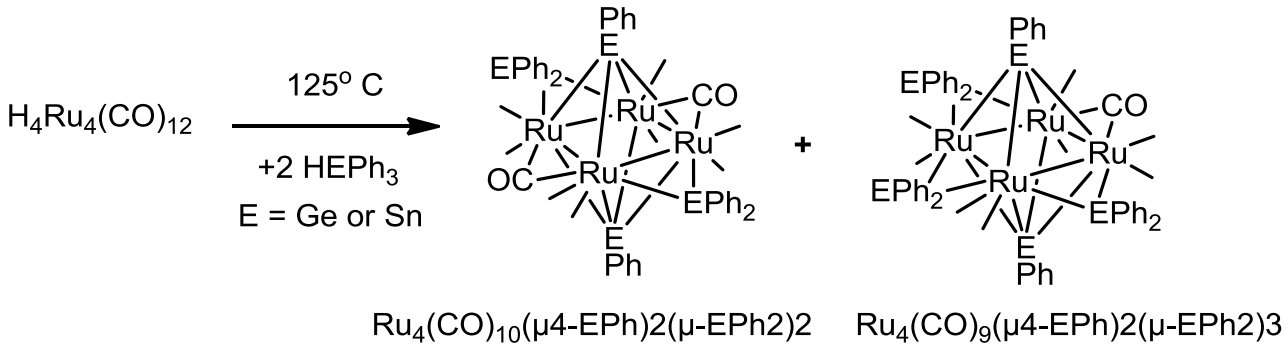

Scheme 4.5. Quadruply bridging EPh compounds $Ru_4(CO)_{10}(\mu_4\text{-}EPh)_2(\mu\text{-}EPh_2)_2$ and $Ru_4(CO)_9(\mu_4\text{-}EPh)_2(\mu\text{-}EPh_2)_3$ are obtained from the reaction of $H_4Ru_4(CO)_{12}$ with excess Ph_3EH in octane reflux.

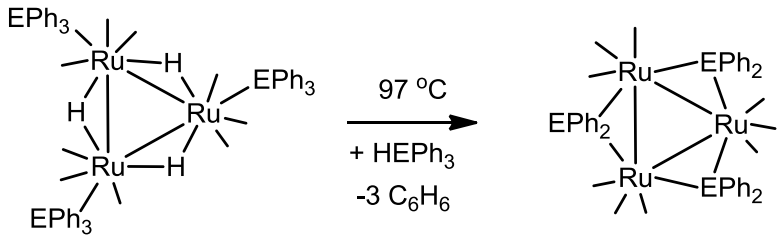

Scheme 4.6. Bridging EPh_2 ligands are formed by heating terminally EPh_3 complexes.

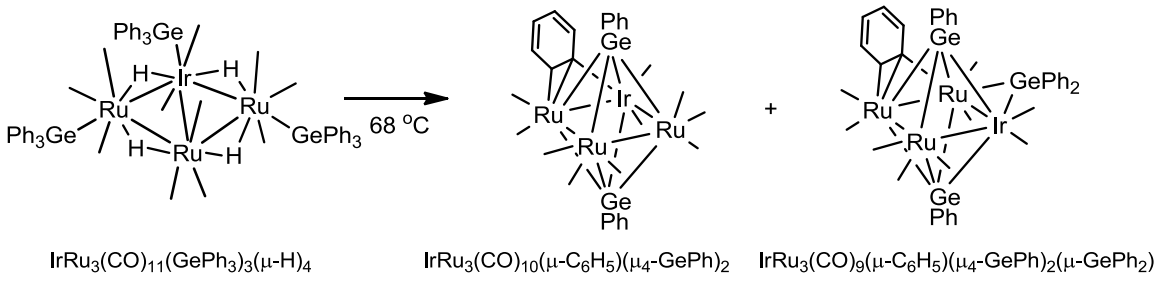

Scheme 4.7. $IrRu_3(CO)_{10}(\mu\text{-}C_6H_5)(\mu_4\text{-}GePh)_2$ and $IrRu_3(CO)_9(\mu\text{-}C_6H_5)(\mu_4\text{-}GePh)_2(\mu\text{-}GePh_2)$ are obtained by heating $IrRu_3(CO)_{11}(GePh_3)_3(\mu\text{-}H)_4$ under hexane reflux.

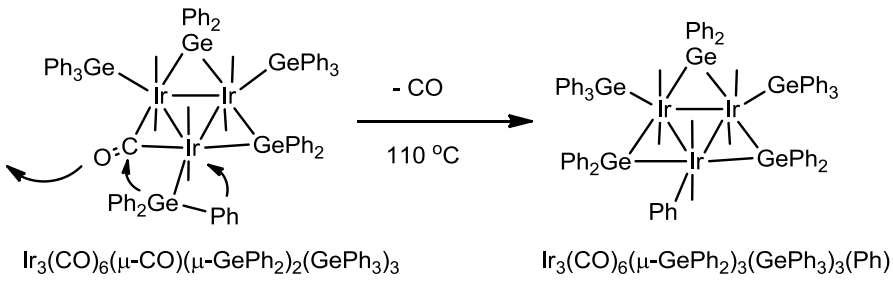

Scheme 4.8. $Ir_3(CO)_6(\mu\text{-}GePh_2)_3(GePh_3)_3(Ph)$ is obtained by α-phenyl cleavage from $Ir_3(CO)_6(\mu\text{-}CO)(\mu\text{-}GePh_2)_2(GePh_3)_3$ upon heating under 110^{o}C

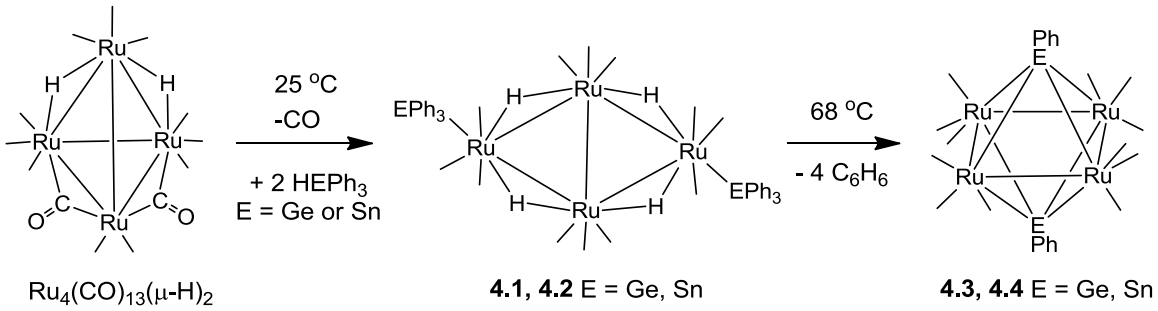

$Ru_4(CO)_{13}(\mu\text{-}H)_2$ **4.1, 4.2** E = Ge, Sn **4.3, 4.4** E = Ge, Sn

Scheme 4.9. $Ru_4(CO)_{13}(\mu\text{-}H)_2$ readily reacts with $HEPh_3$ to yield **4.1** or **4.2**. **4.3** or **4.4** are obtained from **4.1** or **4.2** under hexane reflux, respectively.

Table 4.1. Crystallographic Data for Compounds **4.1**, **4.2** and **4.3**.

Compound	**4.1**	**4.2**	**4.3**
Empirical formula	$Ru_4Ge_2O_{12}C_{48}H_{34}\cdot CH_2Cl_2$	$Ru_4Sn_2O_{12}C_{48}H_{34}\cdot CH_2Cl_2$	$Ru_4Ge_2O_{24}C_{12}H_{10}$
Formula weight	1437.14	1529.34	1039.78
Crystal system	Orthorhombic	Orthorhombic	Triclinic
Lattice parameters			
a (Å)	27.782(5)	28.239(3)	9.1544(3)
b (Å)	11.652(2)	11.8678(14)	9.6436(4)
c (Å)	16.575(3)	16.6154(19)	9.7194(4)
α (deg)	90.00	90.00	73.303(1)
β (deg)	90.00	90.00	83.863(1)
γ (deg)	90.00	90.00	65.546(1)
V ($Å^3$)	5365.4(16)	5568.5(11)	748.07(5)
Space group	*P*bcn(#60)	*P*bcn(#60)	*P*-1(#2)
Z	4	4	1
ρ_{calc} (g/cm^3)	1.78	1.82	2.31
μ (Mo Kα) (mm^{-1})	2.360	2.091	4.009
Temperature (K)	294(2)	294(2)	293(2)
$2\Theta_{max}$ (°)	41.50	33.14	50.04
No. Obs. (I>2σ(I))	3019	4918	2642
No. Parameters	310	306	190
Goodness of fit(GOF)	1.025	1.037	1.049
Max. shift in final cycle	0.001	0.001	0.001
Residuals*: R1; wR2	0.0573; 0.0993	0.0598; 0.0964	0.0345;0.1018
Absor.Corr., Max/min	1.000/0.303	1.000/0.380	1.000/0.653
Largest peak in Final Diff. Map ($e^-/Å^3$)	0.715	0.678	1.789

[a] $R = \Sigma_{hkl}(||F_{obs}| - |F_{calc}||)/\Sigma_{hkl}|F_{obs}|$; $R_w = [\Sigma_{hkl}w(|F_{obs}| - |F_{calc}|)^2/\Sigma_{hkl}wF^2_{obs}]^{1/2}$; $w = 1/\sigma^2(F_{obs})$; $GOF = [\Sigma_{hkl}w(|F_{obs}| - |F_{calc}|)^2/(n_{data} - n_{vari})]^{1/2}$.

Table 4.2. Selected intramolecular angles and bond distances for compound **4.1**.[a]

Distances			**Angles**			
Atom	Atom	Distance(Å)	Atom	Atom	Atom	Angle(deg)
Ru1	Ru2	3.0734(9)	Ge1	Ru2	$Ru1^{i}$	101.65(5)
Ru1	$Ru2^{i}$	3.0130(9)				
Ru2	$Ru2^{i}$	2.8744(12)				
Ru1	Ge1	2.5501(10)				
Ru1	H1	1.98(8)				
Ru1	H2	1.81(5)				
Ru2	H1	1.94(8)				
Ru2	H2	1.75(5)				

[a] Estimated standard deviations in the least significant figure are given in parentheses.

Table 4.3. Selected intramolecular angles and bond distances for compound **4.2**.[a]

Distances			**Angles**			
Atom	Atom	Distance(Å)	Atom	Atom	Atom	Angle(deg)
Ru1	Ru2	3.0434(12)	Sn1	Ru1	Ru2	157.73(4)
Ru1	Ru2^{i}	3.0031(13)				
Ru2	Ru2^{i}	2.8796(16)				
Ru1	Sn1	2.6894(11)				
Ru1	H1	1.88(8)				
Ru1	H2	1.84(9)				
Ru2	H1	1.58(8)				
Ru2	H2	1.48(9)				

[a] Estimated standard deviations in the least significant figure are given in parentheses.

Table 4.4. Selected intramolecular angles and bond distances for compound **4.3**.[a]

Distances			**Angles**			
Atom	Atom	Distance(Å)	Atom	Atom	Atom	Angle(deg)
Ru1	Ru2	2.8830(4)	C24	Ge1	Ru1	126.20(15)
Ru2	Ru1*	2.8850(3)	C24	Ge1	Ru2	126.66(14)
Ru1	Ge1	2.5586(3)				
Ru2	Ge1	2.5559(4)				
Ru1	Ge1*	2.5576(4)				
Ru1	Ge1*	2.5573(4)				
Ge1	C24	1.944(3)				

[a] Estimated standard deviations in the least significant figure are given in parentheses.

REFERENCES

1. (a) Adams, R. D.; Trufan, E., *Phil. Trans. R. Soc. A* **2010**, *368*, 1473-1493. (b) Thomas, J. M.; Johnson, B. F. G.; Raja, R.; Sankar, G.; Midgley, P. A. *Acc. Chem. Res*. **2003**, *36*, 20-30. (c) Braunstein, P.; Rose, J. *Catalysis by Di- and Polynuclear Metal Cluster Complexes*, Adams, R. D.; Cotton, F. A. Eds, Wiley-VCH, New York, **1998**, Ch. 13. (d) Braunstein, P.; Rose, J. *Metal Clusters in Chemistry*, Braunstein, P.; Oro, L.A.; Raithby, P.R. Wiley-VCH, Weinheim, Vol. 2, **1999**, Ch. 2.2, pp 616-677.

2. (a) Ekou, T.; Vicente, A.; Lafaye, G.; Especel, C.; Marecot, P. *Appl Catal. A Gen.*. **2006**, *314*, 73-80. (b) Lafaye, G.; Micheaud-Especel, C.; Montassier, C.; Marecot, *Appl. Catal. A Gen.* **2002**, *230* 19-30. (c) Lafaye, G.; Micheaud-Especel, C.; Montassier, C.; Marecot, *Appl. Catal. A Gen.* **2004**, *257*, 107-117.

3. (a) Burch, R. *J. Catal.* **1981**, *71*, 348-359. (b) Burch, R.; Garla, L. C. *J. Catal.* **1981**, *71*, 360-372. (c) Srinivasan, R.; Davis, B. H. *Platinum Metals Rev.* **1992**, *36*, 151-163. (d) Fujikawa, T.; Ribeiro, F. H.; Somorjai, G. A. *J. Catal.* **1998**, *178*, 58-65. (e) Park, Y.-K.; Ribeiro, F. H.; Somorjai, G. A. *J. Catal.* **1998**, *178*, 66-75. (f) Epron, F.; Carnevillier, C.; Marecot, P. *Appl. Catal.* **2005**, *295*, 157-169. (g) Cortright, R. D.; Dumesic, J. A. *J. Catal.* **1994**, *148*, 771-778. (h) Dautzenberg, F. M.; Helle, J. N.; Biolen, P.; Sachtler, W. M. H. *J. Catal.* **1980**, *63*, 119-128. (i) Huber, G. W.; Shabaker, J. W.; Dumesic, J. A. *Science* **2003**, *300*, 2075-2077. (j) Shabaker, J. W.; Simonetti, D. A.; Cortright, R. D.; Dumesic, J. A. *J. Catal.* **2005**, *231*, 67-76. (k) Guidotti, M.; Dal Aanto, V.; Gallo, A.; Gianotti, E.; Peli, G.; Psaro, R.; Sordelli, L. *Catal. Lett.* **2006**, *112*, 89-95. (l) Cortright, R. D.; Hill, J. M.; Dumesic, J. A. *Catal. Today* **2000**, *55*, 213-223. (m) Hermans, S.; Raja, R.; Thomas, J. M.; Johnson, B. F. G.; Sankar, G.; Gleeson, D. *Angew. Chem., Int. Ed.* **2001**, *40*, 1211-1215. (n) Johnson, B. F. G.; Raynor, S. A.; Brown, D. B.; Shephard, D. S.; Mashmeyer, T.; Thomas, J. M.; Hermans, S.; Raja, R.; Sankar, G. *J. Mol. Catal. A: Chem* **2002**, *89*, 182-183. (o) Hermans, S.; Johnson, B. F. G. *Chem. Commun.* **2000**, 1955-1956. (p) Thomas, J. M.; Johnson, B. F. G.; Raja, R.; Sankar, G.; Midgley, P. A. *Accts. Chem. Res.* **2003**, *36*, 20-30. (q) Adams, R. D.; Blom, D. A.; Captain, B.; Raja, R.; Thomas, J. M.; Trufan, E. *Langmuir*, **2008**, *24*, 9223-9226. (r) Adams, R. D.; Boswell, E. M.; Captain, B.; Hungria, A. B.; Midgley, P. A.; Raja, R.; Thomas, J. M. *Angew. Chem.. int. Ed.*, **2007**, *46*, 8182-8185.

4. (a) Adams, R. D.; Boswell, E. M.; Captain, B.; Patel, M. A. *Inorg. Chem.* **2007**, *46*, 533-540. (b) Adams, R. D.; Captain, B.; Smith Jr., J. L. *Inorg. Chem.* **2005**, *44*, 1413-1420. (c) Adams, R. D.; Captain, B.; Trufan, E. *J. Cluster Sci.* **2007**, *18*, 642-659.

5. (a) Yang, F.; Trufan, E.; Adams, R. D.; Goodman, D. W. *J. Phys. Chem. C.*, **2008**, *112*, 14233-14235. (b) Adams, R. D.; Captain, B.; Trufan, E. *J. Organomet. Chem.* **2008**, *693*, 3593-3602.

6. (a) Adams, R. D.; Captain, B.; Fu, W. *Inorg. Chem.*, **2003**, *42*, 1328-1333. (b) Adams, R. D.; Captain, B.; Fu, W.; Smith, M. D. *Inorg. Chem.* **2002**, *41*, 5593-5601. (c) Adams, R. D.; Captain, B.; Fu, W.; Smith, M. D. *Inorg. Chem.* **2002**, *41*, 2302-2303.

7. Adams, R. D.; Captain, B.; Smith, J. L. Jr., Hall, M. B.; Beddie, C. L.; Webster, C. E. *Inorg. Chem.* **2004**, *43*, 7576-7568.

8. Adams, R. D.; Captain, B.; Herber, R. H.; Johansson, M.; Nowik, I.; Smith Jr., J. L., Smith, M. D. *Inorg. Chem.* **2005**, *44*, 6346-6358.

9. Adams, R. D.; Kan, Y.; Zhang, Q. *Organometallics*, **2011**, *30*, 328-333.

10. Adams, R. D.; Fang, F.; Zhang, Q.; Hall, M. B.; Trufan, E. *Organometallics*, **2012**, *31*, 2621-2630.

11. (a) Anema, S. E.; Lee, S. K.; Mackay, K. M.; McLoed, L. C.; Nickolson, B. K. *J. Chem. Soc., Dalton Trans.* **1991**, 1209-1217. (b) Anema, S. E.; Lee, S. K.; Mackay, K. M.; Nickolson, B. K.; Service, M., *J. Chem. Soc., Dalton Trans.* **1991**, 1201-1202. (c) Lee, S. K.; Mackay, K. M.; Nickolson, B. K., *J. Chem. Soc., Dalton Trans.* **1993**, 715-722. (d) Foster, S. P.; Mackay, K. M.; Nickolson, B. K., *J. Chem. Soc., Chem. Commun.* **1982**, 1156-1157. (e) Gusbeth, P.; Vahrenkamp, H., *Chem. Ber.* **1985**, *118*, 1746-1757.

12. Eady, C. R.; Johnson, B. F. G.; Lewis, J. *J. Chem. Soc., Dalton Trans*, **1977**, 477-485.

13. Adams, R. D.; Captain, B.; Hall, M. B.; Trufan, E.; Yang, X. *J. Am. Chem. Soc.*, **2007**, *129*, 12328-12340.

14. SAINT+, version 6.2a, Bruker Analytical X-ray Systems, Inc., Madison, WI, **2001**.

15. Sheldrick, G. M.; SHELXTL, version 6.1, Bruker Analytical X-ray Systems, Inc., Madison, WI, **1997**.

16. (a) ADF2012, SCM, Theoretical Chemistry, Vrije Universiteit, Amsterdam, The Netherlands, http://www.scm.com. (b) Perdew, J. P.; Ruzsinszky, A.; Csonka, G.I.; Vydrov, O.A.; Scuseria, G. E. *Phys. Rev. Lett.* **2008**, *100*, 136406-136409.

17. (a) Bau, R.; Drabnis, M. H. *Inorg. Chim. Acta* **1997**, *259*, 27-50. (b) Teller, R. G.; Bau, R., *Struc. Bonding* **1981**, 41, 1-82.

18. Lauher, J. *J. Am. Chem. Soc.* **1978**, *100*, 5305-5315.

19. Thimmappa, B. H. S. *J. Cluster Sci.* **1996**, *7*, 1-36.

20. Halet, J.-F.; Hoffmann, R.; Saillard, J.-Y. *Inorg. Chem.* **1985**, *24*, 1695-1700.

CHAPTER 5

Bonding and Reactivity in the New Electronically Unsaturated Hydrogen-Bridged Dimer $[Ru_3(CO)_8(\mu_3\text{-}CMe)(\mu\text{-}H)_2(\mu_3\text{-}H)]_2$

Introduction

Electronic unsaturation in chemical compounds can be expressed in a variety of ways. It is readily recognized in the form of "empty" valence orbitals, such as the one found on the boron atom in BF_3 or in multiple bonds, as found alkenes and alkynes.[1] In metal complexes it can be found in the form of empty orbitals at a "vacant" coordination site[2] or in metal – metal multiple bonds.[3] In the presence of hydrogen, unsaturation can be disguised by the formation of delocalized bonds having hydrogen bridges as found in boranes, such as B_2H_6,[4] or in polynuclear metal complexes, such as the 46-electron triosmium complex $Os_3(CO)_{10}(\mu\text{–}H)_2$,[5] **A,** the 56–electron tetrarhenium complex $Re_3(CO)_{12}(\mu\text{–}H)_4$,[6] **B**, and higher clusters such as the five-metal 68 electron complex $Pt_2Re_3(CO)_9(PtBu_3)_3(\mu\text{–}H)_6$, **C**,[7,8] see Figure 5.1.

In this chapter, a new form of this hydrogen-bridged unsaturation is described, which is located in the linkage between two triruthenium carbonyl clusters in the hexaruthenium carbonyl complex $[Ru_3(CO)_8(\mu_3\text{–}CMe)(\mu\text{–}H)_2(\mu_3\text{–}H)]_2$, **5.1**.

Experimental Section

General Data.

Reagent grade solvents were dried by the standard procedures and were freshly distilled prior to use. Infrared spectra were recorded on a Thermo Nicolet Avatar 360 FT-IR spectrophotometer. Room temperature ^{1}H NMR and $^{31}P\{^{1}H\}$ NMR were recorded on a Bruker Avance/DRX 400 NMR spectrometer operating at 400.3 and 162.0 MHz, respectively. Different temperature 1H NMR for compound **5.1** were recorded on a Varian Mercury 400 spectrometer operating at 399.9 MHz. ^{31}P $\{^{1}H\}$ NMR spectra were externally referenced against 85% o-H3PO4. Mass spectrometric (MS) measurements were performed either by a direct-exposure probe using electron impact ionization (EI) or by electrospray techniques (ES) were made on a VG 70S instrument. $Ru_3(CO)_{12}$ was purchased from STREM. Bis(diphenylphosphino)methane(DPPM) was purchased from Aldrich and used without further purification. $Ru_3(CO)_9(\mu_3\text{-}CMe)\text{-}(\mu\text{-}H)_3$, **5.2**, was prepared according to the previously reported procedures.[9] Product separations were performed by TLC in air on Analtech 0.25 and 0.5 mm silica gel 60 Å F254 glass plates. Dynamic NMR simulations for compound **5.1** were performed by using the SpinWorks program.[10] The exchange rates were determined at six different temperatures in the temperature range -90 to +25 ℃. The activation parameters were determined from a least-squares Eyring plot by using the program Microsoft Excel 2007: $\Delta H^{\ddagger} = 8.73$ kcal.mol-1, $\Delta S^{\ddagger} = 2.54$ cal.mol-1 K-1.

Preparation of $[Ru_3(CO)_8(\mu_3\text{-}CMe)(\mu\text{-}H)_2(\mu_3\text{-}H)]_2$, 5.1.

A 23.5 mg (0.0401mmol) of **5.2** was dissolved in small amount of methylene chloride and placed on 0.5 mm silica gel 60 Å F254 glass plate for 2 hours in the air. The color of the compound on the plate changed from pale yellow to dark orange. The

compound was cut off with silica gel from the plate, then extracted by methylene chloride and remove under a flow of nitrogen. The product was recrystallized by using an 8:1 hexane/methylene chloride solvent mixture at -25^{o}C to yield 10.8mg (48.4% yield) $[Ru_3(CO)_8(\mu_3\text{-}CMe)(\mu\text{-}H)_2(\mu_3\text{-}H)]_2$, **5.1**.

Spectral data for **5.1**: IR νCO (cm^{-1} in CH_2Cl_2): 2093(w), 2077(vs), 2044(sh), 2030(s), 2011(m). ^{1}H NMR (CD_2Cl_2, 25^{o}C, TMS) δ = 4.12 (s, 6H, CH3), -16.88 (s, 2H, hydride), -18.30 (s, 4H, hydride). Mass Spec: EI/MS m/z. 1115, M+, also see Figure 5.2.

Transformations of 5.1 to 5.2.

An 8.6 mg (0.0077 mmol) amount of **5.1** was dissolved in 20 mL of methylene chloride in a 50 mL three neck flask. This solution was purged with CO for 5 min at room temperature. The solution turned from orange to pale yellow. The solvent was then removed in vacuo, and the products were separated by TLC using hexane solvent mixture to yield 8.8 mg of pale yellow **5.2** (97.6% yield).

Reaction of 5.1 with DPPM.

A 7.0 mg (0.0063 mmol) amount of **5.1** was dissolved in 20 mL of methylene chloride in a 50mL three neck flask. To this solution was added 2.4 mg (0.0063 mmol) of DPPM. The color of the solution changed from dark orange to pale yellow immediately. The solvent was then removed in vacuo, and the products were washed twice with hexane. The residue was then dissolved by methylene chloride and isolated as 2.9 mg of pale yellow $[Ru_3(CO)_7(\mu_3\text{-}CMe)\text{-}(\mu\text{-}H)_3]_2(\mu\text{-}dppm)_2$, **5.3** (25% yield).

Spectral data for **5.3**: IR νCO (cm^{-1} in CH_2Cl_2): 2090 (w), 2074 (s), 2026 (vs), 2016 (vs), 2004 (sh), 1960 (m). ^1H NMR (CD_2Cl_2, 25°C, TMS) δ = 7.04-7.45 (m, 40H, Ph), 3.85 (s, 6H, CH3), 4.27 (t, $^3J_{P-H}$ = 6Hz, 4H, CH2), -16.00 (t, $^3J_{P-H}$ = 9.6Hz, 2H, hydride), -16.72 (d, JH-H = 6Hz, 4H, hydride). $^{31}P\{^1H\}$ NMR (CD_2Cl_2, 25°C) δ = 17.57 (s, 8P, P-Ru). Mass Spec: ES+/MS, m/z = 1827.

Reaction of 5.2 with DPPM.

A 16.9 mg (0.0290mmol) amount of **5.2** was dissolved in 30 mL of methylene chloride in a 100mL three neck flask. To this solution was added 11.1 mg (0.0290mmol) of DPPM, and the mixture was stirred for 20h in room temperature. The color of the solution changed from pale yellow to orange. The solvent was then removed in vacuo, and the products were separated by TLC using a 6:1 hexane/methylene chloride solvent mixture to yield in order of elution 3.3 mg of unreacted **5.2**(19.5% yield), 2.2 mg of uncharacterized yellow compound, 8.3 mg of yellow $Ru_3(CO)_7(\mu_3\text{-}CMe)(\mu\text{-}H)_3(\mu\text{-}dppm)$, **5.4** (31.3% yield), and 2.4 mg of uncharacterized orange compound.

Spectral data for **5.4**: IR νCO (cm^{-1} in CH2Cl2): 2090 (w), 2072 (s), 2012 (vs), 1960 (m). ^1H NMR (CD_2Cl_2, 25°C, TMS) δ = 7.01-7.51 (m, 20H, Ph), 4.14 (s, 3H, CH3), 3.77 (doublet of triplets, $^3J_{P-H}$ = 11.2Hz, *J* = 12.9Hz, 1H, one H of CH_2), 3.22 (doublet of triplets, $^3J_{P-H}$ = 11.6Hz, *J* = 12.6Hz, 1H, one H of CH_2), -16.57 (virtual triplet, *J* =19.2Hz, H, hydride), -17.12 (t, $^3J_{P-H}$ = 14Hz, H, hydride). $^{31}P\{^1H\}$ NMR (CD_2Cl_2, 25°C) δ = 29.66 (s, 4P, P-Ru). Mass Spec: EI/MS *m*/*z*. 913, M+.

Crystallographic Analyses:

Red single crystals of **5.1**, yellow single crystal of **5.3** and **5.4** suitable for x-ray diffraction analyses were obtained by slow evaporation of solvent from a hexane/methylene chloride solvent mixture at room temperature, -25 ℃ and 5 ℃, respectively. Each data crystal was glued onto the end of a thin glass fiber. X-ray intensity data were measured by using a Bruker SMART APEX CCD-based diffractometer by using Mo Kα radiation (λ =0.71073 Å). The raw data frames were integrated with the SAINT+ program by using a narrow frame integration algorithm.[11] Correction for Lorentz and polarization effects were also applied using SAINT+. An empirical absorption correction based on the multiple measurement of equivalent reflections was applied using the program SADABS. All structures were solved by a combination of direct methods and difference Fourier syntheses, and were refined by full-matrix least-squares on F2 by using the SHELXTL software package.[12] All non-hydrogen atoms were refined with anisotropic displacement parameters. Hydrogen atoms were placed in geometrically idealized positions and included as standard riding atoms during the least-squares refinements.

Compounds **5.1** and **5.3** both crystallized in the triclinic crystal system. The space group $P\bar{1}$ was assumed for both of them and confirmed by the successful solution and refinement of the structures in both cases.

Compound **5.4** crystallized in the monoclinic crystal system. The space group *P*21/c was identified on the basis of systematic absences in the data and confirmed by the successful solution and refinement of the structure. There was a half of methylene chloride solvent molecule cocrystallized together with compound **5.4** in the asymmetric

unit. Crystal data, data collection parameters, and results of the analyses are listed in Table 5.1.

Computational Details.

All geometry optimizations and vibrational frequency calculations have been performed using the TPSS[13] functional as implemented in the Gaussian 09 software package[14]. The Stuttgart-Dresden (SDD)[15] effective core potential (ECP) was used on the Ru atoms, the 6-31G**[16] basis set for the H atoms and the 6-31G*[16] for the C and O atoms in all calculations. The starting geometry for **5.1** was obtained from the X-ray crystal diffraction analysis. Half a dimer molecule was used as the starting structure for the monomer and a twisted dimer was used as the starting structure for the Intermediate.

The molecular orbital analysis is based on a single point calculation performed using the ADF 2010 program package[17] with the TPSS functional at the previously optimized geometry of the dimer. All-electron Slater-type double-ζ basis sets were used for all atoms. The zeroth-order regular approximate relativistic equation (ZORA)[18] was used for the relativistic-effect correction. In the ADF fragment analysis, the two monomer fragments are frozen in the geometry that they display in the dimer rather than individually optimized as they were above.

Results and Discussion

Compound **5.1** was obtained by a silica gel–induced decarbonylation of the 48 electron complex $Ru_3(CO)_9(\mu_3–CMe)(\mu–H)_3$, **5.2**,[19] and was characterized by a low temperature single-crystal X–ray diffraction analysis. An ORTEP diagram of the

molecular structure of compound **5.1** is shown Figure 5.3. The compound can be viewed as a centrosymmetrically coupled dimer of two 46–electron triruthenium fragments "$Ru_3(CO)_8(\mu_3–CMe)(\mu–H)_3$" each formed by the loss of one CO ligand from a molecule of **5.2**. The two Ru_3 clusters are linked by a long, hydrogen-bridged metal – metal bond, Ru(3) – Ru(3') = 2.9932(5) Å. The Ru – Ru bonds within the Ru_3 triangles are shorter, Ru(1) – Ru(3) = 2.8544(4) Å, Ru(1) – Ru(2) = 2.8650(3) Å, Ru(2) – Ru(3) = 2.8840(3) Å and are similar to those found in **5.2**, 2.841(6) Å and 2.844(6) Å.[20] As in **5.2**, each Ru – Ru bond within the Ru_3 triangles contains a bridging hydrido ligand (located and refined in the structural analysis), but two of these, H(3) and H(3'), serve as triply bridging ligands by extending to the ruthenium atom, Ru(3), in the neighboring Ru_3 triangle. The Ru(2)···Ru(3') distance between the two Ru_3 clusters, 3.627(1) Å, is too long for a direct bonding interaction.

Compound **5.1** contains a total of 92 valence electrons. A six metal cluster with seven metal – metal bonds should have 94 electrons, 6*18 – 7*2, if all of the metal atoms formally have an 18 electron configuration.[21] In order to obtain a clearer picture of bonding in **5.1**, several DFT calculations have been performed: first a geometry optimization starting with the structure as found in the solid state, followed by a vibrational frequency calculation to confirm the stationary point as a minimum, then a fragment analysis was performed to help explain the bonding (details are given in the Supporting Information). To better understand the stability of the dimer, **5.1**, DFT calculations were also performed on the two $Ru_3(CO)_8(\mu_3–CMe)(\mu–H)_3$ monomer units of **5.1**, and the proposed Intermediate that contains the direct Ru(3) – Ru(3') bond, but without triply bridging H(3) or H(3') ligands. The details of the optimized structures for

these three species are shown in Figure 5.4. Our analysis shows that the combination of the two $Ru_3(CO)_8(\mu_3–CMe)(\mu–H)_3$ units to form the Intermediate with only the Ru(3) – Ru(3') bond lowers the Gibbs free energy ($\Delta G^{\ddagger}$) of the system by –2.73 kcal/mol and creates a metal – metal bond at 2.91Å. The rearrangement of this structure into the observed dimer with contributions from the triply bridging H(3) and H(3') lowers the $\Delta G^{\ddagger}$ of the system to –8.96 kcal/mol below that of the two monomers and lengthens the Ru(3) – Ru(3') bond to 3.06Å. These results indicate that the Ru(3) – Ru(3'), H(3) – Ru(3') and H(3') – Ru(3) interactions all contribute to the bonding in **5.1**.

The fragment analysis describes the nature on the bonding between two (labeled A and B) monomers that are frozen in the geometry that they display in the solid state structure, rather than at their optimized geometry as described above. These calculations show that the total (intrinsic) electronic bond energy of –33.40 kcal/mol is comprised mostly of orbital interactions (–31.58 kcal/mol) and a small contribution (–1.82 kcal/mol) from the sum of the electrostatic (attraction in this case) and Pauli repulsions. The source of this orbital stabilization is the fairly strong mixing of the LUMO of the 'monomer' fragments with several occupied fragment orbitals, specifically the HOMO–2, HOMO–8 and HOMO–11. The key features of this mixing are described below and related orbital contour drawings are shown in Figure 5.5. The most significant pair of interaction occurs when the LUMO of one of the monomer fragments accepts electron density from the HOMO-11 of the other fragment, as shown in Figure 5.5(a) for one of the pairs. This mixing leads to significant bonding in the HOMO-27 of the dimer **5.1**, as shown in Figure 5.5(b). The HOMO-8 of each fragment has a similar, but somewhat weaker, interaction with the LUMO of the other fragment, as shown in Figure 5.5(c). This second

interaction enhances the bonding in the HOMO-18 of the dimer **5.1**, shown in Figure 5.5(d). Finally, the LUMO of each fragment also mixes with the HOMO-2 of the other fragment (Figure 5.5(e)), in a way that enhances the bonding from the HOMO-5 of 1, shown in Figure 5.5(f).

The unsaturation of the monomer fragment is concentrated in the LUMO, which is the orbital that a two-electron-donor ligand such as a carbonyl or a phosphine would use to make an additional bond. In the dimer **5.1**, the unsaturation is resolved by electron donation from the HOMO-11, HOMO-8, and HOMO-2 orbitals of the other fragment. Thus, the dimer has both triply bridging H's and direct Ru(3)--Ru(3′) bonding.

Variable temperature ^{1}H NMR spectra of the hydride ligands in **5.1** show that the compound is dynamically active in solution. At low temperature (–90 ^{o}C), the spectrum exhibits three resonances at–16.51 (br, 2H), –16.96 (s, 2H) and –20.68 (br, 2H) for each of the three types of bridging hydride ligands which is in accord with the structure found in the solid state. However as the temperature is raised, the two broad resonances at –16.51 and –20.68, broaden further and merge into a single peak which is the sharp at–18.60 ppm at room temperature, see Figure 5.7. These changes can be explained by a rocking rearrangement motion in which the environments of the triply-bridging hydride ligands H(3) are exchanged a pair–wise fashion with the pair of edge–bridging hydride ligands H(2), but they are not exchanged with the other bridging hydride ligands H(1) as shown in Scheme 5.1, (CO labels are not shown in Scheme 5.1). Alternatively, the molecule could simply dissociate into two $Ru_3(CO)_8(\mu_3–CMe)(\mu–H)_3$ fragments and then recombine in such a way that H(2) and H(3) have been interchanged. Line shape analyses

have provided the following activation parameters: $\Delta H^{\ddagger}$ = 8.7(5) kcal/mol, $\Delta S^{\ddagger}$ = 2.5 cal/K. The small $\Delta S^{\ddagger}$ would suggest a nondissociative mechanism.

Electronically unsaturated compounds generally exhibit higher reactivity than saturated compounds. Such is also the case with **5.1**. When treated with CO at room temperature, compound **5.1** was rapidly converted back to **5.2**, quantitatively. When treated with 1,1–bis(diphenyphosphino)methane, dppm, compound **5.1** was converted to the new compound $[Ru_3(CO)_7(\mu_3–CMe)(\mu–H)_3]_2(\mu–dppm)_2$, **5.3** in 25 % yield at room temperature within 5 min. Compound **5.3** was characterized structurally by a single crystal X–ray diffraction analysis and an ORTEP diagram of its molecular structure is shown in Figure 5.6.

Compound **5.3** is a centrosymmetrical dimer linked by two bridging dppm ligands, each phosphorus atom of the dppm is coordinated to a different Ru_3 cluster. The hydrogen–bridged link between the two triruthenium clusters of **5.1** was completely ruptured and a ten–membered macrocycle which contains two dppm–substituted triruthenium clusters was created in its place, see Scheme 5.2. The Ru – Ru bonding within each Ru_3 triangle, Ru(1) – Ru(3) = 2.8533(14) Å, Ru(1) – Ru(2) = 2.8710(13) Å, Ru(2) – Ru(3) = 2.8445(15) Å, is similar to that in **5.2**.[11]

Notably, there was no formation of compound **5.3** in the reaction between compound **5.2** and dppm at room temperature in 2h, although after 20h, one is able to isolate instead the chelate complex $Ru_3(CO)_7(\mu_3–CMe)(\mu–H)_3(\mu–dppm)$, **5.4** in 31% yield, see Scheme 5.3 and Figure 5.7.

Other molecules with unsaturation such as **5.1** may exist as intermediates or even as isolable compounds in decarbonylation reactions involving hydride containing metal

carbonyl cluster complexes. One such species is the hexaruthenium complex $Ru_6(CO)_{14}[\mu_4–\eta^2–OCH_2CHNC(Me)OC(Ph)]_2(\mu_3–H)_2$ which is held together in part by two bridging hydride ligands and two polydentate bridging oxazoline ligands.[22] Macrocycles such as **5.3** could lead to a new family of complexes that promote bifunctional reactivity by virtue of the two cluster units reacting in concert as a result of their close proximity within the single molecular framework.

Summary

A new hydrogen-bridged unsaturated hexaruthenium carbonyl complex **5.1** has been obtained by a silica gel–induced decarbonylation of **5.2**. Compound **5.1** was converted back to **5.2** when treated with CO. When treated with 1,1–bis(diphenyphosphino)methane, dppm, compound **5.1** was converted to the new compound **5.3**. Compound **5.4** was obtained from the reaction of **5.2** with dppm.

The hydrogen-bridged unsaturation of compound **5.1** was also investigated by computational analyses. The two triply-bridged hydride lower the Gibbs Free Energy of the two monomer unit of **5.1**. The orbital stabilization of **5.1** comes from the mixing of LUMO of each monomer unit with several occupied fragment orbitals, specifically the HOMO-2, HOMO-8, and HOMO-11, of the other fragment.

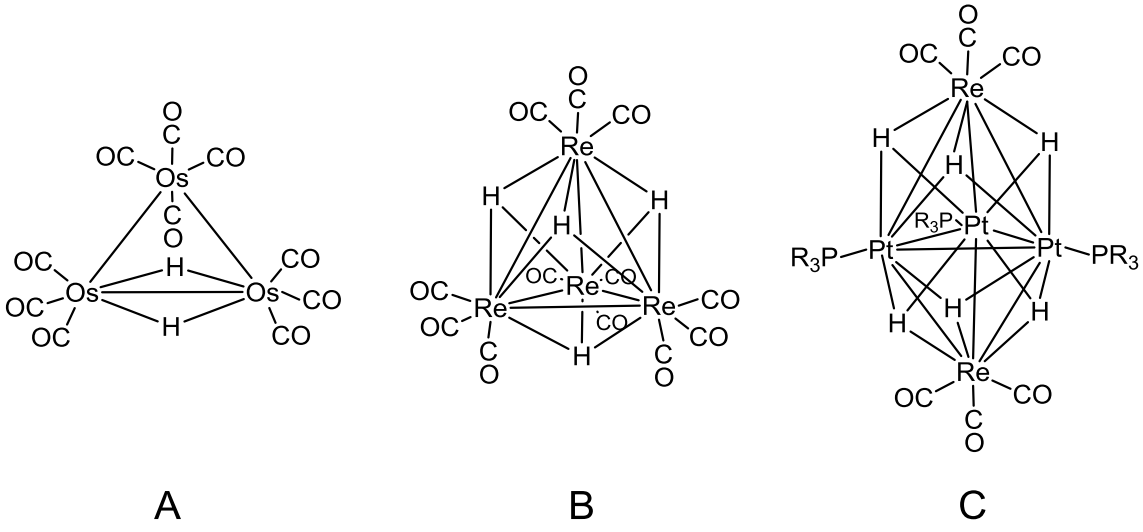

Figure 5.1.Examples of unsaturated polynuclear metal complexes containing bridging hydride ligands.

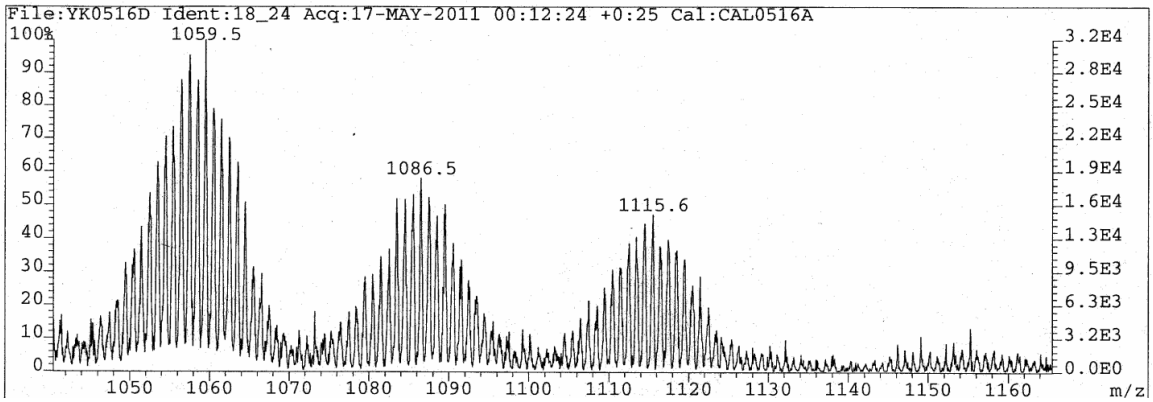

Figure 5.2. Electron impact mass spectrum of compound **5.1**. The parent ion is centered at m/z 1115.6.

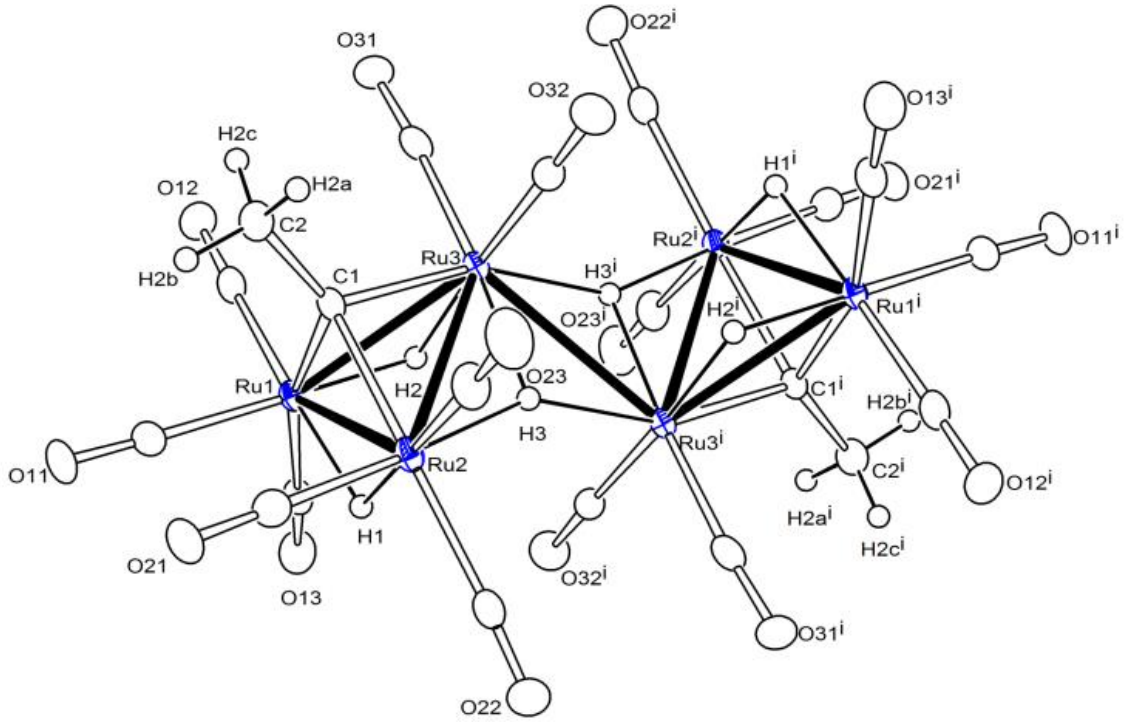

Figure 5.3. An ORTEP diagram of the molecular structure of $Ru_6(CO)_{16}(\mu_3–CMe)_2(\mu–H)_4(\mu_3–H)_2$, **5.1** showing 30% thermal ellipsoid probability.

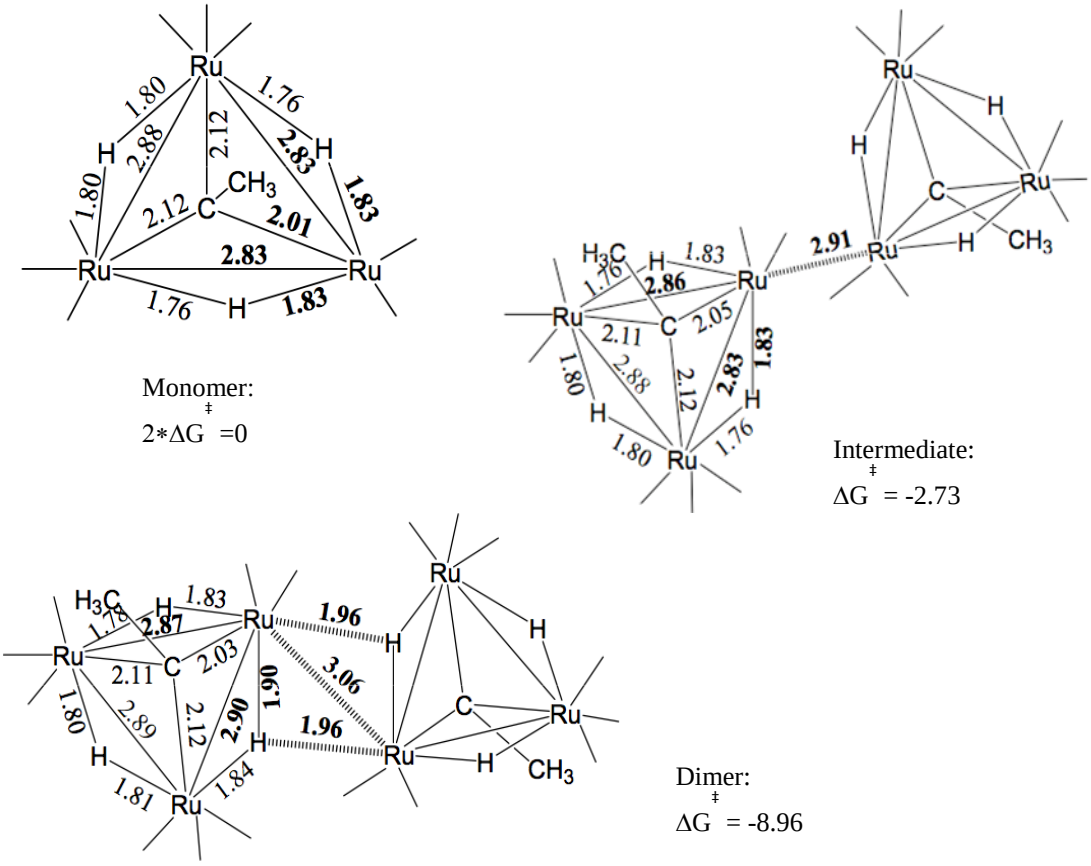

Figure 5.4. Schematic representations of the monomer, the intermediate with the Ru(3)−Ru(3′) bond, and the dimer, showing bond distances of the optimized structures and the relative Gibbs free energies of the systems.

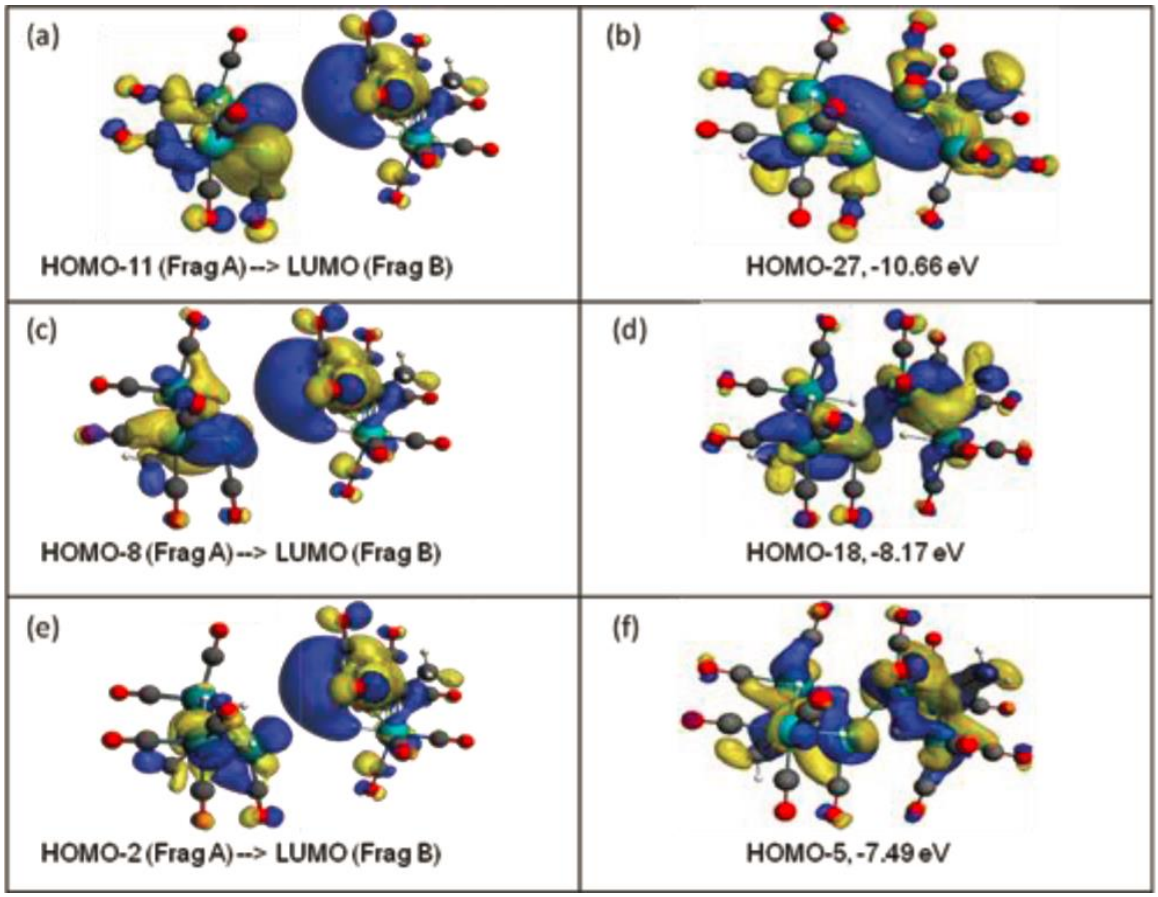

Figure 5.5. Orbital contour diagrams at the isosurface value of 0.03 for the fragment orbitals and 0.02 for the dimer orbitals showing (a) HOMO-11 of fragment A (the electron-donor orbital) in relation to the LUMO of fragment B (the electron-acceptor orbital), (b) HOMO-27, the major MO making a net contribution to the bonding between the two fragments in the dimer **5.1**, (c) HOMO-8 of fragment A (the electron-donor orbital) in relation to the LUMO of fragment B (the electron-acceptor orbital), (d) HOMO-18, a MO making a net contribution to the bonding between the two fragments in the dimer **5.1**, (e) the HOMO-2 of fragment A (the electron-donor orbital) in relation to the LUMO of fragment B (the electron-acceptor orbital), and (f) HOMO-5, the second most important MO making a net contribution to the bonding between the two fragments in the dimer **5.1**. Note that the orientation has the bridging Ru atoms upper right and lower left.

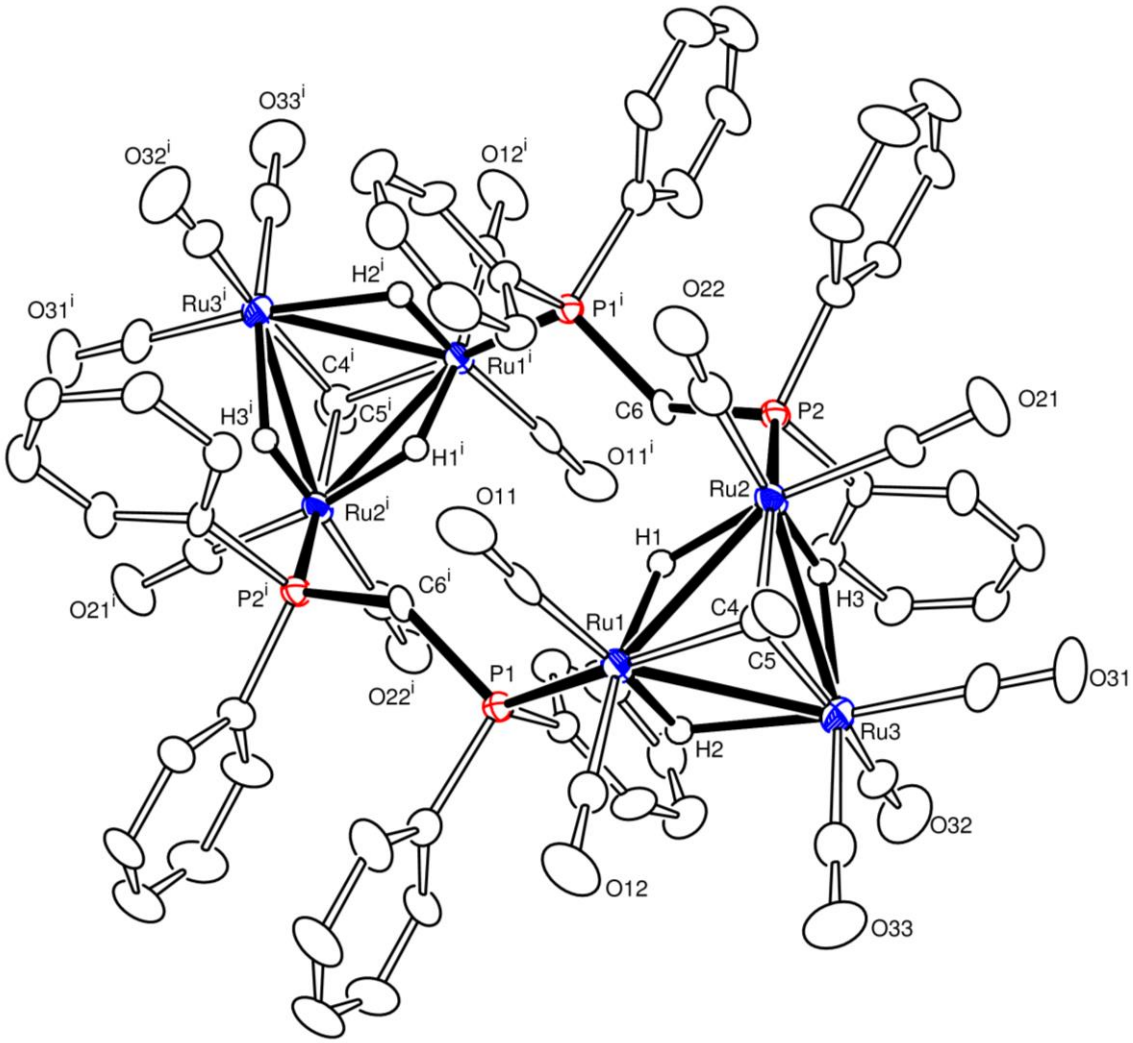

Figure 5.6. An ORTEP diagram of the molecular structure of $[Ru_3(CO)_7(\mu_3\text{–}CMe)(\mu\text{–}H)_3]_2(\mu\text{–}dppm)_2$, **5.3**, showing 30% thermal ellipsoid probability.

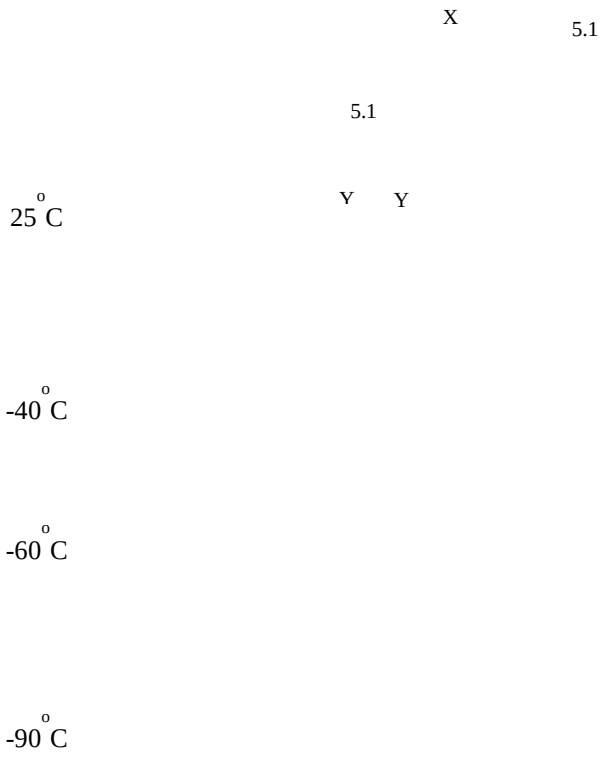

Figure 5.7. A stack of plots of the ^{1}H NMR spectra of compound **5.1** at various temperatures in the hydride region. X marks a resonance of the impurity of the starting material compound **5.2**. The Ys mark the resonances of an unknown trace impurity.

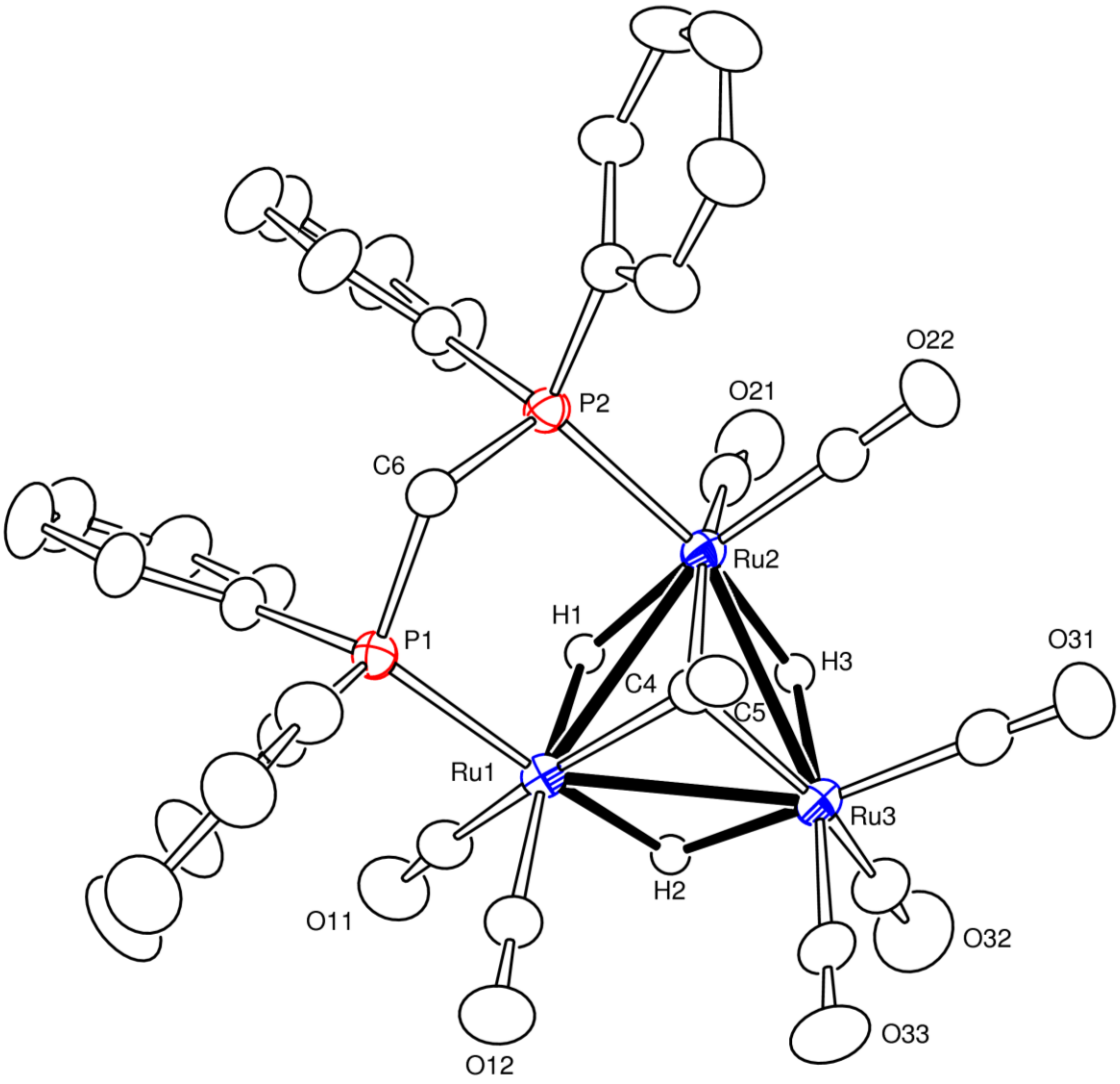

Figure 5.8. An ORTEP diagram of the molecular structure of $Ru_3(CO)_7(\mu_3\text{-}CMe)(\mu\text{-}H)_3(\mu\text{-}dppm)$, **5.4**, showing 30% thermal ellipsoid probability.

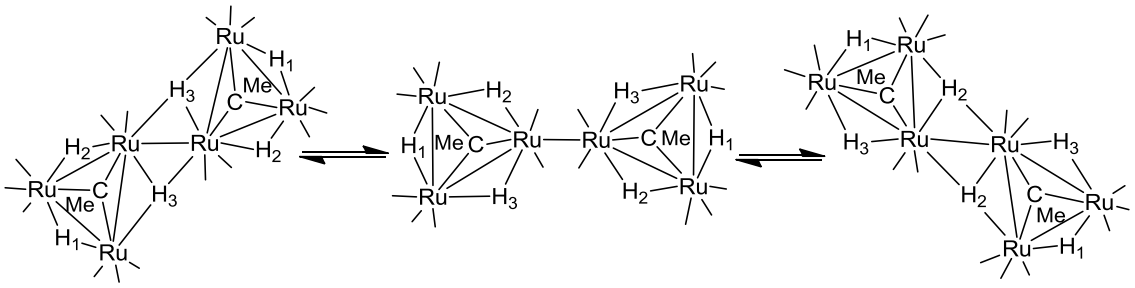

Scheme 5.1. Dynamic activity of **5.1** in solution.

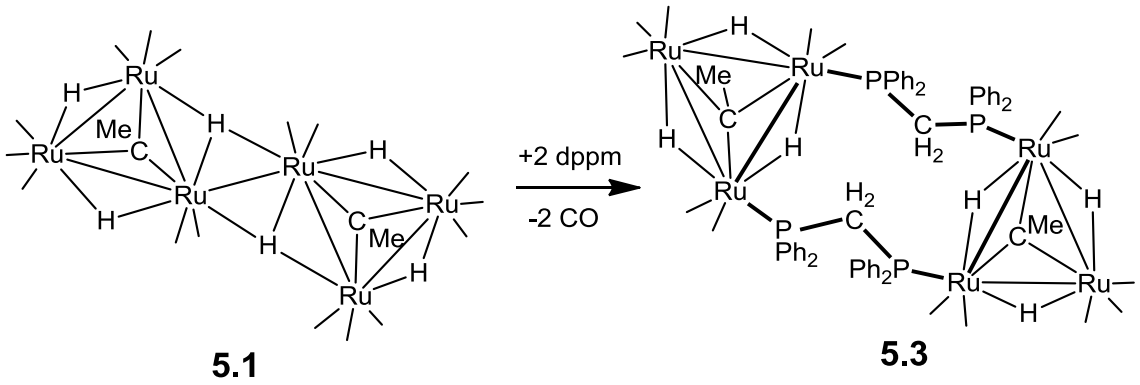

5.1 **5.3**

Scheme 5.2. Formation of **5.3** from **5.1**.

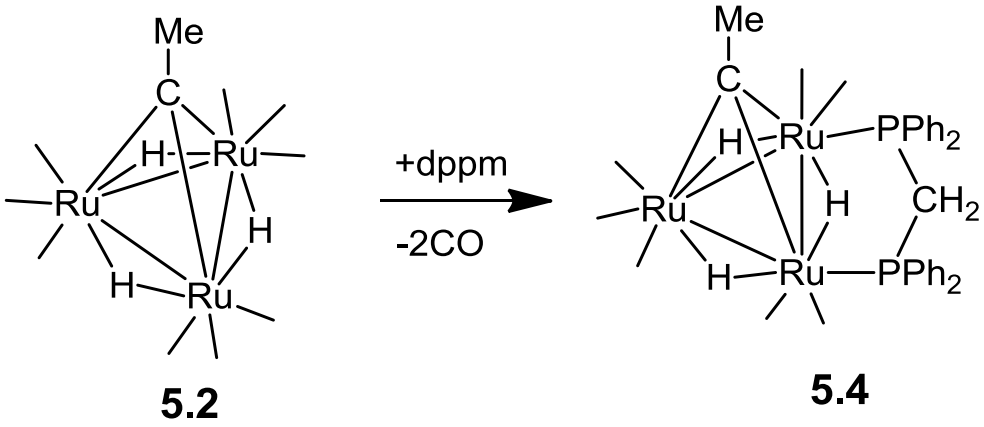

5.2 **5.4**

Scheme 5.3. Formation of **5.4** from **5.2**.

Table 5.1. Crystallographic Data for Compounds **5.1**, **5.3** and **5.4**.

Compound	**5.1**	**5.3**	**5.4**
Empirical formula	$C_{11}H_{11}O_{16}Ru_6$	$C_{34}H_{28}O_7P_2Ru_3$	$C_{34}H_{28}O_7P_2Ru_3$**.**$1/2CH_2Cl_2$
Formula weight	1114.72	913.71	956.18
Crystal system	Triclinic	Triclinic	Monoclinic
Lattice parameters			
a (Å)	8.2723(4)	11.0790(12)	12.1576(5)
b (Å)	8.5713(4)	13.5376(15)	12.4972(5)
c (Å)	11.9281(6)	13.5784(15)	24.5708(10)
α (deg)	108.2640(10)	66.593(2)	90
β (deg)	105.7170(10)	89.780(3)	102.7540(10)
γ (deg)	98.2020(10)	70.765(2)	90
V ($Å^3$)	748.78(6)	1745.5(3)	3641.1(3)
Space group	*P*-1	*P*-1	$P2_1/n$
Z value	1	2	4
ρ_{calc} (g / cm^3)	2.472	1.738	1.744
μ (Mo K_α) (mm^{-1})	3.018	1.418	1.435
Temperature (K)	100(2)	294(2)	294(2)
$2\Theta_{max}$ (°)	50.06	47.62	47.64
No. Obs. ($I > 2\sigma(I)$)	2604	5368	5584
No. Parameters	203	428	428
Goodness of fit (GOF)	1.051	1.013	1.069
Max. shift in cycle	0.001	0.002	0.002
Residuals*: R1; wR2	0.0202;0.0502	0.0753;0.2061	0.0401;0.1019
Absor.Corr, Max/min	1.000/0.801	1.000/ 0.800	1.000/0.689
Largest peak in Final Diff. Map ($e^- / Å^3$)	0.873	0.118	0.983

*$R1 = \Sigma_{hkl}(||F_{obs}| - |F_{calc}||)/\Sigma_{hkl}|F_{obs}|$; $wR2 = [\Sigma_{hkl}w(|F_{obs}| - |F_{calc}|)^2/\Sigma_{hkl}wF^2_{obs}]^{1/2}$; $w = 1/\sigma^2(F_{obs})$; $GOF = [\Sigma_{hkl}w(|F_{obs}| - |F_{calc}|)^2/(n_{data} - n_{vari})]^{1/2}$.

Table 5.2. Selected intramolecular angles and bond distances for compound **5.1**.[a]

Distances			**Angles**			
Atom	Atom	Distance(Å)	Atom	Atom	Atom	Angle(deg)
Ru1	Ru3	2.8544(4)	Ru1	Ru3	Ru2	57.90(2)
Ru1	Ru2	2.8650(3)	Ru1	Ru2	Ru2	58.29(2)
Ru2	Ru3	2.8840(3)	Ru2	Ru1	Ru3	63.51(2)
Ru3	Ru3’	2.9932(5)				
Ru2	Ru3’	3.627(1)				
Ru1	C1	2.094(3)				
Ru2	C1	2.097(3)				
Ru3	C1	2.032(3)				
Ru1	H1	1.78(4)				
Ru1	H2	1.69(4)				
Ru2	H1	1.82(4)				
Ru2	H3	1.81(3)				
Ru3	H2	1.88(4)				
Ru3	H3	1.85(4)				

[a] Estimated standard deviations in the least significant figure are given in parentheses.

Table 5.3. Selected intramolecular angles and bond distances for compound **5.3**.[a]

Distances			**Angles**			
Atom	Atom	Distance(Å)	Atom	Atom	Atom	Angle(deg)
Ru1	Ru3	2.8533(14)	P1	Ru1	Ru2	92.64(3)
Ru1	Ru2	2.8710(13)	P2	Ru2	Ru1	92.39(3)
Ru2	Ru3	2.8445(15)				
Ru1	C4	2.071(11)				
Ru2	C4	2.054(13)				
Ru3	C4	2.072(15)				
Ru1	P1	2.436(3)				
Ru2	P2	2.451(3)				
Ru1	H1	1.67(10)				
Ru1	H2	1.38(14)				
Ru2	H1	1.70(10)				
Ru2	H3	1.33(15)				
Ru3	H3	1.95(16)				
Ru3	H2	2.04(13)				

[a] Estimated standard deviations in the least significant figure are given in parentheses.

Table 5.4. Selected intramolecular angles and bond distances for compound **5.4**.[a]

Distances			**Angles**			
Atom	Atom	Distance(Å)	Atom	Atom	Atom	Angle(deg)
Ru1	Ru3	2.8392(5)	P1	Ru1	Ru2	119.91(8)
Ru1	Ru2	2.8655(5)	P2	Ru2	Ru1	119.39(7)
Ru2	Ru3	2.8533(5)	P1	C6	P2	132.1(6)
Ru1	C4	2.070(5)				
Ru2	C4	2.080(5)				
Ru3	C4	2.112(5)				
Ru1	P1	2.3056(13)				
Ru2	P2	2.3210(12)				
Ru1	H1	1.70(5)				
Ru1	H2	1.81(5)				
Ru2	H1	1.84(5)				
Ru2	H3	1.90(6)				
Ru3	H3	1.79(6)				
Ru3	H2	1.81(5)				

[a] Estimated standard deviations in the least significant figure are given in parentheses.

REFERENCE

1. Gimarc, B. M. *Accts. Chem. Res.* **1974**, *7*, 384 – 392.

2. (a) Crabtree, R. H. *The Organometallic Chemistry of the Transition Metals*, 4th Ed., Wiley-Interscience, Hoboken, **2005**, p 56. (b) Collman, J. P. *Trans. NY Acad. Sci.* **1968**, 479 – 482.

3. Schaefer III, H. F.; King, R. B. *Pure Appl. Chem.* **2001**, *73*, 1059 – 1073.

4. Trinquier, G.; Malrieu, J. P.; Garciacuesta, I. *J. Am. Chem. Soc.* **1991**, *113*, 6465 – 6473.

5. Broach, R. W.; Williams, J. M. *Inorg. Chem.* **1979**, *18*, 314 – 319.

6. Wilson, R. D.; Bau, R. *J. Am. Chem. Soc.* **1976**, *98*, 4687 – 4689.

7. Adams, R. D; Captain, B.; Beddie, C.; Hall, M. B. *J. Am. Chem. Soc.* **2007**, *129*, 986 – 1000.

8. Electronically saturated metal cluster complexes have the following valence electron counts: 48 for triangles with three metal atoms; 60 for a tetrahedron of four metal atoms; 72 for a trigonal bipyramidal cluster of five metal atoms.

9. Canty, A. J.; Johnson, F. G.; Lewis, J. and Norton, J. R., *Chem.Comm*, **1972**, 1331– 1332.

10. (a) SpinWorks 3.1.7, Copyright ., Kirk Marat, University of Manitoba, **2010**. (b) Quirt, A.R.; Martin, J.S. J. Magn. Reson. **1971**, *5*, 318 – 327.

11. SAINT+, version 6.2a, Bruker Analytical X-ray Systems, Inc., Madison, WI, **2001**.

12. G. M. Sheldrick, SHELXTL, version 6.1, Bruker Analytical X-ray Systems, Inc., Madison, WI, **1997**.

13. Tao, J.; Perdew, J. P.; Staroverov, V. N.; Scuseria, G. E. *Phys. Rev. Lett.,* **2003**, *91*, 146401 – 146404

14. Gaussian 09, Revision B.01, M. J. Frisch, G. W. Trucks, H. B. Schlegel, G. E. Scuseria, M. A. Robb, J. R. Cheeseman, G. Scalmani, V. Barone, B. Mennucci, G. A. Petersson, H. Nakatsuji, M. Caricato, X. Li, H. P. Hratchian, A. F. Izmaylov, J. Bloino, G. Zheng, J. L. Sonnenberg, M. Hada, M. Ehara, K. Toyota, R. Fukuda, J. Hasegawa, M. Ishida, T. Nakajima, Y. Honda, O. Kitao, H. Nakai, T. Vreven, J. A. Montgomery, Jr., J. E. Peralta, F. Ogliaro, M. Bearpark, J. J. Heyd, E. Brothers, K. N. Kudin, V. N. Staroverov, T. Keith, R. Kobayashi, J. Normand, K. Raghavachari, A. Rendell, J. C. Burant, S. S. Iyengar, J. Tomasi, M. Cossi, N. Rega, J. M. Millam, M.

Klene, J. E. Knox, J. B. Cross, V. Bakken, C. Adamo, J. Jaramillo, R. Gomperts, R. E. Stratmann, O. Yazyev, A. J. Austin, R. Cammi, C. Pomelli, J. W. Ochterski, R. L. Martin, K. Morokuma, V. G. Zakrzewski, G. A. Voth, P. Salvador, J. J. Dannenberg, S. Dapprich, A. D. Daniels, O. Farkas, J. B. Foresman, J. V. Ortiz, J. Cioslowski, and D. J. Fox, Gaussian, Inc., Wallingford CT, **2010**

15. (a) Bergner, A.; Dolg, M.; Kuechle, W.; Stoll, H.; Preuss, H. *Mol. Phys.*, **1993**, *80*, 1431 – 1441. (b) Kaupp, M.; Schleyer, P. v. R.; Stoll, H.; Preuss, H. *J. Chem. Phys*., **1991**, *94*, 1360 – 1366.

16. Hariharan, P.C.; Pople, J.A. *Theoret. Chimica Acta*, **1973**, *28*,213 – 222.

17. (a) te Velde, G.; Bickelhaupt, F.M.; van Gisbergen, S.J.A.; Fonseca Guerra, C.; Baerends, E.J.; Snijders, J.G.; Ziegler, T. *Journal of Compututational Chemistry*, **2001**, *22*, 931– 967 (b) Fonseca Guerra, C.; Snijders, J.G.; te Velde, G.; Baerends, E.J. *Theoretical Chemistry Accounts*, **1998**, *99*, 391– 403 (c) ADF2010, SCM, Theoretical Chemistry, Vrije Universiteit, Amsterdam, The Netherlands, http://www.scm.com E.J. Baerends, T. Ziegler, J. Autschbach, D. Bashford, A. Bérces, F.M. Bickelhaupt, C. Bo, P.M. Boerrigter, L. Cavallo, D.P. Chong, L. Deng, R.M. Dickson, D.E. Ellis, M. van Faassen, L. Fan, T.H. Fischer, C. Fonseca Guerra, A. Ghysels, A. Giammona, S.J.A. van Gisbergen, A.W. Götz, J.A. Groeneveld, O.V. Gritsenko, M. Grüning, S. Gusarov, F.E. Harris, P. van den Hoek, C.R. Jacob, H. Jacobsen, L. Jensen, J.W. Kaminski, G. van Kessel, F. Kootstra, A. Kovalenko, M.V. Krykunov, E. van Lenthe, D.A. McCormack, A. Michalak, M. Mitoraj, J. Neugebauer, V.P. Nicu, L. Noodleman, V.P. Osinga, S. Patchkovskii, P.H.T. Philipsen, D. Post, C.C. Pye, W. Ravenek, J.I. Rodríguez, P. Ros, P.R.T. Schipper, G. Schreckenbach, J.S. Seldenthuis, M. Seth, J.G. Snijders, M. Solà, M. Swart, D. Swerhone, G. te Velde, P. Vernooijs, L. Versluis, L. Visscher, O. Visser, F. Wang, T.A. Wesolowski, E.M. van Wezenbeek, G. Wiesenekker, S.K. Wolff, T.K. Woo, A.L. Yakovlev

18. (a) van Lenthe, E.; Baerends, E. J.; Snijders, J. G. *J. Chem. Phys.* **1993**, *99*, 4597–4610. (b) van Lenthe, E.; Baerends, E. J.; Snijders, J. G. *J. Chem. Phys.* **1994**, *101*, 9783 – 9792. (c) van Lenthe, E.; Ehlers, A. E.; Baerends, E. J. *J. Chem. Phys.* **1999**, *110*, 8943 – 8953.

19. Canty, A. J.; Johnson, B. F. G.; Norton, J. R.; Lewis, J. *J. C. S., Chem. Commun.* **1972**, 1331 – 1332.

20. Sheldrick, G. M.; Yesinowski, J. P. *J. C. S., Dalton Trans.* **1975**, 873 – 876.

21. Wade, K. in *Transition Metal Clusters*, Johnson, B. F. G., Ed., John Wiley & Sons, Chichester, **1980**, Ch. 3, pp 209 – 264.

22. Bhaduri, S.; Sapre, N.; Jones, P. G. *J. Organomet. Chem.* **1996**, *509*, 105 – 107.

CHAPTER 6

New Osmium-Germanium and Osmium-Germanium-Gold Carbonyl Cluster Complexes: Syntheses, Structures, Bonding and Reactivity

Introduction

Germanium[1] and tin[2] are well known to be valuable modifiers for heterogeneous transition metal catalysts. It has been shown that transition metal – tin complexes can serve as precursors to excellent bi- and multi-metallic supported heterogeneous catalysts.[3] The reactions of $Ir_3(CO)_9(\mu\text{-Bi})$ with $HGePh_3$ and $HSnPh_3$ have yielded the tris-EPh_3, E = Ge and Sn, triiridiumtrihydrido carbonyl complexes $Ir_3(CO)_6(\mu\text{-Bi})(EPh_3)_3(\mu\text{-H})_3$ which were converted to the tris-germylene bridged and tris-stannylene bridged triiridiium complexes, $Ir_3(CO)_6(\mu\text{-Bi})(\mu\text{-}EPh_2)_3$, upon mild heating, Scheme 6.1.[4]

The complexes $Ru_3(CO)_9(EPh_3)(\mu\text{-H})_3$ also eliminate three equivalents of benzene when heated to yield the tris-EPh_2 complexes $Ru_3(CO)_9(\mu\text{-}EPh_2)_3$, E = Ge and Sn, Scheme 6.2.[5,6] It has recently been shown by a computational analysis that the α-cleavage of a phenyl group from a $GePh_3$ ligand occurs at a single iridium atom in the transformation of the triiridium complex $Ir_3(CO)_6(\mu\text{-CO})(\mu\text{-}GePh_2)_2(GePh_3)_3$ to the complex $Ir_3(CO)_6(\eta^1\text{-Ph})(\mu\text{-}GePh_2)_3(GePh_3)_2$, Scheme 6.3.[7]

The reactions of $Os_3(CO)_{10}(NCMe)_2$ with $HGePh_3$ have been investigated and the new compounds $Os_3(CO)_{10}(NCMe)(GePh_3)(\mu\text{-H})$, **6.1** and $Os_3(CO)_{10}(GePh_3)_2(\mu\text{-H})_2$, **6.2** are obtained. Compound **6.1** contains a labile NCMe ligand and this complex was found to react readily with the organo-gold phosphine compounds $RAu(PPh_3)$, R = CH_3 and Ph

to yield the gold-osmium-germylene complex $Os_3(CO)_8(\mu\text{-}CO)(\mu\text{-}O{=}CPh)(\mu\text{-}GePh_2)(\mu\text{-}AuPPh_3)$, **6.4** which also contains a bridging benzoyl ligand and an $AuPPh_3$ group that bridges an Os – Ge bond. Compound **6.4** reacts with PhC_2Ph to yield the complex $Os_3(CO)_7(\mu\text{-}GePh_2)(\mu\text{-}AuPPh_3)[\mu\text{-}(O)CPhCPhCPh)]$, **6.7** which contains a novel bridging oxametallacycle formed by the coupling of PhC_2Ph to the bridging benzoyl ligand. The results of these studies are presented in this chapter.

Experimental Section

General Data.

Reagent grade solvents were dried by the standard procedures and were freshly distilled prior to use. Unless indicated otherwise, all reactions were performed under an atmosphere of nitrogen. Infrared spectra were recorded on a Thermo Nicolet Avatar 360 FT-IR spectrophotometer. ^1H NMR spectra were recorded on a Varian Mercury 300 spectrometer operating at 300.1 MHz. $^{31}P\{^1H\}$ NMR were recorded on a Bruker Avance/DRX 400 NMR spectrometer operating at 162.0 MHz. Mass spectral (MS) measurements were performed either by a direct-exposure probe by using either electron impact ionization (EI) or electrospray techniques (ES) on a VG 70S instrument. $Os_3(CO)_{12}$ and CH_3AuPPh_3 were purchased from STREM. $HGePh_3$ was purchased from Aldrich and was used without further purification. $Os_3(CO)_{10}(NCMe)_2$[8] and $PhAuPPh_3$[9] were prepared according to previously reported procedures. Product separations were performed by TLC in open air on Analtech 0.25 mm or 0.5 mm silica gel 60 Å F_{254} glass plates.

Reactions of $Os_3(CO)_{10}(NCMe)_2$ with $HGePh_3$.

a) *Synthesis of $Os_3(CO)_{10}(NCMe)(GePh_3)(\mu\text{-}H)$,* ***6.1***.

A 29.5 mg (0.0316 mmol) amount of $Os_3(CO)_{10}(NCMe)_2$ were dissolved in 30 mL of methylene chloride in a 100 mL three neck flask. To this solution was added 9.60 mg (0.0315 mmol) of $HGePh_3$ and the mixture was stirred at room temperature until the IR spectra showed that no $Os_3(CO)_{10}(NCMe)_2$ was remaining in the solution (approx. 15 min). Since the reagent $Os_3(CO)_{10}(NCMe)_2$ and the osmium products are air stable, samples can be removed from the reaction solution in order to follow the reaction by the IR spectroscopy. The solvent was then removed *in vacuo*, and the product was isolated by TLC by using a 6/1 hexane/methylene chloride elution solvent mixture to yield 31.2 mg of yellow $Os_3(CO)_{10}(NCMe)(GePh_3)(\mu\text{-}H)$, **6.1** (64% yield).

Spectral data for **6.1**. IR *v*CO (cm^{-1} in methylene chloride): 2102(m), 2065(vs), 2040(s), 2019(s), 2002(s), 1987(m), 1962 (sh). ^1H NMR (CD_2Cl_2, δ in ppm) at 25°C: δ = 7.25-7.57 (m, 15H, Ph), 2.31(s, 3H, CH_3), δ = -12.10 (s, hydride). Mass Spec. ES+/MS 1197 (M^+).

b) *Synthesis of $Os_3(CO)_{10}(GePh_3)_2(\mu\text{-}H)_2$,* ***6.2***.

A 10.2 mg (0.0109 mmol) amount of $Os_3(CO)_{10}(NCMe)_2$ was dissolved in 20 mL of methylene chloride in a 50 mL three neck flask. To this solution was added 8.3 mg (0.0272 mmol) of $HGePh_3$ and the mixture was stirred at room temperature until the IR spectra showed no $Os_3(CO)_{10}(NCMe)_2$ was remaining in the solution (approx. 2h). Since the reagent $Os_3(CO)_{10}(NCMe)_2$ and the osmium product **6.2** are air stable, samples can be removed from the reaction solution in order to follow the reaction by the IR

spectroscopy. The solvent was then removed *in vacuo*, and the product was isolated by TLC by using a 6/1 hexane/methylene chloride elution solvent mixture to yield 15.9 mg of yellow $Os_3(CO)_{10}(GePh_3)_2(\mu\text{-}H)_2$, **6.2** (71% yield).

Spectral data for **6.2**. IR *vCO* (cm^{-1} in CH_2Cl_2): 2127(w), 2099(m), 2056(m), 2044(vs), 2029(m), 1977(w). ^1H NMR (CD_2Cl_2, δ in ppm) at 25 ℃: 7.58-7.26 (m, 30H, Ph), -17.05 (s, hydride); the hydride resonances reveal the presence of two isomers assigned as **6.2** and **6.2'** at -80 ^oC, for isomer **6.2**: δ = -17.121 (d, $^2J_{H\text{-}H}$ = 1.32 Hz), -17.162 (d, $^2J_{H\text{-}H}$ = 1.32 Hz); for isomer **6.2'**: δ = -17.231 (s) and -17.704 (s), the ratio of **6.2**/**6.2'**is 2.3/1 at -80 ^oC. Mass Spec. ES+/MS 1501 (M+K).

*Synthesis of $Os_3(CO)_{10}(GePh_3)_2(\mu\text{-}H)_2$, **6.2** from **6.1**.*

A 25.3 mg (0.0211mmol) of **6.1** was added to a 100 mL three neck flask with a solution of 6.4 mg (0.0210 mmol) $HGePh_3$ in 30 mL CH_2Cl_2. The mixture was then stirred at room temperature until the IR spectrum show no **6.1** remaining in the solution (approx. 30 min). The solvent was then removed *in vacuo*, and the product was isolated by TLC by using a 6/1 hexane/methylene chloride elution solvent mixture to yield a yellow band of **6.2** (10.8 mg, 35% yield).

Synthesis of $Os_5(CO)_{17}(\mu\text{-}GePh_2)$, 6.3.

A 10.7 mg (0.0089 mmol) amount of **6.1** was dissolved in 30 mL of hexane in a 100 mL three neck flask. The solution was heated to reflux for 4 h. After cooling, the solvent was removed *in vacuo*, and the product was then isolated by TLC by using a 6/1 hexane/methylene chloride elution solvent mixture to yield a purple band of

$Os_5(CO)_{17}(\mu\text{-}GePh_2)$, **6.3** (1.06 mg, 9.3% yield) plus traces of a few uncharacterizable products.

Spectral data for **6.3**: IR *v*CO (cm^{-1} in CH_2Cl_2): 2125(w), 2095(w), 2080(m), 2063(m), 2043(vs), 2004(m), 1991 (m). ^1H NMR (CD_2Cl_2, δ in ppm) at 25 ℃: 7.24-7.46 (m, 10H, Ph). Mass Spec. EI/MS *m*/*z*. 1654, M.

Synthesis of $Os_3(CO)_8(\mu\text{-}CO)(\mu\text{-}O{=}CPh)(\mu\text{-}GePh_2)(\mu\text{-}AuPPh_3)$, 6.4.

A 19.5 mg (0.0163 mmol) amount of **6.1** was dissolved in 30 mL of hexane in a 100mL three neck flask. To this solution was added 7.9 mg (0.0166 mmol) of $CH_3Au(PPh_3)$, and the mixture was heated to reflux for 2 h. The color of the solution changed from pale yellow to dark yellow. After cooling, the solvent was removed *in vacuo*, and the product was isolated by TLC by using a 3/1 hexane/methylene chloride elution solvent mixture to yield a dark yellow band of $Os_3(CO)_8(\mu\text{-}CO)(\mu\text{-}O{=}CPh)(\mu\text{-}GePh_2)(\mu\text{-}AuPPh_3)$, **6.4** (18.4 mg, 70% yield).

Spectral data for **6.4**. IR *v*CO (cm^{-1} in CH_2Cl_2): 2098(w), 2073(s), 2033(vs), 2027(vs), 1995(vs), 1975(s), 1877(vw). ^1H NMR (CD_2Cl_2, δ in ppm) at 25°C: 7.87-7.06(m, 30H, Ph). $^{31}P\{^1H\}$ NMR (CD_2Cl_2, 25 ^oC, 85% ortho-H_3PO_4) δ = 60.30 (s, 1P). Mass Spec. ES+/MS 1614 (M^+).

Reaction of 1 with $PhAuPPh_3$.

A 19.2 mg (0.0160 mmol) amount of **6.1** was dissolved in 30 mL of hexane in a 100mL three neck flask. To this solution was added 9.8 mg (0.0183 mmol) of $PhAu(PPh_3)$, and the mixture was heated to reflux for 1.5 h. The color of the solution

changed from pale yellow to orange. After cooling, the solvent was then removed *in vacuo*, and the products were separated by TLC by using a 3/1 hexane/methylene chloride solvent mixture to yield in order of elution 0.6 mg of pale yellow $Os(CO)_4(GePh_3)(AuPPh_3)$, **6.5** (1% yield), 12.4 mg of dark yellow **6.4** (47% yield)), and 0.6 mg of orange $PhOs_4(CO)_{13}(\mu\text{-}GePh_2)(\mu\text{-}AuPPh_3)$, **6.6** (2.6% yield)..

Spectral data for **6.5**: IR *v*CO (cm^{-1} in CH_2Cl_2): 2075(m), 1990(vs). $^{31}P\{^1H\}$ NMR (CD_2Cl_2, 25 ^oC, 85% ortho-H_3PO_4) δ = 53.77 (s,1P, P-Au). Mass Spec. ES+/MS 1105 (M^+).

Spectral data for **6.6**. IR *v*CO (cm^{-1} in CH_2Cl_2): 2107(m), 2060(m), 2049(w), 2028(vs), 1982(m). $^{31}P\{^1H\}$ NMR (CD_2Cl_2, 25 ^oC, 85% ortho-H_3PO_4) δ = 59.09 (s,1P, P-Au). Mass Spec. ES+/MS 1888 (M^+).

Synthesis of $Os_3(CO)_7(\mu\text{-}GePh_2)(\mu\text{-}AuPPh_3)[\mu\text{-}(O)CPhCPhCPh)]$, 6.7.

An 18.5 mg (0.0115 mmol) amount of **6.4** was dissolved in 30 mL of heptane in a 100 mL three neck flask. To this solution was added 3.1 mg (0.0174 mmol) of PhC_2Ph and the mixture was heated to reflux for 10 h. The color was changed from orange to deep red. After cooling, the solvent was then removed *in vacuo*, and the product was isolated by TLC by using a 4/1 hexane/methylene chloride elution solvent mixture to yield a yellow band of unreacted **6.4** (7.7 mg) followed by a red band of $Os_3(CO)_7(\mu\text{-}GePh_2)(\mu\text{-}AuPPh_3)[\mu\text{-}(O)CPhCPhCPh)]$, **6.7** (3.2 mg, 28 % yield).

Spectral data for **6.7**. IR *v*CO (cm^{-1} in hexane): 2063 (w), 2031(vw), 2006(s), 1996(vs), 1985(s), 1965 (w), 1946(m), 1935(m). ^1H NMR (CD_2Cl_2, δ in ppm) at 25 ℃:

7.80-6.81 (m, 40H, Ph). $^{31}P\{^{1}H\}$ NMR (CD_2Cl_2, 25 ^{o}C, 85% ortho-H_3PO_4) δ = 61.32 (s,1P, P-Au). Mass Spec. ES+/MS 1736 (M^+).

Crystallographic Analyses:

Yellow crystals of **6.1** suitable for X-ray diffraction analyses were obtained by slow evaporation of solvent from solutions in pure benzene solvent mixtures at room temperature. Yellow crystals of **6.2**, orange crystals of **6.4**, **6.5**, **6.6** and **6.7** suitable for X-ray diffraction analyses were obtained by slow evaporation of solvent from solutions in hexane/methylene chloride solvent mixtures at room temperature. Green crystals of **6.3** suitable for X-ray diffraction analyses were obtained by slow evaporation of solvent from a hexane solution at room temperature. Each data crystal was glued onto the end of a thin glass fiber. X-ray diffraction intensity data were measured by using a Bruker SMART APEX CCD-based diffractometer by using Mo Kα radiation (λ = 0.71073 Å). The raw data frames were integrated with the SAINT+ program by using a narrow-frame integration algorithm.[10] Corrections for Lorentz and polarization effects were also applied with SAINT+. An empirical absorption correction based on multiple measurements of equivalent reflections was applied by using the program SADABS.[10] All structures were solved by a combination of direct methods and difference Fourier syntheses, and refined by full-matrix least-squares on F^2 by using the SHELXTL software package.[11]All non-hydrogen atoms were refined with anisotropic thermal parameters. All hydride ligands in the complexes were refined with isotropic thermal parameters.

Compounds **6.1**, **6.3** and **6.7** crystallized in the triclinic system. The space group $P\bar{1}$ was assumed and confirmed by the successful solution and refinement for the

structure. For compound **6.1** there was a benzene molecule form the crystallization solvent present in the asymmetric unit. The coordinates, site occupancy factor (sof), and anisotropic thermal parameters for the carbon atoms in the benzene molecule were refined freely. For compound **6.3**, the phenyl rings of C55-C60 and C61-C66 were refined as a regular hexagon with C - C bonds constrained to 1.39 Å. In the crystal of **6.7**, one molecule of methylene chloride from the crystallization solvent was cocrystallized with the complex in the asymmetric unit. This molecule was added to the analysis and was suitably refined by using anisotropic parameters. Compound **6.2** crystallized in the orthorhombic crystal system. The space group *Pbca* was uniquely identified on the basis of the systematic absences observed in the data and by the subsequent successful solution and refinement for the structure.

Compounds **6.4**, **6.5**, **6.6** crystallized in the monoclinic crystal system. The systematic absences in the intensity data indicated the space group *C*2/c or *C*c for **6.4**. The space group *C*2/c was tested and confirmed by the successful solution and refinement for the structure. There was one half molecule of hexane from the crystallization solvent was co-crystallized with the complex in the asymmetric unit; the coordinates, site occupancy factor, and anisotropic thermal parameters for the atoms in the hexane were fixed in the final cycles of refinement. For **5** and **6** the space group $P2_1/n$ was identified uniquely on the basis of the systematic absences observed in the data. For compound **6.5,** the phenyl ring of C27-C32 was refined as a regular hexagon with C - C bonds constrained to 1.39 Å and the carbon atoms were refined with the same anisotropic displacement parameters. Crystal data, data collection parameters, and results of these analyses are listed in Table 6.1.

Computational Details.

All density functional theory (DFT) calculations were performed with the Amsterdam Density Functional (ADF) suite of programs[12a] by using the Hybrid: B3LYP[12b] and meta-GGA: M06-L[12c] functionals for compounds **6.4** and **6.7**, respectively, with valence quadruple-ζ + 4 polarization function, relativistically optimized (QZ4P) basis sets for gold, osmium, and germanium atoms, and double-ζ (DZ) basis sets for phosphorus, carbon, oxygen, and hydrogen atoms with no frozen cores. The molecular orbitals and their energies were determined by single point calculations based on the molecular structures of the compounds as established by the crystal structure analyses.

Results and Discussion

Reactions of $Os_3(CO)_{10}(NCMe)_2$ with $HGePh_3$ have yielded the compounds $Os_3(CO)_{10}(NCMe)(GePh_3)(\mu\text{-}H)$, **6.1** and $Os_3(CO)_{10}(GePh_3)_2(\mu\text{-}H)_2$, **6.2** by the sequential replacement of the NCMe ligands and the oxidative addition of the GeH bonds of one and two $HGePh_3$ molecules to the osmium atoms of the cluster. The yield of **6.2** was increased by using an excess of $HGePh_3$. Compound **6.1** was converted to **6.2** by reaction with an additional quantity of $HGePh_3$. Both products were characterized by IR, ^1H NMR, mass spectra and single-crystal X-ray diffraction analyses. An ORTEP diagram of the molecular structure of **6.1** is shown in Figure 6.1. The structure of compound **6.1** consists of a closed triangular cluster of three osmium atoms. There is one $GePh_3$ ligand coordinated to Os(1). The Os – Ge distance, Os(1) – Ge(1) = 2.5301(6) Å, is slightly longer than the Os – Ge distance, 2.4933(9) Å, to the $GePh_3$ ligand in the complex,

$PtOs_3(CO)_7(PBu^t_3)(\mu\text{-}PBu^t_2)(\mu_4\text{-}CHCMeCH)(GePh_3)(\mu\text{-}H)$.[13] The $GePh_3$ ligand lies in an equatorial position, in the plane of the Os_3 triangle. There is one hydride ligand that bridges the Os(1) – Os(2) bond and one NCMe ligand that occupies an axial coordination site on Os(2), Os(2) – N(1) = 2.107(5) Å. As expected, the hydride-bridged Os – Os bond, Os(1) – Os(2) = 3.0163(3) Å, is significantly longer, than the other two Os – Os bonds, Os(1) – Os(3) = 2.8972(3) Å and Os(2) – Os(3) = 2.8883(4) Å.[14] The Os – Os bond distance found in $Os_3(CO)_{12}$ is 2.877(3) Å.[15] The position of the hydride ligand was located and refined in the analysis, Os(1) – H(1) = 1.74(6) Å, Os(2) – H(1) = 1.76(6) Å. The hydride ligand exhibits a high field shift in the ^{1}H NMR spectrum, δ = -12.10.

An ORTEP diagram of the molecular structure of **6.2** is shown in Figure 6.2. Like **6.1**, the structure of compound **6.2** consists of a closed triangular cluster of three osmium atoms, but it has two $GePh_3$ ligands on adjacent osmium atoms and two hydrido ligands that bridge neighboring Os – Os bonds. Both $GePh_3$ ligands occupy equatorial positions, in the plane of the Os_3 triangle, coordinated to Os(1) and Os(2), Os(1) – Ge(1) = 2.5634(8) Å and Os(2) – Ge(2) = 2.5292(8) Å. The two hydride-bridged Os – Os bonds, Os(1) – Os(2) = 3.0636(4) Å and Os(1) – Os(3) = 3.0884(4) Å are significantly longer than the Os – Os bond that does not have a bridging hydride ligand, Os(2) – Os(3) = 2.9165(5) Å.14 Pomeroy reported a similar bis-$(SnMe_3)Os_3$ complex, $Os_3(CO)_{10}(SnMe_3)_2(\mu\text{-}H)_2$, that was obtained from the reaction of $Os_3(CO)_{10}(\mu\text{-}H)_2$ with $HSnMe_3$.[16]

The ^{1}H NMR spectrum of **6.2** exhibits a single high-field resonance for the two inequivalent hydride ligands at room temperature at δ = -17.05 which is inconsistent with the solid state structure. Suspecting dynamical activity, a variable temperature NMR

study was performed. ^{1}H NMR spectra of **6.2** at various temperatures in the high-field region are shown in Figure 6.3. These spectra reveal that not only are the two hydride resonances of the isomer found in the solid state are averaged, but there is also second isomer present in solution at low temperatures which also exhibits two separate hydride resonances. The two isomers observed at -80 ^{o}C shall be called **6.2** (the major isomer) and **6.2'**, respectively. For isomer **6.2**: δ = -17.121 (d), -17.162 (d); for isomer **6.2'**: δ = -17.231 (s) and -17.704 (s). the ratio of **6.2**/**6.2'**is 2.3/1 at -80 ^{o}C. The first two resonances are mutually coupled doublets, $^{2}J_{H-H}$ = 1.32 Hz; the latter two (**6.2'**) are broad singlets. In addition, it was found that the two isomers are interconverting rapidly on the NMR time scale at intermediate temperatures. This was confirmed by a 2D NOESY spectrum recorded at -80 ^{o}C which showed not only magnetization transfer between the resonances of the two different isomers but also between the two resonances of the major isomer (at -40 ^{o}C), see Figure 6.4 and 6.5. These spectral changes can be explained by either of two mechanisms which differ depending on the identity and structure of the unknown minor isomer. Mechanism (1): Hydride positional isomers. Without repositioning any of the nonhydride ligands, three isomers of **6.2** can be created by repositioning the hydride ligands about the three Os – Os bonds. These structures are represented by **6.2**, **6.2'**, and **6.2"** as shown in Scheme 6.4. It is presumed that structure **6.2** which is the one found in the solid state is the major isomer in solution. The spectra show the presence of only one other isomer in solution at low temperatures. The structure of **6.2'** is tentatively assigned as shown in Scheme 6.4. This isomer is probably more stable than **6.2"** because **6.2'** retains one hydride on the Os – Os bond between the two electron-rich $GePh_3$ ligands. The isomerization between **6.2** and **6.2'** could occur simply shifting the hydride ligand

H2 back and forth between the two Os – Os bonds involving the $Os(CO)_4$ group, process **A**. Low energy migration of hydride ligands between the metal - metal bonds in other trinuclear metal cluster complexes has been observed previously.[17] The barrier to the exchange of the hydrides H1 and H2 within isomer **6.2** itself is a higher energy process because it is still not rapid on the NMR timescale at -20 ^{o}C. Without putting two hydride ligands onto the same Os – Os bond, a minimum of three hydride shifts must occur in order to complete the exchange of H1 and H2 in **6.2**. To do this it is proposed to invoke the third isomer, presumably **6.2"**, which was not observed directly in the solutions. Isomer **6.2"** can be accessed from isomer **6.2** by process **B** shown in the Scheme or by process **C** from isomer **6.2'**. The H1-H2 exchange is completed by shifting atom H2 to the bond between the two $GePh_3$ substituted Os atoms. This can be achieved in one step from **6.2'** shown on the right of Scheme 6.4 and in two steps from **6.2"** shown on the left of Scheme 6.4.

Mechanism (2): $GePh_3$ ligand positional isomers. Isomers of **6.2** could also be formed by repositioning the $GePh_3$ ligands and could be interconverted dynamically via polytopal rearrangements. We have recently observed examples of this in the compounds $Ir_3(CO)_6(\mu\text{-}Bi)(EPh_3)_3(\mu\text{-}H)_3$, E = Ge and Sn, but the temperatures required for those rearrangements are higher than those observed for the isomerization and hydride ligand exchange processes observed in **6.2**.[6] Two plausible $GePh_3$ ligand positional isomers of **6.2** are shown Scheme 6.5. One is the observed solid structure of **6.2**; the other **6.2*** could be formed by repositioning the $GePh_3$ ligand on one of the Os atoms. There are other possible isomers, but isomers that have the bulky $GePh_3$ ligand in equatorial positions should be energetically more favorable for steric reasons. The two isomers **6.2** and **6.2***

can be interconverted by polytopal ligand rearrangements involving the $GePh_3$ ligands. Similar processes have been described for the bis-phosphine complex $Os_3(CO)_{10}(PMe_2Ph)_2$.[18] However, the process shown in Scheme 6.5 does not allow for the observed exchange of the hydride ligands within a given isomer. To explain that observation, either an additional hydride shift processes, e.g. Scheme 6.4, or perhaps a Ge-H "reductive-elimination" coupled with a polytopal rearrangement without dissociation of the $HGePh_3$ ligand would have to be invoked.[17f] These processes cannot be distinguished with the available data.

When a solution of **6.1** in hexane solvent was heated to reflux for 4 h, the higher nuclearity compound $Os_5(CO)_{17}(\mu\text{-}GePh_2)$, **6.3** was obtained in a low yield, 9.3%. Compound **6.3** was characterized by a single crystal X-ray diffraction analysis and an ORTEP diagram of its molecular structure is shown in Figure 6.5. Compound **6.3** contains five osmium atoms arranged in a planar raft-like structure with one $GePh_2$ ligand that bridges the Os(1) – Os(2) bond, Os(1) – Os(2) = 2.8691(7) Å. The six other Os – Os bonds are similar in length, Os(1) – Os(3) = 2.8713(8) Å, Os(1) – Os(4) = 2.8536(7) Å, Os(2) – Os(4) = 2.8376(8) Å, Os(2) – Os(5) = 2.8531(8) Å, Os(3) – Os(4) = 2.8631(7) Å and Os(4) – Os(5) = 2.8804(7) Å. The metal cluster in **6.3** is structurally similar to that found in the two related Os_5 raft cluster complexes $Os_5(CO)_{17}(\mu\text{-}CO)$[19] and $Os_5(CO)_{16}(PMe_3)(\mu\text{-}CO)$[20] both of which have a bridging CO ligand at the site corresponding to the $GePh_2$ ligand in **6.3**. The Os – Ge bond distances, Os(1) – Ge(1) = 2.5115(16) Å and Os(2) – Ge(1) = 2.5286(16) Å, are similar to those found to the edge-bridging $GePh_2$ ligands in the complexes, $Os_4(CO)_9(\mu_4\text{-}GePh)_2(\mu\text{-}GePh_2)_3$ and $Os_4(CO)_8(\mu_4\text{-}GePh)_2(\mu\text{-}GePh_2)_4$.[21] Overall, compound **6.2** contains a total of 76 valence

electrons on the metal atoms which is in accord with the 18 electron rule for a cluster of five metal atoms having seven metal – metal bonds.

It has been recently shown by Adams *et. al.* that organogoldphosphines of the type $PhAu(PPh_3)$, R = Ph and naphthyl, react with $Os_3(CO)_{10}(NCMe)_2$ by displacement of the NCMe ligand and oxidative addition of the Au-C bond of the gold complexes to yield the (organo)(goldphosphine)triosmium carbonyl complexes, $Os_3(CO)_{10}(\mu\text{-}AuPPh_3)[\mu\text{-}R]$.[22] Compound **6.1** was found to react with the compounds $RAu(PPh_3)$, R = CH_3 and Ph, by loss of its NCMe ligand and oxidative addition of the Au-C bond of the gold complexes to yield the compound $Os_3(CO)_8(\mu\text{-}CO)(\mu\text{-}O{=}CPh)(\mu\text{-}GePh_2)(\mu\text{-}AuPPh_3)$, **6.4** (70% yield). One minor product, $Os(CO)_4(GePh_3)(AuPPh_3)$, **6.5** (1% yield) was obtained when $PhAu(PPh_3)$ was used as the gold reagent. The molecular structures of both products were established by single crystal X-ray diffraction analyses.

An ORTEP diagram of the molecular structure of **6.4** is shown in Figure 6.7. Compound **6.4** contains a triangular cluster three osmium atoms, one $Au(PPh_3)$ group, one bridging $GePh_2$ ligand and one bridging benzoyl ligand, O=CPh. There are two long Os – Os bonds, Os(1) – Os(2) = 2.8671(5) Å, Os(1) – Os(3) = 2.8822(5) Å, and one that is significantly shorter, Os(2) – Os(3) = 2.7643(5) Å, the latter contains the bridging benzoyl ligand, Os(2) – O(1) = 2.162(5) Å and Os(3) – C(1) = 2.066(8) Å, and also a bridging CO ligand which could explain the shortness of that Os – Os bond. The $GePh_2$ ligand bridges the Os(1) – Os(2) bond and the Os – Ge bond distances are significantly different, Os(1) – Ge(1) = 2.5021(9) Å, Os(2) – Ge(1) = 2.6107(9) Å, the latter is similar to the Os – Ge bond distances in **6.3**. The $Au(PPh_3)$ group is primarily bonded to Os(1), Os(1) – Au(1) = 2.6757(5) Å, but the Au atom does have a significant

bridging/semibridging interaction to the germanium atom, Au(1) – Ge(1) = 2.7618(10) Å. There are only a few examples of Au – Ge bonds among the known complexes containing $Au(PPh_3)$ groups. These are $Au(GeCl_3)$(P-*o*-$tolyl_3$), Au – Ge = 2.376(1) Å[23] and $Au(GeCl_3)(PPh_3)_3$, Au – Ge = 2.563(1) Å and [2.536(l)] Å,[24] and for both of these compounds, the Ge group has three strongly electron withdrawing Cl atoms. We are unaware of any previous examples of complexes having $Au(PPh_3)$ groups bridging transition metal – Ge bonds, but some years ago Ruiz did report the compound $[Mn_2(CO)_6(dppm)(\mu\text{-}SnCl_2)\{AuP(p\text{-}tol)_3\}_2]$ which was shown to have $AuP(p\text{-}tol)_3$ groups bridging each of the Mn – Sn bonds to the bridging $SnCl_2$ ligand.[25] There are a few examples of hydrogen atoms bridging M – Ge bonds in polynuclear metal complexes.[26]

The phenyl group on the benzoyl ligand must have originated from the phenyl group that was cleaved from the $GePh_3$ ligand in the course of the formation of the $GePh_2$ ligand and not from the $PhAu(PPh_3)$ reagent because the same ligand (benzoyl not acetyl) was formed when the $CH_3Au(PPh_3)$ was used as the reagent. Compound **6.4** contains nine carbonyl ligands and a total of 48 valence electrons (the $Au(PPh_3)$ group is a one electron donor), so each osmium atom achieves the conventional 18 electron configuration. To investigate the character of the Au – Ge interaction further, geometry-optimized DFT molecular orbital calculations were performed on the structures of compound **6.4** by using the B3LYP functional of the Amsterdam Density Functional program library. A significant Au – Ge interaction was confirmed by a significant orbital component found between the Au and Ge atoms in the highest occupied molecular orbital

(HOMO) of **6.4** as shown in Figure 6.9. There is also a significant orbital component between the Au atom and the associated Os atom, Os(1).

An ORTEP diagram of the molecular structure of **6.5** is shown in Figure 6.9. Compound **6.5** contains only one osmium atom, in an $Os(CO)_4$ group, and a $Au(PPh_3)$ group and one $GePh_3$ ligand. Compound **6.5** is clearly the result of a cluster fragmentation process. The Os atom has an octahedral geometry and the $Au(PPh_3)$ and $GePh_3$ groups occupy cis coordination sites, Au(1) – Os(1) – Ge(1) = 89.47(2)^o. However, unlike **6.4**, there does not appear to be any significant bonding interaction between the Au and Ge atoms, Ge(1)$\cdots$Au(1) = 3.6833(8) Å. The Os – Au bonding distance, Os(1) – Au(1) = 2.6574(5) Å, is slightly shorter than that in **6.4**. The Os – Ge distance, Os(1) – Ge(1) = 2.5750(8) Å, is very slightly longer than those in **6.1** and **6.2**. The osmium atom in **6.5** has an 18-electron configuration. An ORTEP diagram of the molecular structure of **6.6** is shown in Figure 6.10. Compound **6.6** contains a butterfly structure of four osmium atoms, one $Au(PPh_3)$ group, one bridging $GePh_2$ ligand and a σ-bonded phenyl group. The σ-bonded phenyl group is a result of the phenyl cleavage from the $GePh_3$ group. Compound **6.6** is probably formed by the combination of **6.5** with **6.4**.

To investigate the reactivity of compound **6.4** further, it was treated with PhC_2Ph in a heptane solution at reflux for 10 h. From this solution, the compound $Os_3(CO)_7($ -$GePh_2)(\mu$-$AuPPh_3)[\mu$-(O)CPhCPhCPh)], **6.7** was obtained in 28% yield. An ORTEP diagram of the molecular structure of **6.7** is shown in Figure 6.11. Compound **6.7** contains a triangular cluster of three osmium atoms, one $Au(PPh_3)$ group, one bridging $GePh_2$ ligand and one bridging η^4-OCPhCPhCPh ligand. The last group was formed by the addition and coupling of one molecule of PhC_2Ph to the carbon atom of the bridging

benzoyl ligand in **6.4**. As in **6.4**, the $Au(PPh_3)$ group bridges one of the Os – Ge bonds to the $GePh_2$ ligand, Au(1) – Ge(1) = 2.7846(12) Å and Os(1) – Au(1) = 2.6803(6) Å. The Os – Ge bond distances, Os(1) – Ge(1) = 2.5143(12) Å and Os(2) – Ge(1) = 2.5992(11) Å, are similar to those in **6.4**. The η^4-OCPhCPhCPh ligand formed a metallacycle by coordination of its two terminal atoms O(1) and C(64) to the metal atom Os(2), Os(2) – O(1) = 2.108(7) Å and Os(2) – C(64) = 2.046(10) Å. All four atoms of the OC_3 chain are π-bonded to Os(3), Os(3) – C(1) = 2.260(10) Å, Os(3) – O(1) = 2.217(6) Å, Os(3) – C(64) = 2.277(9) Å and Os(3) – C(65) = 2.292(9) Å. The formation of bridging metallacycles by the coupling of alkynes is well established,[27] but the formation of heteroatom metallacycles such as that found in **6.7** is very rare, in fact, we have not been able to find any other examples of the coupling of an alkyne to a bridging acyl ligands to form an oxametallacycle. However, there have been some examples of the insertion-coupling of alkynes to terminally-coordinated acyl ligands[28] and η^2–acyl ligands.[29] The nature of the Au – Ge bonding in **6.7** was also investigated by DFT MO calculations. The HOMO and HOMO-2 of **6.7** are shown in Figure 6.12. As seen in **6.4**, there is a significant orbital interaction between the Au and Ge and the Au and Os(1) atoms in both of these orbitals.

Summary

A summary of the results of thess studies is shown in Scheme 6.6. Compounds **6.1** and **6.2** were obtained by the sequential replacement of the two NCMe ligands from $Os_3(CO)_{10}(NCMe)_2$ and the oxidative addition of one and two equivalents of $HGePh_3$ to the cluster. Compound **6.2** can be obtained from **6.1** by reaction with an additional quantity of $HGePh_3$. Compound **6.1** which still contains one labile NCMe ligand was transformed thermally into the Os_5 raft complex **6.3** which contains a bridging $GePh_2$

ligand. Details of the process that led to the growth of the osmium cluster are not available at this time. Compound **6.1** was found to react with the organogold compounds $RAu(PPh_3)$, R = CH_3 and Ph, by loss of its NCMe ligand and oxidative addition of the Au-C bond of the gold complexes to yield the compound **6.4**, **6.6** and one minor product **6.5**. The structural analyses of compounds **6.4** show that the $GePh_3$ ligand was transformed into a bridging $GePh_2$ ligand by cleavage of a phenyl group and an $Au(PPh_3)$ group bridges one of the Os – Ge bonds. The phenyl ligand that was cleaved from the $GePh_3$ group was transferred to a CO ligand to form a bridging benzoyl ligand. Compound **6.4** was found to react with PhC_2Ph to yield the compound **6.7** by coupling of the PhC_2Ph to the benzoyl ligand to form a bridging η^4–oxametallacycle.

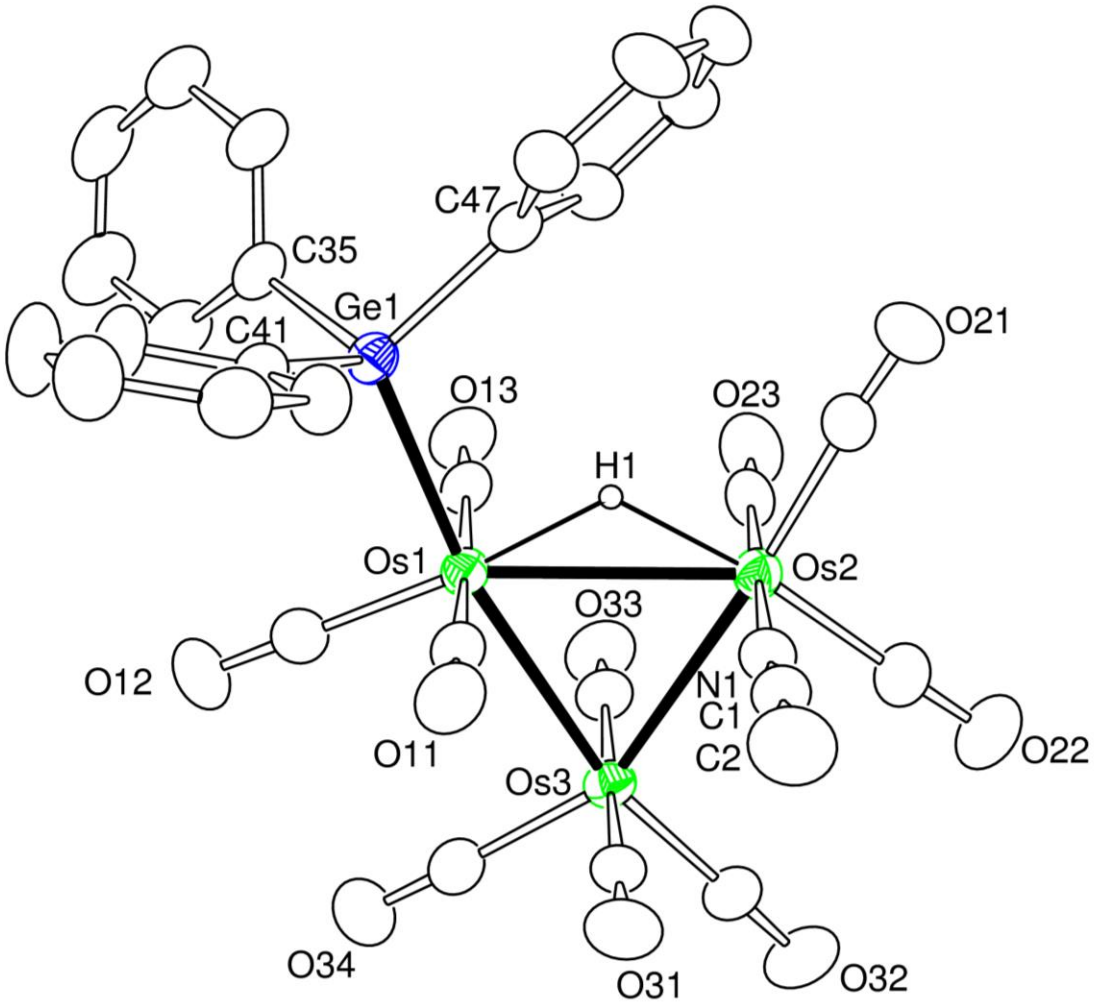

Figure 6.1. An ORTEP diagram of the molecular structure of $Os_3(CO)_{10}(NCMe)(GePh_3)(\mu\text{-}H)$, **6.1** showing 30% thermal ellipsoid probability.

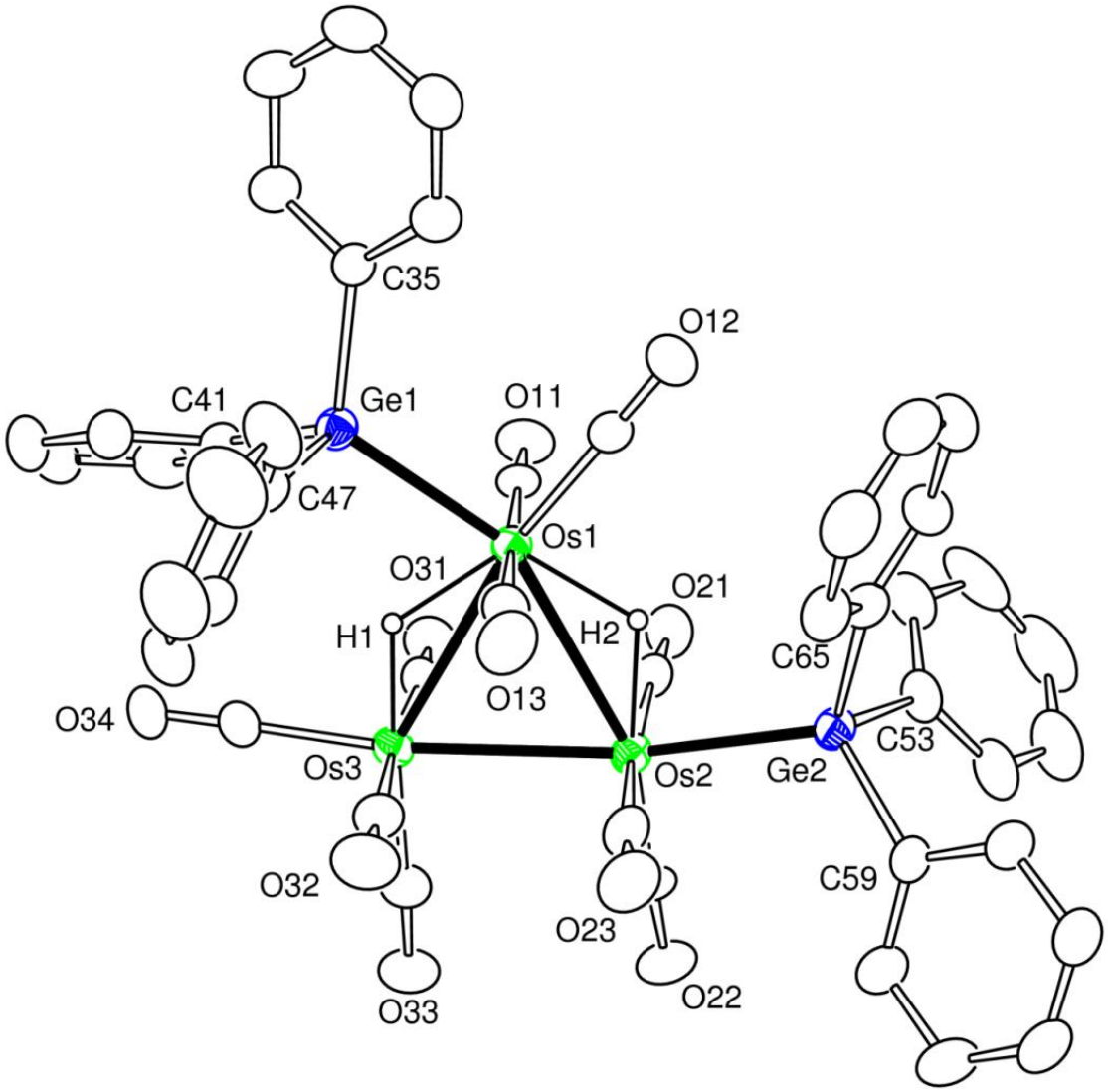

Figure 6.2. An ORTEP diagram of the molecular structure of $Os_3(CO)_{10}(GePh_3)_2(\mu\text{-}H)_2$, **6.2** showing 30% thermal ellipsoid probability.

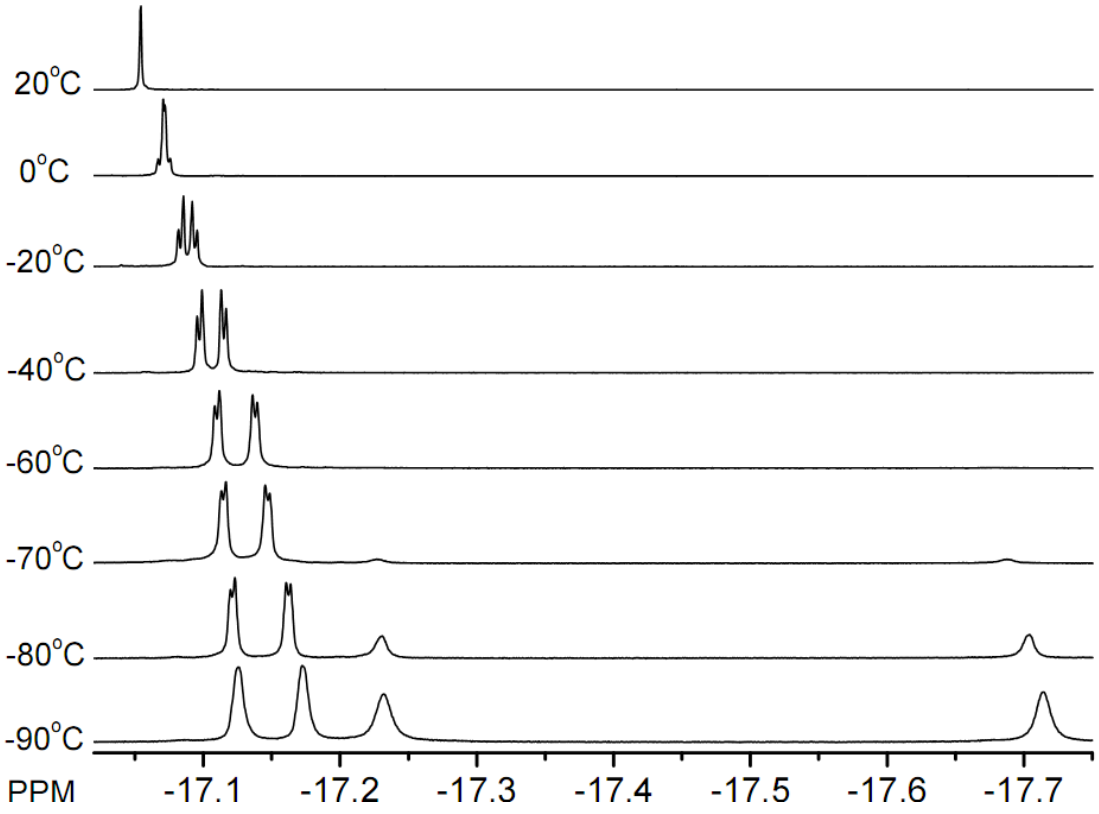

Figure 6.3. Variable temperature ^{1}H NMR spectra for compound **6.2** in CD_2Cl_2 solvent recorded in the high field region of the spectrum.

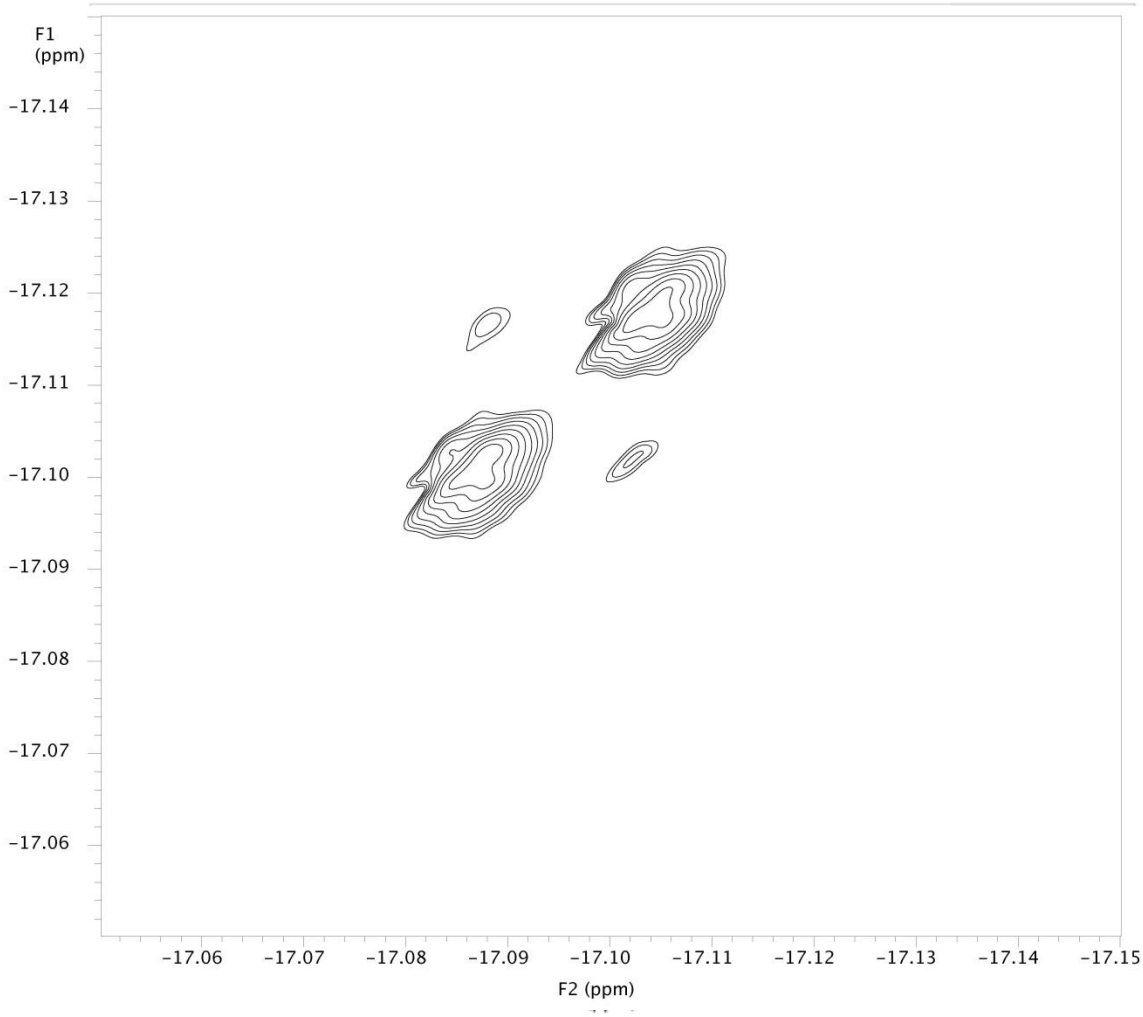

Figure 6.4. A 2D NOESY spectrum of compound **6.2** at -40 ^{o}C.

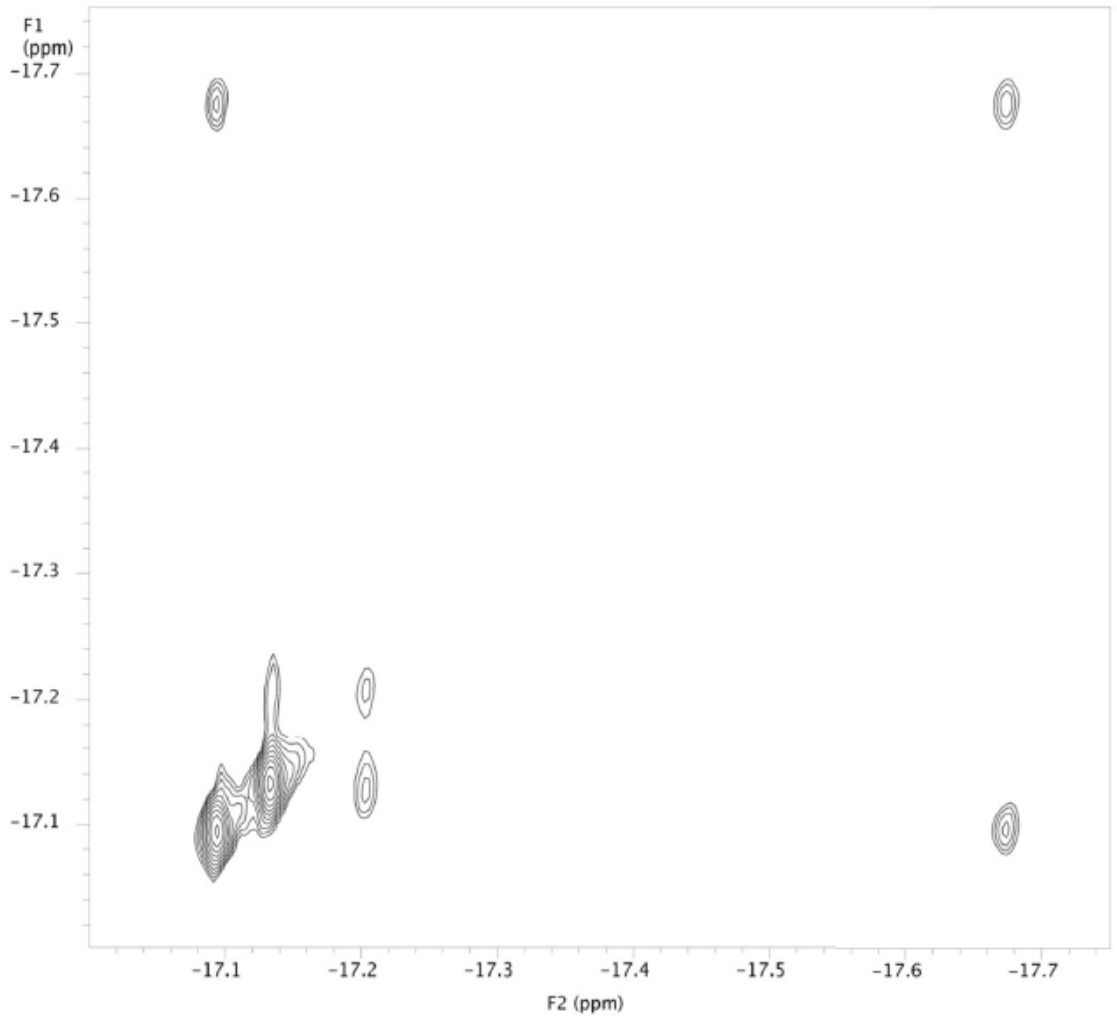

Figure 6.5. A 2D NOESY spectrum of compound **6.2** at -80 ^{o}C.

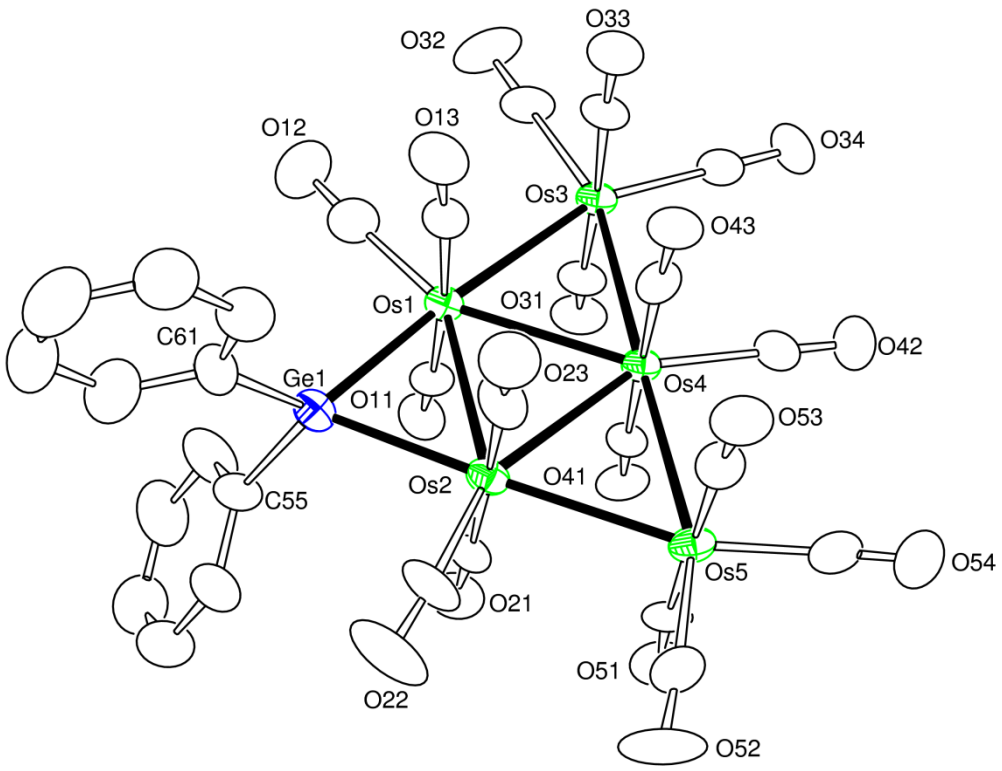

Figure 6.6. An ORTEP diagram of the molecular structure of $Os_5(CO)_{17}(\mu\text{-}GePh_2)$, **6.3** showing 30% thermal ellipsoid probability.

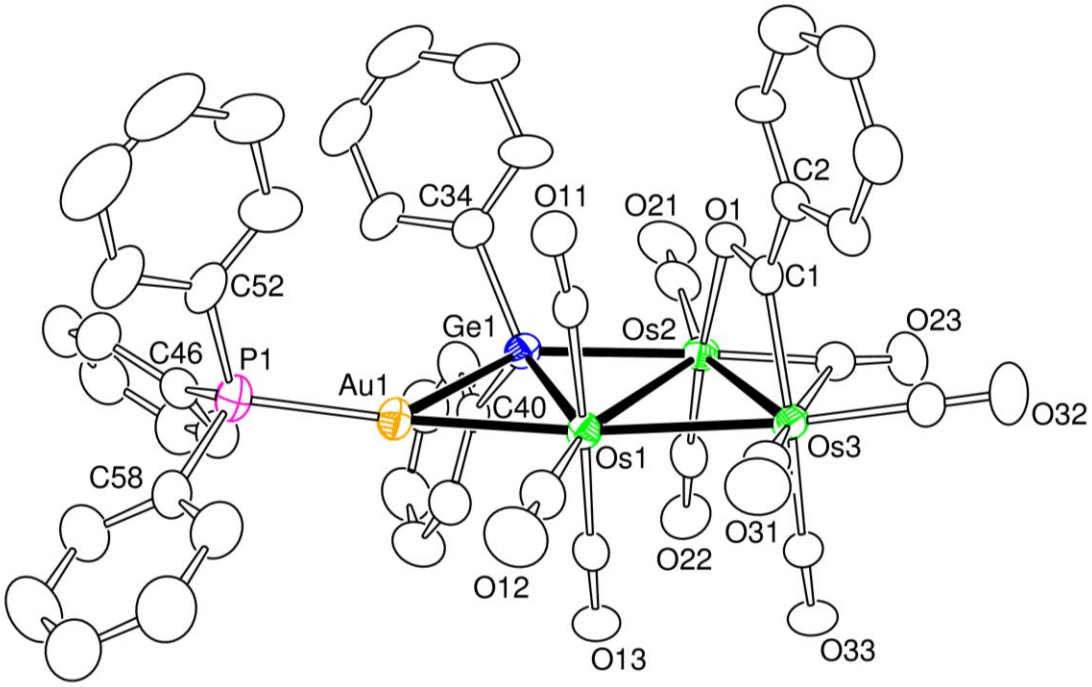

Figure 6.7. An ORTEP diagram of the molecular structure of $Os_3(CO)_8(\mu\text{-}CO)(\mu\text{-}OCPh)(\mu\text{-}GePh_2)(\mu\text{-}AuPPh_3)$, **6.4** showing 30% thermal ellipsoid probability.

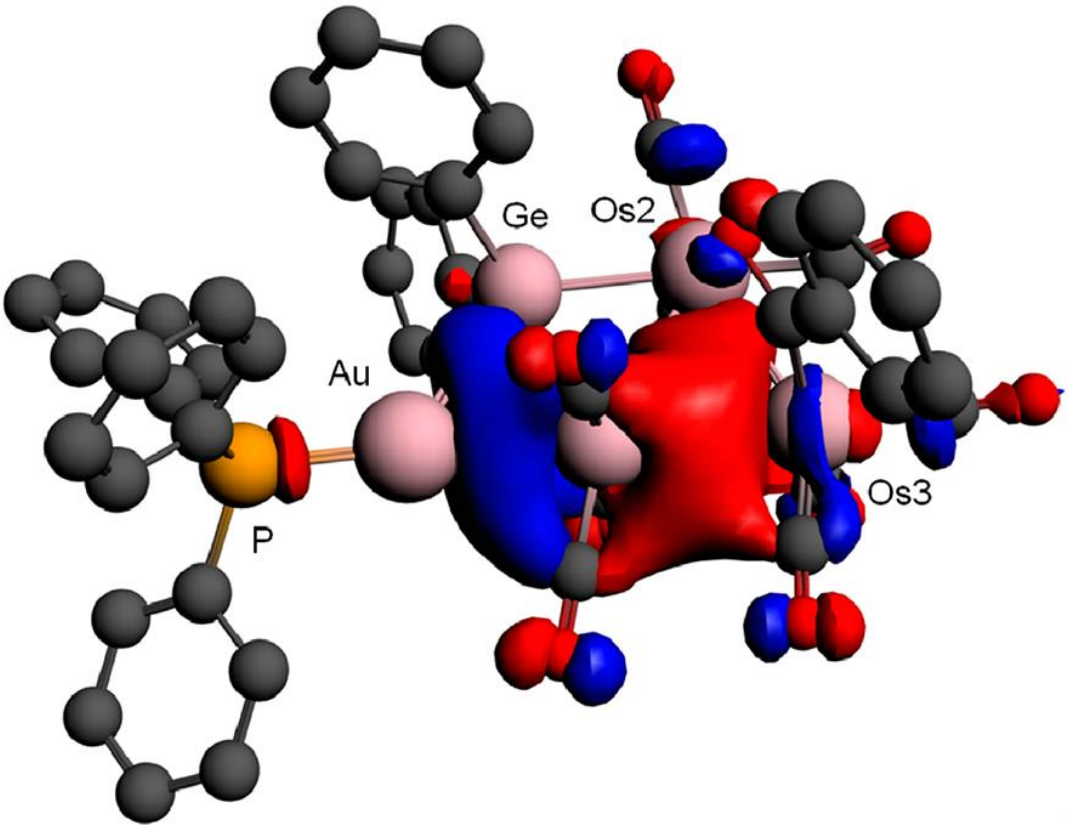

Figure 6.8. The highest occupied molecular orbital of compound **6.4** (Iso = 0.03) shows that a significant component of the orbital is derived from a direct interaction between the Au and Ge atoms.

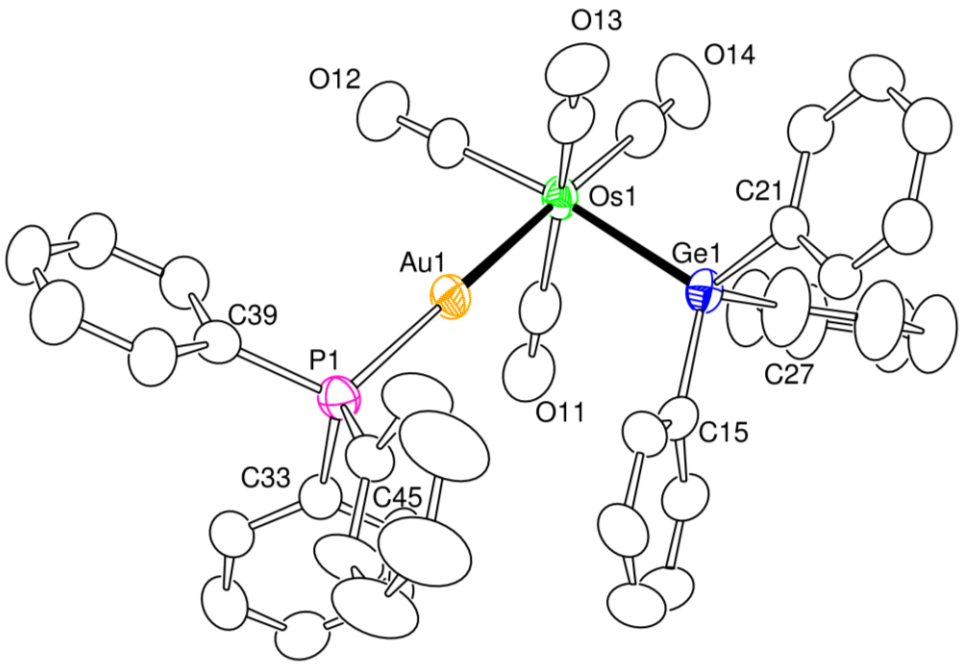

Figure 6.9. An ORTEP diagram of the molecular structure of $Os(CO)_4(GePh_3)(AuPPh_3)$, **6.5** showing 30% thermal ellipsoid probability.

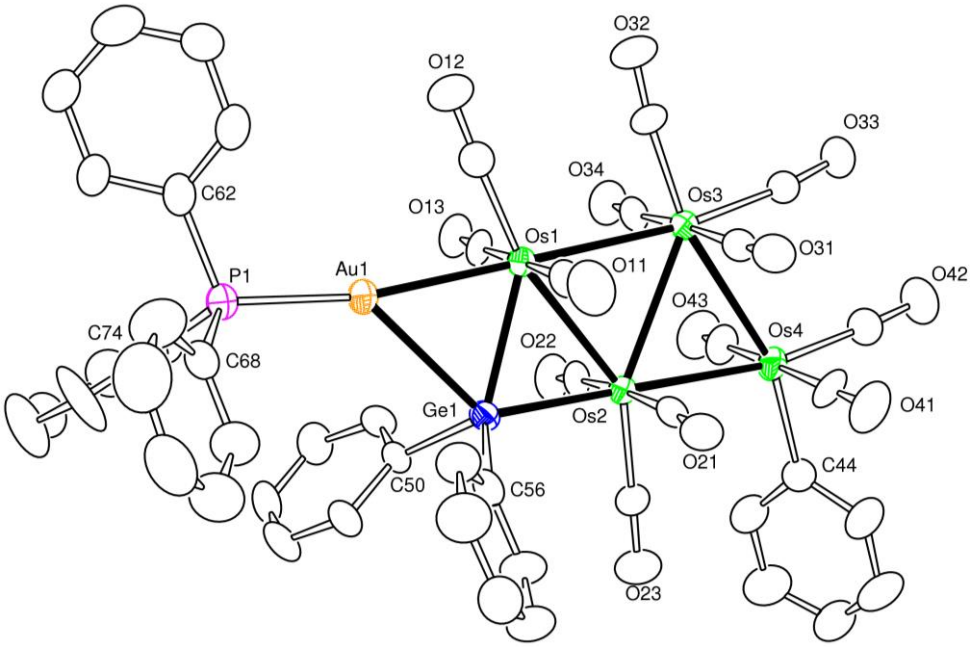

Figure 6.10. An ORTEP diagram of the molecular structure of $PhOs_4(CO)_{13}(\mu\text{-}GePh_2)(\mu\text{-}AuPPh_3)$, **6.6** showing 30% thermal ellipsoid probability.

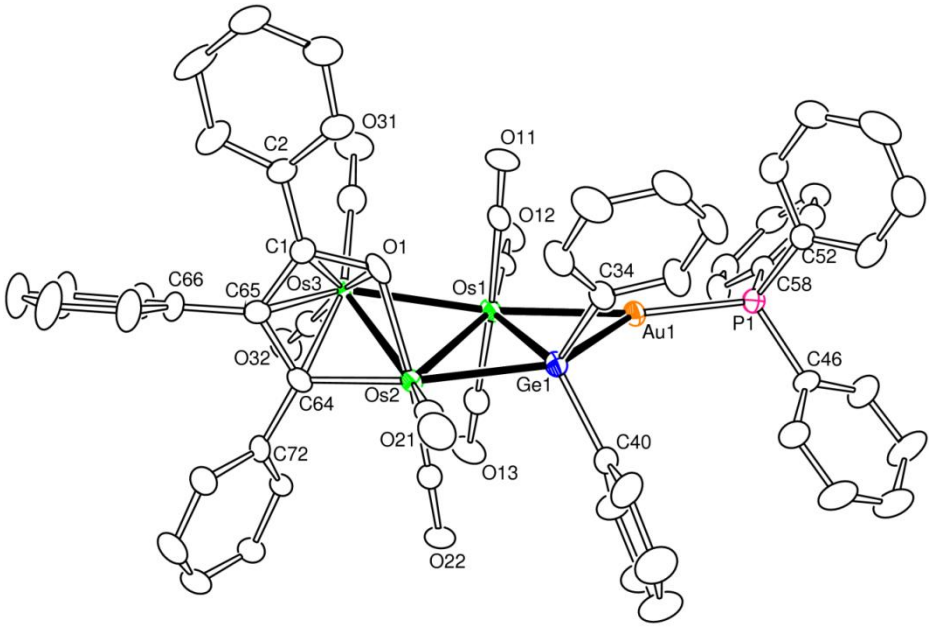

Figure 6.11. An ORTEP diagram of the molecular structure of $Os_3(CO)_7(\mu\text{-}GePh_2)(\mu\text{-}AuPPh_3)[\mu\text{-}OCPhCPhCPh)]$, **6.7** showing 20% thermal ellipsoid probability.

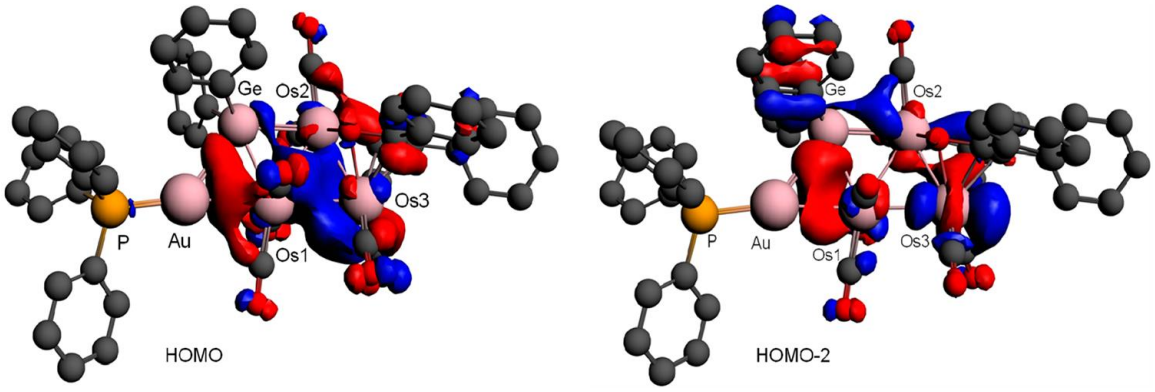

Figure 6.12. The HOMO and HOMO-2 of compound **6.7** (Iso = 0.03) show significant bonding interactions directly between the Au and Ge atoms.

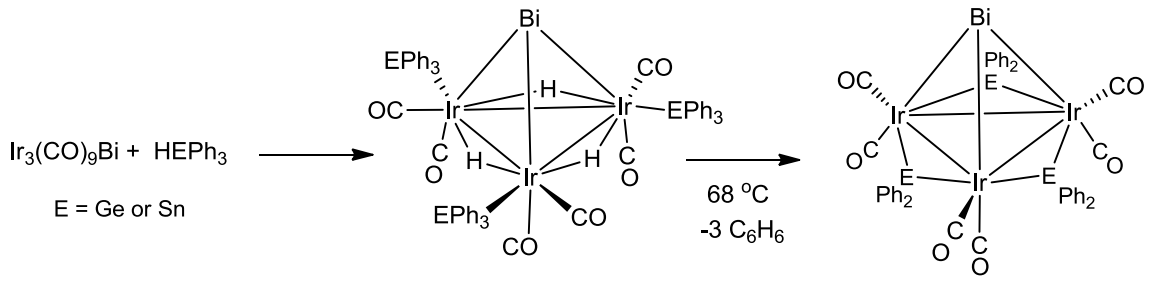

Scheme 6.1.Phenyl cleavage process on Ir-Bi-E cluster.

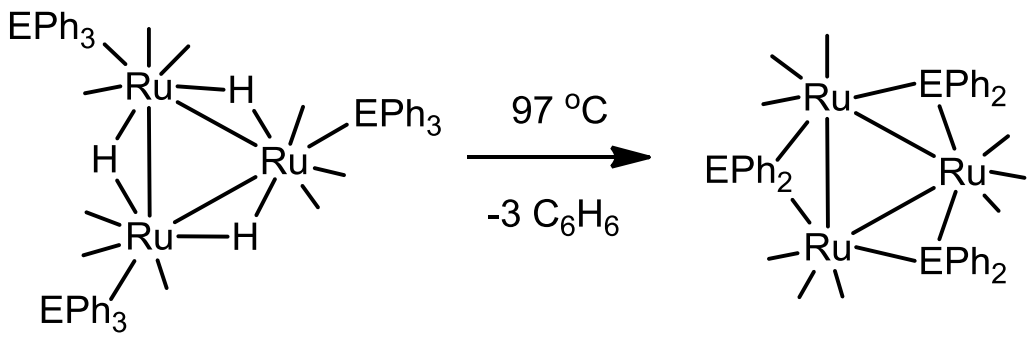

Scheme 6.2. Phenyl cleavage process on $(\mu\text{-H})_3Ru_3(CO)_9(EPh_3)$, E = Ge or Sn.

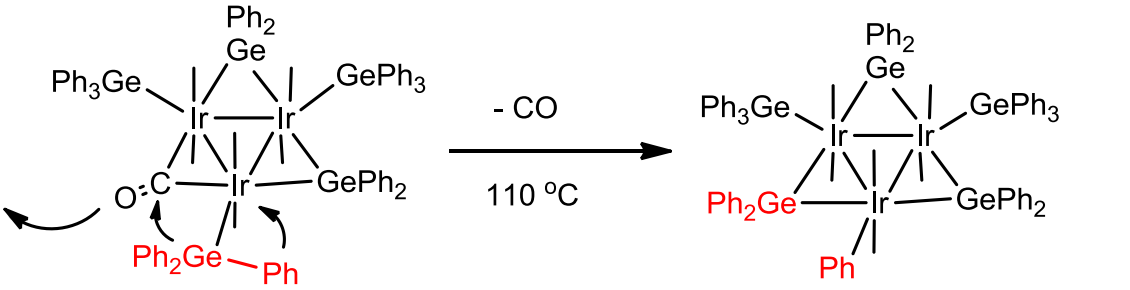

$Ir_3(CO)_6(\mu\text{-}CO)(\mu\text{-}GePh_2)_2(GePh_3)_3$ $Ir_3(CO)_6(\mu\text{-}GePh_2)_3(GePh_3)_3(Ph)$

Scheme 6.3. Phenyl cleavage from $Ir_3(CO)_6(\mu\text{-}CO)(\mu\text{-}GePh_2)_2(GePh_3)_3$

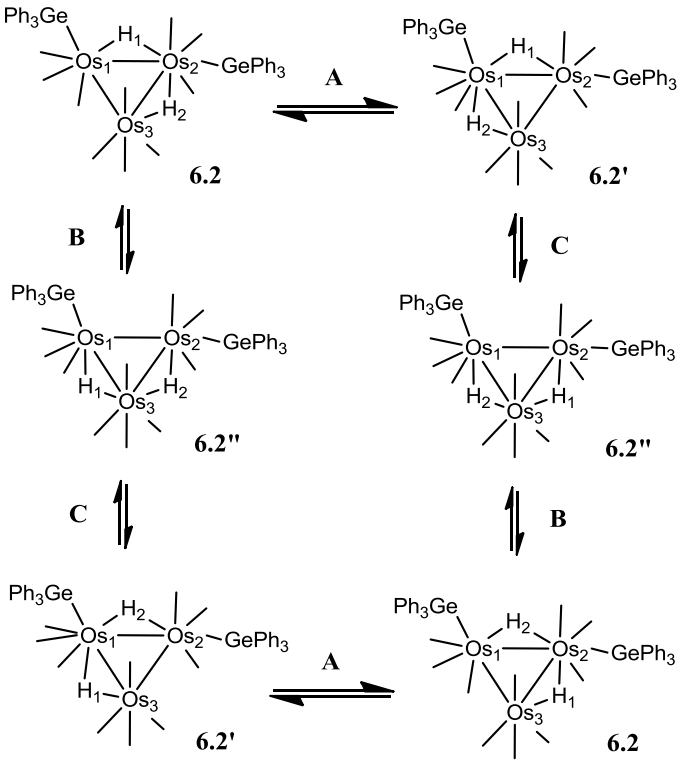

Scheme 6.4. Proposed mechanism(1) for 6.2, 6.2’ and 6.2’’ transformation in solution.

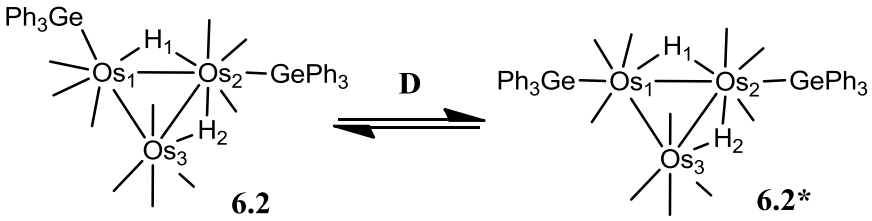

Scheme 6.5. Proposed mechanism(2) for 6.2and 6.2* transformation in solution.

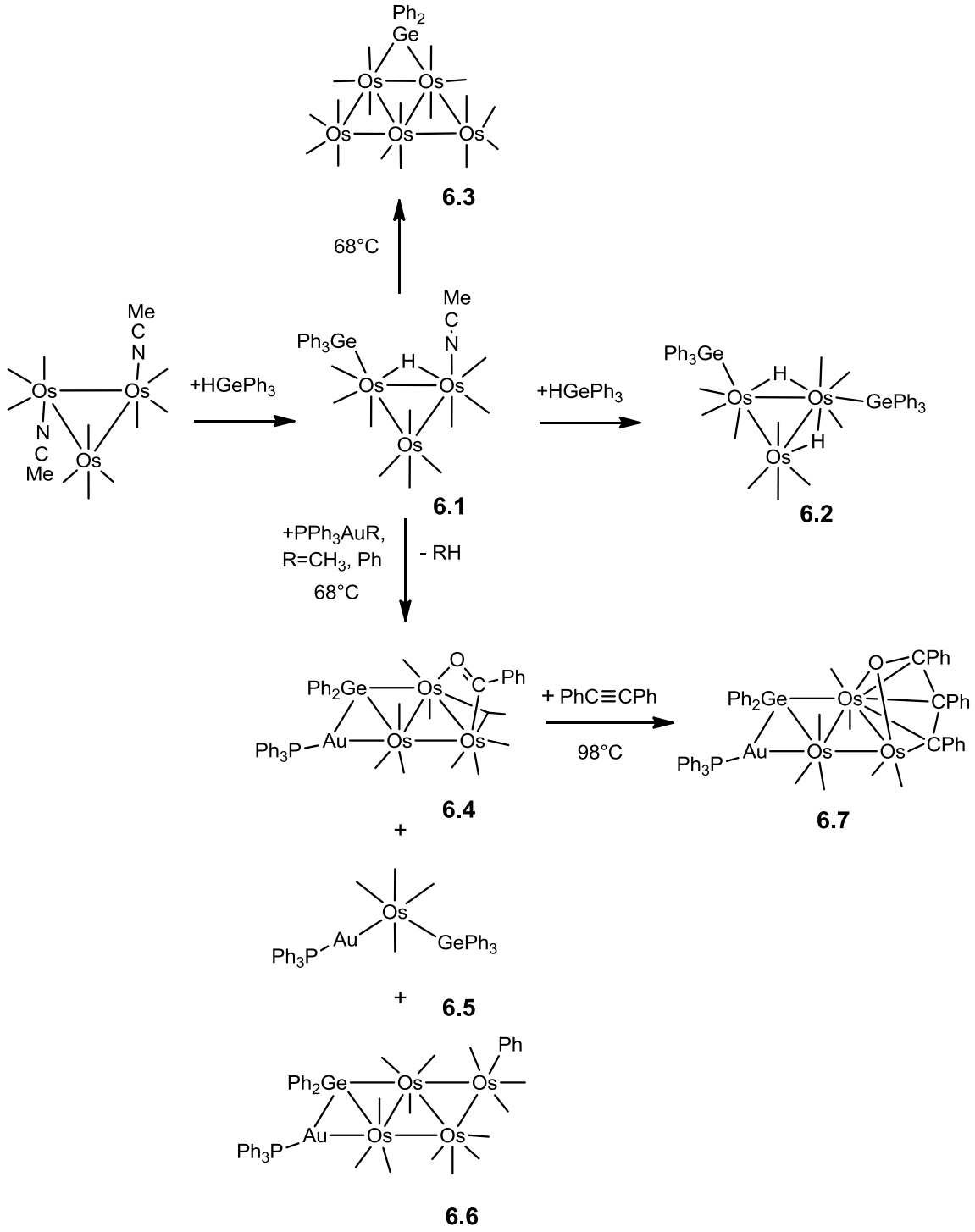

Scheme 6.6. Os-Ge and Os-Ge-Au reactions.

Table 5.1. Crystallographic Data for Compounds **6.1**- **6.7**.

Compound	**6.1**	**6.2**	**6.3**
Empirical formula	$Os_3GeNO_{10}C_{36}H_{25}$	$Os_3Ge_2O_{10}C_{46}H_{32}$	$Os_5GeO_{17}C_{29}H_1$
Formula weight	1274.76	1460.50	1653.96
Crystal system	Triclinic	Orthorhombic	Triclinic
Lattice parameters			
a (Å)	11.1548(4)	18.2230 (11)	10.0493(3)
b (Å)	13.7581(5)	17.1315(11)	10.1132(3)
c (Å)	14.1494(5)	28.6054(18)	18.3249(5)
α (deg)	65.7300(10)	90.00	83.7040(10)
β (deg)	71.5690(10)	90.00	86.8760(10)
γ (deg)	85.3750(10)	90.00	73.4200(10)
V (Å^3)	1874.98(12)	8930.2(10)	1773.65(9)
Space group	*P*-1	*Pbca*	*P*-1
Z value	2	8	2
ρ_{calc} (g / cm^3)	2.258	2.173	3.097
μ (Mo K_α) (mm^{-1})	10.982	9.893	18.749
Temperature (K)	294(2)	294(2)	294(2)
$2\Theta_{max}$ (°)	52.64	54.04	50.06
No. Obs. ($I > 2\sigma(I)$)	6623	7894	6255
No. Parameters	465	556	445
Goodness of fit, GOF*	1.037	1.078	1.023
Max. shift in cycle	0.001	0.000	0.001
Residuals*: R1; wR2	0.0273, 0.0515	0.0373, 0.0503	0.0463, 0.1003
Absor. Corr., Max/min	1.000/0.625	1.000/ 0.698	1.000/0.593
Largest peak in Final Diff. Map (e$^-$ / Å^3)	1.392	0.673	1.816

*$R = \Sigma_{hkl}(\left|\left|F_{obs}\right|-\left|F_{calc}\right|\right|)/\Sigma_{hkl}\left|F_{obs}\right|$; $R_w = [\Sigma_{hkl}w(\left|F_{obs}\right|-\left|F_{calc}\right|)^2/\Sigma_{hkl}wF^2_{obs}]^{1/2}$; $w = 1/\sigma^2(F_{obs})$; GOF = $[\Sigma_{hkl}w(\left|F_{obs}\right|-\left|F_{calc}\right|)^2/(n_{data} - n_{vari})]^{1/2}$.

Table 6.1. (Continued).

Compound	**6.4**	**6.5**	**6.6**	**6.7**
Empirical formula	$Os_3GeAuPO_{10}C_{49}H_{37}$	$OsGeAuPO_4C_{40}H_{30}$	$Os_4GeAuPO_{13}C_{49}H_{30}$	$Os_3GeAuPO_8C_{58}H_{40}\cdot CH_2Cl_2$
Formula weight	1656.91	1065.37	1888.06	1820.95
Crystal system	Monoclinic	Monoclinic	Monoclinic	Triclinic
Lattice parameters				
a (Å)	25.6478(7)	12.6744(16)	18.1098(17)	12.1758(17)
b (Å)	13.3284(4)	10.9674(14)	10.9567(15)	14.985(2)
c (Å)	31.3682(9)	27.570(4)	25.045(3)	17.474(3)
α (deg)	90.00	90.00	90.00	107.190(3)
β (deg)	105.2990(10	101.452(3)	94.142(4)	108.865(3)
γ (deg)	90.00	90.00	90.00	91.232(3)
V ($Å^3$)	10343.0(5)	3756.1(8)	4956.5(10)	2857.9(7)
Space group	*C2/c*	$P2_1/n$	$P2_1/n$	*P*-1
Z value	8	4	4	2
ρ_{calc} (g / cm^3)	2.128	1.884	2.530	2.116
μ (Mo K_α) (mm^{-1})	10.829	8.147	13.856	5.228
Temperature (K)	294(2)	294(2)	294(2)	293(2)
$2\Theta_{max}$ (°)	50.06	50.06	50.06	50.06
No. Obs. ($I > 2\sigma(I)$)	9143	6612	8737	10094
No. Parameters	572	391	622	649
Goodness of fit, GOF*	1.072	1.015	1.037	1.054
Max. shift in cycle	0.001	0.001	0.002	0.001
Residuals*: R1; wR2	0.0397, 0.0747	0.0360, 0.0799	0.0452, 0.0705	0.0432, 0.0951
Absor. Corr., Max/min	1.000/ 0.628	1.000/ 0.724	1.000/ 0.576	1.000/0.650
Largest peak in Final Diff. Map ($e^- / Å^3$)	1.332	1.573	1.597	1.830

*$R = \Sigma_{hkl}(||F_{obs}|-|F_{calc}||)/\Sigma_{hkl}|F_{obs}|$; $R_w = [\Sigma_{hkl}w(|F_{obs}|-|F_{calc}|)^2/\Sigma_{hkl}wF^2_{obs}]^{1/2}$; $w = 1/\sigma^2(F_{obs})$; $GOF = [\Sigma_{hkl}w(|F_{obs}|-|F_{calc}|)^2/(n_{data} - n_{vari})]^{1/2}$.

Table 6.2. Selected intramolecular angles and bond distances for compound **6.1**.[a]

Distances			**Angles**			
Atom	Atom	Distance(Å)	Atom	Atom	Atom	Angle(deg)
Os1	Os2	3.0163(3)	Os2	Os1	Os3	58.434(8)
Os1	Os3	2.8971(3)	Os1	Os2	Os3	58.721(8)
Os2	Os3	2.8883(4)	Os1	Os3	Os2	62.846(8)
Os1	Ge1	2.5301(6)	Ge1	Os1	Os2	111.302(17)
Os2	N1	2.107(5)				
Os1	H1	1.74(6)				
Os2	H1	1.76(6)				

[a] Estimated standard deviations in the least significant figure are given in parentheses.

Table 6.3. Selected intramolecular angles and bond distances for compound **6.2**.[a]

Distances			**Angles**			
Atom	Atom	Distance(Å)	Atom	Atom	Atom	Angle(deg)
Os1	Os2	3.0636(4)	Ge1	Os1	Os3	98.23(2)
Os1	Os3	3.0884(4)	Os2	Os1	Os3	56.597(10)
Os2	Os3	2.9165(5)	Ge2	Os2	Os1	106.44(2)
Os1	Ge1	2.5634(8)	Os1	Os2	Os3	62.131(10)
Os2	Ge2	2.5292(8)	Os1	Os3	Os2	61.272(10)
Os1	H1	1.77(6)				
Os3	H1	1.70(6)				
Os1	H2	1.77(6)				
Os2	H2	1.80(5)				

[a] Estimated standard deviations in the least significant figure are given in parentheses.

Table 6.4. Selected intramolecular angles and bond distances for compound **6.3**.[a]

Distances			**Angles**			
Atom	Atom	Distance(Å)	Atom	Atom	Atom	Angle(deg)
Os1	Os2	2.8691(7)	Os2	Os1	Os4	59.451(18)
Os1	Os3	2.8713(8)	Os1	Os2	Os4	60.004(18)
Os1	Os4	2.8536(7)	Os1	Os3	Os4	59.688(18)
Os2	Os4	2.8376(8)	Os1	Os4	Os2	60.545(18)
Os2	Os5	2.8531(8)	Os2	Os5	Os4	59.327(18)
Os3	Os4	2.8631(7)	Os1	Ge1	Os2	69.39(4)
Os4	Os5	2.8804(7)				
Os1	Ge1	2.5115(16)				
Os2	Ge1	2.5286(16)				

[a] Estimated standard deviations in the least significant figure are given in parentheses.

Table 6.5. Selected intramolecular angles and bond distances for compound **6.4**.[a]

Distances			**Angles**			
Atom	Atom	Distance(Å)	Atom	Atom	Atom	Angle(deg)
Os1	Os2	2.8671(5)	Os1	Au1	Ge1	54.77(2)
Os1	Os3	2.8822(5)	Os1	Ge1	Os2	68.18(2)
Os2	Os3	2.7643(5)				
Os1	Au1	2.6757(5)				
Os1	Ge1	2.5021(9)				
Os2	Ge1	2.6107(9)				
Au1	Ge1	2.7618(10)				
Au1	P1	2.284(2)				
Os2	O1	2.162(5)				
Os3	C1	2.066(8)				
O1	C1	1.293(9)				

[a] Estimated standard deviations in the least significant figure are given in parentheses.

Table 6.6. Selected intramolecular angles and bond distances for compound **6.5**.[a]

Distances			**Angles**			
Atom	Atom	Distance(Å)	Atom	Atom	Atom	Angle(deg)
Os1	Au1	2.6574(5)	Au1	Os1	Ge1	89.47(2)
Os1	Ge1	2.5750(8)				
Au1	P1	2.292(2)				
Ge1	Au1	3.6833(8)				

[a] Estimated standard deviations in the least significant figure are given in parentheses.

Table 6.7. Selected intramolecular angles and bond distances for compound **6.6**.[a]

Distances			**Angles**			
Atom	Atom	Distance(Å)	Atom	Atom	Atom	Angle(deg)
Os1	Os2	2.8726(6)	Os1	Au1	Ge1	55.27(3)
Os1	Os3	2.9372(7)	Os1	Ge1	Os2	68.96(3)
Os2	Os3	2.9125(7)				
Os3	Os4	3.0224(7)				
Os2	Os4	2.8537(7)				
Os1	Au1	2.6936(6)				
Os1	Ge1	2.5635(12)				
Os2	Ge1	2.5099(12)				
Au1	Ge1	2.8274(12)				
Au1	P1	2.298(3)				
Os4	C44	2.101(11)				

[a] Estimated standard deviations in the least significant figure are given in parentheses.

Table 6.8. Selected intramolecular angles and bond distances for compound **6.7**.[a]

Distances			**Angles**			
Atom	Atom	Distance(Å)	Atom	Atom	Atom	Angle(deg)
Os1	Os2	2.8170(6)	Os1	Au1	Ge1	54.74(3)
Os1	Os3	2.7731(6)	Os1	Ge1	Os2	66.84(3)
Os2	Os3	2.7025(7)				
Os1	Au1	2.6803(6)				
Os1	Ge1	2.5143(12)				
Os2	Ge1	2.5992(11)				
Au1	Ge1	2.7846(12)				
Au1	P1	2.305(3)				
Os2	O1	2.108(7)				
Os2	C64	2.046(10)				
Os3	C1	2.260(10)				
Os3	O1	2.217(6)				
Os3	C64	2.277(9)				
Os3	C65	2.292(9)				
O1	C1	1.374(12)				
C1	C65	1.414(13)				
C65	C64	1.451(13)				

[a] Estimated standard deviations in the least significant figure are given in parentheses.

REFERENCE

1. (a) Ekou, T.; Vicente, A.; Lafaye, G.; Especel, C.; Marecot, P. *Appl Catal. A Gen.*. **2006**, *314*, 73-80. (b) Lafaye, G.; Micheaud-Especel, C.; Montassier, C.; Marecot, P. *Appl. Catal. A Gen.* **2002**, *230*, 19-30. (c) Lafaye, G.; Micheaud-Especel, C.; Montassier, C.; Marecot, P. *Appl. Catal. A Gen.* **2004**, *257*, 107-117. (d) Macleod, N.; Fryer, J. R.; Stirling, D.; Webb, G. *Catal. Today* **1998**, *46*, 37-54.

2. (a) Burch, R. *J. Catal.* **1981**, *71*, 348-359. (b) Burch, R.; Garla, L. C. *J. Catal.* **1981**, *71*, 360-372. (c) Srinivasan, R.; Davis, B. H. *Platinum Metals Rev.* **1992**, *36*, 151-163. (d) Fujikawa, T.; Ribeiro, F. H.; Somorjai, G. A. *J. Catal.* **1998**, *178*, 58-65. (e) Park, Y.-K.; Ribeiro, F. H.; Somorjai, G. A. *J. Catal.* **1998**, *178*, 66-75. (f) Epron, F.; Carnevillier, C.; Marecot, P. *Appl. Catal.* **2005**, *295*, 157-169. (g) Cortright, R. D.; Dumesic, J. A. *J. Catal.* **1997**, *148*, 771-778. (h) Dautzenberg, F. M.; Helle, J. N.; Biolen, P.; Sachtler, W. M. H. *J. Catal.* **1980**, *63*, 119-128. (i) Huber, G. W.; Shabaker, J. W.; Dumesic, J. A. *Science* **2003**, *300*, 2075-2077. (j) Shabaker, J. W.; Simonetti, D. A.; Cortright, R. D.; Dumesic, J. A. *J. Catal.* **2005**, *231*, 67-76. (k) Guidotti, M.; Dal Aanto, V.; Gallo, A.; Gianotti, E.; Peli, G.; Psaro, R.; Sordelli, L. *Catal. Lett.* **2006**, *112*, 89-95. (l) Cortright, R. D.; Hill, J. M.; Dumesic, J. A. *Catal. Today* **2000**, *55*, 213-223. (m) Hermans, S.; Raja, R.; Thomas, J. M.; Johnson, B. F. G.; Sankar, G.; Gleeson, D. *Angew. Chem., Int. Ed.* **2001**, *40*, 1211-1215. (n) Johnson, B. F. G.; Raynor, S. A.; Brown, D. B.; Shephard, D. S.; Mashmeyer, T.; Thomas, J. M.; Hermans, S.; Raja, R.; Sankar, G. *J. Mol. Catal. A: Chem* **2002**, *182-183*, 89-97. (o) Hermans, S.; Johnson, B. F. G. *Chem. Commun.* **2000**, 1955-1956. (p) Adams, R. D.; Blom, D. A.; Captain, B.; Raja, R.; Thomas, J. M.; Trufan, E. *Langmuir*, **2008**, *24*, 9223-9226.

3. (a) Thomas, J. M.; Johnson, B. F. G.; Raja, R.; Sankar, G.; Midgley, P. A. *Acc. Chem. Res.* **2003**, *36*, 20-30. (b) Braunstein, P.; Rosé, J. *Catalysis by Di- and Polynuclear Metal Cluster Complexes*, Adams, R. D.; Cotton, F. A. Eds, Wiley-VCH, New York, 1998, Ch. 13. (c) Braunstein, P.; Rosé, *Metal Clusters in Chemistry*, Braunstein, P.; Oro, L.A.; Raithby, P.R. Wiley-VCH, Weinheim, Vol. 2, 1999, Ch. 2.2, pp 616-677. (d) Adams, R. D.; Boswell, E. M.; Captain, B.; Hungria, A. B.; Midgley, P. A.; Raja, R.; Thomas, J. M. *Angew. Chem.. int. Ed.*, **2007**, *46*, 8182 - 8185.

4. Adams, R. D.; Chen, M.; Elpitiya, G.; Zhang, Q. *Organometallics*, **2012**, *31*, 7264-7272.

5. Adams, R. D.; Captain, B.; Trufan, E. *J. Cluster Sci.* **2007**, *18*, 642-659.

6. (a) Adams, R. D.; Captain, B.; Trufan, E. *J. Organomet. Chem*. **2008**, *693*, 3593-3602. (b) Adams, R. D.; Trufan, E. *Phil. Trans. R. Soc. A* **2010**, *368*, 1473-1493.

7. Adams, R. D.; Fang, F.; Zhang, Q.; Hall, M. B.; Trufan, E. *Organometallics*, **2012**, *31*, 2621-2630.

8. Braga, D.; Grepioni, F.; Parisini, E.; Johnson, B. F. G.; Martin, C. M.; Nairn, J. G. M.; Lewis, J.; Martinelli, M., *J. Chem. Soc. Dalton Trans.*, **1993**, 1891-1895.

9. PartyKa, D. V.; Zeller, M.; Hunter, A. D.; Gray, T. G., *Angew. Chem. Int. Ed.* **2006**, 45, 8188 –8191.

10. SAINT+, version 6.2a, Bruker Analytical X-ray Systems, Inc., Madison, WI, 2001.

11. Sheldrick, G. M., SHELXTL, version 6.1, Bruker Analytical X-ray Systems, Inc., Madison, WI, 1997.

12. (a) ADF2012, SCM, Theoretical Chemistry, Vrije Universiteit, Amsterdam, The Netherlands, http://www.scm.com. (b) Stephens P.J.; Devlin F.J.; Chabalowski C.F. and Frisch M.J. *J. Phys. Chem.*, **1994**, 98 (45), 11623–11627. (c) Zhao Y.; Truhlar D. G. *J. Chem. Phys.* **2006**, 125, 194101-194118.

13. Adams, R. D.; Boswell, E. M.; Hall, M. B.; Yang, X. *Organometallics* **2008,** *27,* 4938 – 4947.

14. Bau, R.; Drabnis, M. H. *Inorg. Chim. Acta* **1997**, *259*, 27 - 50. (b) Teller, R. G.; Bau, R., *Struc. Bonding* **1981**, *41*, 1 - 82.

15. Churchill, M. R.; DeBoer, B. G. *Inorg. Chem.* **1977**, *16*, 878.

16. Einstein, F. W. B.; Pomeroy, R. K.; Willis, A. C. *J. Organometal. Chem.* **1986**, *311*, 257−268.

17. (a) Musaev, D. G.; Mowroozi-Isfahani, T.; Morokuma, K.; Abedin, J.; Rosenberg, E.; Hardcastle, K. I. *Organometallics* **2006,** *25,* 203 – 213. (b) Hyder, M. I.; Begum, N.; Sikder, M. D. H.; Hossain, G. M. G.; Hogarth, G.; Kabir, S. E.; Richard, C. J. *J. Organomet. Chem.* **2009**, *694*, 304 – 308. (c) Sharmni, A.; Minazzo, A.; Salassa, L.; Rosenberg, E.; Ross, J. A. B.; Kabir, S. E.; Hardcastle, K. I. *Inorg. Chim. Acta* **2008**, *361*, 1624 – 1633. (d) Deeming, A. J.; Forth, C. S.; Hyder, M.I.; Kabir, S. E.; Nordlander, E.; Rodgers, F.; Ullmann, B. *Eur. J. Inorg. Chem.* **2005**, 4352 – 4350. (e) Keister, J. B.; Frey, U.; Zbinden, D.; Merbach, A. E. *Organometallics* **1991**, *10,* 1497 – 1501. (f) Deeming, A. J.; Hassan, M. M.; Kabir, S. E.; Nordlander, E.; Tocher, D. A. *J. Chem. Soc., Dalton Trans.* **2004**, 3709 – 3714.

18. Deeming, A. J.; Donovan-Mtunzi, S.; Kabir, S. E.; Manning, P. J. *J. Chem. Soc., Dalton Trans.* **1985**, 1037 – 1741.

19. (a)Coughlin, D.; Lewis, J.; Moss, J. R. *J. Organomet. Chem.* **1993**, *444*, C53 – C54. (b) Wang, W.; Einstein, F. W. B.; Pomeroy, R. K. *J. Chem. Soc., Chem. Commun.* **1992**, 1737 – 1738.

20. Wang, W.; Batchelor, R. J.; Einstein, F. W. B.; Lu, C.-Y.; Pomeroy, R. K. *Organometallics* **1993**, *12*, 3598 – 3606.

21. Adams, R. D.; Boswell, E. M.; Captain, B.; Patel, M. A. *Inorg. Chem.* **2007**, *46*, 533–540.

22. Adams, R. D.; Rassolov, V.; Zhang, Q. *Organometallics* **2012**, *31*, 2961−2964.

23. Bauer, A.; Schmidbaur, H. *J. Am. Chem. Soc.* **1996,** *118*, 5324-5325.

24. Bauer, A.; Schier, A.; Schmidbaur, H. *J. Chem. Soc., Dalton Trans.*, **1995**, 2919-2920.

25. Liu, X.-Y.; Riera, V.; Ruiz, M. A.; Lanfranchi, M.; Tiripicchio, A. *Organometallics* **2003**, *22*, 4500−4510.

26. (a) Arii, H.; Nanjo, M.; Mochida, K. *Organometallics* **2008**, *27*, 4147-4151. (b) Adams, R. D.; Smith Jr., J. L. *Inorg.Chem.* **2005**, *44*, 4276-4281. (c) Adams, R. D.; Captain, B.; Smith Jr., J. L. *Inorg.Chem.* **2005**, *44*, 1413-1420. (d) Tanabe, M.; Ishikawa, N.; Osakada, K. *Organometallics* **2006**, *25*, 796-798. (e) Adams, R. D.; Trufan, E. *Organometallics* **2010**, *29*, 4346-4353. (f) Braddock-Wilking, J.; Corey, J.Y.; White, C.; Xu, H.; Rath, N.P. *Organometallics* **2005**, *24*, 4113-4115.

27. (a) Fehlhammer, W. B.; Stolzenberg, H. in Wilkinson, G.; Stone, F. G. A.; and Abel, E. (Eds.), Comprehensive Organometallic Chemistry, Pergamon, Oxford, U.K., 1982, Ch. 31.4. (b) Curtis, C. T.; Stone, F. G. A. *J. Organomet. Chem.* **1968**, *11*, 644−646. (c) Ferrari, R. P.; Vaglio, G. A.; Gambino, O.; Valle, M.; Cetini, G. *J. Chem. Soc., Dalton Trans.*, **1995**, 1998-2001. (d) Adams, R. D.; Qu, B.; Smith, M. D.; Albright, T. A. *Organometallics* **2002**, *21*, 2970−2978.

28. (a) Carmona, E.; Guitierrez-Puebla, E.; Monge, A.; Marin, J. M.; Paneque, M.; Poveas, M. L. *Organometallics* **1984**, *3*, 1438−1440. (b) Reddy, K. R.; Surekha, K.; Lee, G.-H.; Peng, S.-M.; Liu, S.-T. *Organometallics* **2001**, *20*, 5557−5563. (c) Knorr, M.; Strohmann, C.; Braunstein, P.; *Organometallics* **1996**, *15*, 5653−5663.

29. Rusik, C. A.; Collins, M. A.; Gamble, A. S.; Tonker, T. L.; Templeton, J. L. *J. Am. Chem. Soc.* **1989**, *111*, 2550–2560.

CHAPTER 7

Cleavage of Phenyl Groups from $BiPh_3$. The Reactions of $Os_3(CO)_{10}(NCMe)_2$ with $BiPh_3$

Introduction

The cleavage of phenyl groups from the triphenyl Group 15 compounds PPh_3, $AsPh_3$ and $SbPh_3$ in their reactions with triosmium carbonyl complexes goes back to some of the very first reactions of $Os_3(CO)_{12}$ that were studied[1,2]. Cleavage of phenyl groups from $AsPh_3$ and $SbPh_3$ is also facile[3,4]. Recently, complexes containing transition metal – bismuth bonds have attracted attention[5,6]. Transition metal – bismuth catalysts have been shown to exhibit high activity and selectivity for the oxidation and ammoxidation of hydrocarbons.[7,8,9] Adams *et. al.* recently reported the synthesis of dirhenium carbonyl complexes containing $SbPh_2$ and $BiPh_2$ ligands by the cleavage of phenyl rings from $SbPh_3$ and $BiPh_3$ in their reactions with $Re_2(CO)_8[\mu\text{-}\eta^2\text{-}C(H)=C(H)Bu^n](\mu\text{-}H)$, Scheme 7.1(1)[10], Scheme 7.1(2)[11]. These products have been shown to be good catalysts for the ammoxidation of 3-picoline to 3-cyanopyridine[12].

They have also shown that phenyl groups are readily cleaved from $BiPh_3$ in its reaction with $Os_3(CO)_{11}(NCMe)$, Scheme 7.2[13]. In fact, only one product $Os_2(CO)_8(\mu\text{-}BiPh)$ contained any phenyl groups on a Bi atom. Products containing phenyl groups or ligands, such as C_6H_4 and PhCO, derived from them, were abundant. In this chapter, the reaction of $BiPh_3$ with $Os_3(CO)_{10}(NCMe)_2$ is described. These studies have yielded yet another new osmium-bismuth complex as well as some new osmium carbonyl complexes

containing phenyl, benzoyl and benzyne ligands derived from the phenyl groups that were cleaved from the $BiPh_3$. Most interestingly, a high resolution structure analysis of one of the new products $Os_3(CO)_{10}(\mu_3\text{-}CH_4)$, **7.2** which contains a triply-bridging benzyne ligand show a distinct pattern of long and short C-C bonds around the ring of the benzyne ligand. Molecular orbitals for **7.2** were obtained by density functional theory (DFT) calculations and indicate that this bonding pattern can be attributed to a partial localization of the π-bonding in the ring which is enhanced at the shorter C-C bonds.

Experimental Section

General Data.

Reagent grade solvents were dried by the standard procedures and were freshly distilled prior to use. Unless indicated otherwise, all reactions were performed under an atmosphere of nitrogen. Infrared spectra were recorded on a Thermo Nicolet Avatar 360 FT-IR spectrophotometer. ^1H NMR spectra were recorded on a Varian Mercury 300 spectrometer operating at 300.1 MHz. Mass spectral (MS) measurements were performed either by a direct-exposure probe by using electron impact ionization (EI) on a VG 70S instrument. $Os_3(CO)_{12}$ was purchased from STREM. $BiPh_3$ was purchased from Alfa Aesar and was used without further purification. $Os_3(CO)_{10}(NCMe)_2$ was prepared according to the previously reported procedure[14]. Product separations were performed by TLC in open air on Analtech 0.25 mm or 0.5 mm silica gel 60 Å F_{254} glass plates.

Reactions of $Os_3(CO)_{10}(NCMe)_2$ with $BiPh_3$.

A 22.2 mg (0.0238 mmol) amount of $Os_3(CO)_{10}(NCMe)_2$, **7.1** was dissolved in 30 mL of methylene chloride in a 100 mL three neck flask. To this solution was added 10.5 mg (0.0238 mmol) of $BiPh_3$. The solution was heated to reflux for 2h. After cooling, the solvent was removed *in vacuo*, and the products were isolated by TLC by using a 6/1 hexane/methylene chloride elution solvent mixture to yield in order of elution: 1.1 mg of pale yellow $Os_3(CO)_9(\mu\text{-}CO)(\mu_3\text{-}C_6H_4)$, **7.2** (5% yield); 3.0 mg of orange $PhOs_3(CO)_{10}(\mu\text{-}\eta^2\text{-}O{=}CPh)$, **7.3** (12% yield); 2.2 mg of orange $HOs_5(CO)_{18}(\mu\text{-}\eta^2\text{-}C_6H_4)(\mu_4\text{-}Bi)$,[13] **7.4** (9% yield); 2.5 mg of $HOs_6(CO)_{20}(\mu\text{-}\eta^2\text{-}C_6H_4)(\mu_4\text{-}Bi)$, **7.5** (11% yield).

Spectral data for **7.2**: IR *v*CO (cm^{-1} in hexane): 2099 (vw), 2082 (w), 2077 (w), 2060 (vs), 2024 (s), 2012 (s), 1998 (w), 1983 (vw), 1844 (w). ^1H NMR (CD_2Cl_2, δ in ppm) at 25 ℃: δ = 7.65 (m, 2H, C_6H_4), δ = 6.72 (m, 2H, C_6H_4). Mass Spec. EI/MS m/z. 928 (M^+).

Spectral data for **7.3**. IR *v*CO (cm^{-1} in methylene chloride): 2111(m), 2096(w), 2059 (vs), 2027 (s), 2003 (m), 1986 (m), 1942 (w). ^1H NMR (CD_2Cl_2, δ in ppm) at 25°C: δ = 7.22-7.84 (m, 10H, Ph). EI/MS m/z. 1034 (M^+).

Spectral data for **7.5**. IR *v*CO (cm^{-1} in hexane): 2126 (w), 2089 (m), 2082 (m), 2073 (s), 2056 (w), 2044 (vs), 2020 (m), 2015 (m), 2009 (m), 2850 (w). ^1H NMR (CD_2Cl_2, δ in ppm) at 25°C: δ = 6.59-7.08 (m, 4H, C_6H_4), δ = -14.54, -14.59 (s, hydride). EI/MS m/z. 1988 (M^+).

Thermal transformations of 7.3.

A 7.4mg (0.0072mmol) amount of **7.3** was dissolved in 10mL of hexane in a 50mL three neck flask. The solution was heated to reflux for 5 h. After cooling, the

solvent was then removed *in vacuo*, and the product was isolated by TLC by using a 6/1 hexane/methylene chloride elution solvent mixture to yield in order of elution: 0.7 mg of **7.2** (10.5% yield); 3.2 mg of $Os_3(CO)_{10}(\mu\text{-}\eta^2\text{-}O{=}CPh)_2$, **7.6**[15] (42% yield).

Spectral data for **7.6**: IR *v*CO (cm^{-1} in hexane): 2099 (w), 2068 (vs), 2048 (m), 2016 (vs), 2005 (s), 1998 (m), 1989 (w), 1983 (m), 1975 (w), 1954 (vw). Mass Spec. EI/MS m/z. 1062 (M^+).

Crystallographic Analyses:

Yellow single crystals of **7.2** and orange single crystals of **7.3** suitable for x-ray diffraction analyses were obtained by slow evaporation of solvent from solutions in hexane/methylene chloride solvent mixtures at -30°C. Dark green single crystals of **7.5** suitable for x-ray diffraction analyses was obtained by slow evaporation of solvent from solutions in hexane/methylene chloride solvent mixtures at room temperature. Yellow single crystals of **7.6** suitable for x-ray diffraction analyses were obtained by slow evaporation of solvent from solutions in hexane solvent mixtures at -30°C. Each data crystal was glued onto the end of a thin glass fiber. X-ray diffraction intensity data were measured by using a Bruker SMART APEX CCD-based diffractometer by using Mo Kα radiation (λ = 0.71073 Å). The raw data frames were integrated with the SAINT+ program by using a narrow-frame integration algorithm[16]. Corrections for Lorentz and polarization effects were also applied with SAINT+. An empirical absorption correction based on the multiple measurement of equivalent reflections was applied by using the program SADABS[16]. All structures were solved by a combination of direct methods and difference Fourier syntheses, and refined by full-matrix least-squares on F^2 by using the

SHELXTL software package[17]. All non-hydrogen atoms were refined with anisotropic thermal parameters. The hydride ligand in compound **7.5** was also refined with anisotropic thermal parameters.

Compounds **7.2** crystallized in orthorhombic system. The space group *P*na2_1 was indicated by the systematic absences in the data and confirmed by the successful solution and refinement for the structure. Compounds **7.3, 7.5** and **7.6** crystallized in monoclinic system. The space group *P*2_1/c in compound **7.3**, *P*2_1/n in compound **7.5** and **7.6** were identified by the systematic absences in the data and confirmed by the successful solution and refinement for the structure, respectively. Crystal data, data collection parameters, and results of these analyses are listed in Table 7.1.

Computational Details.

Density functional theory (DFT) calculations were performed with the Amsterdam Density Functional (ADF) suite of programs[18] by using the PBEsol functional[19] with valence quadruple-ζ + 4 polarization function, relativistically optimized (QZ4P) basis sets for osmium and valence triple-ζ + 2 polarization function (TZ2P) basis sets for carbon, oxygen, and hydrogen atoms with small frozen cores. The molecular orbitals for **7.2** and their energies were determined by a single point calculation based on the structure found in the crystal. Electron densities at the bond critical points around the C_6 ring were calculated by using the Bader Quantum Theory of Atoms In a Molecule (QTAIM) model and the AIMAll software package.

Results

Four products $Os_3(CO)_{10}(\mu_3\text{-}C_6H_4)$, **7.2** (5% yield), $Os_3(CO)_{10}Ph(\mu\text{-}\eta^2\text{-}O{=}CPh)$, **7.3** (12% yield), $HOs_5(CO)_{18}(\mu\text{-}\eta^2\text{-}C_6H_4)(\mu_4\text{-}Bi)$,[13], **7.4** (9% yield) and $HOs_6(CO)_{20}(\mu\text{-}\eta^2\text{-}C_6H_4)(\mu_4\text{-}Bi)$, **7.5** (11% yield) were obtained all in low yields from the reaction of **7.1** with $BiPh_3$ in a methylene chloride solution at reflux for 2h. Three of the products, **7.2**, **7.3** and **7.5** are new and were characterized by a combination of IR, NMR, mass spec and single crystal x-ray diffraction analyses. Compound **7.4** was obtained previously from the reaction of $Os_3(CO)_{11}(NCMe)$ with $BiPh_3$[13].

An ORTEP diagram of the molecular structure of **7.2** is shown in Figure 7.1. Compound **7.2** contains three osmium atoms, nine linear terminal carbonyl ligands, one bridging carbonyl ligand and a triply bridging C_6H_4 benzyne ligand. It is related to the $Os_3(CO)_9(\mu_3\text{-}C_6H_3R)(\mu\text{-}H)_2$, R = H, CH_3, Cl, $HC_2(H)Ph$, family of compounds that was reported by Johnson and Lewis many years ago[20]. The primary difference between **7.2** and the Johnson - Lewis compounds is that **7.2** has ten CO ligands and no hydride ligands, while the Johnson - Lewis compounds have nine CO ligands and two hydride ligands. The osmium-osmium bond distances in **7.2** are Os(1) – Os(2) = 2.8526(3) Å, Os(1) – Os(3) = 2.7631(4) Å and Os(2) – Os(3) = 2.7506(4) Å, while $Os_3(CO)_9(\mu_3\text{-}C_6H_4)(\mu\text{-}H)_2$ has two Os – Os bonds that are much longer, 3.026(2) [3.041(2)] Å, 2.866(2) [2.849(2)] Å and 2.751(2) [2.751(2)] Å[20]. The two long bonds in $Os_3(CO)_9(\mu_3\text{-}C_6H_4)(\mu\text{-}H)_2$ can be attributed to effects of the hydride ligands that bridge those bonds[21]. The coordinated C – C triple bond in **7.2**, C(1) – C(6) is 1.406(9) Å in length. Because of the high quality of this structure analysis, the alternating pattern of long and short C – C bond distances about the C_6 ring, C(1) – C(2) = 1.438(9)Å, C(2) – C(3) = 1.375(10)Å, C(3) – C(4) = 1.405(10)Å, C(4) – C(5) = 1.361(10)Å, C(5) – C(6) = 1.428(10)Å, seems

to be a true result and could be explained by the existence of partial localizations of the π–bonding in the ring induced by interruption in the delocalization of the π–bonding at the C(1) – C(6) bond due to the coordination of these atoms to the metal atoms. This idea was supported by density functional theory (DFT) calculations that were performed on the structure as found in the solid state. Two molecular orbitals, the HOMO and the HOMO-2, shown in Figure 7.2, show a clear pattern of enhanced π-bonding between the two pairs of atoms, C(2) – C(3) and C(4) – C(5), which exhibit the shortest of the C – C ring bond distances.

The bonding in **7.2** was further analyzed by calculating the electron densities at the bond critical points (BCPs) in the optimized structure by using the QTAIM method. Selected electron densities at important BCPs are shown in Figure 7.6. The electron densities at the BCPs in the C(2) – C(3) and C(4) – C(5) bonds are 0.3182 and 0.3187 e/bohr3, while that in the C(1) – C(2) and C(5) – C(6) are 0.2972 and 0.2894, respectively. Such electron densities indicate that the C(2) – C(3) and C(4) – C(5) bond strength is approximately 10% greater of the strength of the C(1) – C(2)and C(5) – C(6) bond. These bond indices further confirm enhanced π-bonding at C(2) – C(3) and C(4) – C(5) bond.

An ORTEP diagram of the molecular structure of **7.3** is shown in Figure 7.3. Compound **7.3** contains three osmium atoms, ten CO ligands, one of which is a semi-bridging CO ligand, and two phenyl rings; one of which is σ–bonded to one of the osmium atoms and the other is bonded to a CO group in the form of a bridging benzoyl ligand. The three metal atoms are arranged in a triangle: Os(1) - Os(2) = 2.8141(7), Os(1) - Os(3) = 2.9020(6), Os(2) - Os(3) = 2.8606(7). The short Os(1) – Os(2) bond is the one

that contains the semi-bridging CO ligand C(11)-O(11) and the bridging benzoyl ligand: Os(2) - C(1) = 2.087(11) Å, Os(1) - O(1) = 2.129(7) Å and C(1) - O(1) = 1.287(12) Å. The phenyl ligand is terminally coordinated to Os(1), Os(1) – C(4) = 2.125(10) Å. Two other osmium carbonyl cluster complexes containing σ–phenyl ligands, $Os_4(CO)_{15}Ph(\mu_4$-Bi) with Os - C = 2.178(7) and $Os_5(CO)_{19}Ph(\mu_4$-Bi) with Os - C = 2.152(13) Å, were obtained from the reaction of $BiPh_3$ with $Os_3(CO)_{11}$(NCMe), see Scheme 7.2 [13]. Leong obtained some osmium cluster complexes containing σ–phenyl ligands by cleaving a phenyl group from a $SbPh_3$ ligand[4].

An ORTEP diagram of the molecular structure of **7.5** is shown in Figure 7.4. Compound **7.5** contains six osmium atoms in groups of four and two. The two groups are bridged by a spiro-μ_4-Bi atom, Os(1) - Bi(1) = 2.7644(12) Å, Os(2) - Bi(1) = 2.7085(13) Å, Os(5) - Bi(1) = 2.7203(12) Å and Os(6) - Bi(1) = 2.7235(13) Å. Four compounds containing spiro-μ_4-Bi atoms were obtained in the reaction of $BiPh_3$ in its reaction with $Os_3(CO)_{11}$(NCMe), Scheme 7.2 [13]. One of those was the compound **7.4** which was also obtained in this reaction. The Os – Bi distances in those compounds are similar to those found in **7.5**. The Os – Os bond distances in **7.5** are not unusual, except for the elongated Os(5) – Os(6) bond of 3.0309(13) Å in the Os_2 group. This bond is bridged by a hydride ligand which was located and refined crystallographically, Os(5) - H(1) = 1.71(19) Å, Os(6) - H(1) = 2.01(19) Å which could explain the unusual Os – Os bond length[21]. Interestingly, the ^{1}H NMR spectrum of **7.5** exhibits two high-field resonances, δ = -14.54, -14.59, for the hydride ligand which suggests the existence of two isomers for the compound in solution. There is μ-η^2-C_6H_4 ligand bridging the osmium atoms in the two atom group, Os(5) - C(1) = 2.12(3), Os(6) – C(2) = 2.11(3). μ-η^2-C_6H_4 ligands are rare,

but one was also found in the compound $HOs_5(CO)_{18}(\mu\text{-}C_6H_4)(\mu_4\text{-}Bi)$, **7.7**, Os(1)-C(2) = 2.110(11) Å, Os(2)-C(1) = 2.132(12) Å which was obtained from the reaction of $Os_3(CO)_{11}(NCMe)$ with $BiPh_3$.[13] Leong also obtained some examples of $\mu\text{-}\eta^2\text{-}C_6H_4$ ligands in some osmium carbonyl cluster complexes formed by the cleavage of phenyl rings from $SbPh_3$ ligands[22]. The spiro-Bi atom in **7.5** acts as a 5-electron donor and formally all of the metal atoms in **7.5** have 18 electron configurations.When compound **7.3** was heated to reflux in hexane solvent for 5 h, it was transformed into compound **7.2** in 10.5% yield) and the compound $Os_3(CO)_{10}(\mu\text{-}\eta^2\text{-}O{=}CPh)_2$, **7. 6** in 42% yield. Compound **7.6** was obtained by Kaesz many years ago by the reaction of $Os_3(CO)_{12}$ with phenyl lithium followed by the oxidation with $(Me_3O)(SbCl_6)$ or $CuBr_2$ [15], but this molecule has never been characterized structurally by X-ray crystallographic methods. An ORTEP diagram of the molecular structure of **7.6** is shown in Figure 7.5. Compound **7.6** contains a triangular cluster of three osmium atoms with ten linear terminal carbonyl groups and two benzoyl ligand that bridge the atoms Os(1) and Os(2). The benzoyl ligands serve as three electron donors so the metal atoms have a total of 50 valence electrons and thus all of the metal atoms achieve 18 electron configurations with the existence of only two Os – Os bonds, Os(1) - Os(3) = 2.8720(6) Å and Os(2) - Os(3) = 2.8810(7) Å. The Os(1) - Os(2) distance of 3.652(1) Å is clearly a nonbonding interaction. The two benzoyl ligands are paired antisymmetrically such that the oxygen atom of one is bonded to Os(1) and the oxygen atom of the other is bonded to Os(2); Os(1) - O(1) = 2.112(6) Å, Os(2) - O(2) = 2.100(7) Å.

Discussion

A summary of the reactions and products obtained in this study is shown in the Scheme 7.3. Four products were formed from the reaction of **7.1** with $BiPh_3$. Compounds **7.4** and **7.5** contain spiro-μ_4-Bi atoms formed by the cleavage of all of the phenyl groups from the $BiPh_3$. Products **7.2** and **7.3** contain the phenyl rings that were cleaved from the $BiPh_3$, although the ring in **7.2** is actually a triply bridging C_6H_4 ligand formed by the cleavage and elimination of one hydrogen atom from the ring. A high quality structural analysis of **7.2** coupled with a DFT computational analysis indicate that there is a significant degree of localization of the π-bonding in that ring. Compound **7.2** was also obtained in a low yield by heating **7.3**. It is anticipated that **7.2** was formed by the elimination of benzaldehyde from **7.3**, but that was not confirmed experimentally. The compound **7.6** was also obtained from the thermal treatment of **7.3**. The formation of **7.6** requires formally the addition of an equivalent of CO, presumably provided by small amounts of CO formed by degradation of some **7.3** and then a coupling of the CO to its phenyl group to produce the second benzoyl ligand found in **7.6**.

Conclusions

The cleavage of phenyl groups from $BiPh_3$ by activated osmium carbonyl cluster complexes is facile and leads to products containing naked bridging bismuth atoms and coproducts containing the phenyl rings. Similar results were found in our studies of the reactions of $BiPh_3$ with activated rhenium carbonyl complexes[11]. Evidence has been presented that shows a pattern of alternating long and short C – C distances in the bridging benzyne ligand in **3** that is consistent with a significant amount of localized π-

bonding in the ring that is induced by the coordination of the triple bond of the ring to the metal atoms.

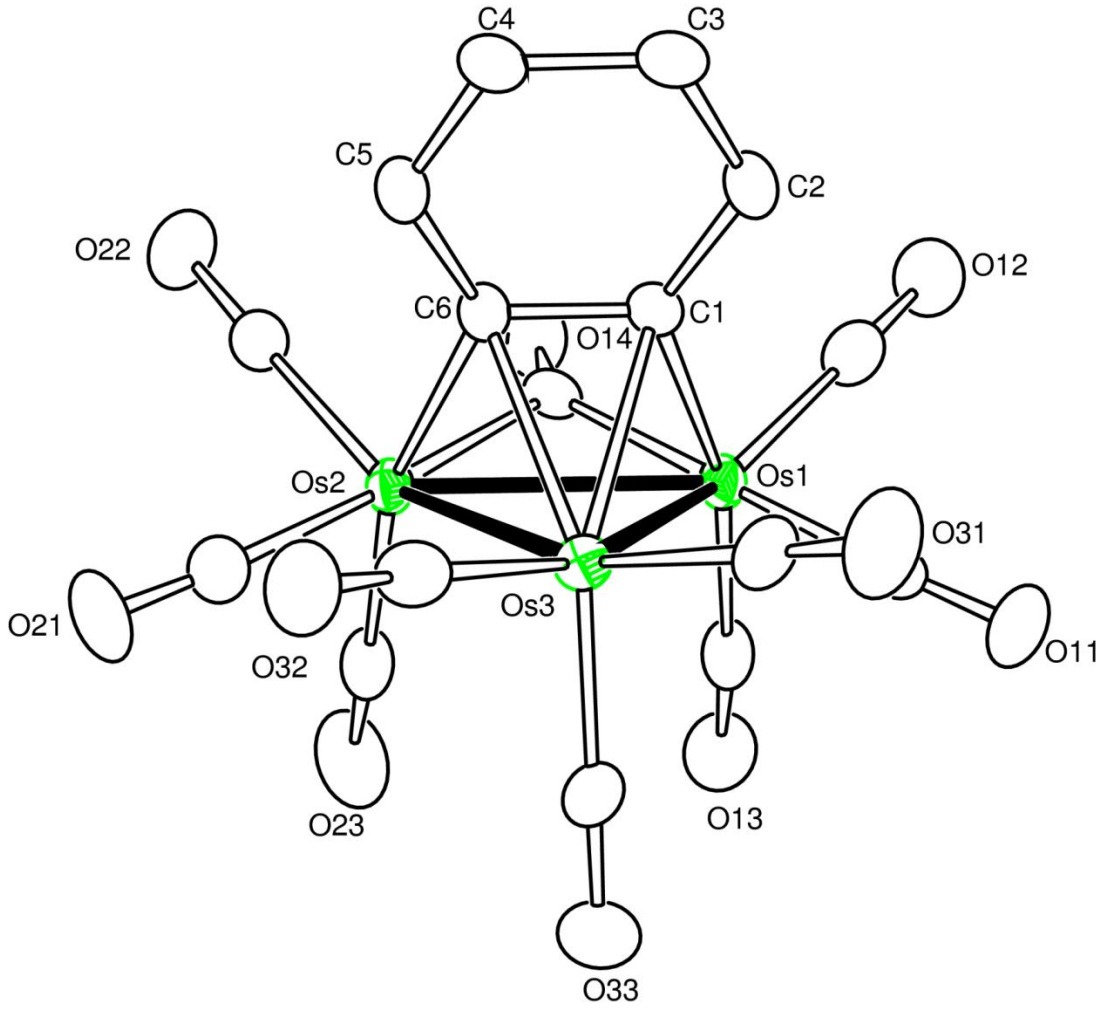

Figure 7.1. An ORTEP diagram of the molecular structure of $Os_3(CO)_9(\mu\text{-}CO)(\mu_3\text{-}C_6H_4)$, **7.2** showing 40% thermal ellipsoid probability.

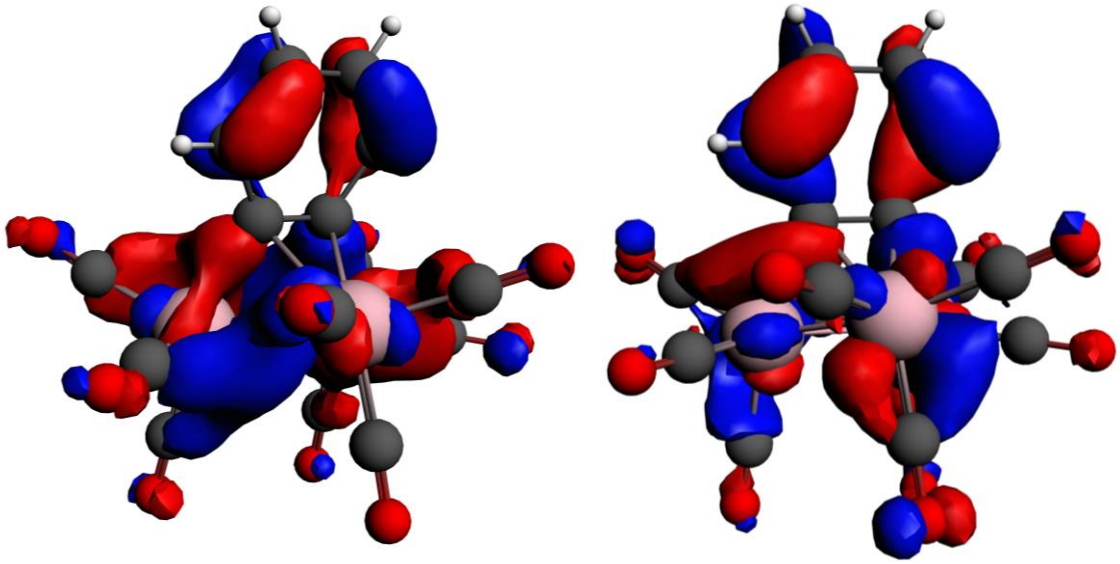

HOMO, -5.48 eV HOMO-2, -6.54

Figure 7.2. Diagrams of the HOMO and HOMO-2 with their energies for compound **7.2** showing the π-bonding in the C_6H_4 ring.

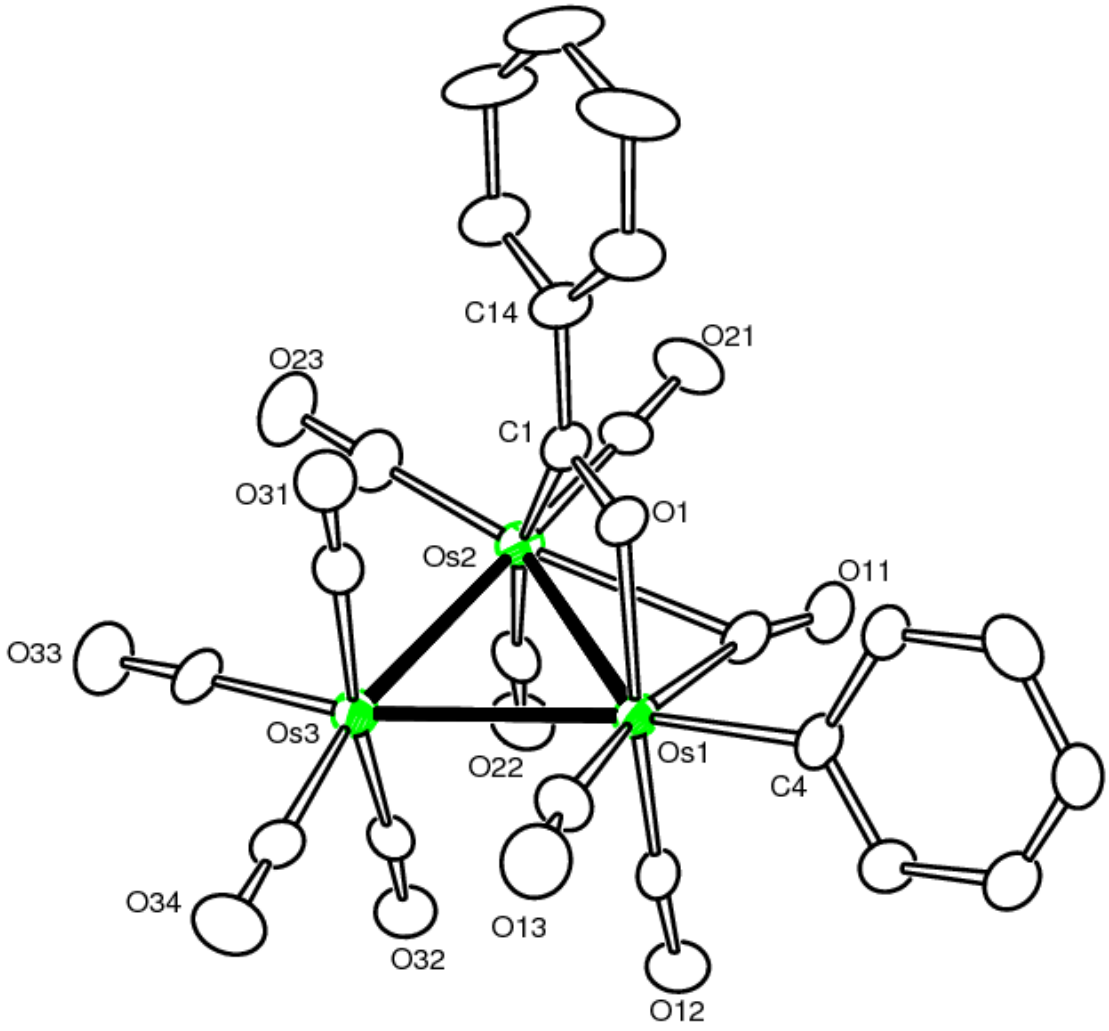

Figure 7.3. An ORTEP diagram of the molecular structure of $PhOs_3(CO)_{10}(\mu\text{-}\eta^2\text{-}O{=}CPh)$, **7.3** showing 30% thermal ellipsoid probability.

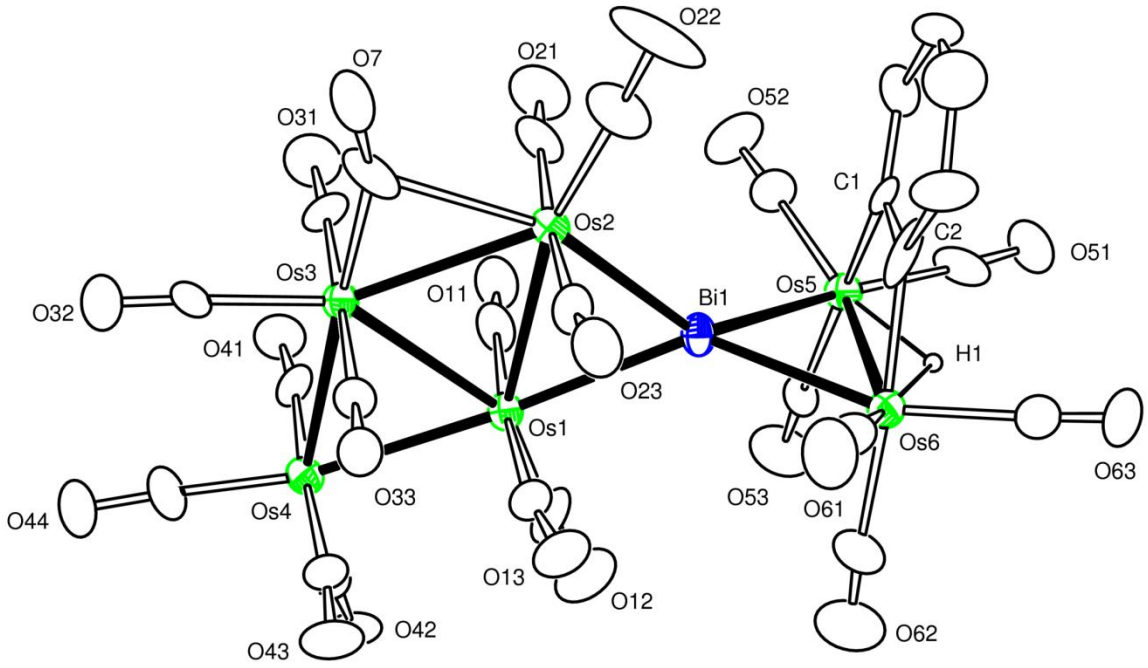

Figure 7.4. An ORTEP diagram of the molecular structure of $Os_6(CO)_{20}(\mu\text{-}\eta^2\text{-}C_6H_4)(\mu_4\text{-}Bi)(\mu\text{-}H)$, **7.5** showing 30% thermal ellipsoid probability.

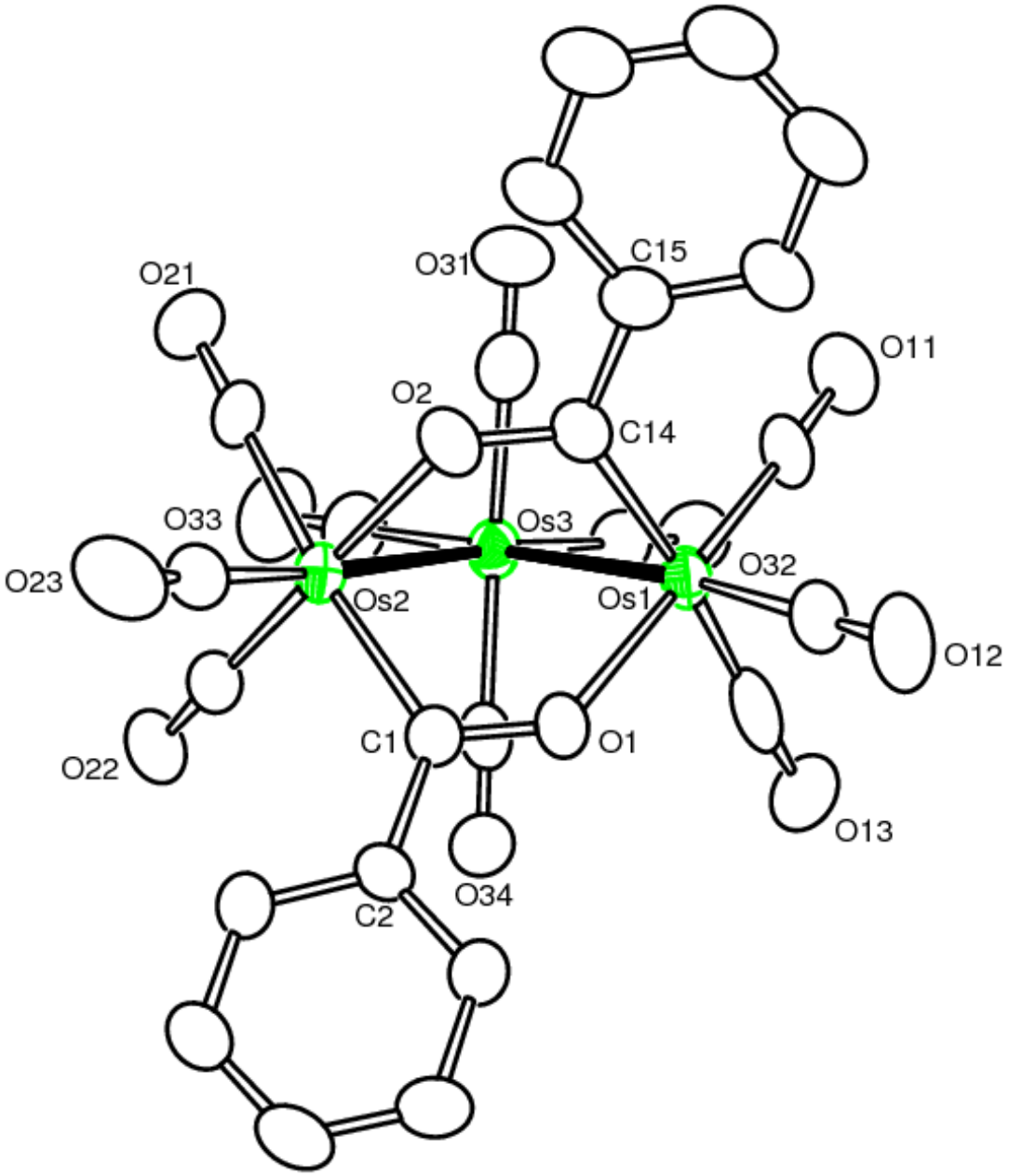

Figure 7.5. An ORTEP diagram of the molecular structure of $Os_3(CO)_{10}(\mu\text{-}\eta^2\text{-}O{=}CPh)_2$, **7.6** showing 30% thermal ellipsoid probability.

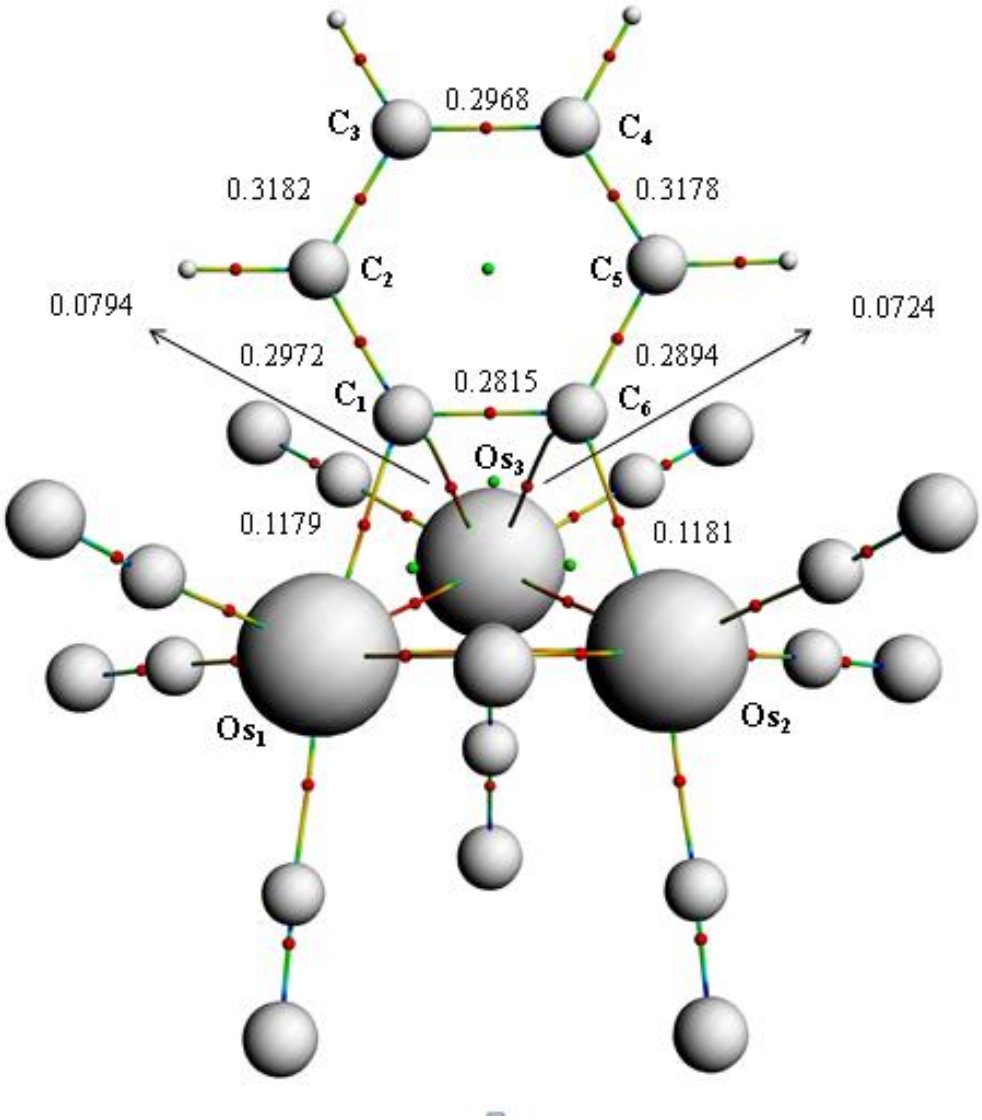

Figure 7.6. Selected electron densities at bond critical points calculated by QTAIM using optimized structure of **7.2**.

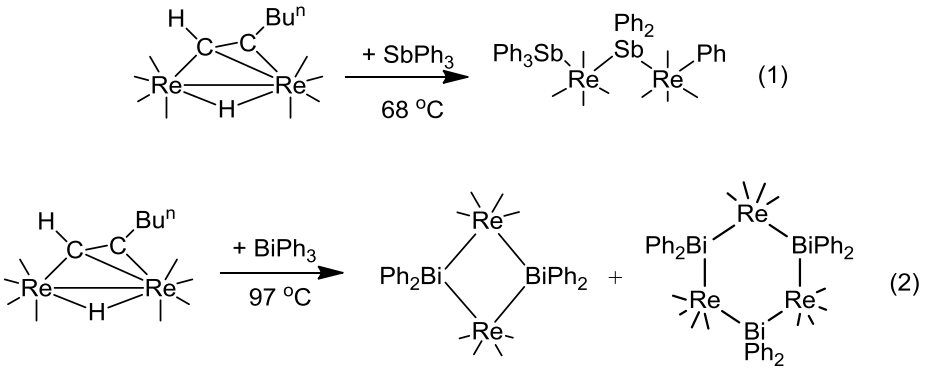

Scheme 7.1.The synthesis of Re-Bi complexes

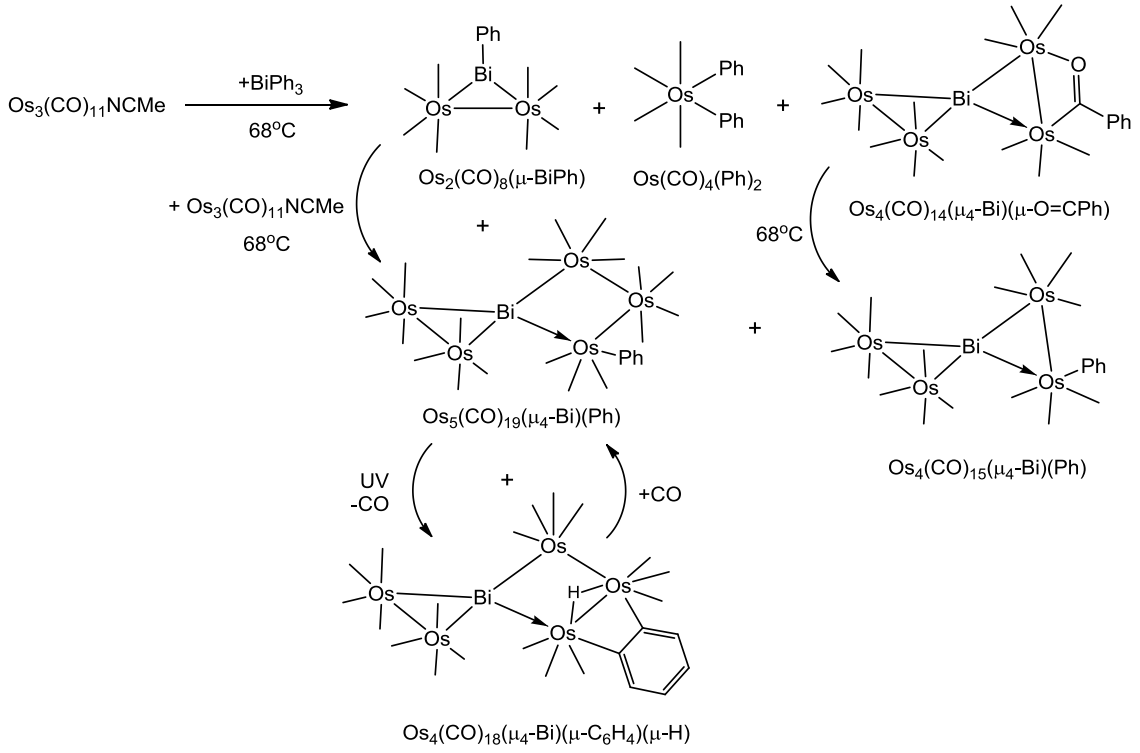

Scheme 7.2. The reaction of $Os_3(CO)_{11}(NCMe)$ with $BiPh_3$ and the transformation of the OsBi cluster complexes.

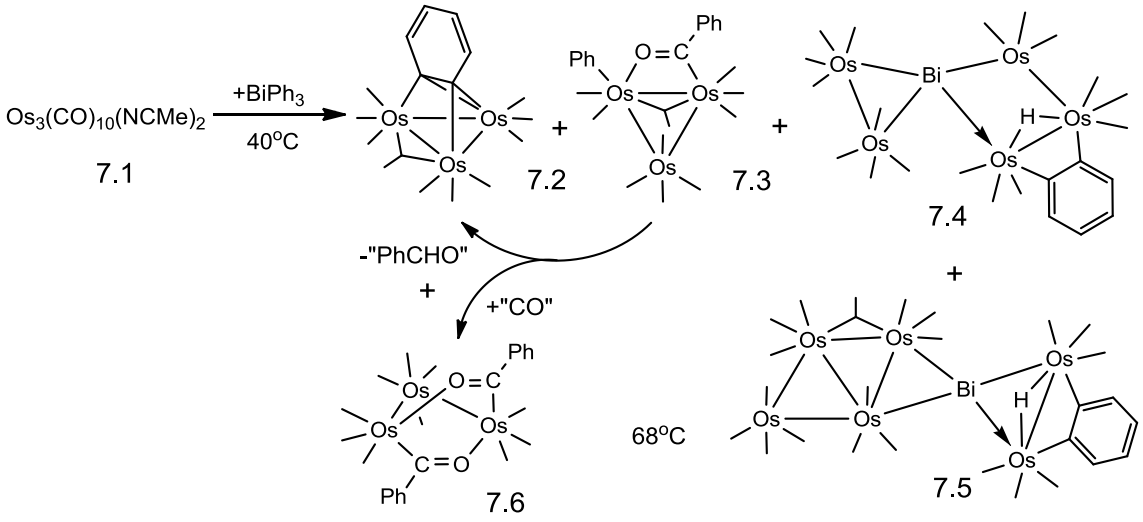

Scheme 7.3. The reaction of $Os_3(CO)_{11}(NCMe)_2$ with $BiPh_3$ and the transformation of the OsBi cluster complexes.

Table 7.1. Crystallographic Data for Compounds **7.2**, **7.3**, **7.5** and **7.6**.

Compound	**7.2**	**7.3**	**7.5**	**7.6**
Empirical formula	$Os_3O_{10}C_{16}H_4$	$Os_3O_{11}C_{23}H_{10}$	$Os_6BiO_{17}C_{29}H_{10}$	$Os_3O_{12}C_{24}H_{10}$
Formula weight	926.79	1032.91	1987.48	1060.92
Crystal system	Orthorhombic	Monoclinic	Monoclinic	Monoclinic
Lattice parameters				
a (Å)	13.9465(3)	10.9741(10)	9.6005(4)	16.766(3)
b (Å)	8.9230(2)	28.833(3)	24.3314(10)	9.4626(14)
c (Å)	15.2811(3)	8.4711(8)	16.4283(7)	16.991(3)
α (deg)	90.00	90.00	90.00	90
β (deg)	90.00	110.460(2)	102.0420(10)	99.243(3)
γ (deg)	90.00	90.00	90.00	90
V ($Å^3$)	1901.65(7)	2511.3(4)	3753.1(3)	2660.6(7)
Space group	*P*na2_1, No.33	*P*2_1/c, No.14	*P*2_1/n, No.14	*P*2_1/n, No.14
Z value	4	4	4	4
ρ_{calc} (g / cm^3)	3.237	2.732	3.517	2.649
μ (Mo K_α) (mm^{-1})	20.048	15.200	24.977	14.354
Temperature (K)	294(2)	294(2)	294(2)	294(2)
$2\Theta_{max}$ (°)	56.06	50.06	50.06	50.06
No. Obs. (I > 2σ(I))	3363	4429	6624	4689
No. Parameters	263	334	475	352
Goodness of fit GOF*	1.035	1.070	1.090	1.071
Max. shift in cycle	0.001	0.000	0.001	0.001
Residuals*: R1; wR2	0.0190, 0.0326	0.0423, 0.0759	0.0637, 0.1201	0.0368, 0.0793
Absor.Corr., Max/min	1.000/0.749	1.000/ 0.703	1.000/0.523	1.000/0.646
Largest peak in Final Diff. Map ($e^{-}/Å^3$)	0.496	1.369	2.935	1.387

*$R = \Sigma_{hkl}(||F_{obs}| - |F_{calc}||)/\Sigma_{hkl}|F_{obs}|$; $R_w = [\Sigma_{hkl}w(|F_{obs}| - |F_{calc}|)^2/\Sigma_{hkl}wF^2_{obs}]^{1/2}$; $w = 1/\sigma^2(F_{obs})$; GOF = $[\Sigma_{hkl}w(|F_{obs}| - |F_{calc}|)^2/(n_{data} - n_{vari})]^{1/2}$.

Table 7.2. Selected intramolecular angles and bond distances for compound **7.2**.[a]

Distances			**Angles**			
Atom	Atom	Distance(Å)	Atom	Atom	Atom	Angle(deg)
Os1	Os2	2.8526(3)	Os3	C6	C1	109.5(5)
Os1	Os3	2.7631(4)	Os1	C1	C6	110.3(4)
Os2	Os3	2.7506(4)				
Os1	C1	2.119(8)				
Os3	C1	2.335(6)				
Os2	C6	2.121(7)				
Os3	C6	2.316(7)				
C1	C6	1.406(9)				
C1	C2	1.438(9)				
C2	C3	1.375(10)				
C3	C4	1.405(10)				
C4	C5	1.361(10)				
C5	C6	1.428(10)				

[a] Estimated standard deviations in the least significant figure are given in parentheses.

Table 7.3. Selected intramolecular angles and bond distances for compound **7.3**.[a]

Distances			**Angles**			
Atom	Atom	Distance(Å)	Atom	Atom	Atom	Angle(deg)
Os1	Os2	2.8141(7)	Os2	C1	O1	112.7(7)
Os1	Os3	2.9020(6)	Os1	O1	C4	88.0(4)
Os2	Os3	2.8606(7)				
Os1	C1	2.087(11)				
C1	O1	1.287(12)				
Os1	O1	2.129(7)				
Os1	C4	2.125(10)				
Os1	C11	1.957(13)				
Os2	C11	2.615(13)				

[a] Estimated standard deviations in the least significant figure are given in parentheses.

Table 7.4. Selected intramolecular angles and bond distances for compound **7.5**.[a]

Distances			**Angles**			
Atom	Atom	Distance(Å)	Atom	Atom	Atom	Angle(deg)
Os1	Os2	2.9511(13)	Os2	Bi1	Os1	65.25(3)
Os1	Os3	2.8875(12)	Os5	Bi1	Os6	67.66(3)
Os1	Os4	2.8268(13)				
Os2	Os3	2.8853(13)				
Os3	Os4	2.8972(13)				
Os5	Os6	3.0309(13)				
Os1	Bi1	2.7644(12)				
Os2	Bi1	2.7085(13)				
Os5	Bi1	2.7203(12)				
Os5	H1	1.71(19)				
Os6	H1	2.01(19)				
Os6	Bi1	2.7235(13)				
Os5	C1	2.12(3)				
Os6	C2	2.11(3)				

[a] Estimated standard deviations in the least significant figure are given in parentheses.

Table 7.5. Selected intramolecular angles and bond distances for compound **7.6**.[a]

Distances			**Angles**			
Atom	Atom	Distance(Å)	Atom	Atom	Atom	Angle(deg)
Os1	Os2	3.652(1)	Os2	Os3	Os1	78.808(15)
Os1	Os3	2.8720(6)				
Os2	Os3	2.8810(7)				
Os2	C1	2.086(9)				
C1	O1	1.256(10)				
Os1	O1	2.112(6)				
Os1	C14	2.091(10)				
C14	O2	1.296(11)				
Os2	O2	2.100(7)				

[a] Estimated standard deviations in the least significant figure are given in parentheses.

REFERENCE

1. Bradford, C.W.; Nyholm, R.S.; Gainsford, G.J.; Guss, J.M. P.R. Ireland and R. Mason, *J. Chem. Soc., Chem. Commum.* **1972**, 87 - 89.

2. Gainsford, G. J.; Guss, J. M.; Ireland, P.R.; Mason, R.; Bradford, C.W.; Nyholm, R. S. *J. Organomet. Chem.* **1972**, *40*, C70 – C72.

3. Tay, C. T.; Leong, W. K. *J. Organomet. Chem.* **2001**, *625*, 231–235.

4. Leong, W. K.; Chen, G. *Organometallics* **2001**, *20*, 2280-2287.

5. Braunschweig, H.; Cogswell, P.; Schwab, K. *Coord. Chem. Rev.* **2011**, *255*, 101-117.

6. Whitmire, K. H. *J. Cluster Sci.* **1991**, *2*, 231-258.

7. Hanna, T. A. *Coord. Chem. Rev.* **2004**, *248*, 429-440.

8. Grasselli, R. K.; Burrington, J. D.; Buttrey, D. J.; DeSanto Jr., P..; Lugmair, C. G.; Volpe, A. F. Jr.; Weingand, T. *Topics in Catal.* **2003**, *23*, 5 – 22.

9. Goddard W. A.; Chenoweth, III, K.; Pudar, S.; van Duin, A. C. T.; Cheng, M.-J. *Topics in Catal.* **2008**, *50*, 2 – 18.

10. Adams, R. D.; Captain, B.; Pearl Jr., W. C., *J. Organomet. Chem.* **2008**, *693*, 1636-1644.

11. Adams, R. D.; Pearl Jr., W. C, *Inorg.Chem.* **2009**, *48*, 9519-9525.

12. Raja, R.; Adams, R. D.; Blom, D. A.; Pearl, W. C. Jr.; Gianotti, E.; Thomas, J. M. *Langmuir*, **2009**, *25*, 7200-7204.

13. Adams, R. D.; Pearl Jr., W. C., *Inorg. Chem.* **2010**, *49*, 7170-7175.

14. Braga, D.; Grepioni, F.; Parisini, E.; Johnson, B. F. G.; Martin, C. M.; Nairn, J. G. M.; Lewis, J. ; Martinelli, M. *J. Chem. Soc. Dalton Trans.*, **1993**, 1891-1895.

15. Jensen, C. M.; Chen, Y-J.; Knobler, C. B.; Kaesz, H. D. *New J. Chem.*, **1988**, *12*, 649-660.

16. SAINT+ Version 6.2a. Bruker Analytical X-ray System, Inc., Madison, Wisconsin, USA, **2001**.

17. Sheldrick, G. M. SHELXTL Version 6.1; Bruker Analytical X-ray Systems, Inc., Madison, Wisconsin, USA, **1997**.

18. ADF2012; SCM Theoretical Chemistry, Vrije Universiteit, Amsterdam, The Netherlands, http://www.scm.com.

19. Perdew, J. P.; Ruzsinszky, A.; Csonka, G. I.; Vydrov, O. A.; Scuseria, G. E. *Phys. Rev. Lett.* **2008**, *100*, 136406.

20. Goudsmit, R. J.; Johnson, B. F. G.; Lewis, J.; Raithby, P. R.; Rosales, M. J. *J. Chem. Soc., Dalton Trans.* **1983**, 2257-2261.

21. Bau, R.; Drabnis, M. H. *Inorg. Chim. Acta* **1997**, *259*, 27-50. (b) Teller, R. G.; Bau, R. *Struc. Bonding* **1981**, *41*, 1-82.

22. Chen, G.; Deng, M.; Lee, C. K. D.; Leong, W. K.; Tan, J.; Tay, C. T. *J. Organomet. Chem.* **2006**, *691*, 387–394.

REFERENCES

Dine, T. J.; Rochester, C. H.; Thomson, J. *Catalysis and surface characterization*; The Royal Society of Chemistry, Cambride, **1992**.

Shriver, D. F.; Kaesz, H. D.; Adams, R. D. *The Chemistry of Metal Cluster Complexes*; VCH Publisher, Weinheim, **1990**.

Mingos, D. M. P.; Wales, D. J. *Introduction of Cluster Chemistry*; Prentice Hall, New York, **1990**.

Knozinger, H.; Guczi, L.; Gates, B. C. *Metal Clusters in Catalysis*; Elsevier, New York, **1986**.

Johnson, B. F. G., *Transition Metal Clusters*; Wiley, New York, **1980**.

Chisholm, M. H.; Early Transition Metal Clusters with π-Donor Ligands; VCH Publishers, New York, **1995**.

Johnson, B. F. G. *Coord. Chem. Rev.* **1999**, *190-192*, 1269.

Cotton, F. A.; Wilkinson, G.; Murillo, C. A.; Bochmann, M.; *Advanced Inorganic Chemistry*, six ed., Wiley, New York, **1999**.

Thayer, J. S. *Organometallic Chemistry*, VCH Publishers, **1988**.

Mond, L.; Langer, C.; Quincke, F. *J. Chem. Soc.* **1890**, 749.

Abel, E. *J. Organomet. Chem.* **1990**, *383*, 11.

Mingo, D. M. P. *Accts. Chem. Res.* **1984**, *17*, 311-319.

Muetterties, E. L.; Rhodin, T. N.; Band, E.; Brucker, C. F.; Retzer, W. R. *Chem. Rev.* **1979**, *79*, 91.

Muetterties, E. L. *Bull. Soc. Chim. Belg.* **1976**, *85*, 451.

Muetterties, E. L. *Bull Soc. Chim. Belg.* **1975**, *84*, 959.

Amoroso, A. J.; Gade, L. H.; Johnson, B. F. G.; Lewis, J.; Raithby, P. R.; Wong, W. T. *Angew. Chem. Int. Ed. Engl.* **1991**, *24*, 697.

Bradley, J. S. *J. Am. Chem. Soc.* **1966**, *88*, 3491.

Adams, R. D.; Cotton, F. A. *Catalysis by Di- and Polynuclear Metal Cluster Complexes*, Wiley-VCH, New York, 1998, chapter1, p4

Adams, R. D.; Barnard, T. S.; Li, Z.; Wu, W.; Yamamoto, J. H. *J. Am. Chem. Soc.* **1994**, *116*, 9103.

Shephard, D. S.; Maschmeyer, T.; Thomas, J. M.; Sankar, G.; Ozkaya, D.; Zhou, W.; Oldroyd, R. D.; Bell, R. G. *Angew. Chem. Int. Ed. Engl.* **1997**, *36*, 2242.

Parkyns, N. D. in *Proceddings, 3rd International Congress on Catalysis.*

Sachtler, W. H. M.; Schuit, G. C. A.; Zwietering, P. Eds. North-Holland, Amsterdam, 1965, p. 164.

Sinfelt, J. H. *Bimetallic Catalysts: Discoveries, Concepts, and Applications*; Wiley, New York, 1983.

Sinfelt, J. H. *Adv. Chem. Eng.* 1964, *5*, 37.

Ichikawa, M. *Adv. Catal.* **1992**, *38*, 283.

Goodman, D. W.; Houston, J. E. *Science,* **1987**, *236*, 403

Adams, R. D.; Babin, J. E.; Tasi, M.; Wang, J. G. *Organometallics* **1988**, *7*, 755.

Castiglioni, M.; Giordano, R.; Sappa, E. *J. Organomet. Chem.* **1988**, *342*, 111.

Castiglioni, M.; Giordano, R.; Sappa, E. *J. Organomet. Chem.* **1987**, *319*, 167.

Dombek, B. D. *Organometallics* **1985**, *4*, 1707.

Xiao. J.; Puddephatt, R. J. *Coord. Chem. Rev.* **1995**, *143*, 457.

Dees, M. J.; Ponec, V. *J. Catal.* **1989**, *115*, 347.

Rice, R. W.; Lu, K. *J. Catal.* **1982**, *77*, 104.

Rasser, J. C.; Beindorff, W. H.; Scholten, J. F. *J. Catal.* **1979**, *59*, 211.

Sinfelt, J. H. *Sci. Am.* **1985**, *253*, 90.

Sinfelt, J. H.; Via, G. H. *J. Catal.* **1979**, *56*, 1.

Nashner, M. S.; Frenkel, A. I.; Adler, D. L.; Shapley, J. R.; Nuzzo, R. G. *J. Am. Chem. Soc.* **1997**, *119*, 7760.

Hills, C. W.; Nashner, M. S.; Frenkel, A. I.; Shapley, J. R. Nuzzo, R. G. *Langmuir*, **1999**, *15*, 690.

Ekou, T.; Vicente, A.; Lafaye, G.; Especel, C.; Marecot, P. *Appl Catal. A Gen.*. **2006**, *314*, 73-80.

Lafaye, G.; Micheaud-Especel, C.; Montassier, C.; Marecot, P. *Appl. Catal. A Gen.* **2002**, *230*, 19-30.

Lafaye, G.; Micheaud-Especel, C.; Montassier, C.; Marecot, P. *Appl. Catal. A Gen.* **2004**, *257*, 107-117.

Macleod, N.; Fryer, J. R.; Stirling, D.;Webb, G. *Catal. Today* **1998**, *46*, 37-54.

Burch, R. *J. Catal.* **1981**, *71*, 348-359.

Burch, R.; Garla, L. C. *J. Catal.* **1981**, *71*, 360-372.

Srinivasan, R.; Davis, B. H. *Platinum Metals Rev.* **1992**, *36*, 151-163.

Fujikawa, T.; Ribeiro, F. H.; Somorjai, G. A. *J. Catal.* **1998**, *178*, 58-65.

Park, Y.-K.; Ribeiro, F. H.; Somorjai, G. A. *J. Catal.* **1998**, *178*, 66-75.

Epron, F.; Carnevillier, C.; Marecot, P. *Appl. Catal.* **2005**, *295*, 157-169.

Cortright, R. D.; Dumesic, J. A. *J. Catal.* **1994**, *148*, 771-778.

Huber, G. W.; Shabaker, J. W.; Dumesic, J. A. *Science* **2003**, *300*, 2075-2077.

Cortright, R. D.; Hill, J. M.; Dumesic, J. A. *Catal. Today* **2000**, *55*, 213-223.

Hermans, S.; Raja, R.; Thomas, J. M.; Johnson, B. F. G.; Sankar, G.; Gleeson, D. *Angew. Chem., Int. Ed.* **2001**, *40*, 1211-1215.

Johnson, B. F. G.; Raynor, S. A.; Brown, D. B.; Shephard, D. S.; Mashmeyer, T.; Thomas, J. M.; Hermans, S.; Raja, R.; Sankar, G. *J. Mol. Catal. A: Chem* **2002**, *182-183*, 89-97.

Hermans, S.; Johnson, B. F. G. *Chem. Commun.* **2000**, 1955-1956.

Dumitriu, D.; Bârjega, R.; Frunza, L.; Macovei, D.; Hu, T.; Xie, Y; Pârvulescu, V.I.; Kaliaguine, S. *J. Catal.* **2003**, *219*, 337–351.

Zhao, J.; Qian, G., Li, F.; Zhu J.; Ji ,S.; Li, L. *Chin. J. Catal.*, **2012**, *33*, 771–776.

Qian, G.; Ji, D.; Lu, G.; Zhao, R.; Qi, Y.; Suo, J, *J. Catal.* **2005**, *232*, 378–385.

Dautzenberg, F. M.; Helle, J. N.; Biolen, P.; Sachtler, W. M. H. *J. Catal.* **1980**, *63*, 119-128.

Biloen, P.; Helle, J. N.; Verbeek, H.; Dautzenberg, F. M.; Sachtler, W. M. H. J. Catal, 1980, 63, 112

Guidotti, M.; Dal Aanto, V.; Gallo, A.; Gianotti, E.; Peli, G.; Psaro, R.; Sordelli, L. *Catal. Lett.* **2006**, *112*, 89-95.

Shabaker, J. W.; Simonetti, D. A.; Cortright, R. D.; Dumesic, J. A. *J. Catal.* **2005**, *231*, 67-76.

Adams, R. D.; Blom, D. A.; Captain, B.; Raja, R.; Thomas, J. M.; Trufan, E. *Langmuir*, **2008**, *24*, 9223-9226.

Grasselli, R. K. *J. Chem. Ed.* **1986**, *63*, 216-221.

Kirkland, J. B., Niacin, in *Handbook of Vitamins*, Rucker, R.; Zempleni, J.; Suttie, J.W.; McCormick, D.B. (Eds.), 4th ed., Taylor and Francis, New York, **2007**, pp 191–232. *Catal. Lett.* **2006**, *112*, 89-95.

Ali, K. M.; Wonnerth, A.; Huber, K.; Wojta, J. *Brit. J. Pharmacology* **2012**, *167*, 1177-1194.

Grundy, S. M. *Am. J. Cardiol.* **1992**, *70*, I27-I32.

Raja, R.; Adams, R. D.; Blom, D. A.; Pearl, Jr., W. C.; Gianotti, E.; Thomas, J. M. *Langmuir* **2009**, *25*, 7200–7204.

Holt, M. S.; Wilson, W. L.; Helson, J. H. *Chem. Rev.* **1989**, 89, 11-49.

Adams, R. D.; Trufan, E. *Organometallics* **2010**, *29*, 4346-4353.

Adams, R. D.; Trufan, E. *Phil. Trans. R. Soc. A* **2010**, *368*, 1473–1493.

Thomas, J. M.; Johnson, B. F. G.; Raja, R.; Sankar, G.;Midgley, P. A. *Acc. Chem. Res.* **2003**, *36*, 20.

Braunstein, P. Rose, J. In Catalysis by Di- and Polynuclear Metal Cluster Complexes; Adams, R. D.; Cotton, F. A., Eds.;Wiley-VCH: New York, **1998**; Chapter 13.

Braunstein, P.; Rose, J. Metal Clusters in Chemistry; Braunstein, P.; Oro, L.A.; Raithby, P. R., Eds.; Wiley-VCH: Weinheim, **1999**; Vol. 2, Chapter 2.2, pp 616-677.

Adams, R. D.; Captain, B.; Trufan, E.; Zhu, L. *J. Am. Chem. Soc.*, **2007**, *129*, 7545.

Adams, R. D.; Captain, B.; Zhu, L. *Organometallics,* **2006**, *25*, 4183-4187.

Adams, R. D.; Fang, F.; Zhang, Q. *Organometallics*, **2012**, *31*, 2621-2630.

Adams, R. D.; Captain, B.; Smith, J. L., Jr.; Hall, M. B.; Beddie, C. L.; Webster, C. E. *Inorg. Chem.* **2004**, *43*, 7576-7578.

Adams, R. D.; Captain, B.; Fu, W.; Smith, M. D. *Inorg. Chem.* **2002**, *41*, 5593-5601.

Adams, R. D.; Boswell, E. M.; Captain, B.; Hungria, A. B.; Midgley, P. A.; Raja, R.; Thomas, J. M. *Angew. Chem. Int. Ed.* **2007**, *46*, 8182-8185.

Adams, R. D.; Boswell, E. M.; Captain, B.; Patel. M. A. *Inorg. Chem.* **2007**, *46*, 533-540.

Carty, A. J.; Taylor, N. J.; Coleman, A. W.; Lappert, M. F.; *J. Chem. Soc. Chem. Commun.* **1979**, 639.

Holmes, N. J.; Levason, W.; Webster, M. *J. Organomet. Chem.* **1997**, *545-546*, 111.

Schumann, H.; Eguren, L. *J. Organomet. Chem.* **1991**, *403*, 183.

Holmes, N. J.; Levason, W.; Webster, M. *J. Organomet. Chem.* **1999**, *584*, 179-184.

Champness, N. R.; Levason, W. *Coord. Chem. Rev.* **1994**, 133, 115.

Gemelin Handbuch der Anorganische Chemie, Bismut Organischen Verbindungen. Springer, New York 1977.

Adams, R. D.; Pearl, Jr., W. C. *Inorg. Chem.* **2010**, *49*, 7170–7175.

Cortright, R. D.; Dumesic, J. A. *Appl. Catal. A General* **1995**, *129*, 101-115.

Cortright, R. D.; Dumesic, J. A. *J. Catal.* **1995**, *157*, 576-583.

Mallat, T.; Baiker, A. *Appl. Catal. A General* **2000**, *200*, 3-22.

Yoshikawa, K.; Iwasawa, Y. *J. Molec. Catal.* **1995**, *100*, 115-127.

Gerstosio, V.; Santini, C. C.; Taoufik, M.; Bayard, F.; Basset, J.-M.; Buendia, J.; Vivat, M. *J. Catal.* **2001**, *199*, 1-8.

Ruiz-Martinez, J.; Sepulveda-Escribano, A.; Anderson, J. A; Rodriguez-Reinoso, F. *Catal. Today* **2007**, *123*, 235-244.

Hungria, A. B.; Raja, R.; Adams, R. D.; Captain, B.; Thomas, J. M.; Midgley, P. A.; Golvenko, V.; Johnson, B. F. G. *Angew. Chem. int. Ed.*, **2006**, *45*, 4782-4785.
Thomas, J. M.; Adams, R. D.; Boswell, E. M.; Captain, B.; Grönbeck, H.; Raja, R. *Faraday Disc.* **2008**, *138*, 301-315.

Adams, R. D.; Captain, B.; Trufan, E. *J. Organomet. Chem.* **2008**, 693, 3593-3602.

Adams, R. D.; Captain, B.; Fu, W.; Smith，M. D. *Inorg. Chem.*, **2002**, *41*, 2302-2303.

Suss-Fink, G.; Haak, S.; Ferrand, V.; Stoeckli-Evans, H. *Dalton Trans.* **1997**, 3861-3865.

SAINT+ Version 6.2a. Bruker Analytical X-ray System, Inc., Madison, Wisconsin, USA, **2001**.

Sheldrick, G. M. SHELXTL Version 6.1; Bruker Analytical X-ray Systems, Inc., Madison, Wisconsin, USA, **1997**.

Churchill, M. R.; Hutchinson, J. P. *Inorg. Chem.*, **1978**, *17*, 3528-3535.

Bau, R.; Drabnis, M. H. *Inorg. Chim. Acta* **1997**, *259*, 27-50.

Teller, R. G.; Bau, R. *Struc. Bonding*, **1981**, *41*, 1-82.

Churchill, M. R.; Hollander, F. J.; Hutchinson, J. P. *Inorg. Chem.* **1977**, *16*, 2655.

Suss-Fink, G.; Haak, S.; Ferrand, V.; Neels, A.; Stoeckli-Evans, H. *J. Organomet. Chem.* **1999**, 580, 225-233.

Farrugia, L. J.; Miles, A. D.; Stone, F. G. A. *J. Chem. Soc., Dalton Trans.* **1984**, 2415-2422.

Hoferkamp, L. A.; Rheinwald, G.; Stoeckli-Evans, H.; Suss-Fink, G. *Organometallics* **1996**, *15*, 704-712.

Shima, T.; Suzuki, H. *Organometallics* **2005**, *24*, 1703-1708.

Alvarez, M. A.; Garcia, M. E.; Martinez, M.E.; Ramos, A.; Ruiz, M.A. *Organometallics* **2009**, *28*, 6293-6307.

Takaoka, Mendiratta, A.; Peters, J. C. *Organometallics* **2009**, *28*, 3744–3753.

Feldman, J. D.; Peters, J. C.; Tilley, T. D., *Organometallics* **2002**, *21*, 4065-4075.

Litz, K.E.; Banaszak Holl, M. M.; Kampf, J. W.; Carpenter, G. B. *Inorg. Chem.*, **1998**, *37*, 6461–6469.

Tokitoh, N.; Manmaru, K.; Okazaki, R., *Organometallics* **1999**, *13*, 167–171.
Pu, L.; Twamley, B.; Haubrich, S.T.; Olmstead, M. M.; Mork, B. V.; Simons, R. S.; Power, P. P., *J. Am. Chem. Soc.* **2000**, *122*, 650-656.

Ponec, V. and Bond, G. C. in *Catalysis by Metals and Alloys*, *Stud. Surf. Sci. Catal.* **1998**, *95*, Ch. 13.

Tiong Sie, S. in *Catalytic Naphtha Reforming*, G.J. Antos, A.M. Aitani, J.M. Parera (Eds.), Science and Technology, Marcel Dekker Inc., New York, **1995**, Ch. 6.

Thomas, J. M.; Johnson, B. F. G.; Raja, R.; Sankar, G.; Midgley, P. A. *Acc*. *Chem*. *Res*. **2003**, *36*, 20-30.

Adams, R. D.; Captain, B.; Smith, Jr., J. L. *Inorg. Chem.* **2005**, *44*, 1413 – 1420.

Adams, R. D.; Captain, B.; Trufan, E. *J. Cluster Sci.* **2007**, *18*, 642-659.

Adams, R. D.; Kan Y., Trufan, E.; Zhang, Q. *J. Cluster Sci.* **2010**, *21*, 371-378.

Adams, R. D.; Pearl Jr., W. C. *J. Organomet. Chem.* **2011**, *696*, 1198-1210.

Cabeza, J. A.; Franco, R. J.; Llamazares, A.; Riera, V.; Perez-Carreiio, E.; Van der Maelen, J. F. *Organometallics* **1994**, *13*, 55-59.

Delavaux, B.; Chaudret, B.; Dahan, F.; Poilblanc, R. *Organometallics* **1985**, *4*, 935-937.

Harding, M. M.; Nicholls, B. S.; Smith, A. K. *J. Chem. Soc. Dalton* Trans. **1983**, 1479-1481.

Jans, J.; Naegeli, R.; Venanzi, L. M.; Albinati, A. *J. Organomet. Chem.* **1983**, *247*, C37-C41.

Taylor, N. J.; Chieh, P. C.; Carty, A. J. *J. Chem. Soc. Chem. Commun.* **1975**, 448.

Bradford, C. W.; Nyholm, R. S.; Gainsford, G. J.; Guss, J. M.; Ireland, P. R.; Mason, R. *J. Chem. Soc.*, *Chem. Commun.* **1972**, 87-89.

Bradford, C. W.; Nyholm, R. S. *J. Chem. Soc. Dalton* Trans. **1973**, 529-533.

Akita, M.; Hua, R.; Oku, T.; Tanaka, M.; Moro-oka, Y. *Organometallics* **1996**, *15*, 4162-4177.

Watson, W. H.; Poola, B.; Richmond, M.G., *Organometallics* **2005**, *24*, 4687-4690.

Takanori Matsuda, T.; Kadowaki, S.; Yamaguchi, Y.; Murakami, M. *Org. Lett.* **2010** , *12*, 1056-1058.

Corriu, R. J. P.; Moreau, J. J. E. *J. Chem. Soc., D* **1971**, 812.

Esteruelas, M. A.; Martin, M.; Oro, L. A. *Organometallics* **1999**, *18*, 2267-2270.

Kinoshita, H.; Nakamura, T.; Kakiya, H.; Shinokubo, H.; Matsubara, S.; Oshima, K. *Org. Lett.* **2001**, *3*, 2521-2524.

Marciniec, B .; Lawicka, H.; Majchrzak, M.; Kubicki, M.; Kownacki, I. *Chem. Eur. J.* **2006**, *12*, 244-250.

David-Quillot, F.; Thiery, V.; Abarbri, M.; Thibonnet, J.; Besson, T.; Duchene, A. *Trans. Metal Chem.* **2007**, *30*, 235-244.

Ichinose, Y.; Oda, H.; Oshima, K.; Utimoto, K. *Bull. Chem. Soc. Jpn.* **1987**, *60*, 3468-3470.

Mochida, K.; Wada, T.; Suzuki, K.; Hatanaka, W.; Nishiyama , Y.; Nanjo, M.; Sekine, A.; Ohashi, Y.; Masato Sakamoto, M.; Yamamoto, A., *Bull. Chem. Soc. Jpn.* **2001**, *74*, 123-137.

Yang, F.; Trufan, E.; Adams, R. D.; Goodman, D. W. *J. Phys. Chem. C.,* **2008**, *112*, 14233-14235.

Adams, R. D.; Captain, B.; Fu, W. *Inorg. Chem.*, **2003**, *42*, 1328-1333.

Adams, R. D.; Captain, B.; Herber, R. H.; Johansson, M.; Nowik, I.; Smith Jr., J. L., Smith, M. D. *Inorg. Chem.* **2005**, *44*, 6346-6358.

Adams, R. D.; Kan, Y.; Zhang, Q. *Organometallics*, **2011**, *30*, 328-333.

Anema, S. E.; Lee, S. K.; Mackay, K. M.; McLoed, L. C.; Nickolson, B. K. *J. Chem. Soc., Dalton Trans.* **1991**, 1209-1217.

Anema, S. E.; Lee, S. K.; Mackay, K. M.; Nickolson, B. K.; Service, M., *J. Chem. Soc., Dalton Trans.* **1991**, 1201-1202.

Lee, S. K.; Mackay, K. M.; Nickolson, B. K., *J. Chem. Soc., Dalton Trans.* **1993**, 715-722.

Foster, S. P.; Mackay, K. M.; Nickolson, B. K., *J. Chem. Soc., Chem. Commun.* **1982**, 1156-1157.

Gusbeth, P.; Vahrenkamp, H., *Chem. Ber.* **1985**, *118*, 1746-1757.

Eady, C. R.; Johnson, B. F. G.; Lewis, J. *J. Chem. Soc., Dalton Trans*, **1977**, 477-485.

Adams, R. D.; Captain, B.; Hall, M. B.; Trufan, E.; Yang, X. *J. Am. Chem. Soc.*, **2007**, *129*, 12328-12340.

ADF2012, SCM, Theoretical Chemistry, Vrije Universiteit, Amsterdam, The Netherlands, http://www.scm.com.

Perdew, J. P.; Ruzsinszky, A.; Csonka, G.I.; Vydrov, O.A.; Scuseria, G. E. *Phys. Rev. Lett.* **2008**, *100*, 136406-136409.

Lauher, J. *J. Am. Chem. Soc.* **1978**, *100*, 5305-5315.

Thimmappa, B. H. S. *J. Cluster Sci.* **1996**, *7*, 1-36.

Halet, J.-F.; Hoffmann, R.; Saillard, J.-Y. *Inorg. Chem.* **1985**, *24*, 1695-1700.

Gimarc, B. M. *Accts. Chem. Res.* **1974**, *7*, 384 – 392.

Crabtree, R. H. *The Organometallic Chemistry of the Transition Metals*, 4th Ed., Wiley-Interscience, Hoboken, **2005**, p 56.

Collman, J. P. *Trans. NY Acad. Sci.* **1968**, 479 – 482.

Schaefer III, H. F.; King, R. B. *Pure Appl. Chem.* **2001**, *73*, 1059 – 1073.

Trinquier, G.; Malrieu, J. P.; Garciacuesta, I. *J. Am. Chem. Soc.* **1991**, *113*, 6465 – 6473.

Broach, R. W.; Williams, J. M. *Inorg. Chem.* **1979**, *18*, 314 – 319.

Wilson, R. D.; Bau, R. *J. Am. Chem. Soc.* **1976**, *98*, 4687 – 4689.

Adams, R. D; Captain, B.; Beddie, C.; Hall, M. B. *J. Am. Chem. Soc.* **2007**, *129*, 986 – 1000.

Canty, A. J.; Johnson, F. G.; Lewis, J. and Norton, J. R., *Chem.Comm*, **1972**, 1331–1332.

SpinWorks 3.1.7, Copyright ., Kirk Marat, University of Manitoba, **2010**.

Quirt, A.R.; Martin, J.S. J. Magn. Reson. **1971**, *5*, 318 – 327.

Tao, J.; Perdew, J. P.; Staroverov, V. N.; Scuseria, G. E. *Phys. Rev. Lett.*, **2003**, *91*, 146401 – 146404

Gaussian 09, Revision B.01, M. J. Frisch, G. W. Trucks, H. B. Schlegel, G. E. Scuseria, M. A. Robb, J. R. Cheeseman, G. Scalmani, V. Barone, B. Mennucci, G. A. Petersson, H. Nakatsuji, M. Caricato, X. Li, H. P. Hratchian, A. F. Izmaylov, J. Bloino, G. Zheng, J. L. Sonnenberg, M. Hada, M. Ehara, K. Toyota, R. Fukuda, J. Hasegawa, M. Ishida, T.

Nakajima, Y. Honda, O. Kitao, H. Nakai, T. Vreven, J. A. Montgomery, Jr., J. E. Peralta, F. Ogliaro, M. Bearpark, J. J. Heyd, E. Brothers, K. N. Kudin, V. N. Staroverov, T. Keith, R. Kobayashi, J. Normand, K. Raghavachari, A. Rendell, J. C. Burant, S. S. Iyengar, J. Tomasi, M. Cossi, N. Rega, J. M. Millam, M. Klene, J. E. Knox, J. B. Cross, V. Bakken, C. Adamo, J. Jaramillo, R. Gomperts, R. E. Stratmann, O. Yazyev, A. J. Austin, R. Cammi, C. Pomelli, J. W. Ochterski, R. L. Martin, K. Morokuma, V. G. Zakrzewski, G. A. Voth, P. Salvador, J. J. Dannenberg, S. Dapprich, A. D. Daniels, O. Farkas, J. B. Foresman, J. V. Ortiz, J. Cioslowski, and D. J. Fox, Gaussian, Inc., Wallingford CT, **2010**

Bergner, A.; Dolg, M.; Kuechle, W.; Stoll, H.; Preuss, H. *Mol. Phys.*, **1993**, *80*, 1431 – 1441.

Kaupp, M.; Schleyer, P. v. R.; Stoll, H.; Preuss, H. *J. Chem. Phys.*, **1991**, *94*, 1360 – 1366.

Hariharan, P.C.; Pople, J.A. *Theoret. Chimica Acta*, **1973**, *28*,213 – 222.

te Velde, G.; Bickelhaupt, F.M.; van Gisbergen, S.J.A.; Fonseca Guerra, C.; Baerends, E.J.; Snijders, J.G.; Ziegler, T. *Journal of Compututational Chemistry,* **2001**, *22*, 931–967.

Fonseca Guerra, C.; Snijders, J.G.; te Velde, G.; Baerends, E.J. *Theoretical Chemistry Accounts*, **1998**, *99*, 391– 403.

ADF2010, SCM, Theoretical Chemistry, Vrije Universiteit, Amsterdam, The Netherlands, http://www.scm.com E.J. Baerends, T. Ziegler, J. Autschbach, D. Bashford, A. Bérces, F.M. Bickelhaupt, C. Bo, P.M. Boerrigter, L. Cavallo, D.P. Chong, L. Deng, R.M. Dickson, D.E. Ellis, M. van Faassen, L. Fan, T.H. Fischer, C. Fonseca Guerra, A. Ghysels, A. Giammona, S.J.A. van Gisbergen, A.W. Götz, J.A. Groeneveld, O.V. Gritsenko, M. Grüning, S. Gusarov, F.E. Harris, P. van den Hoek, C.R. Jacob, H. Jacobsen, L. Jensen, J.W. Kaminski, G. van Kessel, F. Kootstra, A. Kovalenko, M.V. Krykunov, E. van Lenthe, D.A. McCormack, A. Michalak, M. Mitoraj, J. Neugebauer, V.P. Nicu, L. Noodleman, V.P. Osinga, S. Patchkovskii, P.H.T. Philipsen, D. Post, C.C. Pye, W. Ravenek, J.I. Rodríguez, P. Ros, P.R.T. Schipper, G. Schreckenbach, J.S. Seldenthuis, M. Seth, J.G. Snijders, M. Solà, M. Swart, D. Swerhone, G. te Velde, P. Vernooijs, L. Versluis, L. Visscher, O. Visser, F. Wang, T.A. Wesolowski, E.M. van Wezenbeek, G. Wiesenekker, S.K. Wolff, T.K. Woo, A.L. Yakovlev

van Lenthe, E.; Baerends, E. J.; Snijders, J. G. *J. Chem. Phys.* **1993**, *99*, 4597–4610.

van Lenthe, E.; Baerends, E. J.; Snijders, J. G. *J. Chem. Phys.* **1994**, *101*, 9783 – 9792.

van Lenthe, E.; Ehlers, A. E.; Baerends, E. J. *J. Chem. Phys.* **1999**, *110*, 8943 – 8953.

Sheldrick, G. M.; Yesinowski, J. P. *J. C. S., Dalton Trans.* **1975**, 873 – 876.

Wade, K. in *Transition Metal Clusters*, Johnson, B. F. G., Ed., John Wiley & Sons, Chichester, **1980**, Ch. 3, pp 209 – 264.

Bhaduri, S.; Sapre, N.; Jones, P. G. *J. Organomet. Chem.* **1996**, *509*, 105 – 107.

Adams, R. D.; Chen, M.; Elpitiya, G.; Zhang, Q. *Organometallics*, **2012**, *31*, 7264-7272.

Braga, D.; Grepioni, F.; Parisini, E.; Johnson, B. F. G.; Martin, C. M.; Nairn, J. G. M.; Lewis, J.; Martinelli, M., *J. Chem. Soc. Dalton Trans.*, **1993**, 1891-1895.

PartyKa, D. V.; Zeller, M.; Hunter, A. D.; Gray, T. G., *Angew. Chem. Int. Ed.* **2006**, 45, 8188 –8191.

Stephens P.J.; Devlin F.J.; Chabalowski C.F. and Frisch M.J. *J. Phys. Chem.*, **1994**, 98 (45), 11623–11627.

Zhao Y.; Truhlar D. G. *J. Chem. Phys.* **2006**, 125, 194101-194118.

Adams, R. D.; Boswell, E. M.; Hall, M. B.; Yang, X. *Organometallics* **2008,** *27*, 4938 – 4947.

Churchill, M. R.; DeBoer, B. G. *Inorg. Chem.* **1977**, *16*, 878.

Einstein, F. W. B.; Pomeroy, R. K.; Willis, A. C. *J. Organometal. Chem.* **1986**, *311*, 257−268.

Musaev, D. G.; Mowroozi-Isfahani, T.; Morokuma, K.; Abedin, J.; Rosenberg, E.; Hardcastle, K. I. *Organometallics* **2006,** *25*, 203 – 213.

Hyder, M. I.; Begum, N.; Sikder, M. D. H.; Hossain, G. M. G.; Hogarth, G.; Kabir, S. E.; Richard, C. J. *J. Organomet. Chem.* **2009**, *694*, 304 – 308.

Sharmni, A.; Minazzo, A.; Salassa, L.; Rosenberg, E.; Ross, J. A. B.; Kabir, S. E.; Hardcastle, K. I. *Inorg. Chim. Acta* **2008**, *361*, 1624 – 1633.

Deeming, A. J.; Forth, C. S.; Hyder, M.I.; Kabir, S. E.; Nordlander, E.; Rodgers, F.; Ullmann, B. *Eur. J. Inorg. Chem.* **2005**, 4352 – 4350.

Keister, J. B.; Frey, U.; Zbinden, D.; Merbach, A. E. *Organometallics* **1991**, *10*, 1497 – 1501.

Deeming, A. J.; Hassan, M. M.; Kabir, S. E.; Nordlander, E.; Tocher, D. A. *J. Chem. Soc., Dalton Trans.* **2004**, 3709 – 3714.

Deeming, A. J.; Donovan-Mtunzi, S.; Kabir, S. E.; Manning, P. J. *J. Chem. Soc., Dalton Trans.* **1985**, 1037 – 1741.

Coughlin, D.; Lewis, J.; Moss, J. R. *J. Organomet. Chem.* **1993**, *444*, C53 – C54.

Wang, W.; Einstein, F. W. B.; Pomeroy, R. K. *J. Chem. Soc., Chem. Commun.* **1992**, 1737 – 1738.

Wang, W.; Batchelor, R. J.; Einstein, F. W. B.; Lu, C.-Y.; Pomeroy, R. K. *Organometallics* **1993**, *12*, 3598 – 3606.

Adams, R. D.; Rassolov, V.; Zhang, Q. *Organometallics* **2012**, *31*, 2961−2964.

Bauer, A.; Schmidbaur, H. *J. Am. Chem. Soc.* **1996,** *118*, 5324-5325.

Bauer, A.; Schier, A.; Schmidbaur, H. *J. Chem. Soc., Dalton Trans.*, **1995**, 2919-2920.

Liu, X.-Y.; Riera, V.; Ruiz, M. A.; Lanfranchi, M.; Tiripicchio, A. *Organometallics* **2003**, *22*, 4500−4510.

Arii, H.; Nanjo, M.; Mochida, K. *Organometallics* **2008**, *27*, 4147-4151.

Adams, R. D.; Smith Jr., J. L. *Inorg.Chem.* **2005**, *44*, 4276-4281.

Tanabe, M.; Ishikawa, N.; Osakada, K. *Organometallics* **2006**, *25*, 796-798.

Braddock-Wilking, J.; Corey, J.Y.; White, C.; Xu, H.; Rath, N.P. *Organometallics* **2005**, *24*, 4113-4115.

Fehlhammer, W. B.; Stolzenberg, H. in Wilkinson, G.; Stone, F. G. A.; and Abel, E. (Eds.), Comprehensive Organometallic Chemistry, Pergamon, Oxford, U.K., 1982, Ch. 31.4.

Curtis, C. T.; Stone, F. G. A. *J. Organomet. Chem.* **1968**, *11*, 644−646.

Ferrari, R. P.; Vaglio, G. A.; Gambino, O.; Valle, M.; Cetini, G. *J. Chem. Soc., Dalton Trans.*, **1995**, 1998-2001.

Adams, R. D.; Qu, B.; Smith, M. D.; Albright, T. A. *Organometallics* **2002**, *21*, 2970−2978.

Carmona, E.; Guitierrez-Puebla, E.; Monge, A.; Marin, J. M.; Paneque, M.; Poveas, M. L. *Organometallics* **1984**, *3*, 1438−1440.

Reddy, K. R.; Surekha, K.; Lee, G.-H.; Peng, S.-M.; Liu, S.-T. *Organometallics* **2001**, *20*, 5557−5563.

Knorr, M.; Strohmann, C.; Braunstein, P.; *Organometallics* **1996**, *15*, 5653−5663.

Rusik, C. A.; Collins, M. A.; Gamble, A. S.; Tonker, T. L.; Templeton, J. L. *J. Am. Chem. Soc.* **1989**, *111*, 2550–2560.

Gainsford, G. J.; Guss, J. M.; Ireland, P.R.; Mason, R.; Bradford, C.W.; Nyholm, R. S. *J. Organomet. Chem.* **1972**, *40*, C70 – C72.

Tay, C. T.; Leong, W. K. *J. Organomet. Chem.* **2001**, *625*, 231–235.

Leong, W. K.; Chen, G. *Organometallics* **2001**, *20*, 2280-2287.

Braunschweig, H.; Cogswell, P.; Schwab, K. *Coord. Chem. Rev.* **2011**, *255*, 101-117.

Whitmire, K. H. *J. Cluster Sci.* **1991**, *2*, 231-258.

Hanna, T. A. *Coord. Chem. Rev.* **2004**, *248*, 429-440.

Grasselli, R. K.; Burrington, J. D.; Buttrey, D. J.; DeSanto Jr., P..; Lugmair, C. G.; Volpe, A. F. Jr.; Weingand, T. *Topics in Catal.* **2003**, *23*, 5 – 22.

Goddard W. A.; Chenoweth, III, K.; Pudar, S.; van Duin, A. C. T.; Cheng, M.-J. *Topics in Catal.* **2008**, *50*, 2 – 18.

Adams, R. D.; Captain, B.; Pearl Jr., W. C., *J. Organomet. Chem.* **2008**, *693*, 1636-1644.

Adams, R. D.; Pearl Jr., W. C, *Inorg.Chem.* **2009**, *48*, 9519-9525.

Jensen, C. M.; Chen, Y-J.; Knobler, C. B.; Kaesz, H. D. *New J. Chem.*, **1988**, *12*, 649-660.

Goudsmit, R. J.; Johnson, B. F. G.; Lewis, J.; Raithby, P. R.; Rosales, M. J. *J. Chem. Soc., Dalton Trans.* **1983**, 2257-2261.

Chen, G.; Deng, M.; Lee, C. K. D.; Leong, W. K.; Tan, J.; Tay, C. T. *J. Organomet. Chem.* **2006**, *691*, 387–394.